Hydrological Modelling of the Transboundary Brahmaputra River for Strategic Water Management under Climate Change

A thesis submitted in partial fulfillment of the requirement

for the award of the degree of

Doctor of Philosophy

By

Pulendra Dutta

Department of Civil Engineering
Indian Institute of Technology Guwahati
2020

Department of Civil Engineering
Indian Institute of Technology Guwahati
Guwahati-781039, Assam, India

Certificate

It is certified that the work containing in this thesis entitled "**Hydrological Modelling of the Transboundary Brahmaputra River for Strategic Water Management under Climate Change**" by **Pulendra Dutta**, **Roll Number 166104038** (QIP), a student in the Department of Civil Engineering, Indian Institute of Technology Guwahati for the award of Doctor of Philosophy has been carried out under my supervision and that this work has not been submitted elsewhere for a degree.

Date:

(**Arup Kr Sarma**)

Professor,

Department of Civil Engineering

Indian Institute of Technology Guwahati

Guwahati-781039, Assam (India)

Declaration of Authorship

I, **Pulendra Dutta**, declare that this thesis titled "**Hydrological Modelling of the Transboundary Brahmaputra River for Strategic Water Management under Climate Change**" and the works presented in it has been carried out by me under the supervision of **Prof. Arup Kr. Sarma**, Civil Engineering Department, Indian Institute of Technology Guwahati. This work has not been submitted for the award of any other degree.

Date:

(**PULENDRA DUTTA**)

Department of Civil Engineering

Indian Institute of Technology Guwahati

Guwahati-781039, Assam, India

Acknowledgment

I would like to express my deep sense of gratitude and sincere thanks to my Supervisor Prof. Arup Kr. Sarma, Professor, Civil Engineering Department, Indian Institute of Technology Guwahati, for his invaluable guidance and constant support throughout my research work.

I am grateful to the Chairman of my Doctoral Committee Prof. Chandan Mahanta, HOD, Civil Engineering Department, Indian Institute of Technology Guwahati, for his valuable suggestions and kind support in the completion of my research works. I am very much thankful to the members of my Doctoral Committee Prof. Sashindra Kr. Kakoty, Professor, Mechanical Engineering Department, IITG, and Dr. Sreeja P., Associate Professor, Civil Engineering Department, IITG, for their valuable suggestions and kind support during my research works.

I am obliged to the government of Assam and Jorhat Engineering College for sponsoring me to undergo the Ph.D. research under the QIP scheme. Besides, I am thankful to the Indian Institute of Technology Guwahati for providing the chance to carry out my research under magnificent facilities and a beautiful environment.

I acknowledge the support of the Indian Meteorological Department and Central Water Commission for providing me hydro-climatological data required for my works.

Finally, I am indebted to my friends and well-wishers namely Gilbert, Deepsikha, Gaurav, Anupal, Amit, Dipima, Jeffrey, Jayashree, Bandita, Sagarika and many more who have directly or indirectly extended helping hands during my research works.

Pulendra Dutta

Dedicated to my

(*Wife*) Dr. Ajanta Dutta

(*Son*) Victor Kashyap

(*Daughter*) Beauty Nandini

ABSTRACT

Water is the basis of life on earth and iver is one of the prime sources where people get a large portion of water for their uses. The Brahmaputra is one of the major rivers of south Asia that majestically flows for catering to the people of its basin covering four nations viz. China, India, Bangladesh and Bhutan. The physica-climatological complexities and transboundary issues of the Brahmaputra river basin pose a huge challenge for drawing the effective benefits of the water resources. Besides, the study of this basin encounters difficulties due to limited information of hydro-climatological variables. In the absence of observed data, the researchers can utilize the globally available satellite based data, although their reliability is of concern. Of course, we could identify a weather dataset consisting of global gridded CFSR data, IMD data and stations data over Tibet as the best suitable combination to provide a reasonably acceptable hydrologic assessment of the Brahmaputra basin.

Hydrologic models can be used as a tool for water resources management of this data-scarce basin, although their calibration demand spatially observed data for such a large river basin. Moreover, a hydrologic model established for a large basin should be made capable to replicate the basin hydrology even at sub-basin levels. All these issues are incorporated in the present study based on hydrologic modeling approach in SWAT platform. The purpose of the study is to derive science-based elements required for water resources managements at desired locations across the Brahmaputra basin. The basin scale impact analysis using SWAT hydrologic model has provided a reasonably acceptable outcomes at the basin as well as its sub-basin levels.

Man-made activity within the jurisdiction of a river leads to change in its basin hydrology to subsequently impact on the hydraulic behaviour. In the absence of cooperation among the basin sharing nations, it becomes difficult to understand the extent of impacts on the lower riparian countries due to dams and reservoirs constructed in the upper riparian

country. This study presents quantifications of such impacts due to water diverted from a specified location, based on the results of the hydrologic model simulated with a provision of a dam and reservoir. The impact of such a reservoir on water resources parameters like stream flow, sediments, etc. are found to be significant corresponding to 10%, 25%, 50%, and 80% water diversion scenarios adopted in the analyses.

The Brahmaputra river basin characterized by glaciers at its source and ocean at its mouth is susceptible to global climate change. The present study projects the climatic variables for future periods and evaluates the probable impacts on the basin hydrology based on the GCMs. The uncertainties associated with the GCMs were handled by applications of interpolation followed by bias correction methods. Man-Kendall and Sen's slope trend analyses depict the Brahmaputra basin would undergo significant changes in the climatic pattern that will consequently impact on the streamflow till the end of the current century. As such, implications of these impacts that need to be strategically managed for the greater interest of obtaining the utmost benefits of water resources of this mighty basin are also forwarded to help the stakeholders.

List of Contents

List of Figures

List of Tables

List of abbreviations

95 PPU	: 95 Percent prediction uncertainty
ANN	: Artificial neural network
BB	: Brahmaputra basin
BP	: Base period
CMIP5	: Coupled model inter-comparison project phase 5
CC	: Climate change
CN	: Curve number
CWC	: Central Water Commission (India)
FAO	: Food and Agricultural Organization
GA	: Genetic algorithm
GCM	: Global climate model
GIS	: Geographic information system
HEC-HMS	: Hydrologic Engineering Center - Hydrologic Modeling System
HEC-RAS	: Hydrologic Engineering Center – River Analysis System
IDF	: Intensity duration frequency
IDWA	: Inverse distance weighted average
IMD	: Indian Meteorological department
IPCC	: Inter-governmental panel on climate change
IRS	: Indian remote sensing
LISS	: Linear imaging self-scanning sensor
LULC	: Landuse and landcover
NDVI	: Normalized difference vegetation index
NS	: Statistically non-significant
NSE	: Nash-Sutcliff efficiency

PCP	: Precipitation
RCM	: Regional climate model
RCP	: Representation concentration pathways
RMSE	: Root mean square error
SCS	: Soil conservation services
SRTM	: Shuttle radar topographic mission
SS	: Sen's slope
SUFI2	: Sequential uncertainty parameter fitting approach
SWAT	: Soil and Water Assessment Tool
SWAT-CUP	: SWAT- calibration and uncertainty program
TAMU	: Texas A & M University
USLE	: Universal soil loss equation
VIC	: Variable infiltration capacity
WMS	: Watershed modelling system
WQI	: Water quality index
WR	: Water resources
WRD	: Water Resources Department of Assam

List of symbols

A	: Area
F1	: Future 1
F2	: Future 2
F3	: Future 3
I-B	: Indo-Bangladesh
I-C	: Indo-China
NS	: Statistically non-significant
PCP	: Precipitation
R^2	: Coefficient of determination
S	: Statistically significant
Slr	: Solar radiation
TMax	: Maximum temperature
TMin	: Minimum temperature
Wnd	: Wind velocity

Chapter 1

Introduction

1.0 Background

Ever since the earth was inhabited, the survival of humans and other living creatures have depended on the natural resources that exist freely in nature. Natural resources are the basis of life on earth. However, they are not evenly distributed all over the world. Natural resources are available to sustain the very complex interaction between the living as well as the non-living things. In fact, natural resources are continuously facing a significant threat probably due to the increasing population. Overpopulation demands industrial growth that leads to the consumption of more raw materials and natural resources. Even though natural resources are the basic support structures of life, its abundance or scarcity can come with a lot of trouble and conflict.

Water resources are the sources of water that are potentially useful to life for existence. Salient uses of water include household, agriculture, industrial, environmental and recreational activities. All these uses virtually require fresh water obtained from surface and groundwater sources. As compared to the groundwater, surface water is mostly used by people worldwide, as they are easily accessible. River, lake, pond and wetland are some of the freshwater sources available on the earth surface. Although rivers account for only a small amount of freshwater, this is where humans get a large portion of their water from. A river traverses along a long path, and its basin includes several places consisting of streams, lakes, forests, dwellings, and landscapes, etc. As such, maintaining ecology within a natural river basin is necessary for the sustainability of all living beings.

The ecological balance of a natural river basin is disturbed primarily by human interventions. Human needs have historically taken priority over environmental apprehensions while managing water and other natural assets. Natural beings do not follow political restrictions, so laws and other policy activities in majority cases, are not aligned with the definite wishes of plants, animals, and water. Therefore, a natural river basin

should be so managed that its original system remains merely undisturbed while deriving benefits from its water resources.

Effective river basin management policy requires consideration of multi-dimensional aspects of nature as well as man-made activities, for deriving the utmost benefits from the water resources. With the advent of computer tools, studies related to such management have nowadays become easier where multiple objectives in terms of hydrologic, hydraulic, economic, social and ecological analysis can be incorporated in a single platform. In fact, there could be a challenge to understand the basin hydrology for a watershed having complex characteristics like the transboundary Brahmaputra river basin.

The Brahmaputra river basin is characterized by high spatial variations, in terms of topography, weather components, landuse, and land cover. Originating at high altitudes in Tibet, the Brahmaputra river merges into the Bay of Bengal in Bangladesh. So, the source of this mighty river is glacier-fed, whereas the mouth is driven by a high rate of evaporation. Understanding the Brahmaputra basin has always been challenging due to its complex characteristics, both hydraulically and hydrologically (Rao et al., 2009). The Brahmaputra basin is shared by four countries namely China, India, Bangladesh, and Bhutan. The challenge of hydrologic studies of the Brahmaputra basin lies in obtaining correct and adequate input information, especially hydro-climatic data mainly due to transboundary issues. This is because the data scarcity situations widely impact the results of hydrologic studies (Tabari et al. 2012; Chen et al., 2018).

The Brahmaputra river is the youngest among the major rivers in the world, and it is also known as a moving ocean. The Brahmaputra is one of the highly sediment-laden rivers of the world (Goswami, 1985). Locating in the area of high structural instability (Lahiri and Sinha, 2012), the Brahmaputra river carries the largest amount of water and silt among all Indian rivers. The mean annual flow of this mighty river is about 600 billion cubic meters, at its outfall at Bangladesh (Sarma and Singha, 2017). Despite the severe hazards like flood and bank erosion faced by the inhabitants, this basin has enormous potential towards various sectors of water resources including hydropower generation (Singh et al., 2004). The Brahmaputra is the lifeline for many people living along its bank, especially India and Bangladesh regions. However, this is probably the least exploited river in terms of research and management, and there is no comprehensive management policy to date, for this

important river basin. Exploring the Brahmaputra basin hydrologically and hydraulically, by consideration of versatile and complex basin characteristics coupled with the transboundary issues and impact of global climate change is the need of time.

1.1 Purpose of the study

Water basin is a biophysical unit for hydrological analysis, to generate the basis of governance for water resources management. Interestingly, every river basin of the world possesses its unique characteristics. Hydrological models serve as a tool for hydrologic assessment from a river basin, and as such, they should be made capable to represent the basin hydrology in the best possible ways. The versatile complexities and transboundary issues of the Brahmaputra river basin pose a huge challenge to the researchers, engineers, environmentalists, and policymakers, to culminate the effective benefits while managing the water resources. In the absence of available information beyond the national boundary, it becomes difficult to establish a suitable hydrologic model and even to validate at ungauged locations. This complexity is escalated if certain man-made activities are performed at the upper riparian countries that may likely impact the lower riparian country. Hydrology changed upstream would surely impact on the hydrology downstream. Besides, the Brahmaputra river basin characterized by glaciers at its source and ocean at its mouth is susceptible to global climate change. It, therefore, is necessary to incorporate all possible components while assessing the hydrologic parameters of a data-scarce and complex river basin. Especially, the evaluations for impacts due to transboundary effects and future climate change are the need of time. This would facilitate the stakeholders with pieces of information required for managing the water resources of the Brahmaputra.

1.2 Research objectives

Following research objectives have been laid in the present work:

1] Hydrologic assessment at gauged and un-gauged locations by establishing a hydrologic model for the entire Brahmaputra basin.

2] Basin-scale impact studies of the hydrologic model established in the present study.

3] Quantifications of transboundary effects.

4] Assessment of climate change impact on precipitation and temperature of the Brahmaputra river basin, for the present and future periods.

5] Projection of Brahmaputra streamflow as per IPCC emission scenarios.

1.3 Organization of the thesis

The present research work is divided into several chapters as explained below:

- ***Chapter 2*** describes the brief literature review of the works already done by the researchers worldwide, on the topics selected for the present works. Initially, all kinds of literature related to the hydrological aspects of Brahmaputra basin and/or its part were reviewed to identify the potential scopes of research. Later, literatures in the lines of study scopes so identified were reviewed and presented in the subsequent sections. Finally, a critical appraisal of the reviewed literature was done to identify the present research objectives.
- ***Chapter 3*** enlists the study area, and various input datasets used in the present study. The descriptions of datasets along with its processing are also presented in this chapter. As the satellite data often bears certain systemic errors, their applicability was tested before application, and they are presented in Sec. 3.3.
- ***Chapter 4*** describes the processes involved during the development, calibration, and validation of the hydrologic model. The model results are also presented in this chapter, along with the relevant discussion. The model applicability in water resources management of the Brahmaputra river basin has also been presented in this chapter.
- ***Chapter 5*** comprises the detailed description of the basin impact study of the SWAT (Soil and Water Assessment Tool) model. Here, the applicability of a hydrologic model was tested to understand if a model established for a large river basin would provide acceptable outputs for its sub-basins of smaller areas, at the tributary level.
- ***Chapter 6*** describes the probable transboundary effects of the Brahmaputra river. The subsequent impacts at the lower riparian country (India) due to certain flow

augmentation activities at the upper riparian country (China) are evaluated and presented in this chapter.

- ***Chapter 7*** is a description of evaluations for the climate change impacts on the weather variables, especially precipitation and temperature. Here, the detailed procedures like interpolation, bias correction, and uncertainty analysis, etc., of the GCM (Global climatic model) data are presented. Besides, their trend pattern analyses, w.r.t. the IPCC emission scenarios, for the present and future periods are presented in this chapter.
- ***Chapter 8*** describes how the streamflow of the Brahmaputra River is projected for future periods. Here, climate change impact on streamflow with relevant results and discussions are presented corresponding to the IPCC emission scenarios.
- ***Chapter 9*** provides the conclusion and discussion of the entire research works. Finally, the future scopes of research are also presented to conclude the thesis.

######## ########

Chapter 2

Literature Review

2.0 Introduction

This chapter presents the relevant literature of the studies already conducted across the globe, in regards to hydrological modeling, climate change issues and its impacts on water resources, transboundary river issues, etc. Initially, all kinds of literature for the studies regarding the Brahmaputra river basin and its sub-basins are reviewed, to identify the scope of studies at a glance, for this mighty river basin. For this, the resources available at all possible kinds of sources in soft (i.e. online) as well as hard (i.e. library of institutions/ universities etc.) forms are collected. The pieces of literature of the past studies are organized in such a way to cover all the salient objectives of the present area.

2.1 Studies on Brahmaputra river basin

An integrated approach for effective management of the water resources of the river Brahmaputra is essentially needed due to its international character which originates in Tibet, flows through China and India before reaching Bangladesh and finally merging into the Bay of Bengal. The Brahmaputra has been causing a serious threat to life and property lying in the basin. As an approach to mitigate the flood hazard, Latif (1969) carried out a detailed hydrographical and hydrological investigation and is of the opinion for providing embankments on both the banks of the Brahmaputra.

The Brahmaputra river in Assam, characterized by high seasonal variability in flow, sediment transport, and channel configuration, is currently experiencing a secular period of aggradations. In a study, Goswami (1985) found that suspended load budget indicates the overall aggradation of the 607 km Assam reach of the Brahmaputra between Ranaghat and Jogighopa by about 16 cm during the period 1971- 1979, whereas about 70% of the suspended sediment inflow into the reach being retained in the channel. The current high

rate of the denudation of river may be caused due to rapid uplift of the mountain system, recent earthquake activity and high susceptibility of geologic formations to erosion by running water along with the effectiveness of the monsoon rainfall regime. Brahmaputra River is located in the area of high structural instability as the large numbers of earthquakes have been evidenced in the Himalayan catchment through which it flows (Lahiri and Sinha, 2012).

The pattern and pathways of sediment transport (both bedload and suspended load) and the evolution of channel planform are all strongly affected by secondary currents. Richardson and Thorne (1998) forwarded a study to understand the effect of secondary current on channel morphology around a braided bar in the Brahmaputra by measuring flow velocities using Acoustic Doppler Current Profiler. In another study, Kotoky and Sarma (2001) forwarded sedimentologic, geomorphologic and hydrological assessment on the Brahmaputra river channel from Majuli to Kaziranga. This study presented evaluations of suspended load characteristics, erosion, and deposition, hydrology and sediment transport pattern based on hydrographs, flood frequency analysis, and sediment rating analysis along with an evaluation of wetlands. Bezbaruah et al. (2003) also added a similar study based on toposheets and IRS imageries. They revealed that the low lying nature combined with frequent shifting of stream channels (Gogoi et al., 2012) in a relatively short time has given rise to the development of numerous swampy areas.

The South Asian river basins are quite different geologically, hydrologically, geomorphologically, hydrodynamically than the other rivers of America (Sikder et al., 2016). For extracting the morphological characteristics of the middle reach of the Brahmaputra river, a 2-dimensional hydrodynamic and sediment transport model was forwarded by considering the flow variation, sediment rating curve and bed material composition (Ravindra and Dutta, 2011). In another study, a hydraulic and sediment transport modelling was carried out by Nandi and Mahanta (2014), and found 23 cm aggradations & 150 cm degradation between Pandughat and Pancharatna, during 2008-2010. Besides, Fischer (2015) attempted to investigate the sensitivity of sediment transport on the Brahmaputra river. In another approach for sediment analysis, Singh and Sarma (2014) forwarded a study related to scouring around the Saraighat bridge piers, where sediment analyses were carried out using different empirical equations. They considered

hydraulic characteristics of the Brahmaputra river. Phukan et al (2012) highlighted the various causes of bank erosion of the Brahmaputra, the 2nd largest river in the world after the Yellow River in China in terms of sediment transport per unit drainage area. Riverbank erosion leads to many damages to the people living aside the river line which are well elaborated by Das et al. (2014).

The experimental studies (Singh et al., 2003; Talukdar, 2013) carried out an experimental based study on a transboundary river basin to understand the erosion pattern. Bank sediments and suspended loads were collected from different locations starting from the Himalayan Front to Bangladesh for the Brahmaputra and its major tributaries. Chemical and isotopic compositions of the sediments are used to trace sediment provenance and to understand erosion patterns in the basin. The study revealed that the composition of Brahmaputra is stable and the Siang-Tsangpo River is the major source of sediment to the whole Brahmaputra.

The geomorphologic studies (Kathar and Sarma, 2009; Sarma and Ashagrie, 2012) reveal that the Brahmaputra river bank is very prone to erosion. The river banks get eroded during high flood seasons and cause a threat to the people living aside the river bank. However, this kind of hazard can be controlled by the application of certain structural measures as suggested by Garimella and Sarma (2007). Generally, hydraulic and sedimentologic analyses are based on Lacey's regime equation, although its applicability is to be checked for the Brahmaputra river having unique characteristics. In such a study, Swamee et al. (2008) developed a regime equation for this mighty river and revealed that the Brahmaputra river follows the structure of Lacey's regime equations, but the values of the coefficients were found to be little different than the original ones. Here, the coefficients stand higher for area and perimeter, whereas the velocity coefficient was found to be greater than that in the original equations. Interestingly, the coefficients for hydraulic radius were found to be of the same order as the original.

Several studies regarding erosion/ deposition patterns were carried out (Jain, 2003; Kotoky et al., 2003; Sarma and Phukan, 2006) for 'Majuli', the world's largest river island. The land area of Majuli follows a consistently decreasing trend from 735.01 sq. Km (1920) to 577.65 sq. Km (1998). Even, application of radiogenic study, based on chemical analysis of river sediments (Singh et al., 2003; Bora and Mahanta, 2006; Kotoly et al., 2006; Sarma

et al., 2007; Sarma and Acharjee, 2012) were forwarded to understand the erosion/ deposition of Majuli. The erosion rate (8.76 km^2/yr) is higher than the deposition rates (1.87 km^2/yr) of Majuli island (Dutta et al., 2010). The agencies like WRD, Brahmaputra Board, etc. are adopting various structural measures to the sub-basins of the Brahmaputra, aiming to prevent bank erosion. The usefulness of permeable groynes in the Brahmaputra and its tributaries are claimed by those departments. A combination of a series of groynes (Kalita and Sarma, 2014) helps control the Brahmaputra riverbank erosion.

The Brahmaputra river system consists of numerous sub-basins. There have been several studies (Perambudoor, 2005; Girija et al., 2007; Kamal and Sarma, 2008; Shil, 2010; Mahanta et al., 2011; Hazarika and Das, 2014; Bora and Goswami, 2015; etc.) in connection with the tributaries like 'Bharalu', 'Subansiri'. 'Pagladiya', Ghorajan', 'Dhansiri' etc. etc. These studies include the determination of peak runoff, sediment yield, water quality assessment, bank line migration, etc. using various approaches such as theoretical, experimental, analytical, etc. Even the areas like geographical setting and their associated physical, ecological and socio-economic characteristics of the sub-basins were covered in certain of these studies. The Brahmaputra basin tributaries exhibit quite different characteristics (Devi and Goswami, 2014) than the other Himalayan rivers. Here, the flood characteristics of rivers are different and therefore, post-flood analyses (Sarma and Sarma, 2010; Roy and Hussain, 2014) play an important role in river restoration. The Brahmaputra basin has also been studied (Bhatt et al., 2013), for accurate assessment of losses in regards to life and property due to floods.

With the advent of computer software, the studies of watershed hydrology have become easier nowadays. Apart from the other available tools like HEC-RAS, HEC-HMS, Mike 11, SWAT, etc., autoregression and time series models (Maheswari and Sarma, 2005) have widely been used for hydrodynamic studies of the Brahmaputra basin and/or its part. A real-time forecast model for stage (Sankhua et al., 2006) and streamflow (Reddy and Sreeja, 2011) was found helpful in predicting the flood events of the Brahmaputra river and its tributaries. Even, genetic algorithm (GA), ANN model (Sharma et al., 2004) are found to be suitable for prediction of the studies of a braided river like the Brahmaputra. However, this study may be advanced through the use of a three-layered ANN model (Singh et al., 2004). The use of the ANN model provides both accuracy and speed

(Siddiquee and Hossain, 2015) over the traditional hydrodynamic modelling in predicting river water levels of the Brahmaputra.

The flows of the Brahmaputra basin are highly seasonal and influenced by monsoon rainfall. Realizing that, meteorological behaviour of the basin was introduced by Chowdhury and Ward (2004) along with the hydrological behaviour, to take stock of variation of streamflow along the river channel. The monsoon flood is very serious (Derry et al., 2007) in the Brahmaputra plain. The hydro-meteorological behaviour in the upstream (India) leading to serious issues of water resources in the downstream (Bangladesh) is presented in this study. The hydro-meteorological variability of the basin including headwater regions in India and their role in the streamflow in the downstream area in Bangladesh are explored based on the climatic patterns of both the countries. The Brahmaputra river basin mass balance model, if developed in combination with the radar altimetry data, provides a better result for predicting flood events (Finsen et al., 2014). This enables the direct use of radar altimetry data for real-time modelling and hydrological forecasting.

The success of a hydraulic project depends upon the knowledge of the accurate peak flow before its design and construction. Flood frequency analysis can be forwarded using L-Moments (Kumar and Chatterjee, 2005) for estimation of the peak flow. Homogeneity of the North Brahmaputra region is developed using discordance measure coupled with heterogeneity measure based on L-Moments for 13 gauge sites of the basin. A total of 500 simulations were performed using Kappa Distribution for computing the heterogeneity measure. Comparative flood frequency analysis was carried out employing L-Moments based on the commonly used frequency distribution. Regional flood frequency relationship was developed for estimation of peak flood for various return periods. Hazarika and Sarma (2013) used meteorological data from GCM and 10 IMD stations including the Barak basin and compared both Fuzzy clustered data sets. GCM data provides a better result of clustering while identifying the homogeneous climatic region.

There have been several studies made on the mighty Brahmaputra regarding bank line migration, erosion/ deposition, streamflow forecasting, geological investigation, etc. Apart from these, certain researches have so far carried out a certain assessment of the water quality. A study of this kind has been formulated by Mandal (2005) for an urban stretch of

20 km of the Brahmaputra river covering upstream and downstream and the entire length of the Guwahati city to understand the water characteristics. Water samples were collected from seventeen sites during several seasons over seven months. The samples were analyzed for water quality evaluation through the application of Water Quality Indices (WQI). To support and strengthen the findings so analyzed, an analysis of the data based on multiple regression was done to examine whether seasonal or spatial variation in different parameters can be explained and predicted based upon their interrelationship in terms of source and mobility. Kriging map was also developed for the prediction of water quality zoning. Similar studies (Reddy, 2005; Hanumagutti, 2006) under the same area of the Brahmaputra river for assessing the quality of water using QUAL2K with emphasis on widespread geological sources that contribute to loads of mineral substances (Sulphate and Phosphate). A regional perspective is provided with river water quality being interpreted concerning catchment geography.

Saxena and Mahanta (2006) presented a study for the distribution of heavy metals in the Brahmaputra floodplain. Sediments were collected from various locations near Guwahati of the Brahmaputra river and tested for heavy metals like Cu, Mn, Fe, and Al by using Scanning Electron Microscope (SEM) and Atomic Absorption Spectroscopy (AAS). The concentrations so obtained were plotted in a GIS to assess the present distribution pattern of metal in the river. The study on the distribution and solid phase of toxic heavy metals of bed sediments concludes addition towards the pollution level of Brahmaputra (Hoque et al., 2011; Sailo and Mahanta, 2014) carried out a study on an unexplored part of the river Brahmaputra basin which is characterized by alluvial deposits and contains high organic carbon. The groundwater of the Brahmaputra basin is enriched by soluble ions and arsenic (Verma et al., 2015), leading to health hazards to its inhabitants.

For proper management of the water resources of a river basin, the understanding of river dynamics is an important parameter. A systematic analysis of river dynamics using ANN robust model using Survey of India toposheets and IRS images coupled with the application of GIS may be helpful to investigate the fluvial-morphology of the river (Sankhua, 2005; Sarma, 2005) for monitoring and management of the Brahmaputra river system. The Brahmaputra river bed morphology in space and time during 1957-1988 (Swamee et al., 2008) changed exponentially. There has been a significant decrease in bed level of upper

reach as compared to the lower reach due to tectonic setting. A similar study for an alluvial reach of the Brahmaputra at 'Palashbari' area, using various bank protection measures was carried out by Mukherjee and Sarma (2006) with the help of mathematical modelling software MIKE 21C. The sensitivity of the eddy viscosity and Chezy coefficient was also evaluated in this study. Though few studies are being earlier made on certain short sections only, Sarkar et al (2012) covered a relatively long reach of the Brahmaputra from Dibrugarh to Dhubri to understand the river dynamics using RS & GIS techniques. The channel configuration has been mapped from 1990-2008 using IRS 1A LISS-I & IRS-O6 LISS- III satellite images. Results show that there are sharp changes in fluvial landform in recent years resulting in considerable land loss. Gogoi and Goswami (2013) have contributed a similar study on the Subansiri river, one of the largest among the Trans-Himalayan tributaries of the Brahmaputra river in Assam. The rate of Brahmaputra bank erosion depends upon the hydrodynamic & morphological conditions of the river near the bank, and its value is high during high flows and when the flood stage is on the receding phases (Prasad and Dutta, 2009). High overflow and consequent sediment discharge during the rainy season are the prime factors for the bank line migration of Brahmaputra (Chetry, 2014).

Though the engineering and technological aspects are indeed needed, the other aspects like social, economic, ecological, political, etc. should also be paid similar importance for proper management of the water resources. Such kind of concept has been forwarded by Blackmore (2006) for consideration by researchers, planners, and the implementing authorities citing a comprehensive management structure to lead the Brahmaputra basin into the 21st century. The Brahmaputra river basin provides the basis for the production of food and fiber that supports millions of people living in the northeastern part of India. On the other hand, the Brahmaputra regularly continues to pose a real threat to peoples' existence and livelihood through periodically devastating floods. It is therefore very needed of the time for developing comprehensive management involving the riparian states, for extraction of the natural resources, considering economic, social, ecological and political aspects to the best possible extent. However, the basin remains both under-developed and sub-optimally managed as there is no single approach that can be simply "rolled out" and applied to the Brahmaputra basin (Hazarika, 2012).

The applicability of innovative techniques in understanding 2D seismic survey used for hydrocarbon explorations in a logistically difficult, hazardous and environmentally protected river bed area is discussed by Mandal et al. (2006) aiming to protect the ecology and the bio-diversity of the Brahmaputra basin. The use of air guns, hydrophone etc. creates noise pollution which may lead to an unbalance of the flora and fauna of the river basin. The environmental degradation of the Brahmaputra has led to declining in river animals (Wakid, 2009; Deori and Abujam, 2015), especially fish and river dolphins, as well as the land animals (Bora et al., 2010) in the Brahmaputra river basin.

The peculiarities of the hydrological regime have led the mouth of the mighty Brahmaputra as one of the most vulnerable areas on earth as to natural disasters. The main features of natural as well as the climatic conditions are studied by Mikhailov and Dotsenko (2006) for the mouth of the river Brahmaputra. Characterization of the drainage system, assessment of water and sediment runoff for the river is presented in addition to the hydrological regime.

The global climate change is responsible for the change in land cover and its subsequent impact on the watershed characteristics of the Brahmaputra basin is to be properly evaluated (Kumar and Dutta, 2008). A change detection technique has been proposed and evaluated for time-series NDVI data. The impact of climatic change coupled with the change in land use/ land cover on flood vulnerability of the Brahmaputra basin (Ghosh and Dutta, 2011) has been presented to predict flood in 2070. The morpho-dynamic behaviour of the river was addressed based on sediment transport, soil erosion and variation in run-off due to that change in land use/ land cover to assess the basin characteristics by Sarma et al (2011). The global climate change would be responsible to impact on the Brahmaputra basin weather variables (Deka and Sarma, 2011) and river runoff (Gupta et al., 2011). The impact of climate change on the water cycle leads to intensifying the hydrological and its associated processes (Patil, 2013; Apurv et al., 2015; Gain and Giupponi, 2015) of this mighty basin. Interestingly, all these studies w.r.t. the climate change impacts over the Brahmaputra basin has been carried out for a definite part only. However, certain studies (Akhtar et al., 2011; Aktar et al., 2015; Alam et al., 2016; Mohammad et al., 2017) considered the entire Brahmaputra basin, but the emphasis was paid to the Bangladesh area only, and no spatial analyses was forwarded.

2.2 Hydrologic modelling

Watershed studies have wide applications of computer-based hydrologic as well as water quality models that use various input information like landuse, soil, topography, weather data etc, and process to produce output. However, the choice of input data has a large impact on decision making in any hydrologic assessment for water resource management and planning. Moreover, the watershed characteristics and processes being simulated in a model are one of the salient issues to understand by the model practitioners for simulating the real world situations from the watershed (Daggupati et al., 2015). The model should be made capable to capture hydrologic processes, spatially across the basin to produce water balance within reasonable limits (Seibert and McDonnell, 2002; Yen et al., 2014).

With the advent of numerous software tools, hydrologic modelling has nowadays become easier to assess the real ground situations by using correct input data. Unfortunately, hydrologic modelling often suffers difficulties due to the scarcity of hydro-climatological data. The effects of data scarcity on hydrologic model results have been forwarded by many researchers (Yu et al., 2011; Tabari et al., 2012; Ploeg et al., 2012; Valdivieso and Sendra, 2014). In an attempt, Brath et al. (2004) found a spatial scarcity of weather data has many influences on model results and concluded that using a higher density of raingauges in the model provides better simulation results. Whereas, in another study, Chen et al. (2018) described temporal scarcity of data as a concern for obtaining poorer simulation results. However, the missing variables may be generated to use in the hydrologic model, although their reliability is yet a big concern. Nyeko (2015) adopted different techniques in generating missing model parameters especially solar radiation, saturated soil hydraulic conductivity, available soil water content, USLE erodability factor and moist soil albedo; and used in a semi-distributed hydrologic model of a data-scarce basin located in Uganda. Besides, the different hydrologic processes within a basin can be modeled by explicitly training the missing data as constraints in mathematical programming (Pande et al., 2012). Even, the process of calibration and validation of a hydrologic model is again a major challenge at the un-gauged sections where discharge data is not available. In the absence of adequate flow data, researchers can adopt an internal mass balance method for validation (Jang et al., 2012) of model results. However, attaining satisfactory simulation and

calibration results from such models for a basin with scarce data has always been difficult, and often remains less satisfactory.

Watershed simulation models are widely used across the globe to investigate the water-related issues incorporating land use and climate change impacts, pollutant load assessment and the best management practices (Stone et al., 2001; Kannan et al., 2005; Tuppad et al., 2010; Jha and Gassman, 2014). Watershed models are key tool for addressing a wide spectrum of watershed problems (Singh and Frevert, 2006). In the event of various presently available software to build hydrologic and water quality models, choosing the appropriate one to help to fulfill the study objectives is important. A comparative assessment of 22 different hydrologic and water quality models have been forwarded by Moriasi et al. (2012), highlighting the key aspects, including calibration and validation. In an attempt, Borah and Bera (2004) compared SWAT model with several other hydrologic and water quality models and found that SWAT is a promising model for continuous simulations. They found that SWAT is efficient in predicting annual and monthly flow volumes and pollutant losses. In another study, Shepherd et al. (1999) compared 14 different watershed models and found SWAT to be the most suitable for the estimation of phosphorus loss from low land in the UK. Moreover, SWAT is more consistent than Hydrologic Simulation Program-Fortran (HSPF) in the prediction of streamflow for different climatic conditions and can suitably be used in investigating long term impacts of climate variability on surface water resources (VanLiew and Garbrecht, 2003). In another approach, the flow estimation was accurately found (Srinivasan et al., 2005) in SWAT model for 39.5 ha experimental watershed in east-central Pennsylvania as compared to Soil Moisture Distribution Routing (SMDR) model. It is, therefore, Soil and Water Assessment Tool (SWAT) is found to be more suitable for modeling the transboundary Brahmaputra river basin. In addition to that, the SWAT model is computationally efficient and capable of continuous simulation over long periods (Arnold et al., 2012). Whereas SWAT is a continuous, semi-distributed process-based river model, and it considers spatially detailed input/output parameters and describes interactions between elementary units of various hydrological processes (Lempert and Ostrowski, 2002).

2.3 Rainfall comparison

Rainfall is the main driving variable for hydrological assessment of a catchment. Accurate rainfall data is essentially needed for modeling a watershed. Although Hydrological models are capable to provide the necessary information about the ground response, it is extremely difficult to establish models and generate representative water resource availability information without adequately accurate climate (temperature, rainfall, evaporation, etc.) input information. In the light of sufficient data, rainfall characteristics especially variability and trend are important for water resource schemes (Nyatuame et al., 2014). Effective stormwater management plans depend on reliable rainfall intensity-duration-frequency (IDF) relationships (Trefry et al., 2005). The ground observations for meteorological data are sparse, especially in developing and underdeveloped countries due to a lack of available resources (Hughes, 2006). Precipitation data is principal information in most hydro-climatological studies. In large parts of the world, however, observed precipitation records are often scarce, discontinuous and frequently contain discrepancies (Koutsouris et al., 2016). Although longer records are found in gauge observations (Yatagai et al., 2009) they do not provide a reliable spatial representation of precipitation (Gruber and Levizzani, 2008). The distribution of global precipitation was not well documented up to a few years ago, both because of its wide spatial and temporal variability (Xie and Arkin, 1995). Nowadays various countries have developed tools for estimating the gridded data with better spatial and temporal representations. Since observational rainfall datasets over land areas for most of Asia lack, Yatagai et al. (2008, 2009) have generated a high-resolution rain gauge-based daily precipitation gridded dataset for East, Middle East, and Russia. Similar attempts have been made to develop and improve global gridded precipitation data in recent years (e.g. New et al., 2000; Mitchell and Jones, 2005).

Remote sensing techniques, such as those using radar or satellites, are useful for monitoring rainfall over large mountainous and oceanic regions. Though these data provide more homogeneous quality, their time series accuracy and precision is lower than the existing and corresponding gauge-based ground observations data sets (Schulz et al., 2009).

The choice of input data in any hydrologic assessment study has a large impact on decision making in water management and planning. In the event of a large number of global

precipitation data available, its' evaluation and inter-comparison are needed to justify applicability for both research and resource planning (Koutsouris et al., 2016). There have been many region-specific studies (Todd et al., 1999; Thorne et al., 2001; Grimes and Diop, 2003), wherein statistical and other analyses were carried out for the use of satellite rainfall data. Goyal (2014) applied Mann-Kendell and Sen's slope estimator test to check the applicability of India water portal metadata (provided by IMD) to help provide rational regulatory and policy concerning water resources.

The use of synthetic weather data derived from satellite or so has gained importance, while its' reliability is to be checked before developing a hydrological model. Wilk et al. (2006) forwarded some of the issues of using the synthetic data together with the historical rainfall data in the river flow simulation studies. There have been many studies to evaluate the gridded precipitation data against gauge data (Sapiano and Arkin, 2009; Dinku et al., 2011; Romilly and Gebremichael, 2011; Liechti et al., 2012; Guo and Liu, 2016; Rossi et al., 2017). The amount of disagreement between the radar estimates and the gauge rainfall is much significant (Barnston and Thomas, 1983; Masunga et al., 2002). While comparing the Doppler radar outcomes with the actual rain gauge data, Espinosa et al (2015) concluded that possible topographic interference may be necessary for most storm events based upon the use of radar data. Satellite estimates of TRMM outcomes do not conform to good agreements while compared with the high resolution gridded precipitation data sets of Iran (Javanmard et al., 2010). Again, TRMM data is found over-estimated in some stations while under-estimated in some other stations over Bolivia when compared to gauge rainfall data (Blacutt et al., 2015). However, TMPA satellite products tend to under-estimate the rain gauge rainfalls over Italy (Rossi et al., 2017). Because the global precipitation data do not tally with the corresponding actual gauge precipitation, this study has been forwarded to evaluate and analyze the number of discrepancies between them to help in the choice of the data.

2.4 Climate change

2.4.1 Greenhouse gas emissions and Climate change

Life on Earth depends on the Sun. The Sunlight passes through the air and clouds of the earth's atmosphere, to reach the surface. This energy is absorbed in the surface and then radiated upward in the form of infrared heat. This heat is then absorbed by the greenhouse gases and radiated back toward the surface, and making our plant a warmer and habitable. Water vapour is the most important greenhouse gas. However, there is a substantial contribution from carbon dioxide and smaller contributions from ozone, methane, and nitrous oxide. Greenhouse gases from human activities are the most significant driver of observed climate change since the mid-20th century. Earth's natural greenhouse effect is crucial to supporting life. Human activities, however, mainly the burning of fossil fuels and clear-cutting of forests, have accelerated the greenhouse effect causing global warming. Besides, rapid industrial growth plays an important role in accelerating global warming.

The science related to climate change is assessed by the IPCC (Intergovernmental Panel on Climate Change), a body of the United Nations. The IPCC was created in 1988, to provide policymakers with a regular scientific assessment on climate change and its subsequent impact, and to put forward adaptions as well as mitigation measures. In its fifth assessment report (AR5), the IPCC adopted four Representative Concentration Pathways (RCP), the greenhouse gas concentrations trajectory. These RCP scenarios include RCP2.6, RCP4.5, RCP6, and RCP8.5, and they are labeled after a possible range of radiative forcing values in W/m^2. The RCP2.6 is known as the low radiative forcing scenario with value as 2.6 W/m^2. The radiative forcing in RCP8.5 increases throughout the 21st century before reaching a level of about 8.5 W/m^2 at the end of the century.

As per the AR5 of IPCC, global warming is currently increasing at the rate of 0.2^{0}C per decade. The global climate change continues to impact the hydro-meteorological variables of a watershed. For instance, a decrease in rainfall over an area generally results in a drought-like situation. The drought may still intensify with an increase in precipitation if the stronger evaporation rate is driven by the increase in temperature (Prudhomme et al., 2014). Thus the mechanism by which the variability of climatic components is being driven by the global climate changes should be analyzed. Of course, climate change impacts are not uniform throughout all places. It depends upon the factors causing global warming. Even, it depends upon the sensitivity of climate variables. An area of high altitude is more

sensitive to temperature (Li Li et al., 2008) since it is fed by snow and ice (Barman and Bhattacharjya, 2015). There would likely to increase in the number of spells with higher rainfall and longer duration (Apurv et al., 2015) in the coming decades, over the Brahmaputra basin.

The reliability of climate change projections depends upon the spatially available data over an area, and more the available data sets, better is the accuracy. Kerim and Sarma (2017) suggested the use of average values of numerous spatial weather station data instead of only one station data for reliable prediction of the climate variables under climate change. Because of the severe effects of climate change, reliability on the stationary assumption of the hydroclimatic variable has become questionable, and therefore, the non-stationarity concept has gained significant attention in the research community in terms of better planning and risk management. Das and Umamahesh (2017) incorporated uncertainty analysis between Stationary & Non-stationary variables on the Wainganga Basin of Godavari river to assess the impact of climate change. Extreme Value Theory (EVT) was applied for stationary analysis and the Bayesian inference method was applied to provide a framework to quantify the predictive uncertainties in nonstationary modelling. Non-stationary estimates of lower return period for streamflow provided relatively better results. The study of the impact of climate change on hydrological variables depends on projections of future climate provided by various Global Climate Models (GCM). However, we hardly use GCM outputs directly because they produce error/biases due to their limited spatial resolution and various thermodynamic and climate system processes. Even in cases of Regional Climate Models (RCMs), where the climate is simulated by taking into account the regional characteristics of the area under investigation, there are observed biases between the simulation and the in-situ measurements (Lazoglou et al., 2019). Hence they cannot be used directly as input to any semi-distributed or lumped hydrological model. If used directly the error between the GCM output concerning historical observations is often observed to be large (Ramirez-Villegas et al., 2013). Therefore, often these GCM models have to be downscaled to an appropriate (generally to higher) resolution (Von Storch et al., 1993). However, issues of uncertainties of future climate data of various downscaled GCM outputs are not yet avoidable (Chen et al., 2011). Taking into account these uncertainties along with other factors such as time constraints, human resources, and computational

constraints, downscaling of GCM models is not a straight forward or simple task especially for the Brahmaputra basin with 69 available gauge stations. To tackle this problem, one approach may be to use the Bias-correction and spatial interpolation methods to improve the GCM output of Brahmaputra river basin (Shrestha et al., 2017). Interpolation of climate data using different methods from the neighboring points to a required point has been carried by many people in the past. For instance, Yussouf & Stensrud (2006) employed Cressman scheme interpolating method to interpolate the 12day mean bias value from neighboring points to a given station. Mohammadi et al. (2017) used inverse distance squared weighting and gradient inverse distance method to interpolate the data from the neighboring observations to any desired location. Using a similar concept, the climate variables viz. precipitation, maximum temperatures, and minimum temperatures are interpolated from the neighboring available data points to the desired location and then corrected for bias. The biased corrected outputs are then used for future climate change impact studies. These outcomes are thought to be useful for decision-makers to support their decisions on climate adaption measures.

2.4.2 CC impacts on water resources

This section presents a detailed survey about certain salient works done by researchers across the globe. It includes the studies related to climate change impact on water resources of the world. Besides, the studies in context to the Indian river basin are also covered in this section.

The increase in greenhouse gas concentrations in the atmosphere has led to a change in climate conditions. As a result, the hydrological cycle is intensified, leading to more intense precipitation events in terms of intensity, frequency and the associated severity of floods. Climate variability and change beyond a few decades ahead have significant social, economic, and environmental implications. Temperature change due to climate change would rise to impact the watershed hydrology in the coming days (Shivam et.al., 2016). The hydrologic response study requires a suitable set of data and models and a proper methodology. Selecting historical data, different models including hydrologic and climate models are an important task for accurate assessment of regional hydrologic response. Eum

et al. (2011) presented a complete engineering procedure for climate change flood risk assessment for the Upper Thames River basin. It is an integrated approach involving Climate-Hydrologic-Hydraulic models to evaluate floodplain mapping under the changing climatic conditions. The results showed an increase in floods due to climate change. The importance of regional climate models (RCM) for the estimation of climate change impacts over a particular area has been elaborated by some researchers (Yates and Strzepek, 1998). Global climate change is responsible for alterations of Hydrologic Variables which consequently may lead to change in WR management practices. Phan et al. (2011) forwarded a study on Song Cau watershed in Northern Vietnam, for assessment of the impact of climate change on Stream Discharge as well as Sediment Yield by using the SWAT hydrologic model. GCM with different emission scenarios as per IPCC was used to downscale and predict the future climate and the model result shows changes in the streamflow and sediment discharge. A similar kind of study was carried for the Sutlej basin, India (Singh et al., 2015) and Malaprabha river basin (Mudbhatakal et al., 2017). In a study, Duong et al. (2016) found the seasonal streamflow of Vu Gia-Thu Bon catchment (Vietnam) may increase upto 200% in the rainy season, during 2091-2100, whereas a decrease upto 30% would happen during the dry periods. Assessing the impacts of water resources in Tanzania, Adhikari et al. (2017) found the surface runoff would increase upto 94.1% and 159%, at the country level and the watershed level respectively, till the end of the current century.

Hydrologic models are not able to compute unsteady flood flows and the hydraulic models are sometimes found less effective in uncertainty estimation in the modelling outcomes (Singh and Goyal, 2017). Here, a hydrologic model namely SWAT was used to compute the future flow scenario using downscaled GCM data and prediction of unsteady flow is presented under a climate change scenario. The projected outputs from SWAT (outflow, water level) are then incorporated into the Hydrodynamic model (MIKE11) to develop rating curve equations at outlets. The results predict an increase of flow velocity from historical value of 6.5m/s to 8.5 m/s during 2100. The results from both the models may be used for future planning & management of the Teesta river.

Exploring the impacts of climate change on hydrologic and institutional water availability from a river basin for the numerous users is an important task for water resource

management agencies. Wurbs et al. (2005) described a case study investigation of the potential effects of climate-change on assessments of water-supply capabilities and focusing on whether and how climate change considerations should be incorporated in the Water Availability Model (WAM) system on Brazos River Basin (US). The study uses two models, one climate model and the other is the hydrologic model (SWAT). Water availability in 2050 was checked and found as compared to the requirements at some specified locations. They found that the future climate scenario would result in decreased mean streamflows with greater variability across the basin, thus affecting the water availability until the year 2050. Pervez and Henebry (2015) have also forwarded a similar study on Brahmaputra basin aiming to assess the future freshwater availability by adopting sensitivity analysis of climate models and LULC change. The results predicted strong increasing trends for total water yield, streamflow, and groundwater recharge, indicating more potential of flooding during August–October of the 21st century. The change of land use land cover is induced by urban growth which ultimately affects the watershed hydrology. A similar study was forwarded by Pumo et al. (2017) and described how climate and land use changes may interact and affect the fundamental hydrological dynamics. They also concluded that the processes governing basin hydrological response may change with spatial scale.

The scientific community is facing important basic questions about the implications of long-term climate change for freshwater resources. Potential effects include seasonal shifts in streamflow; changes in extreme flow events of surface and groundwater, changes in the fate and transport of nutrients and sediments [IPCC, 2007a]. A study on 20 large watersheds (US) was carried out by Johnson et al. (2012) to analyze the impact of climate change on water quality. The study includes the sensitivity of different watershed models and several climate models in assessing the streamflow water quality from the basin. Miller et al. (2012) also presented a similar study for the San Juan River Basin (Mexico) to assess the water quality. In another study, Draper & Kundell (2007) presented a dialogue based detailed discussion about the transboundary water sharing issues relevant to the IPCC 4th Assessment report'2007. The salient highlight of this discussion were risks imposed by climate change to transboundary water-sharing agreements identification, agreements most

at risk are identified and the hurdles due to legal aspects and policy of countries to share water resources.

Incorporation of drought characteristics to a basin under climate change was done by Madadgar and Moradkhani (2013) using COPULA, a multivariable probability distribution method. The impact of climate change on future droughts is evaluated using five general circulation models (GCMs) under one emission scenario and streamflow forecast done by the ANN model. Some indices like Streamflow Drought Index (SDI), Standardized Precipitation Index (SPI) are calculated for analysis. Despite more intense extreme events that are expected to occur in most parts of the globe in the future, the results of this study show that the Upper Klamath River Basin in the Pacific Northwest (US) will experience less intense droughts affected by climate change. A complete assessment for the risk due to the changing climate over the Bangladesh area of the Brahmaputra basin was studied by Gain & Giupponi (2015). They observed that water scarcity occurs, not only due to the limitation of resources, i.e. the shortage in the availability of freshwater relative to water demand but also depends upon social factors. The social & ecological system coupled with the dynamic behavior of the river is incorporated in this study to calculate Water Scarcity Index (WSI). Results show that water scarcity risk is expected to slightly increase and to fluctuate remarkably as a function of the hazard signal.

Simonovic and Li (2003) forwarded a study to address the future climate change scenario and its subsequent impact on flood protection structures specially dykes, reservoirs within the Red River basin (Canada). Assessment is done w.r.t. flood flows, flood level and capacity of structures. An original hydrologic model has been developed for the hydrological study. Several GCMs were used for projecting the future climate scenario under several emission scenarios as per the IPCC, to incorporate the uncertainty analysis for climate models. Another study on urban stormwater infrastructure design has also been presented by Forsee & Ahmad (2011) for Las Vegas Valley under a climate change scenario. 100 years design storm depth was calculated by using the Flood Frequency Analysis based on data generated through climate projections of several RCMs. The projected changes in design-storm depths were incorporated into a HEC-HMS model. Hydrologic simulation results showed exceedences of the prevailing design standard.

Soil moisture is an important parameter for the growth of natural vegetation and crops. Tavakoli and Smedt (2012) carried out a study on Vermilion basin that is about 95% dominated by Agricultural land, to assess the impact of climate change on agricultural production. The study was carried out to predict the soil moisture and streamflow for future periods by using a distributed rainfall-runoff model (WetSpa) to calibrate for streamflow and validate for soil moisture. They found the future Soil moisture in the basin would decline, due to climate changes, and this will ultimately affect agricultural production.

Climate change may impact the stream temperature which ultimately leads to the survival of aquatic life. A study of this kind was studied for some U.S. Streams by Stephen and Sinokrot (1993). A Heat Transfer Model was used to calculate the heat exchange between air and water. The model is very sensitive to air temperature and solar radiation. The output of the model aids in the study of aquatic life survival. A similar approach was presented by Lee et. al. (2014) for Nakdong river (Korea). A rainfall-runoff model TANK was used to calibrate and validate the historical data. Indicators of Hydrologic Alterations (IHA)-- (1) magnitude, (2) timing, (3) frequency, (4) duration and (5) rate of change were presented to conclude the aquatic ecosystem. The results of this study showed an increase in stress on the aquatic ecosystem due to extremely high streamflow.

Climate change leads to variation in spatial and temporal precipitation patterns. Such a variation may affect the quantity and quality of available water resources, thereby increasing the competition among various users like agriculture, ecosystems, settlements, industry, and energy sectors. Islam & Gan (2014) addressed a Multimodal analysis for future outlook of surface water management of the S.S. River Basin of Alberta. Climate scenario was projected by 3 different GCM forced by several emission scenario as reported by IPCC. The annual maximum streamflow simulated through Modified Interaction Soil Biosphere-Atmosphere (MISBA) model was used as input in Water Resources Management Model (WRMM) to simulate changes to the number of deficits years out of 68 years (1928–1995) of historical data. Another model "Irrigation District Model (IDM)" was run to project the irrigation water demand. This study describes the use of multimodal analysis in WR management for present and future periods.

The conflicting trajectories of water–energy–food (WEF) nexus are highly relevant for water policy and planning, especially for the transboundary rivers like the Brahmaputra.

To assess the impact of changing climate on this basin, Yang et al. (2016) carried out a hydro-economic model analysis. The study includes the development of a new model, called "BRAhmaputra HydroEconomic MOdel (BRAHEMO)" to address the flow scenario. The results indicate an increase in streamflow and easing of conflicts at the WEF nexus in the basin. As the conventional optimization techniques can't be used for net economic benefits from a transboundary river, due to its inability to quantify political and social aspects, this study attempted an alternative approach based on explicit recognition of the limited ability of several models. The authors capitalized on the recent climate change risk assessment for presenting Ex-post scenario analysis under 'Nexus Thinking' (as per World Economic Forum, WEF). Economic assessment of Jucar basin (Spain) due to impact of climate change impacts are incorporated by Bou et al. (2017) employed various models like climate, hydrology, crop water requirements, statistical, water management. The rainfall-runoff model is used to present the flow scenario of Jucar basin (Spain). Results show that the system is vulnerable to global change. The economic assessment through the use of a Hydro-economic model depicts that adaptation actions can save €3–65 million per year.

2.5 Critical appraisal

It has been observed through the search of the above literature that there is ample scope of study concerning the mighty Brahmaputra. The Brahmaputra plain has been studied in numerous aspects, although majorities are done at a tributary level rather than the main stem. Some of these studies include quantification of the channel processes, erosion and deposition pattern, fluvial morphology, geomorphologic, development of wetlands, hydrodynamic model, Laboratory study on Brahmaputra river water & sand. Apart from the engineering studies, certain other aspects like social, economic, political, ecological, religious importance, preservation of wild as well as water animals, the involvement of local communities living aside the river banks of the Brahmaputra basin are also highlighted in various studies. However, climate change and its impact on the entire Brahmaputra basin is hardly been addressed comprehensively, and therefore planned to forward in this study, to add towards the Brahmaputra research.

Based on the literature reviewed regarding climate change studies worldwide, it is observed that a river basin is susceptible to climate change effects. Herein, several climate change impact assessment done by the researchers worldwide have been discussed to explore the possible mechanism for climate change studies. The global climate change impacts the hydro-meteorological variables of a watershed, during both the present and future periods. The hydrological response from a river basin could only be possible through the use of a hydrological model. As such, several rainfall-runoff models have been reviewed (Sec. 2.2) for its effectiveness; whereas the SWAT model is found to be more suitable for the present basin. Furthermore, the present basin lacks observed hydro-climatic data due to which the use of global datasets would be compulsory. The applicability of the global datasets to a basin should, therefore, be justified as evidenced in section 2.3. This could be achieved by comparing the global datasets, especially rainfall values to certain gauge records. So, it is clear from the literature above that the present study could be planned to forward by developing a hydrologic model in SWAT platform, to assess the flow scenario at various gauged and un-gauged locations. The impact of climate change on the hydro-climatic components of the Brahmaputra river basin during the present, as well as the future periods, would be taken up as salient objectives of the present study. As the development of a "comprehensive management strategy" for the Brahmaputra river basin is the need of time, the present study would consider an assessment of the transboundary effects. Especially, the assessment of the hydrological impacts on the lower riparian country (i.e. India) due to certain man-made activities in the upper riparian country (i.e. China) is expected to provide significant findings of the proposed studies.

######## ########

Chapter 3

Study Area and Input data

3.0 Introduction

The mighty Brahmaputra river basin has been taken up as the study area (*Fig. 3.1*) of the present research work. It includes the entire river reach starting from its source at Tibet to the mouth at the Bay of Bengal. This chapter is presented to discuss the study area including its climate and hydrology. Later this chapter, we have presented the input data used for the present study objectives along with their processing to make them useful in hydrological modelling.

3.1 Brahmaputra Basin: an Overview

The Brahmaputra River originates in the Chemayungdung mountain ranges which is located nearly sixty miles away from south-east of Mansarovar lake in the Mount Kailash range in Southern Tibet. A spring called 'Tamchok Khambab' spills from the glaciers which later gather breath and volume to become the 'Tsangpo', the highest river in the world. From its source, the river runs nearly 1100 km in easterly direction between the Himalayas range to the south and Kailash range to the north. After passing 'Pi' in Tibet, the river suddenly turns north and thereafter it again turns south-flowing through a deep gorge (*Fig. 3.2*) to finally enter India. 'Tsangpo' is also popularly known as 'Yarlung Zangbo' by the Chinese.

Out of its total length of 2,880 km, the Brahmaputra covers a major part of its journey in Tibet as 'Tsangpo' River flowing 1625 km, parallel to the main range of Himalayas before entering India through Arunachal Pradesh (India). Here, the river is popularly known as 'Siang' river and makes a very rapid descend from its original height in Tibet to finally appear in plains where it is called 'Dihang'. It flows for about 35 km and is joined by two other major tributaries 'Dibang' and 'Lohit' at Kobo, a place in the west of Sadiya, Assam (India). From this confluence point, the river is known as the 'Brahmaputra' till it crosses

Assam below Dhubri and enters Bangladesh as ‘Jamuna’. In Assam, the Brahmaputra is popularly known as ‘Luit’, which has been derived from the original Sanskrit name ‘Louhitya’. In Bangladesh, the Jamuna river is joined by ‘Teesta’, one of the largest tributaries of Bangladesh. Below Teesta, one anabranch originates due east which finally merges into the mainstem of the Brahmaputra.

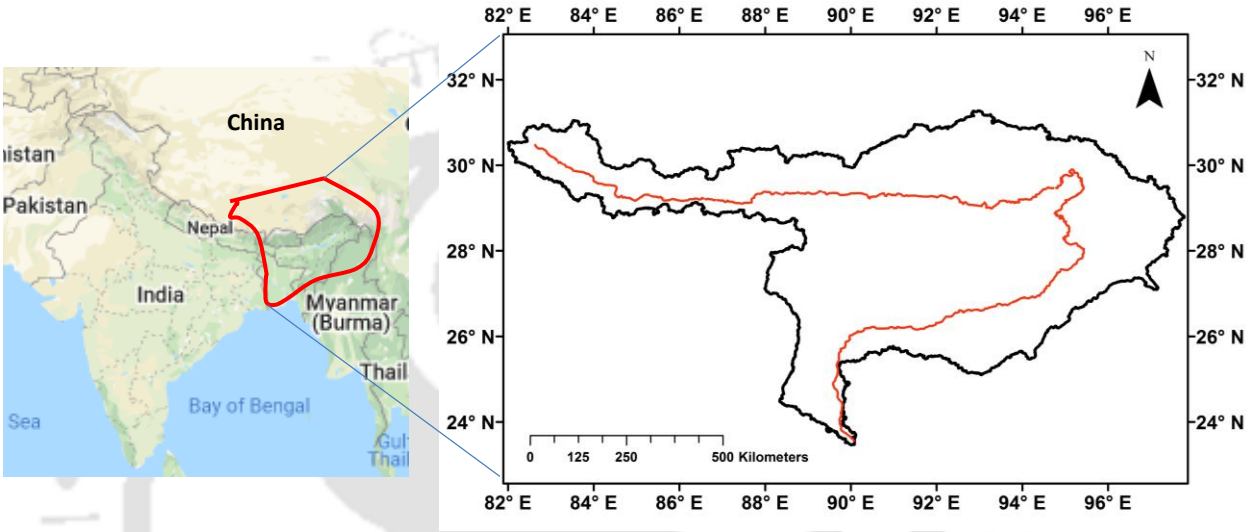

Fig. 3.1 Brahmaputra river basin

The “Ganges”, another major river of India, and popularly known as “Padma” in Bangladesh joins the mainstem of the Brahmaputra near Daulatdia, Bangladesh. After traveling a distance of around 95 Km from this point, the Brahmaputra is joined by the ‘Surma’, another major river of Bangladesh at the location called ‘Rajrajeswar’. From this point, the Brahmaputra is popularly pronounced as ‘Meghna’ which finally merges into the Bay of Bengal to end its journey.

Fig 3.2 The Great Bend of Tsangpo (Source: http://greenbuzz.net)

The mighty Brahmaputra flows majestically in the Assam Valley for a distance of about 720 km which is joined by a large number of tributaries on both the north south banks. Some major tributaries like Jiadhal, Manas, Subansiri, Kameng, Pagladiya etc. on the north bank and Dhansiri, Kapili, Dikhow, Digaru, Krishnai, Dudhnoi etc. on the south bank pay their tribute to the master river.

While traversing through India following the journey of 918 km long, the Brahmaputra river is astonishingly wide in some areas. In Upper Assam, near Dibrugarh the river is 16 km wide whereas in lower Assam at Pandu (Guwahati), the river is 1.2 km wide, but the Brahmaputra river becomes very wider (nearly 18 km) in the immediate downstream of Pandu. The Brahmaputra has been widening its (riverbed) size continuously from the last century. According to a report of the Water Resources Department, Assam, the Brahmaputra river is spreading over 6000 sq km in 2008, whereas this value was only 4000 sq km in the year 1920.

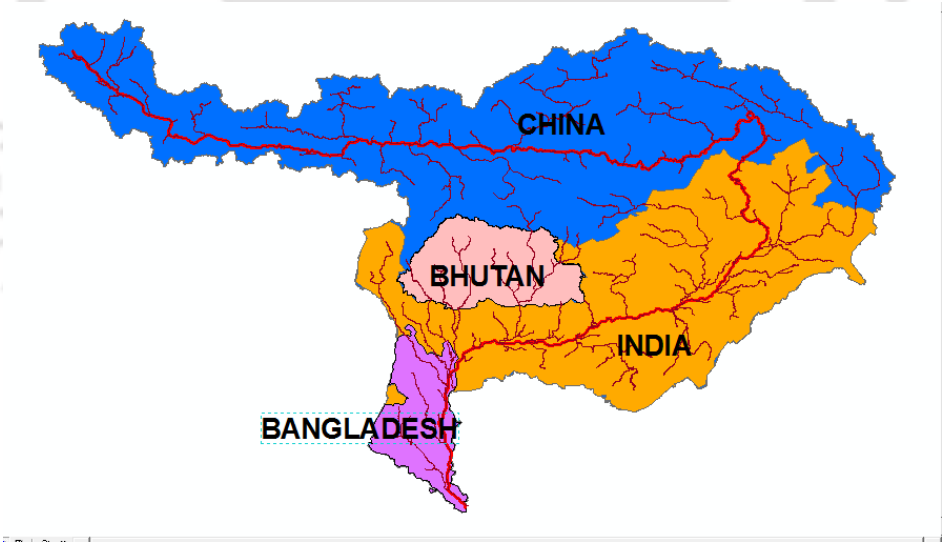

Fig. 3.3 Brahmaputra basin sharing co-nations

The word 'Brahmaputra' means 'son of Lord Brahma' and as such the Brahmaputra basin attains its mythological importance for devotees, especially Hindus, Jains, and Buddhists. The Brahmaputra River has its history of flow through the dense forests and tribal settlements. A seldom-run river, it offers beautiful scenery and great wildlife in a less-

visited corner of the sub-continent that attracts tourists from around the world. The various adventurous sports held in the Brahmaputra River have helped India's poor to high-end adventure reputation, especially rafting. The basin has the enormous potential to become one of the hot-spot in terms of tourism, hydropower generation, agricultural production, navigation etc. Fishermen utilize the river and the other water bodies within the basin as their income source.

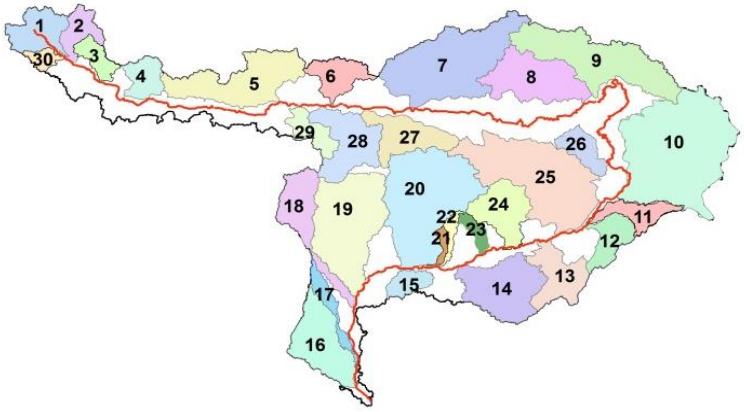

Fig. 3.4 Brahmaputra basin and its Salient sub-basins

People with different traditions, culture, language & religion along with other living creatures as well as a wide variety of flora and fauna habitating altogether in the beautiful landscape have led the Brahmaputra basin an exceedingly incredible one. Although the severe hazard caused by the Brahmaputra like flood and bank erosion is also much pronounced which results in huge loss of life and property every year. Comprehensive management is the need of time to extract the best possible utilization of the water resources out of the Brahmaputra basin. Though the study on the mighty Brahmaputra had been started quite long back and the formal research had gained its momentum during the late sixties of the last century. The Brahmaputra basin is shared by four nations namely China, India, Bangladesh, and Bhutan (*Fig 3.3*). The Brahmaputra poses a huge challenge to the researchers, engineers, environmentalists, and policymakers to culminate the effective benefits while managing the water resources, due to its versatile complexity and transboundary effects.

3.1.1 Basin characteristics

The Brahmaputra river basin covers an area of 5,42,450 km^2 (Dutta and Sarma, 2020), corresponding to an outlet (Lat: 23.576N; Long: 89.442E) at Bangladesh. Out of the total drainage area, China occupies the highest (≈ 50%), followed by India (≈ 36%), and Bangladesh and Bhutan shares almost equally (≈ 7%). Being braided and meandering river in a quite bit, the Brahmaputra frequently forms temporary sand bars. The tectonic activity in this region is quite significant that is associated with the Himalayan uplift and development of the Bengal fore-deep. Several researchers have hypothesized that the underlying structural control on the location of the major river systems of Bangladesh. In 1959, Morgan and Melntire (source: Wikipedia) found a zone of 'structural weakness' along the present course of the Ganga-Jamuna-Padma rivers, which may be due to either a subsiding trough or a fault at depth. As well, it is mentioned in the same source that the width changes in the Jamuna may respond to these faults and they may also cause increased sedimentation upstream of the fault. The tectonic and climatic context is thought to produce large water and sediment discharges in the Brahmaputra river, especially the Bangladesh part, by the high rates of Himalayan uplift.

The Brahmaputra basin is fed by glaciers at the Himalayan range and merges into the Bay of Bengal. The river bed slope is very steep (≈ 2.82 m/Km) in Tibet, and gets reduced to about 0.1m/Km in Assam valley. Due to this sudden flattening of river slope, the river becomes braided in the Assam valley. The Brahmaputra is one of the largest rivers in the world and ranks fifth (https://waterresources.assam.gov.in) with respect to its average discharge. The average annual discharge of this mighty river during the dry season is about 4420 m^3/s, at Pandughat (26.176872N; 91.687088E). As per Wikipedia (https://en.wikipedia.org), the Ganga-Brahmaputra system has the third-greatest average discharge (roughly 30,770 m^3 per second) of the world's rivers; and the river Brahmaputra alone supplies about 19,800 m^3 per second of the total discharge. The rivers' combined suspended sediment load of about 1.87 billion tonnes per year is the world's highest.

3.1.2 Climate

The meteorological conditions of the transboundary Brahmaputra river basin are widely different in the upper riparian country (Tibet) than the lower riparian countries (India, Bangladesh), and lie in different climatic zones. The climate of the Brahmaputra valley varies from the harsh, cold, and dry conditions found in Tibet to the generally hot and humid conditions prevailing in Assam state and Bangladesh. Tibetan winters are severely cold, with average temperature is below 32 ^{0}F (0 ^{0}C), while summers are mild and sunny. The upper river valley lies in the rain shadow of the Himalayas, and precipitation there is relatively light. The mean annual rainfall over the entire catchments including Tibet and Bhutan is about 2500 mm. The rainfall in the Brahmaputra basin is mainly due to the South-West monsoon. Interestingly, merely 85% out of the total annual rainfall of the Brahmaputra basin occurs during the months from May to September.

3.1.3 Hydrology

The hydrology of the Brahmaputra River is characterized by its significant rates of sediment discharge. Starting from the source until it enters into Assam, India, the Brahmaputra river flows along a steep slope of hills and mountains. This stretch of the river possesses high current in streamflow. The Brahmaputra flow is large and varies significantly which causes rapid channel aggradations and thereby results in accelerated rates of basin denudation. The course of the Brahmaputra has changed continually over time. Along with the lower courses within India and Bangladesh, the land undergoes constant erosion and deposition of silt. Thus, deposition results in the formation of bars and sand bars at the edge of the flood plain. The basin is subjected to vast inundation during the wet monsoon months. Floods overtopping or breaching the levees make sedimentary fluvial deposits on the flood plain of the Brahmaputra. The hydrology of this mighty river basin is susceptible to the impacts of the global climatic change. Besides, tidal surges accompanying tropical cyclones sweeping inland from the Bay of Bengal periodically bring great destruction to the delta region.

3.2 Data

Table 3.1 List of input data used in the present study

Sl No	Input data		Source
	Required	**Used in this study**	
1	Digital elevation model (DEM)	SRTM DEM of 90 m spatial resolution (release by NASA)	*Downloaded:* www.dwtkns.com/srtm
2	Land use and land cover map	Global Land Cover map of 0.5 km spatial resolution	*Downloaded:* https://landcover.usgs.gov/global_climatology.php
3	Soil map	Global soil map of 0.9 km spatial resolution	*Downloaded:* www.fao.org/soils-portal/soil-survey/soil-maps
4	Weather data (5 different sets)	(a) Observed data at 6 IMD Stations	*Obtained* from Indian Meteorological Department
		(b) Observed data at 8 Stations over Tibet (China)	*Obtained* through a collaborative academic research project
		(c) Observed data at Tea Estate Stations	*Collected* from various Tea Estates of Assam
		(d) Global gridded CFSR data	*Downloaded:* https://globalweather.tamu.edu/
		(e) Global gridded IMD data	*Downloaded:* https://swat.tamu.edu/software/links/india-dataset
5	Discharge data	Observed discharge data for 5 locations (i.e. Bhomoraguri, Pandughat, Pancharatna, Golaghat, Chowldhoaghat)	*Obtained* from Central Water Commission, Govt. of India
6	Global climatic model (GCM)	GCM data obtained from CMIP5 archive	*Downloaded:* https://esgf-node.llnl.gov/search/cmip5/

Initially, the present study involves the establishment of a suitable hydrological model for the entire Brahmaputra river basin. A watershed model requires adequate and long-term data of hydro-meteorological variables. Indeed, modelling the Brahmaputra watershed with huge data scarcity is a major challenge. Especially, precipitation being the main

variable to impact the results of hydrological modelling, their adequacy in terms of spatial and temporal availability is a must. Apart from the precipitation, a hydrologic model requires several other data of weather variables like temperature, humidity, wind, solar radiation, etc. that control the basin hydrology. Besides, the water balance of a watershed depends upon the topography, land use, land cover, soil characteristics, etc. A complete list of input data used in the present study is presented in *Table 3.1*. The sources of different data are also indicated in this list.

3.2.1 Data description

3.2.1.1 Topography, landuse and soil data

The present study uses several data as input to the hydrologic model developed in the SWAT (Soil and Water Assessment Tool) platform. The basin's topographic information was obtained by using the DEM (Digital Elevation Model) of 90m spatial resolution. The DEM belongs to SRTM (Shuttle Radar Transmission Mission) archive and provided by NASA (National Aeronautics and Space Administration), USA.

Table 3.2 Landuse/ land cover classes for the Brahmaputra river basin.

LEGEND	SWAT SYMBOL	DESCRIPTION
0	WATR	Water
1	FOEN	Evergreen needle leaf forest
2	FOEB	Evergreen broadleaf forest
3	FODN	Deciduous needle leaf forest
4	FODB	Deciduous broadleaf forest
5	FOMI	Mixed Forest
6	MIGS	Mixed Grassland/Shrubland
7	SHRB	Shrubland
8	TUWO	Wooded Tundra
9	SAVA	Savanas
10	GRAS	Grassland
11	WETL	Wetland Mixed
12	CRGR	Cropland/ Grassland
13	URBN	Urban and Built up
14	CRWO	Cropland/Wooded Mosaic
15	ICES	Snow and Ice
16	BSVG	Barren and Sparsely vegetated

The Brahmaputra, being the transboundary river, we are unable to collect any information regarding the land use and land cover as well as the soil characteristics for its basin, beyond the national boundary, due to transboundary issues. As such, we are bound to rely on global data regarding this information. The global data were downloaded from the respective links as shown in *Table 3.1* and then clipped to the Brahmaputra basin shape. While extracting the global soil map (*Fig. 4.4b*), it was found to have as many as 39 soil classes within the Brahmaputra basin. Here, each soil class is given different names representing different soil characteristics, and they are known as the "SWAT soil classes". Besides, we found as many as 16 classes of landuse/ landcover, after extracting the global map for the Brahmaputra basin. The list of these SWAT land classes is shown in *Table 3.2*, describing the meaning of each.

3.2.1.2 Climatic data

Weather components, especially precipitation are the driving variable to impact the results of the hydrological analysis. As such, they should be so used to represent fine spatial and temporal resolution. Accurate weather data, preferably the ground observational records always provide better results in hydrologic simulations. However, we are unable to gather a single set of weather data, representing the spatial and temporal variations over the entire basin, due to transboundary issues. Therefore, we have collected weather data from all possible sources locally and globally, to make them useful in the present hydrologic analysis. There are altogether five sets of weather data used in our study as listed in *Table 3.2*.

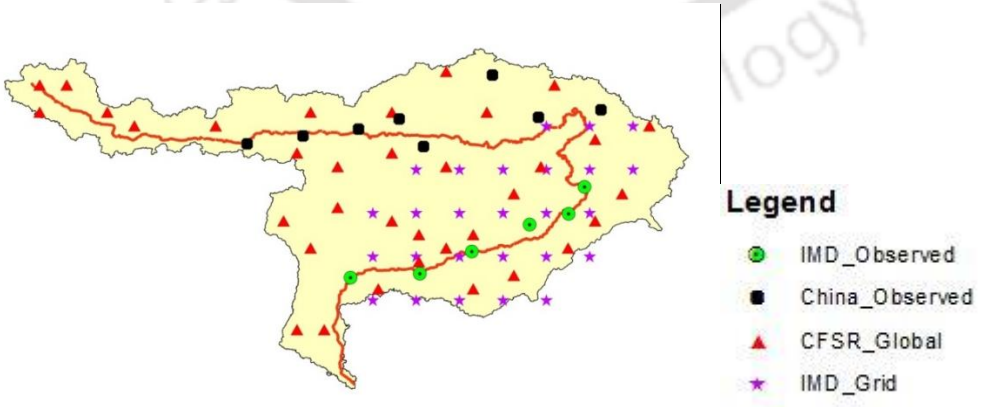

Fig. 3.5 Weather stations used in present hydrological analysis.

The details of the weather data used in the present study are described as follows:

- The first weather datasets include observed data at 6 gauge stations over Indian territory, and collected from the Indian Meteorological Department (IMD). These daily datasets consist of four variables (precipitation, max/ min temperature, wind), and we could collect them for 25 years (1991-2015) periods.
- The second dataset includes the measured weather data at 8 gauge stations over Tibet region (China), obtained through an academic collaborative project, and it contains six variables (precipitation, max/min temperature, wind, solar, humidity) spanning over 22 years (1991-2012) records, on daily basis.
- Thirdly, the weather datasets were collected from various Tea gardens across Assam, India. This dataset provides precipitation and max/min temperature on a daily record basis. These data are found unsuitable for using them into the present hydrological studies, due to insufficient records temporarily, but they are used in the evaluation of the satellite rainfalls, as shown in the next section (*Sec. 3.3*).
- The fourth set of weather variables is the Climate Forecast System Reanalysis (CFSR) data, provided by Texas A&M University (TAMU) as gridded global, high resolution coupled atmosphere-ocean-land surface-sea ice system weather data, on daily basis. These weather data consist of six variables: precipitation (pcp), maximum/minimum temperature (tmp), relative humidity (hmd), solar (slr) and wind (wnd), and available for 36 years (1979-2014).
- And, finally, the IMD gridded weather data generated by Dr. Balaji Narasimhan, Associate Professor, IIT Madras has been used as the fifth weather dataset. These data, on a daily basis contain only three variables (pcp, tmp min/max) and available up to the year 2005.

The weather stations considered for the hydrological analysis are shown in *Fig. 3.5*. Here, we omitted the third dataset i.e. the Tea garden data, as they were not used as input to the modelling purposes, rather they were used for rainfall comparison only.

3.2.1.3 Discharge data

The hydrological model established in this study was calibrated and validated with respect to discharge obtained from the Central water commission (CWC), govt. of India, as gauge data. These data were obtained corresponding to five locations namely Bhomoraguri, Pandughat, Pancharatna, Golaghat and Chowldhoaghat, the first three belong to the main stem whereas the later two belongs to tributary outlets. The lengths of available discharges at all locations are not uniform. As such, calibration and validation periods for all these locations would not be possible to consider the same.

3.2.1.4 GCM data

As for the Global Climatic Model (GCM) data are concerned, we downloaded them from Coupled Model Inter-comparison Project Phase 5 (CMIP5) archive, based on availability for the present and the future periods. Three GCMs were selected for obtaining the climatic data starting from the year 1991 till the end of the current century. The details of the GCM data are described later (*Chapter 7*) in this report.

3.3 Evaluation of Satellite data

The challenge of water resource schemes lies in obtaining accurate ground observations. Although the hydrological models can serve this purpose, they require an adequately accurate climate (temperature, rainfall, evaporation, etc.) input information. Out of all the weather components, rainfall is the main driving variable to widely impact the results of hydro-climatologic studies. The planning of water resource schemes depends on rainfall characteristics especially the variability and trend as well as a reliable rainfall intensity-duration-frequency (IDF) relationship. In large parts of the world, however, the observed precipitation records are often scarce, discontinuous and frequently contain discrepancies, particularly in the developing and under-developed countries. In cases longer records are available in certain gauge observations; they fail to provide a reliable spatial depiction. The Brahmaputra river basin, encompassing four countries have a poor rain gauge network. Moreover, it is difficult to obtain the available data, due to hurdles of data sharing policy between the basin sharing co-nations. So, the use of satellite data becomes inevitable for the hydro-climatic applications of this river basin.

The satellites-based data provide more homogeneous quality, but, their time series accuracy and precision are lower than the corresponding gauge-based ground observations. Due to the fact that the global precipitation data, in many cases do not merely match with the actual gauge observations, it is necessary to evaluate the global gridded precipitation records. The accuracies of gridded precipitation data sets should be evaluated, as they can be affected by systematic errors. Therefore, a preliminary assessment of the satellite precipitation products is important to understand their qualifications for a specific region before putting into an application.

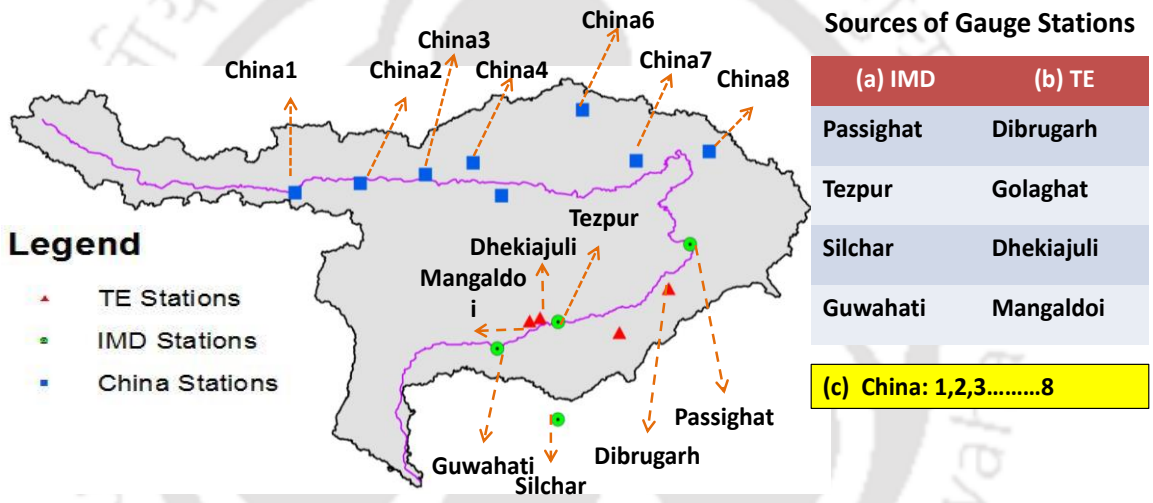

Fig. 3.6 Raingauges considered for rainfall comparison

3.3.1 Methods for Evaluation of Satellite data

The daily rainfall values of the global datasets are compared with the corresponding values of the gauge datasets during 2006-2011 and in terms of statistical as well as regression analysis. Due to the lack of continuous data in the gauge records, longer periods could not be taken up for this study. Fortunately, no gap-filling was required for the gridded global data. However, a very few days if found with missing values in the gauge records are ignored and omitted in this study. Because of lacking required actual gauge data, more stations could not be taken up in this study. Here, "gauge" means the observed rainfall values at raingauges; whereas, "global" means the satellite rainfall data of global stations. Out of the two satellite data (i.e. CFSR and IMD grid) of precipitations, we have evaluated

the CFSR data only. The other one i.e. IMD gridded data has not been evaluated since they were derived based on the satellite records as well as the IMD station data, and in Indian context as well.

3.3.2 Results and discussions

The comparison corresponds to observed values at 16 raingauges (*Fig. 3.6*) though the global CFSR daily precipitation is available at numerous grid points within the basin boundary. We were bound to restrict our use only to these stations due to data scarcity. We understand that the precipitation data of only 16 raingauges spanning over a short duration (2006-2011) are insufficient to conclude a comparative remark for such an almighty river basin. However, this study would surely make sense since we considered the observed data from three different sources (i.e. IMD, TE and China).

3.3.2.1 Statistical comparison

Here, the statistics of rainfall values of wet days during a year are calculated separately and then averaged during 2006-2011, for both the gauge and global data sets. Wet days are considered as those days which actually experience rainfall ($R > 0$) events according to the gauge observations.

Table 3.3 shows the comparison in statistical values of the daily rainfall data sets between the gauge and global weather stations considered over India for example, because similar trends were observed for the other weather stations over China territory of the Brahmaputra basin. It is evident from this table that there is a significant difference between the annual average rainfall values of the gauge and global data. All the global stations recorded lesser annual rainfall value than that of the gauge stations except 'Guwahati' station. This difference might arise because rain gauge represents point data whereas the gridded data represent areal average values. Surprisingly, the annual mean rainfall value for Dhekiajuli station is only 6.88 mm at the global records against 15.16 mm at the gauge records, indicating the highest dissimilarity among all stations concerned. Even the maximum rainfall value recorded on a specific day during a year has a significant variation between both the data sets. High magnitudes in standard deviation and variance indicate that the

data points are highly spread out from the mean as well as from one another. Moreover, high skewness values indicate non-symmetry in gauge records at majority of the stations.

Table 3.3 Summary of Rainfall statistics indicating average values over 6 years wet days Rainfall data during 2006-2011 (for the IMD and TE stations).

Station Name	**Source**	**Annual (mm)**	**Mean (mm)**	**Maximum (mm)**	**Standard Deviation (mm)**	**Variance (mm^2)**	**Skewness**
Guwahati	Gauge	1854	13.26	113.62	18.69	349.31	3.44
	Global	2492.4	17.82	116.41	23.52	547.75	1.72
Passighat	Gauge	3895.3	22.69	186.34	30.72	943.72	2.87
	Global	3577.8	19.13	131.56	21.65	468.93	1.81
Silchar	Gauge	3328.3	17.81	127.40	21.20	449.44	3.63
	Global	3263.2	17.46	152.93	24.67	608.44	3.61
Tezpur	Gauge	1738.3	11.86	91.73	16.45	270.60	3.04
	Global	1721.2	11.74	109.42	17.85	318.62	3.85
Dhekiajuli	Gauge	1563.1	15.16	70.25	14.49	209.96	2.55
	Global	709.6	6.88	80.67	12.09	146.17	2.91
Golaghat	Gauge	1398.5	13.74	78.84	15.20	231.04	2.08
	Global	831.2	8.17	76.36	13.67	186.86	1.97
Mangaldoi	Gauge	1612.9	12.99	95.73	15.86	251.22	3.03
	Global	1436.3	11.56	123.67	17.30	299.29	1.45
Dibrugarh	Gauge	1409	10.61	63.75	11.31	127.91	3.02
	Global	725	5.45	53.29	9.06	82.01	3.34

3.3.2.2 Scatter plot

The extent of correlation between two sets of data can be visualized through a scatter plot. A scatter plot (*Fig. 3.7*) of wet days' rainfall during the year 2006 for global data sets against the corresponding values of the gauge data sets for certain weather stations is shown for example. A similar trend was observed for the other stations, and other years too. The points as plotted in this figure are randomly scattered for all the weather stations and hardly concentrating near the 1:1 line and a similar pattern was noticed for the other periods too. The values of the correlation coefficient (R^2) are poor for all the stations. It may be concluded from this analysis that the gauge and the global datasets can't be correlated on

the basis of daily values. Henceforth, the comparison is further analysed based on the monthly as well as annual rainfall values.

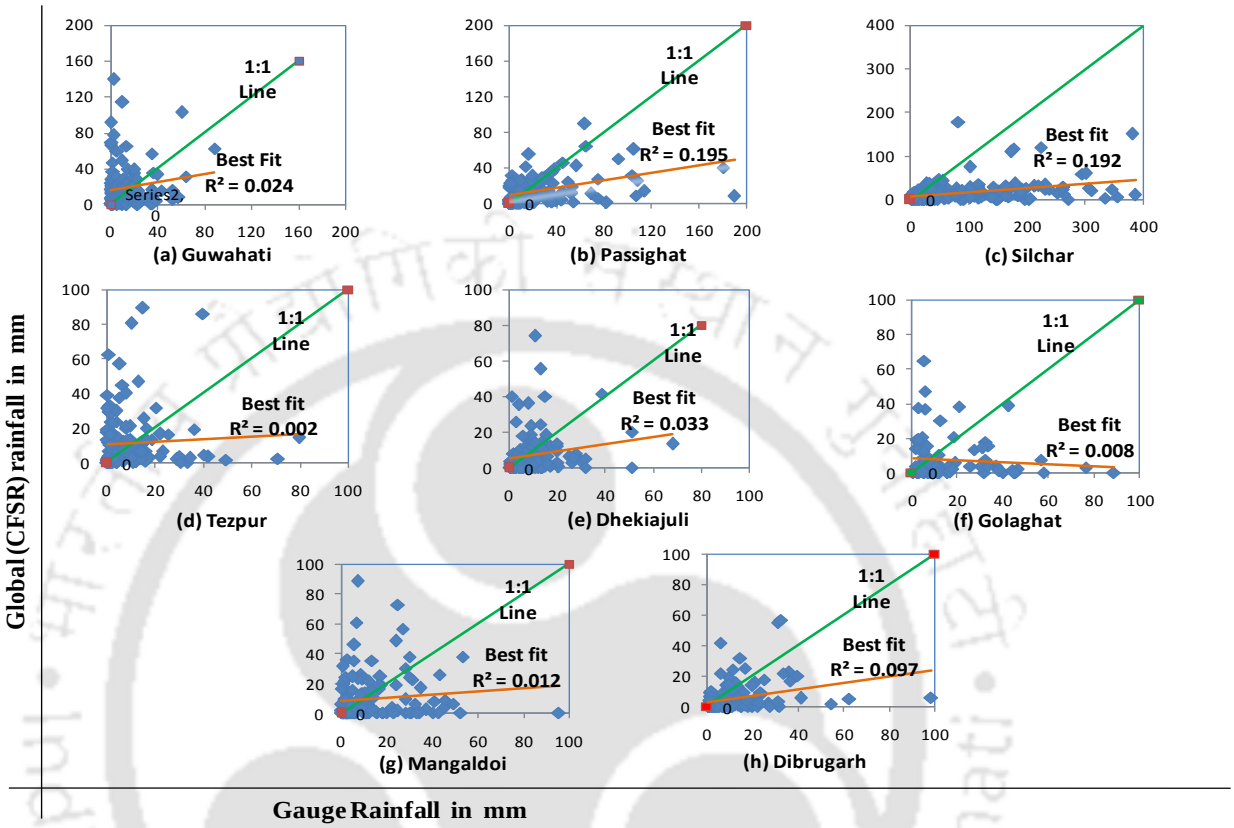

Fig. 3.7 Scatter plot of wet days rainfall during 2006 for the IMD and TE stations.

3.3.2.3 Comparison on monthly rainfall

The station-wise monthly rainfall values of the eight stations over India are shown in *Fig. 3.8* considering a period of 6 years. Here, the wet days' rainfall values are summed up over a particular month during a year, to obtain the total monthly value and then averaged over the entire period of 6 years. It is evident from these plots that the monthly average rainfall values at the gauge stations are higher than that of the global stations with little exceptions in few months of certain stations. While considering all the eight weather stations within the Indian Territory of the Brahmaputra basin as a lump, the final results show the global observations falling below the gauge observations for all the months. Even, a similar trend

is also observed for the other eight stations within the China portion of the basin when considered as a whole during the study period.

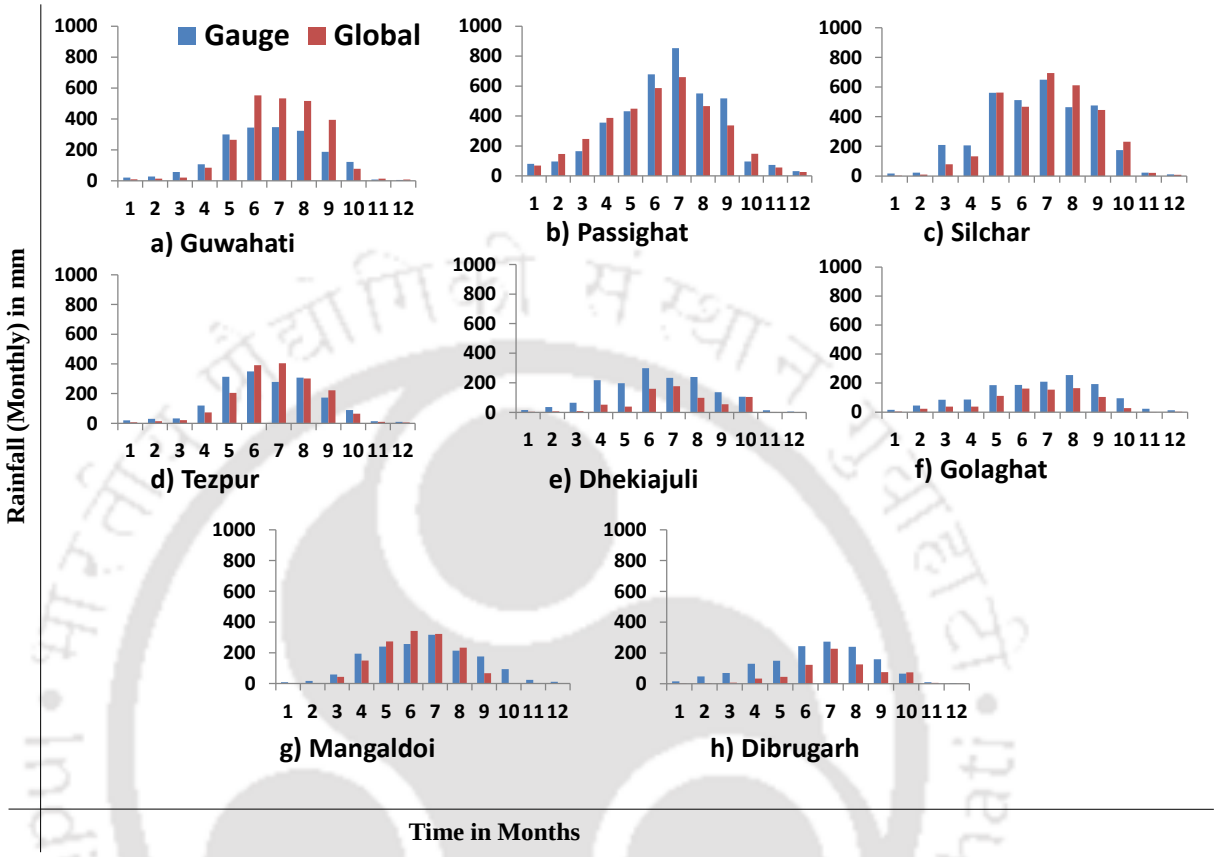

Fig. 3.8 Station-wise mean monthly rainfalls (2006-2011) at stations IMD & TE.

3.3.2.4 Comparison of annual rainfall

The annual average rainfall at each weather station is shown in *Fig. 3.9*. Here, the wet days' rainfalls are summed up during individual years and then averaged over 6 years of data at the corresponding stations. While comparing the gauge and global observations, the annual average rainfalls at China8 &Guwahati stations show the opposite trend as the other stations do. On calculating the average of all the weather stations within India portion as well as Chinese portion of the basin, the global values are found to be under-estimated. Even, the global value is only 1106 mm against 1297 mm at gauge measurements, when averaged over all the 16 stations considered for the present study area.

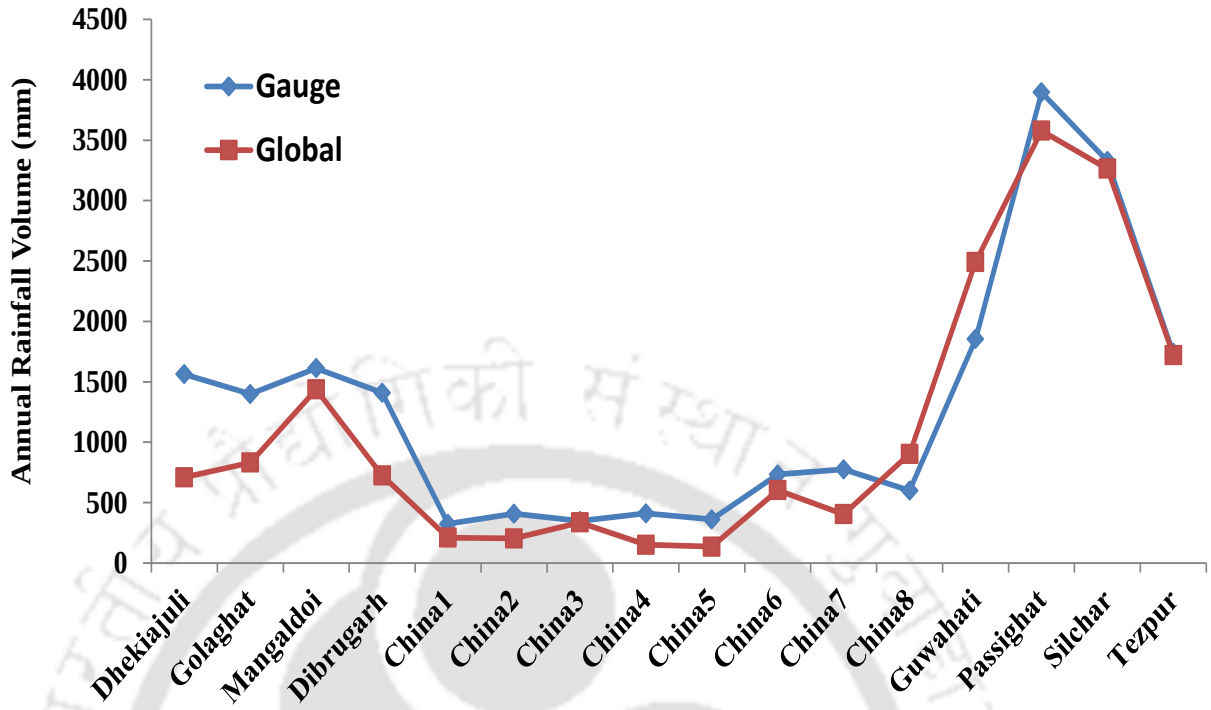

Fig. 3.9 Station-wise Annual Rainfall depths (mm) during 2006-2011.

3.3.2.5 Regression analysis

Regression models are adopted for analyzing the cumulated rainfalls of both the global and gauge datasets. The cumulated rainfall is one of the most significant parameters in analyzing the triggering of different hydrological processes. To analyze the correlation between cumulated rainfalls, Rossi et al. (2017) forwarded two types of regression models as follows:

Linear regression: $\mathbf{R = a\,T}$ ---------- (Eq. 3.1)

Power Law regression: $\mathbf{R = T^b}$ ---------- (Eq. 3.2)

Here, R and T represent cumulated rainfall of measured data by the global and gauge observations and ‘a’ and ‘b’ are the coefficients of linear and power law regressions respectively.

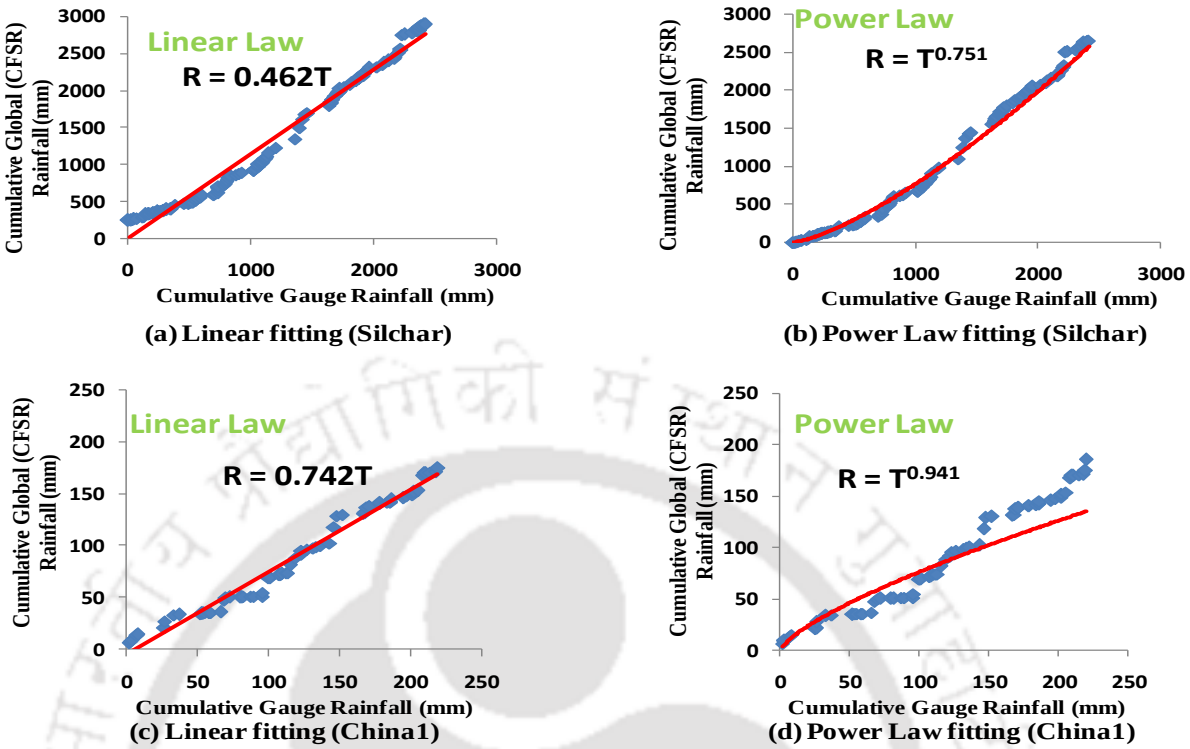

(A) Linear fitting [(a) and (c)] and Power Law fitting [(b) and (d)] between cumulative wet days' rainfall of CFSR Global and the corresponding Gauge observations during the year 2006.

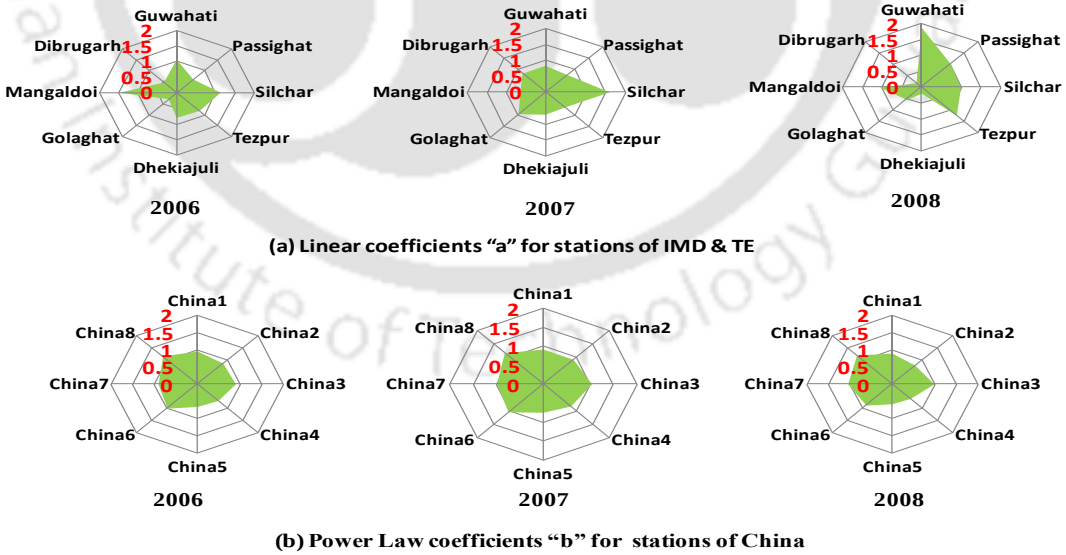

(B) Values of Coefficients: (a) Linear "a" for stations considered over India; (b) Power Law "b" for stations considered over China during the years 2006; 2007 and 2008.

Fig. 3.10 Rainfall comparison based on regression analysis.

As an example, the linear correlations [*Fig. 3.10(A)a,c*] between the cumulative wet day rainfalls at 'Silchar' and 'China1' stations and the power-law correlations [*Fig. 3.10(A)b,d*] for the same values at these two weather stations are shown for the datasets of the year 2006 only. Here, the cumulated rainfalls of the global data and gauge data are plotted to the best possible fit. The linear regression coefficients 'a' for the respective stations are 0.462 and 0.742; both fall below 1, indicating that the global values are under-estimated than the corresponding gauge observations. The values of linear regression coefficients "a" for each station considered over India are shown in figure [*Fig. 3.10(B)a*] for only three years i.e. 2006, 2007 and 2008, as for example. Similar observations of "a" were found during other periods, and at other stations of Tibet. These figures clearly indicate a wide variation in the values while linearly fitting the global values concerning the gauge ones. Similar observations are found even in power-law fitting between the duo, and at all the stations over India and Tibet. Herein, power coefficient "b" is shown [*Fig. 3.10(B)b*] for the Tibet weather stations, as for instance. The value of "b" for majority stations are lesser than 1.0 which again indicates under-estimations in the global observations. Here, "a" and "b" values are shown for three years i.e. 2006, 2007 and 2008 only for example, whereas a similar observation was found during the other years too.

The regression coefficients widely vary from station to station, and even year to year, for all Indian stations. The average value of linear regression coefficients for all stations was found to be 0.821, indicating cumulated rainfall for the global datasets falls below the gauge observations of India. A similar trend was observed through the power-law regression analysis where the mean value was obtained as 0.952, implying a power of all the gauge datasets of India. This indicates lower magnitudes in the global datasets. As for China, data are concerned, almost all the weather stations show "a" value lesser than unity, indicating lower in the CFSR global values except two stations (i.e. China6 & China8). However, the mean value for the linear coefficients of all the China stations while considered as a lump is only 0.802. This means that the CFSR global rainfall values are under-estimated than the actual observation at raingauges. It is evident from this analysis that both the regression coefficients fall below 1.0, and it indicates lower magnitudes in the global CFSR datasets than the gauge datasets of the study area.

3.4 Conclusion

The present study includes a hydrological assessment from the Brahmaputra river basin, apart from several other objectives. The hydrological analysis essentially requires adequate and correct input information. Especially, precipitation being the main driving variable to impact the results of hydrological simulations, their availability in terms of adequacy and reliability is desirable. As the satellite based estimations of weather data may suffer certain systematic errors, their reliability should be checked before application in any water resource schemes. As such, the CFSR satellite precipitation was evaluated in terms of statistical as well as the regression analyses. It is obvious from the results that the CFSR precipitation is under-estimated than the actual ground observations of the Brahmaputra basin. This information would be helpful during the development of the hydrologic model (*Chapter 4*) for the present basin. There is a chance to obtain under-estimated outputs during hydrological analysis, provided the CFSR data alone would be used for the present basin. Therefore, certain measures would be necessary for obtaining reasonable matching with the ground situations during the model simulations. And, the performance of CFSR data are enhanced by using them, in combination with other datasets while establishing the hydrological model.

######## ########

Chapter 4

Hydrologic Model Development & Results

4.0 Introduction

A robust hydrological assessment is a challenging task in regions of limited hydro-climatological information. This level of uncertainty is further augmented in studies of flood hydrology for regions having wide variations in physical and hydro-meteorological characteristics. Hydrological models can serve the purpose of hydrologic assessment from river basins having limited input information. They can provide outputs at both gauged and un-gauged locations, and across the basin. Moreover, they can be used as a tool for estimating the variables required for water resources management practices of a data-scarce watershed.

Understanding the Brahmaputra basin has always been challenging due to its complex characteristics, both hydraulically and hydrologically (Rao et al. 2009). The Brahmaputra river basin possesses very complex stream network systems. This mighty river basin is characterized by high spatial variations of topography, landuse, soil properties, and weather components. The Brahmaputra is a transboundary river, the basin of which occupies four different nations namely China, India, Bangladesh, and Bhutan. As such, the challenge to model this basin lies in hydro-climatic information across and beyond the national boundary. This is because the data scarcity situations widely impact the hydrologic model results. As well, the performance of hydrologic models is dependent on utilizing accurate, long-term input data series. The present chapter enumerates the development of a hydrologic model that would be capable to capture the Brahmaputra basin characteristics hydrologically and hydraulically. Subsequently, the results of the hydrologic model are discussed in the later portion of this chapter.

4.1 Hydrologic model

A hydrologic model should be made capable to capture the basin hydrology in the best suitable manner. Of course, the performance of the model depends on using accurate hydro-climatic information along with the other input data. With the advent of computer software, modelling a river basin has nowadays become easier. Presently, there are numerous hydrologic models available to model the hydrology of a basin. These are:

- SWAT (Soil and Water Assessment Tool).
- VIC (Variable Infiltration Capacity).
- WMS (Watershed Modelling System).
- HEC-HMS (Hydrologic Engineering Center - Hydrologic Modeling System).
- ANN (Artificial Neural Network).

All the above models are capable and can be used to derive the rainfall-runoff processes a river basin, with certain advantages and limitations. In this study, we have implemented the SWAT model for the Brahmaputra basin.

4.2 Why SWAT?

The flow production in the present basin is estimated by implementing the Soil and Water Assessment Tool (SWAT) model, which has earlier been successfully applied by many researchers across the globe. Some of such studies include flow and sediment simulation (Rosenberg et al., 1999; Srinivasan et al., 2005; Zhang et al., 2008; Valdivieso and Sendra, 2014; Daggupati et al., 2015; Dahal et al., 2016), as well as a quantitative and qualitative assessment of water quality (Fohrer et al., 2001; Grizzetti et al., 2003; Bekiaris et al., 2005; Abbaspour et al., 2007; Guse et al., 2015; Chen et al., 2018). Another reason for using SWAT is that it is computationally efficient and capable of continuous simulation over long periods (Borah and Bera, 2004; Arnold et al., 2012). As well, the SWAT model has a provision of using several weather components like precipitation, temperature, wind, humidity, solar radiation etc., which can best describe the hydrologic cycle of a river basin. Even it can be applied for small as well as large watersheds.

4.3 SWAT description

SWAT is a continuous, semi-distributed process-based river model, and describes interactions between the elementary units of various hydrological processes. Gassman et al. (2007) stated SWAT as a physically-based model that simulates the physical processes through the input parameters like topography, land use, climate variables, and soil properties. In SWAT, a watershed is divided into some sub-watersheds, which are then further subdivided into hydrologic response units (HRUs). The HRUs represent an area consisting of dominant land use, soil characteristics, topography, and management practices. A basin or even its sub-basins may consist of several HRUs.

SWAT model first delineates the basin boundary, and then estimates the hydrologic parameters of each HRU. Indeed, SWAT provides several outputs (i.e. hydrologic parameters) like runoff, water quality parameters, sediments, etc. The contributions of each HRU are then aggregated for the sub-basin, by weighted average methods. All such parameters are routed to the outlets of sub-basin, and finally to the main basin. The water balance equation in SWAT can be written (Neitsch et al., 2011) as the following equation (*Eq. 4.1*).

$$SW_t = SW_0 + \sum_{i=1}^{t} [R_{day} - Q_{sur} - E_a - W_{seep} - Q_{gw}] \qquad \text{(Eq. 4.1)}$$

Here, SW_t = Final water content (mm H_2O)

SW_0 = Initial water content (mm H_2O)

t = time in days

R_{day} = amount of precipitation on day i (mm H_2O)

Q_{surf} = Amount of surface runoff on day i (mm H_2O)

Ea = Amount of evapotranspiration on day i (mm H_2O)

W_{seep} = Amount of percolation and by-pass flow exciting the soil profile bottom on day "i" (mm H_2O)

Q_{gw} = Amount of return flow on day 'i' (mm H_2O)

SWAT uses soil conservation services - curve number (SCS-CN) method for estimation of runoff from a watershed. This method was suggested by United States Development of Agriculture (USDA), and can be represented by the equations. (*Eq. 4.2/4.3)*.

$$Q_{Sur} = \frac{(R-Ia)^2}{(R-Ia+S)^2} \quad \text{(Eq. 4.2)}$$

or,
$$Q_{Sur} = \left[\frac{R-0.2S}{R+0.8S}\right]^2 \quad \text{(Eq. 4.3)}$$

Where Q_{sur} is the total surface runoff (mm),

R is the daily rainfall (mm),

I_a is the initial abstractions before runoff (mm) and can be approximated as 0.2S,

S is a retention parameter (mm) based on the soil, landuse and land cover.

$$S = \frac{25400}{CN} - 254 \quad \text{(Eq. 4.4)}$$

Here, CN is the curve number for the day.

SWAT uses weather data, topographic data, soil data, and landuse/land-cover data as input variables, and produces outputs such as runoff, sediments, water quality parameters, etc. It requires the input variables on a daily time-step basis, whereas it has provision to provide outputs on daily, monthly and annual basis.

4.4 SWAT model for Brahmaputra basin

4.4.1 Model Preparation

The step involved in the development of the SWAT model is illustrated in *Fig. 4.1*. First of all, the DEM is loaded into the SWAT project to generate the stream network of the river. SWAT is a physically-based model that simulates the physical processes through the input parameters like topography, land use, climate variables, and soil properties. Based on the DEM, it captures the topographic features like elevation and slope. The stream network (*Fig 4.2a*) is generated for the threshold drainage area of 2000 km^2. Out of 41

manually added outlets, 34 outlets have been chosen for major tributaries at certain defined locations, whereas the other 7 outlets are chosen at some salient points on the main stem. Here, the multiple outlets are added to the stream network to keep provision for spatial input consideration (*Fig 4.2b*). The main basin, as well as the sub-basins boundaries, are then delineated for the final outlet at (23.576N: 89.44E) within Bangladesh. The entire Brahmaputra basin (*Fig 4.2c*) area has been obtained as 542450 square kilometers, out of which China occupies the highest (~50%) followed by India (~36%); and the other two countries i.e. Bangladesh and Bhutan shares almost equally (~7%).

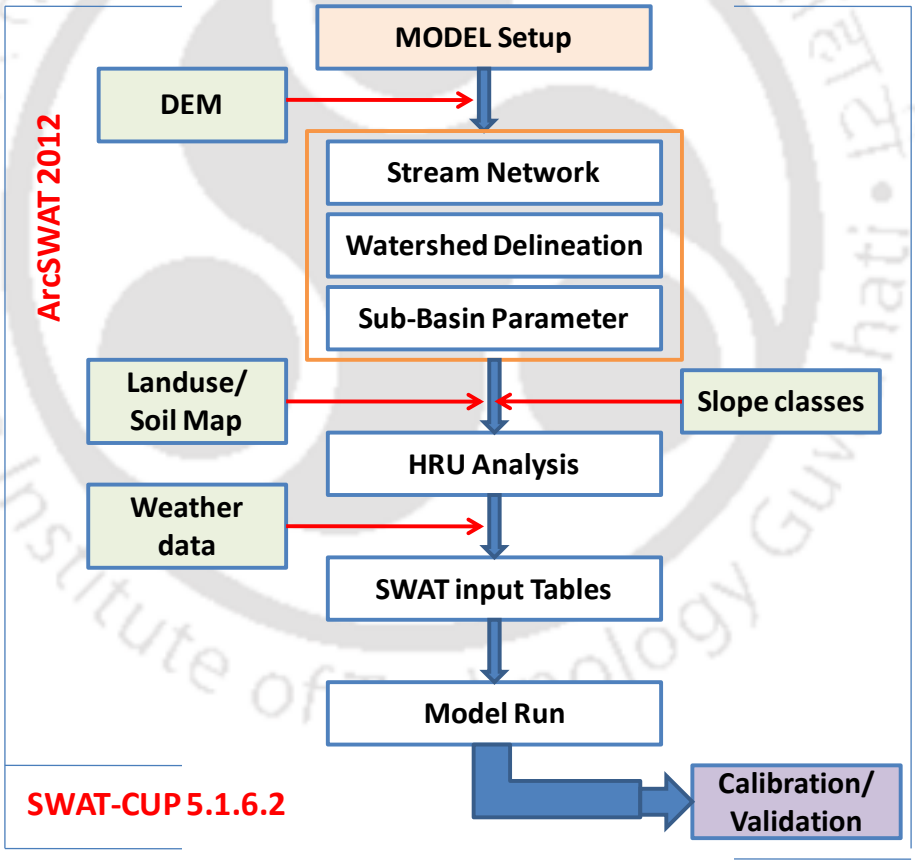

Fig. 4.1 Flow chart showing steps during SWAT model development

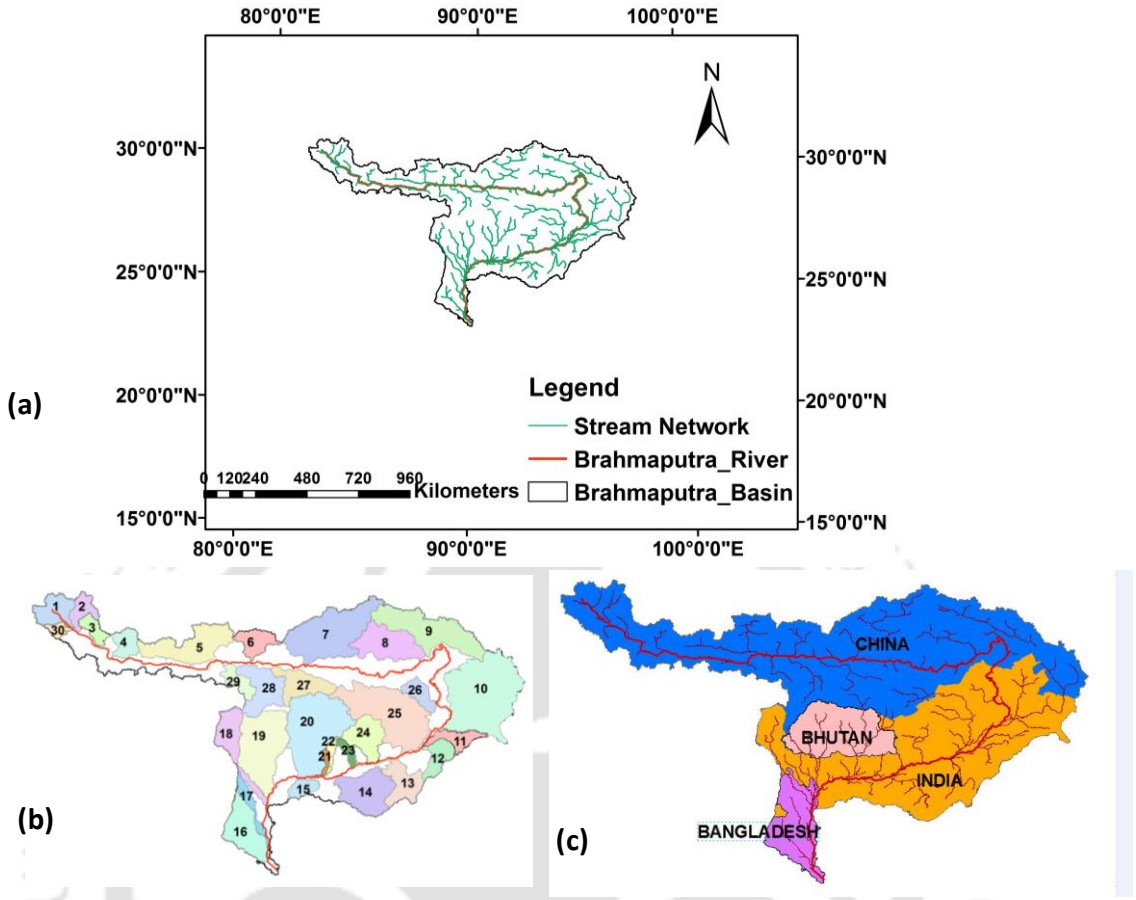

Fig. 4.2 Brahmaputra River Basin: (a) Stream network; (b) Sub-basins of major tributaries; (c) Co-nations of Brahmaputra Basin.

In SWAT, a watershed is divided into multiple sub-watersheds, which are then further subdivided into hydrologic response units (HRUs). The HRUs represent an area consisting of dominant land use, soil characteristics, topography, and management practices. Based on DEM (*Fig. 4.3a*), land use (*Fig. 4.4a*), soil (*Fig. 4.4b*), and slope (*Fig. 4.3b*), the whole Brahmaputra basin is discretized into 40 numbers of sub-basins excluding the main, which are further sub-divided into 1578 numbers of HRUs.

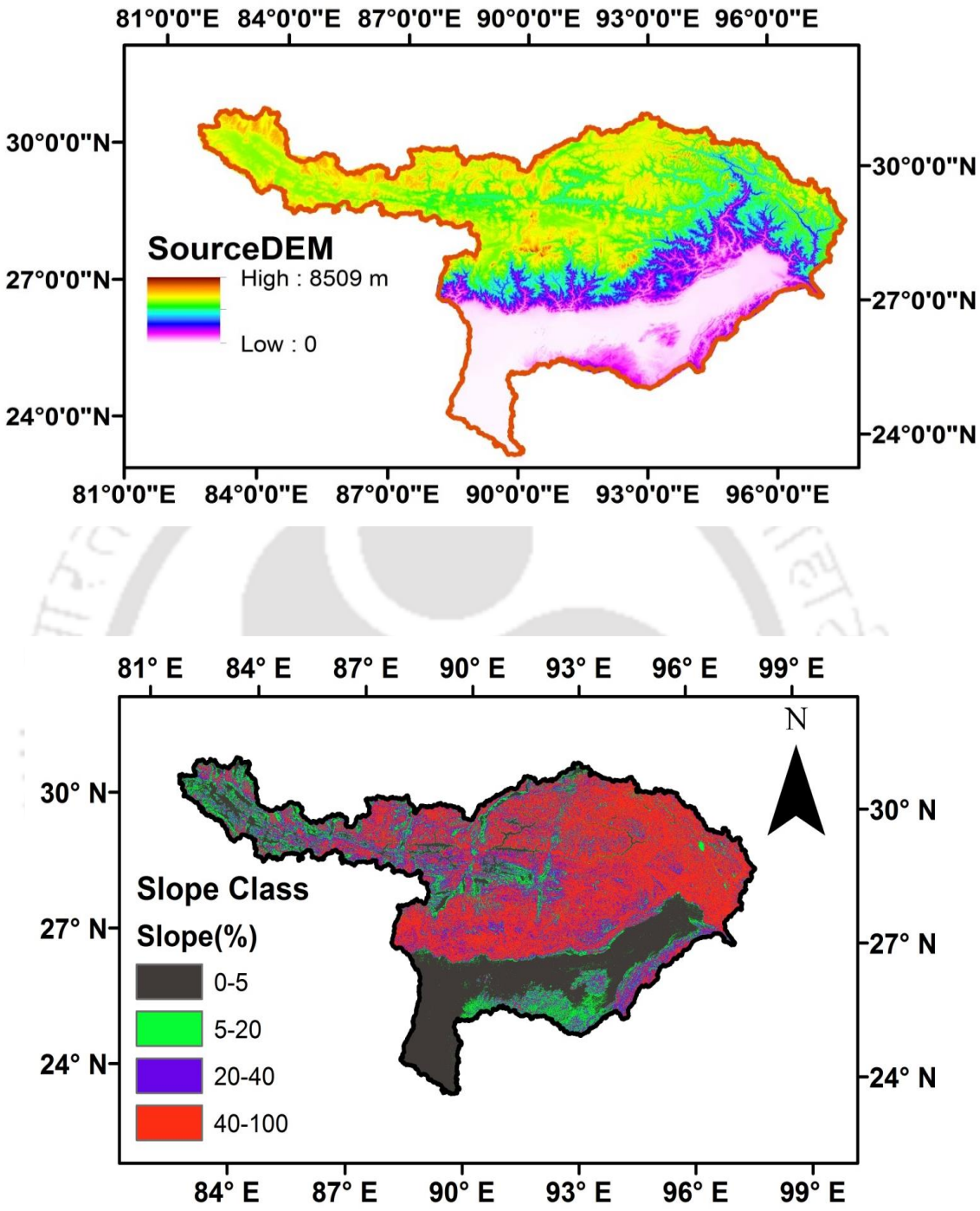

Fig. 4.3. [a] DEM (top) and [b] Slope map (bottom) of the Brahmaputra basin.

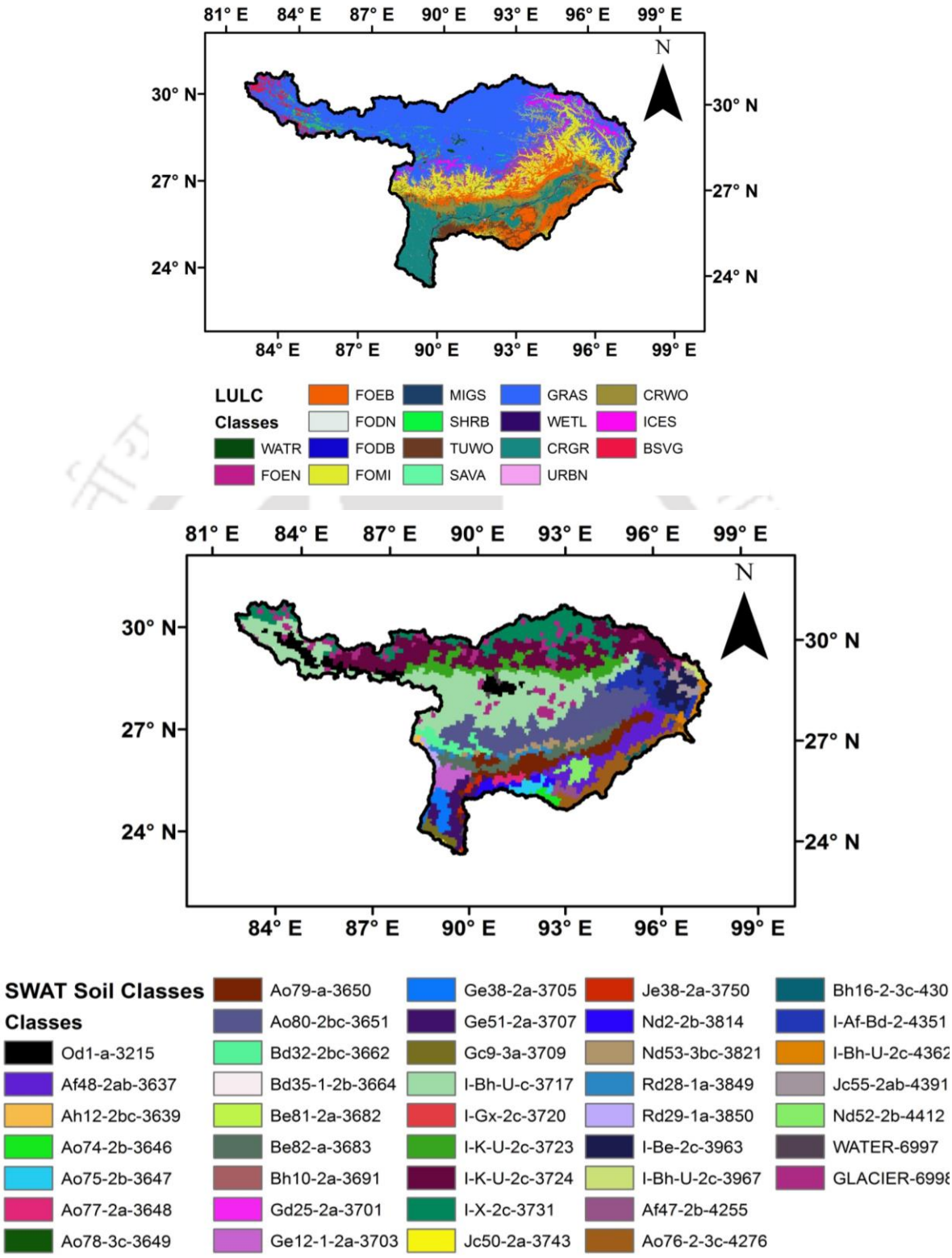

Fig. 4.4 [a] LULC map (top), and [b] Soil map (bottom) of Brahmaputra basin. Here, the names of classes of LULC/soil belong to the SWAT database.

After HRU analysis, the SWAT model requires weather information on a daily time-step basis. It has a provision to input several weather variables like precipitation, temperature, wind, humidity, solar radiation, etc. Then all the input tables within SWAT setup are ready for simulation. Once the simulation is complete, the model is calibrated and validated in SWAT-CUP platform.

Table 4.1 List of SWAT models developed in the present study and their data usage. The calibration periods (CP) and validation periods (VP) are also shown in this table.

S.N.	Model #	Landuse	Soil	Weather	CP	VP
1	MODEL_1	MODIS-based Global Land Cover map with 0.5 km spatial resolution	FAO soil map of 0.9 km spatial resolution	CFSR	1999-2008	2009-2012
2	MODEL_2			CFSR + IMD Stn	1999-2008	2009-2012
3	MODEL_3			CFSR + China Stn	1999-2008	2009-2012
4	MODEL_4			CFSR + (IMD + China) Stn	1999-2008	2009-2012
5	MODEL_5			CFSR + IMD grid	1993-2001	2002-2005
6	MODEL_6			CFSR + IMD grid + China Stn	1993-2001	2002-2005

In the present study, a total of six numbers of SWAT models (*Table 4.1*) were developed. Initially, the evaluations of various datasets are carried out based on the simulation results of SWAT model, setup independently for different input datasets (*Table 4.1*). Subsequently, a proper dataset suitable for the data-scarce Brahmaputra basin is identified. Finally, the SWAT model using the suitable dataset is forwarded for the subsequent analysis such as spatial calibration/ validation, streamflow projection, transboundary effects, etc.

4.4.2 Parameterization, uncertainty and sensitivity analyses

The simulation results of SWAT model are calibrated and validated in SWAT-CUP platform. Here, SUFI2 algorithm is applied for model parameterization, sensitivity analysis as well as uncertainty analysis. The model calibration is performed using the concept of 'aggregate parameter selection' (Yang et al., 2007) that is understood by defining a

parameter change whether ‘replace’ or ‘relative’ or ‘absolute’. SWAT-CUP comprises all sources of uncertainties related to model, parameter and data error.

Parameter uncertainty is usually caused as a result of inherent non-uniqueness of parameters, in inverse modeling, due to wrong data inputs and parameterizations. Here, the parameters mean the variables involved during the calibration processes. Inverse modeling (Abbaspour et al., 2007) approach is effectively used for hydrologic model calibration.

Table 4.2 List of sensitive parameters

Sl	Parameter	Description	Range		Best fit
			Min	Max	
1	R__SOL_AWC	Average available soil water content	0.125	0.348	0.196
2	R__ALPHA_BF	Base flow recession factor in days	0.054	0.503	0.246
3	V__GW_DELAY	Ground water delay time in days	0	128.800	79.162
4	V__GW_REVAP	Ground water revap coefficient	0.110	0.184	0.135
5	R__CN2	SCSII curve number	-0.545	-0.173	-0.354
6	V__SMTMP	Snowmelt base temperature in degree Celsius	0.970	4.920	1.276
7	V__ESCO	Soil evaporation compensation factor	0.828	0.897	0.888
8	V__GWQMN	Threshold water depth in shallow aquifer requires for	1.457	2.753	1.875
9	A__REVAPMN	Threshold water depth in shallow aquifer requires for	0	127.083	111.516

Note: R: Relative; V: Replace; A: Absolute

The sensitivity of a parameter is defined as how significant the parameter is, for the basin. A parameter is said to be sensitive, if, for a little change in its value, there is an influence on the calibration results. Sensitivity analysis helps to identify the significance level of a particular parameter, for the calibration processes. There are two types of sensitivity analysis like ‘global’ and ‘one-at-a-time’ analysis. In our study, we applied the ‘global’ sensitivity analysis which means all the selected parameters are run simultaneously, and the significance level is determined for each of them. Here, sensitivity is determined by using a multiple regression approach, which regresses Latin hypercube generated

parameters against the objective function. To know the rank of the significance level of a parameter, generally, two tests are applied in SWAT-CUP, and they are 'P-value test' and statistical 't-test'. P-value zero (0) signifies sensitivity rank as 'unity', meaning the parameter is highly sensitive. The list of sensitive parameters identified for calibrating discharges of the Brahmaputra basin is presented in *Table 4.2*.

SUFI2 follows an iterative process to update the old value of the parameter and estimates one new value for that parameter. Whereas it adopts sequential fitting processes for incorporating the parameter uncertainty, and parametric errors are identified in terms of over-estimations or under-estimations. Moreover, it utilizes a prior knowledge of the parameter coefficient and quality data checks to minimize the uncertainty. Initially, the algorithm considers a large uncertainty range to ensure the observed values lie within 95PPU (95% prediction uncertainty) band, for the first iteration. The parameter uncertainty range is brought narrower for the second iteration. SUFI2 aims at minimizing the over-estimations and/or under-estimations of modeling outcomes through parameterizations and tries to bracket most of the observed data within 95PPU, with the smallest possible uncertainty band. Likewise, iterations are continued until the calibration results become satisfactory.

4.4.3 Evaluation of SWAT model

The performance of SWAT model is evaluated based on some statistical parameters as discussed follows:

1. **Determination coefficient** **(R^2)**:- The determination coefficient is a statistical test that represents a correlation between the observed and the simulated values. It gives an idea about how well the variance of measured values is replicated by the model simulations and can range from 0 to 1 where 0 indicates no correlation and 1 represents perfect correlation.

$$R^2 = \left[\frac{\Sigma(Oi-Oavg)(Pi-Pavg)}{\sqrt{[\Sigma(Oi-Oavg)^2 \ \Sigma(Pi-Pavg)^2]}} \right]^2 \qquad \text{(Eq. 4.5)}$$

Where, Oi = Observed value at time i

Oavg = Mean of observed value for i = 1..... n

Pi = Simulated value at time i

Pavg = Mean of simulated value for i = 1.....n

n = No. of records

2. **Nash-Sutcliffe coefficient (NSE)**:- NSE provides an idea about how well the simulated output matches the measured data along a 1:1 line. A perfect fit between the simulated and the measured data is indicated by an NSE value of 1 (Surfleet et al. 2012). This value can range from $-\infty$ to 1.

$$\text{NSE (or, NS)} = 1 - \frac{\Sigma(Oi - Pi)^2}{\Sigma(Oi - Oavg)^2} \qquad \text{(Eq. 4.6)}$$

3. **Present bias (PBIAS)**:- It measures the mean tendency of the simulated data to be larger or smaller than the observed ones. For the PBIAS, another statistical test, the optimal value is 0.0, indicating accurate model simulation. Low PBIAS value represents a better simulation. Negative values indicate model overestimation bias, and positive values indicate model underestimation bias (Gutpa et al. 1999). The model performance for streamflow is defined as satisfactory if PBIAS ± 25 (Moriasi et al. 2007).

$$\text{PBIAS} = \frac{\Sigma(Oi - Pi)}{\Sigma Oi} \times 100\% \qquad \text{(Eq. 4.7)}$$

4. **P-factor and R-Factor:-** P-factor is the percentage of observed data enveloped by Model results (i.e. 95PPU). In SUFI2, most of the observations are expected to lie within the envelope. Its value should be larger than 70%. On the other hand, R-factor is the thickness of the Model envelope (i.e. 95PPU). The thickness of the envelope should be as small as possible. Its value ranges from 0 to infinity, and should be around 1 for acceptance of a model. It is the measure of uncertainty.

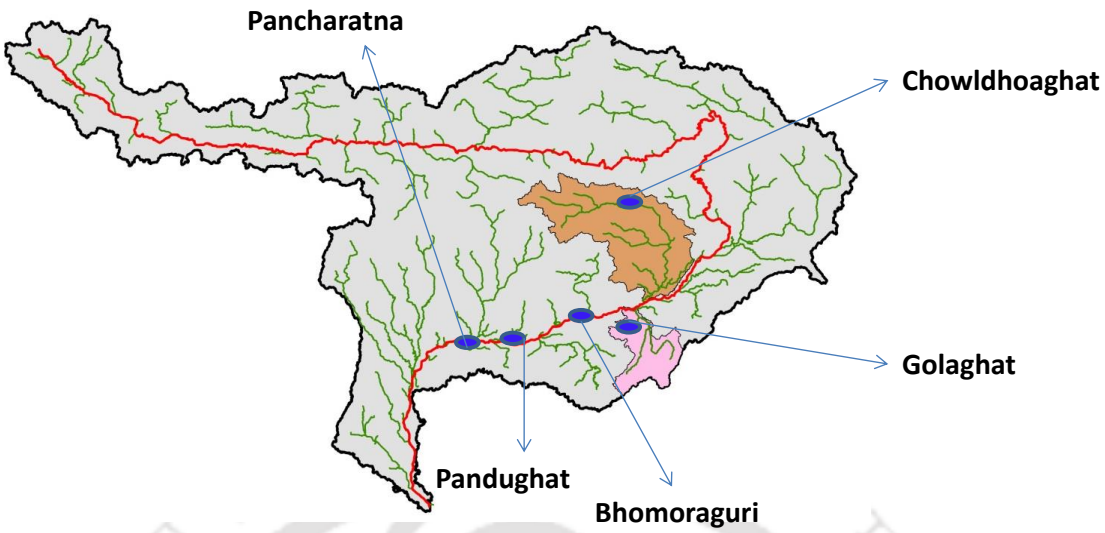

Fig. 4.5 Locations for Calibration and validation

4.5 Model results and discussions

4.5.1 Simulation results

Initially, all the SWAT models (*Table 4.1*) were established as per the descriptions given earlier. It is very important to use adequately correct data while establishing a hydrologic model, without which reasonably valid outputs be rarely achieved. The simulation results, without calibration and validation of the respective SWAT models, are compared to have an idea about the model performance based on data usage. The *Fig.4.6* shows a scatter plot between the simulated and observed flows for the models at Pancharatna (*Fig. 4.5*), for example. Similar trends were also observed at all other outlets. This plot provides an idea of how the simulated flow is different from the observed ones. A perfect match between the duos represents a straight 1:1 line.

It is evident from *Fig. 4.6* that the MODEL_1 that uses only the CFSR global stations datasets exhibits the least correlation (R^2 = 0.607) value, indicating the highest disagreement between the measured and simulated flows out. The flows out of MODEL_2 & MODEL_3 that use observed station data of IMD and China respectively too did not provide good resemblance with the observed flow data. Here, although there are improvements in model outputs, significantly wide changes have not been observed, due to the non-capturing of all the observed weather datasets by the 2nd and 3rd SWAT models.

This is because only the weather station close to the geometric center of sub-watersheds is picked-up by SWAT. On combining all the observed weather datasets with the global CFSR dataset as used in MODEL_4, however, the correlation further improved with R^2 value as 0.65.

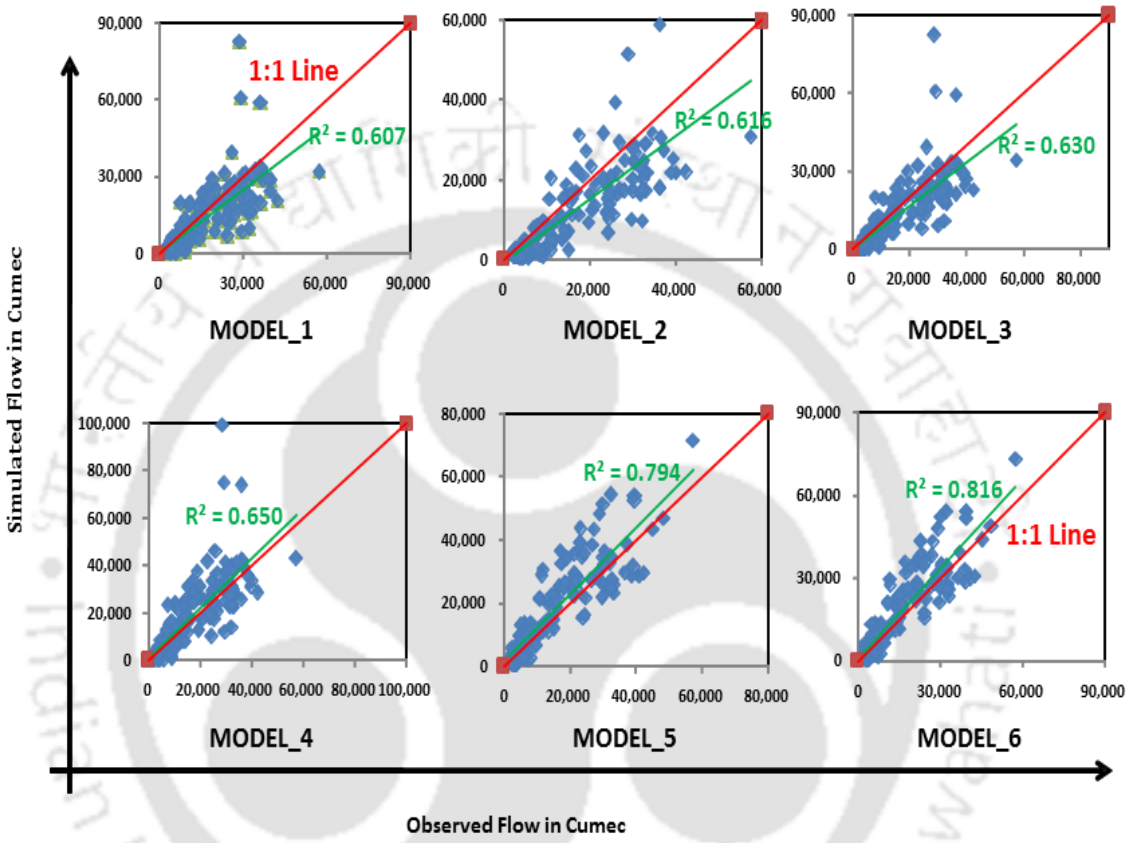

Fig. 4.6 Scatter plot of monthly simulated flows (m^3/s) against the corresponding measured discharges (m^3/s) at Pancharatna for all SWAT models. Here, simulated values indicate the monthly outputs obtained from model run (1991-2012, for the first four models; and 1991-2005, for the last two models) without calibration and validation.

The simulation result of the MODEL_5 has surprisingly improved while the IMD gridded data are added to the global CFSR weather data. Furthermore, the MODEL_6 provided the best correlation ($R^2 = 0.816$) value among all models developed in this study. This analysis indicates the MODEL_6 that uses the global CFSR dataset in conjunction with the IMD gridded, as well as the observed data over China, provided the best performances in simulating the discharges, and it, therefore, may be taken up as a default model for the present basin.

4.5.2 Calibration & Validation results

4.5.2.1 Single-Outlet Calibration/Validation

The calibration and validation of the SWAT models are done in SWAT-CUP platform that tries to capture most of the measured data within 95% prediction uncertainty (95PPU) during iteration.

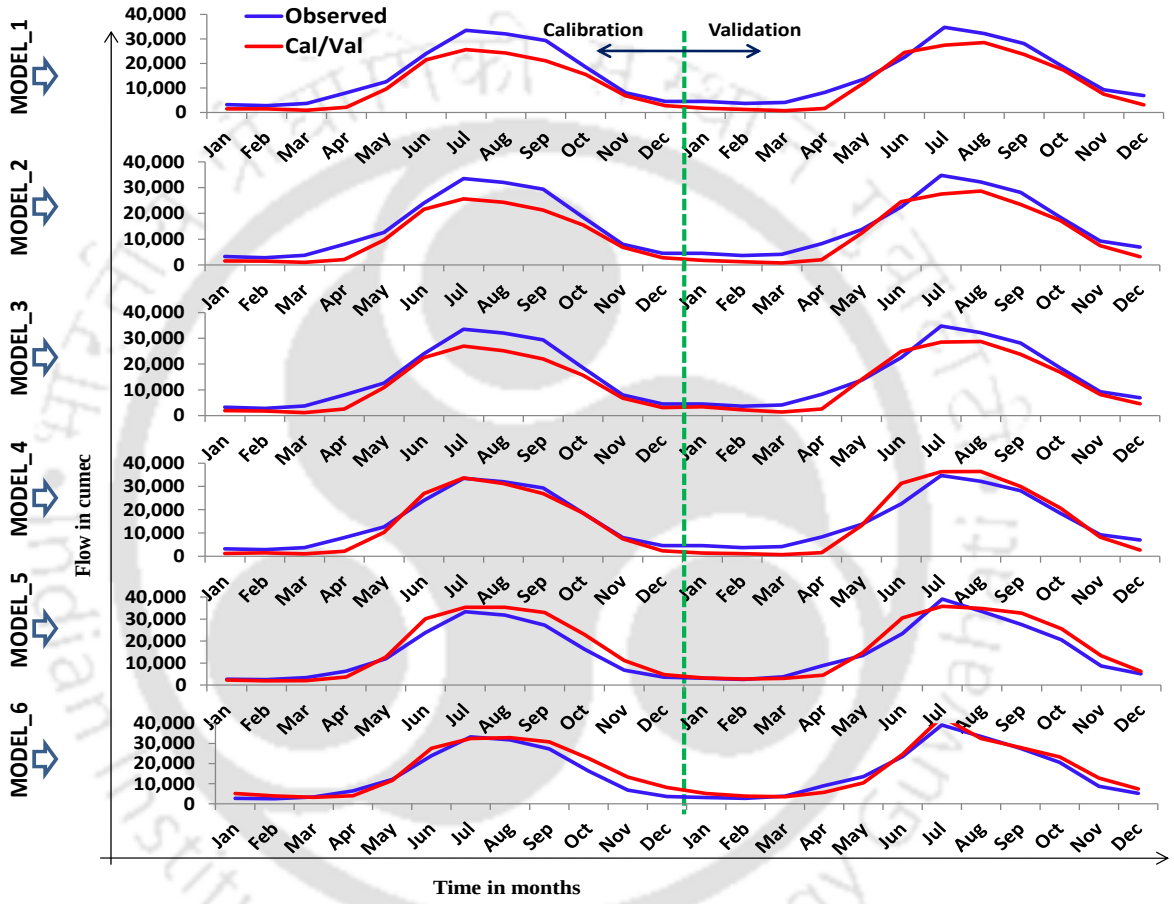

Fig. 4.7 Results of Single-outlet Calibration and validation at "Pancharatna" of all the SWAT models (i.e. MODEL_1-6). Here, the discharge values of calibration (or validation) are averaged to obtain the month-wise values.

The two indices as "P-factor" and "R-factor" are used for the goodness of fit between the simulated and the observed values. Whereas, the P-factor is the fraction of observed data bracketed by 95PPU band and varies from 0 to 1, where 1 indicates a cent percent bracketing by 95PPU. On the other hand, R-factor is the thickness of the Model envelope

(i.e. 95PPU) and should be around 1, but a value of <1.5 is acceptable (Abbaspour et al., 2007) for this index.

Initially, all the SWAT models are calibrated and validated at a single outlet basis. In the present analysis, we show the calibrated and validated results at Pancharatna (*Fig. 4.7*) outlet only, as a continuous graph for simplicity and clarity of presentation. Here, only the monthly average values over calibration (or validation) periods are shown, rather than the complete time series plot, to maintain the data secrecy policy of the CWC. The first four models (*Fig. 4.7*) i.e. MODELs_1,2,3,4 were calibrated for 10 years (1999-2008) and validated for 4 years (2009-2012) by skipping 8 years (1991-1998) for initiation of the hydrologic response. While the last two models (*Fig. 4.7*) i.e. MODELs_5,6 were calibrated for 9 years (1993-2001) and validated for 4 years (2002-2005). Although more the skipping periods better is the initial response, we could not make it longer for the last two models due to the limitation of model input data, and 2 years (1991-1992) period only was provided for them.

Table 4.3 Statistics of Single-output-calibration and validation at Pancharatna for all SWAT models

Model #	Calibration Statistics				Validation Statistics			
	R^2	NS	P-factor	R-factor	R^2	NS	P-factor	R-factor
MODEL_1	0.78	0.68	0.60	0.63	0.77	0.70	0.71	0.74
MODEL_2	0.78	0.69	0.60	0.65	0.77	0.70	0.70	0.73
MODEL_3	0.80	0.73	0.59	0.60	0.78	0.74	0.67	0.70
MODEL_4	0.81	0.72	0.74	1.07	0.79	0.64	0.80	1.27
MODEL_5	0.82	0.70	0.60	0.62	0.73	0.66	0.60	0.46
MODEL_6	0.79	0.74	0.90	0.97	0.86	0.84	0.81	0.88

It is understood from the results that the MODEL_1 provides the least satisfactory output, as evidenced by the calibration statistics in *Table 4.3*. Here, the value of R^2 (0.78) is fair, but the other values like NS (0.68); P-factor (0.60); R-factor (0.63) are relatively inferior for acceptance of the model. On checking the validation statistics, however, slightly better performances were noticed. The statistics of MODEL_2 and MODEL_3 are found to comply with satisfactorily. However, the MODEL_4 provided the best statistics among the first four models, during both the calibration as well as validation. Surprisingly, the

MODEL_5 which showed good agreement during the simulation (*Fig.4.6*) failed to produce good statistics during calibration and validation, although they were carried out by using the same sensitive parameters (*Table 4.2*) as the previous ones. Among all, MODEL_6 is found to perform the best, since it provides a very good strength of statistics for all the parameters, even during both the calibration and validation (*Table 4.3*). This fair result is due to using a proper combination of input datasets in this model (MODEL_6), as compared to the others used in the other models (MODELs_1-5). The R-factor (0.97) value during calibration (*Table 4.3*) is nearly equal to the desired value (1.00). It indicates a very good measure of parameter uncertainty. As such, this model i.e. MODEL_6 is found to be the best, among all the SWAT models developed in this study. Therefore, MODEL_6 only has been extended for the subsequent analyses.

4.5.2.2 Multi-Outlet Calibration/Validation

The calibration at a single site is judicious for the small watershed only, because of homogeneous watershed characteristics. On the contrary, a large watershed needs a multi-site calibration to represent heterogeneous characteristics. The single-site calibration if done on a large watershed may result in a combination of under/over-estimation for values (Qi and Grunwald 2005), due to consideration of homogeneous characteristics over the entire basin. To have a better intra-watershed spatial accuracy, the present study includes multi-site calibration/validation at five outlets (*Fig. 4.5*) simultaneously. This spatial accuracy is done only for the best SWAT model identified earlier (*Sec. 4.5.1* and *Sec. 4.5.2.1*) i.e. MODEL_6, assuming that the other models would not lead to better performances, even during the multi-site calibration and validation.

The time series plots (*Fig. 4.8*) show the results of multi-outlet calibration and validation, as a continuous graph for simplicity in the presentation. Due to the non-symmetry of available discharge data length, different calibration periods were chosen for the individual outlets. However, the validation periods for all the sites were chosen the same as 4 years (2002-2005).

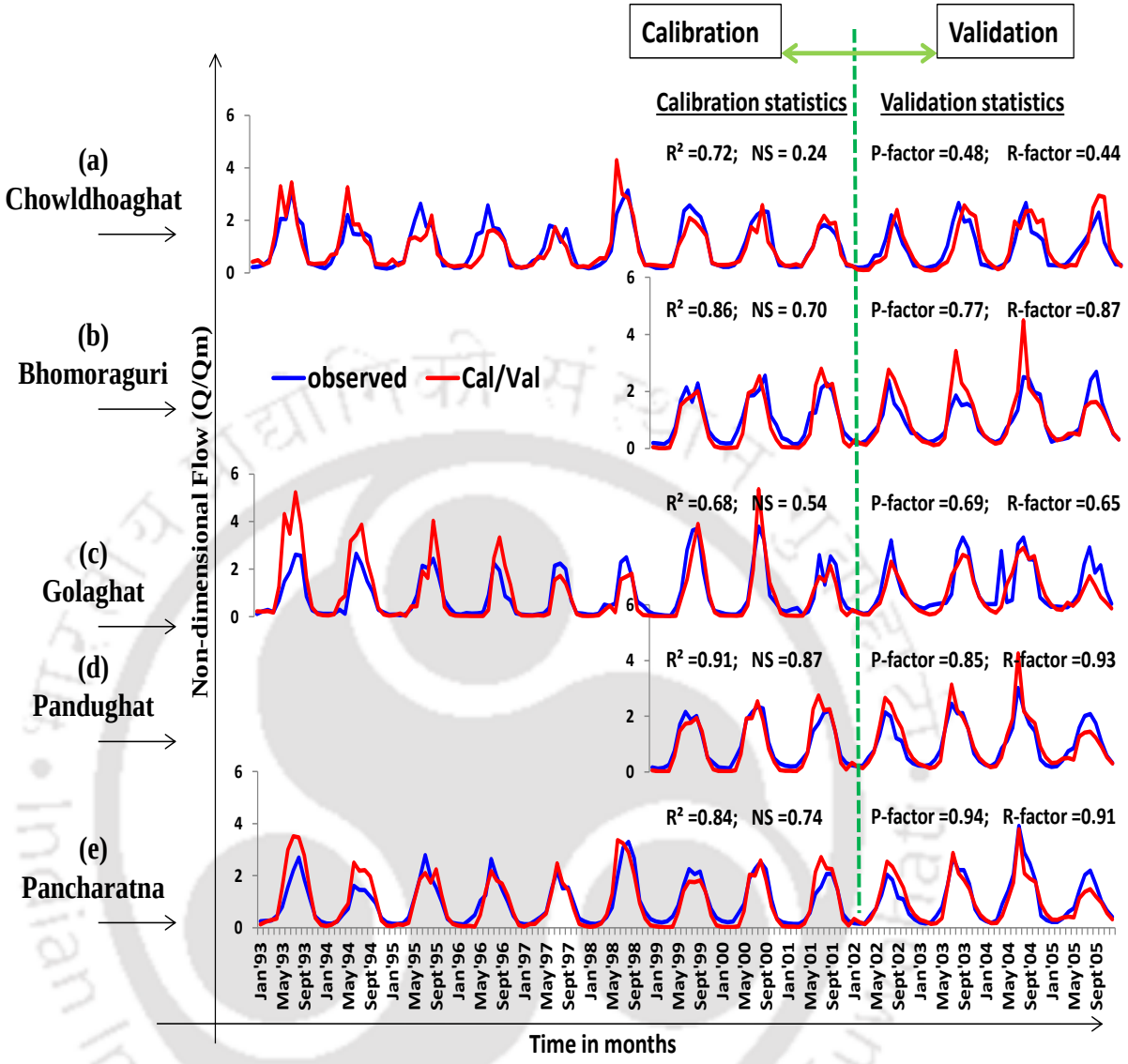

Fig. 4.8 Results of Multi-outlet calibration and validation results of MODEL_6. The calibration and validation results of the monthly model are plotted in a single plot showing the Non-dimensional flow (Q/Q_m) values. Here, Q represents flow (simulated or observed) and Q_m represents the mean flow value of the respective series.

Due to its complex characteristics, a large watershed may not be expected to produce good statistics against each outlet during multi-site calibration, however, a balance among the statistical parameters are required for reasonable acceptance of a model. During this spatial analysis (*Fig. 4.8e*), the most downstream outlet (i.e. Pancharatna) is found to conform good statistics during calibration (R^2 = 0.84; NS = 0.74) and validation (P-factor = 0.94; R-factor = 0.91). Similarly, the model is found to produce satisfactory statistics at the other

two mainstem outlets viz. Bhomoraguri (*Fig. 4.8b*) and Pandughat (*Fig. 4.8d*). However, the calibration results at Pancharatna, especially the value of R^2 (0.84) is relatively low as compared to Bhomoraguri (0.86) and Pandughat (0.91). This is probably due to the different lengths of the warm-up period kept for the initiation of watershed responses by the hydrologic models. The warm-up period for Pancharatna is only 2 years (1991-1992) against 8 years (1991-1998) for the later two outlets. Interestingly, the results at the tributary outlets (*Fig. 4.8a,c*) are found relatively poor than the results at the main stem outlets. Especially, the value of NS at Chowldhoaghat outlet is only 0.24, the lowest among the corresponding values at the other outlets. This is due to low values of river discharges at the tributary outlets, as compared to the mainstem values. A little change in flow values during calibration/validation may lead to a wide impact on the statistical parameters. Anyway, it becomes unfair to seek good statistics at all the locations, during spatial calibration and validation, due to heterogeneous basin characteristics. Overall, the spatial calibration/validation results of the MODEL_6 may be termed as satisfactory.

4.6 Model application in water resources management

SWAT model provides location-specific hydrologic information across a river basin which may be utilized by the water resource managers for planning and designing of hydraulic structures. This information belongs to the quantitative and qualitative assessment of river flows. A list of certain parameters is enumerated in *Table 4.4* corresponding to a location (LAT: 29.15485N; LONG: 95.006979E) named as 'Indo-China Border'. Here, monthly values are obtained from the outputs of the final run of the MODEL_6 which are then averaged during 1991-2005.

The SWAT hydrologic model output for river flows at the salient location widely varies from a very low value (28.0 m^3/s) in February to a very high value (8364.8 m^3/s) in June. Similarly, wide outputs have also been noticed for the sediment concentration with the maximum value (445.815 mg/L) during June month. Whereas, high values of sediment concentration may lead to loss of aquatic habitats, wetlands, and recreation attributes. Moreover, it becomes a concern for human health and erosion hazards.

Table 4.4 Parameters for water resources management practices and their mean values at a certain location (LAT: 29.15485N; LONG: 95.006979E) within the Brahmaputra river basin. The figures are obtained as output from the final run of the SWAT model suitably adopted in the present study i.e. MODEL_6.

Months	Flow value m^3/s	Sediment Concentration mg/L	Organic Nitrogen mg/L	Organic Phosphorous mg/L	Nitrate mg/L	Ammonium mg/L	Mineral Phosphorous mg/L	Dissolved Oxygen mg/L
Jan	100.4	44.075	0.000	0.000	0.001	0.002	0.000	4.758
Feb	28.0	24.060	0.565	0.074	0.001	0.002	0.001	3.646
Mar	44.1	11.129	5.870	0.778	0.003	0.010	0.009	0.937
Apr	711.2	45.566	7.417	1.598	0.059	0.535	0.046	0.271
May	6878.2	252.269	7.036	1.529	0.014	0.698	0.073	0.215
Jun	8364.8	445.815	4.586	0.754	0.018	0.408	0.069	1.599
Jul	4920.0	382.623	8.508	1.097	0.046	0.069	0.032	6.927
Aug	4994.2	310.185	8.869	1.189	0.053	0.107	0.029	3.836
Sep	4266.5	278.100	6.373	0.850	0.049	0.044	0.015	5.388
Oct	2439.8	172.431	0.479	0.064	0.019	0.001	0.003	5.280
Nov	909.9	64.991	0.000	0.000	0.001	0.000	0.000	1.037
Dec	312.4	55.787	0.000	0.000	0.001	0.001	0.000	2.217

The water quality parameters like nitrogen, phosphorous, nitrates, ammonium, dissolved oxygen, etc. may be a concern for human and plant health. Based on the qualitative analysis for those parameters, the processes and cost of treatment of water, if derived for water supply projects, can be ascertained. Although the present model is capable of providing quite a lot of information regarding water quantity and quality at all desired locations across the basin, the present analysis is shown corresponding to one outlet only, for example. Such information provided by the hydrologic models at the desired location may be utilized by the water resource managers. As such, hydrologic models serve the purpose of deriving information at locations of no historical records, especially at the locations beyond the national boundary for such a transboundary river basin.

4.7 Conclusion

There is acute data scarcity for the Brahmaputra river basin. The rain gauge network in the Brahmaputra basin is not adequate since the spatial variations of rainfall are very wide across the basin. Moreover, it is difficult to obtain the hydro-climatic information beyond the national boundary, due to transboundary issues. In the absence of sufficient and long-term data, hydrologic modelling of this mighty river basin has always been challenging. Interestingly, the combination of several sets of weather data could lead to providing satisfactory results of the hydrologic model. The CFSR datasets while used in combination with IMD gridded and China station data is proved to the best suitable for the present basin, and among the available datasets to our end. This information would be helpful to the research community.

Due to data scarcity situations, the planners and managers of water resources are not able to develop a comprehensive management policy for the Brahmaputra river basin. The results of the present modelling study would facilitate them by providing the necessary information.

From the present study, MODEL_6 is found to provide the best satisfactory results in simulating the Brahmaputra basin hydrology, among all models developed in this study. Therefore, this model is considered as the default hydrologic (SWAT) model for the subsequent study objectives. As such, we would extend this model (i.e. MODEL_6) only for application in the subsequent objectives. While analyzing the basin-scale impact, transboundary effect, and even impacts of climate change, etc., the model used will mean this MODEL_6 only, for all cases.

######## ########

Chapter 5

Basin Scale Impact Studies of SWAT Model

5.0 Introduction

Watersheds can be desegregated in geographic space and their processes in time. Indeed, one of the key differences between lumped and distributed models is the processes in which they take spatial variability into account. The distributed, physically based watershed hydrologic models become indispensable for having correct predictions of the hydrologic parameters across the basin. The physically-based semi-distributed SWAT hydrologic model has successfully been applied to the small watersheds (Bekiaris et al., 2005; Srinivasan et al, 2005; Bracmort et al, 2006; Abbaspour et al, 2007; Jha, 2009, etc.) as well as the mid-sized watershed for simulating flow, sediment, and water quality. Even, SWAT has wide applications towards large watersheds (Lee et al, 2011). A hydrologic model established for a large watershed, however, may not provide justified outputs for its sub-watersheds.

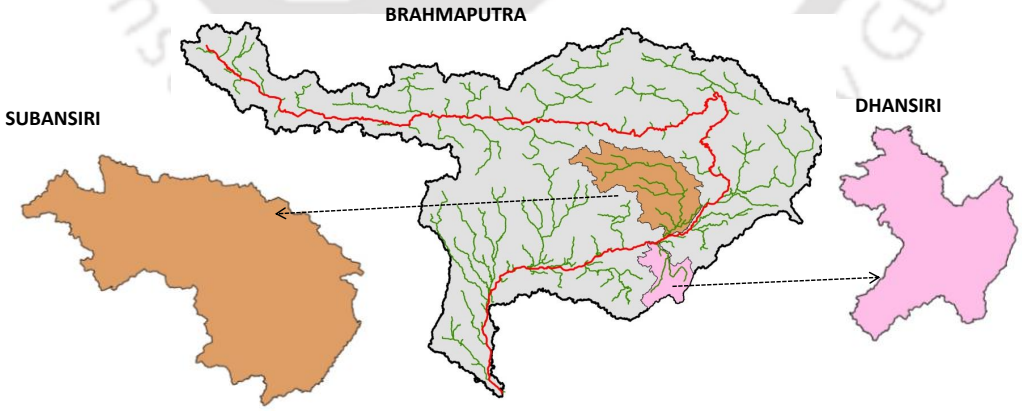

Fig. 5.1 Brahmaputra basin and two of its sub-basins viz. Subansiri basin and Dhansiri basin.

This section of the study investigates whether the SWAT model established for the large Brahmaputra basin would provide acceptable outputs at the sub-basins i.e. tributary outlets. Here, two sub-basins (*Fig. 5.1*) namely '*Dhansiri River basin'* on the southern bank and '*Subansiri River basin'* on the northern bank of the Brahmaputra has been considered.

Table 5.1 Sensitive parameters utilized during calibration of SWAT models.

S.N.	Parameter	Description
1	SOL_AWC[1,2]	Average available soil water content
2	ALPHA_BF[1,2]	Baseflow recession factor in days
3	GW_DELAY[1,2]	Groundwater delay time in days
4	GW_REVAP[1,2]	Groundwater revap coefficient
5	CN2[1,2]	SCSII curve number
6	SMTMP[1]	Snowmelt base temperature in ^{0} Celsius
7	ESCO[1,2]	Soil evaporation compensation factor
8	GWQMN[1,2]	Threshold water depth in shallow aquifer requires for return flow to occur
9	REVAPMN[1,2]	Threshold water depth in shallow aquifer requires for revap to occur

Note: 1 stands for sensitive parameters used for main (Brahmaputra) model [Case-I, Case-II]
2 stands for sensitive parameters used for both the sub-models (Dhansiri & Subansiri) [Case-III].

5.1 Methodology

Initially, a SWAT hydrologic model has been established for the large Brahmaputra basin. The detailed procedures for establishing this model has earlier been discussed in *Chapter 4*. This model was calibrated and validated at various locations including 'Golaghat' (an outlet at Dhansiri River) and 'Chowldhoaghat' (an outlet at Subansiri River). Later, individual SWAT models for these two tributaries have been established. The process of making the sub-watershed models in SWAT platform is exactly similar to the main model. And, the input datasets for these models are kept same as the main SWAT model. This means the simulation processes of the Dhansiri model and the Subansiri model are kept the same as that of the Brahmaputra model. However, the process of calibration and validation of the sub-watershed models are considered by adopting two different ways:

(1) First, calibration/ validation are done using the *same set of parameters and same magnitudes* as those used in the main model [i.e. Brahmaputra basin model (*Chapter 4*)];

(2) Second, calibration/ validation is done using the *different set of parameters with different magnitudes* as those used in the main model.

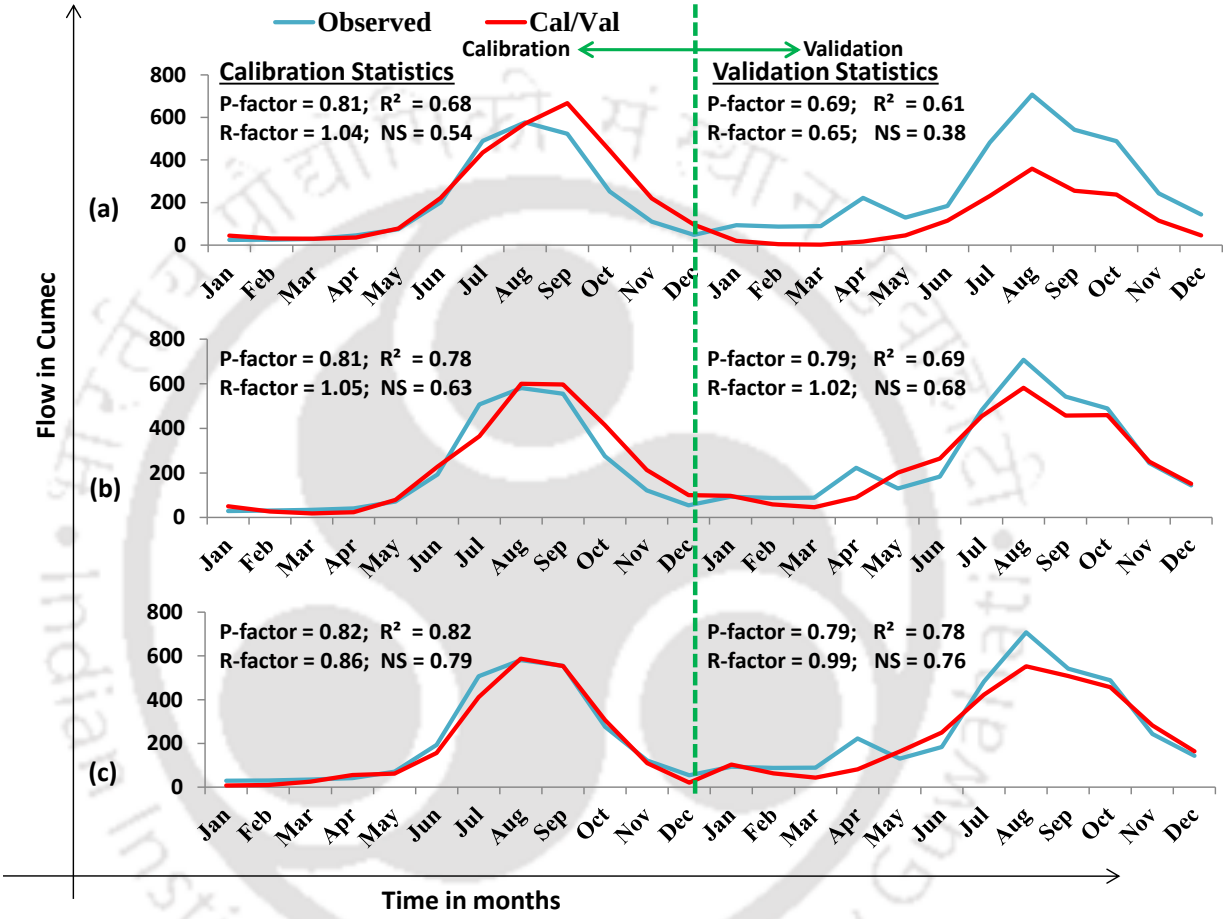

Fig. 5.2 Calibration (1993-2001) and Validation (2002-2005) results at Golaghat (Dhansiri Basin): (a) *Case-I*: From multi-outlet calibration/validation results of the **Brahmaputra Basin model** using nine sensitive parameters; (b) *Case-II*: Single-outlet calibration/validation of the **Dhansiri Basin model** using the same set of parameters and same magnitudes as Case-I; (c) *Case-III*: Single-outlet calibration/validation of the **Dhansiri Basin model** using the different set of parameters than Case-I.

Finally, the results of the main model are compared with the results of the sub-watershed models corresponding to the two outlets i.e. 'Golaghat' and 'Chowldhoaghat'. For this, we have considered three cases: (a) Case-I: outputs obtained from the main model calibrated using nine sensitive parameters [*Table 5.1*]; (b) Case-II: outputs obtained from individual

sub-watershed models calibrated using the same sensitive parameters as case-I; (c) Case-III: outputs obtained from individual sub-watershed models calibrated using different sensitive parameters [*Table 5.1*] than Case-I/II.

5.2 Results and discussions

5.2.1 Model results for Dhansiri basin

Fig 5.2 shows the time series plot of calibration and validation results of the different SWAT models for the Dhansiri River basin. Here, *Case-I* represents the results obtained from the large Brahmaputra basin model corresponding to the 'Golaghat' outlet. It is observed that the calibration statistics are reasonably fair for P-factor (0.81), R-factor (1.04), R^2 (0.68) and NS (0.54). On the other hand, the validation statistics were found relatively inferior in magnitudes, as compared to the corresponding magnitudes of the calibration statistics. This may be due to the shorter length of the validation period than the calibration period. This calibration/ validation has been done by using nine sensitive parameters as used in the main (Brahmaputra) model (*Table 5.1*). These sensitive parameters while used for the calibration/ validation of the separate Dhansiri model produces different outputs that are shown in Case-II. Here, the values of the statistical measures get improved. For example, R^2 and NS values during calibration stand higher at (0.78; 0.63) than the corresponding values (0.68; 0.54) as in Case-I. Even, the validation statistical values get improved too. The Dhansiri model calibrated using different sensitive parameters as in Case-III (*Fig. 5.2*) provides a better strength of statistical parameters than the other two cases i.e. Case-I/II. The R-factor (0.78) during validation (Case-III) signifies a good measure of model strength.

5.2.2 Model results for Subansiri basin

The SWAT model results corresponding to the "Chowldhoaghat" outlet of the Subansiri River is shown in *Fig.5.3*. It is observed that the Brahmaputra basin SWAT (*Fig. 5.3a*) model provides the least satisfactory results as compared to the individual models for the Subansiri model (*Fig.5.3b,c*). For instance, the P-factor value during the calibration of the

main model is only 0.27 (Case-I) against 0.57 (Case-II) and 0.62 (Case-III). Similarly, the R^2 value during validation of the main model is only 0.65 (Case-I) against 0.75 (Case-II) and 0.80 (Case-III). So, it becomes clear that a separate SWAT model of the Subansiri river provides better results at 'Chowldhoaghat' than the results of the large Brahmaputra basin model at the same outlet.

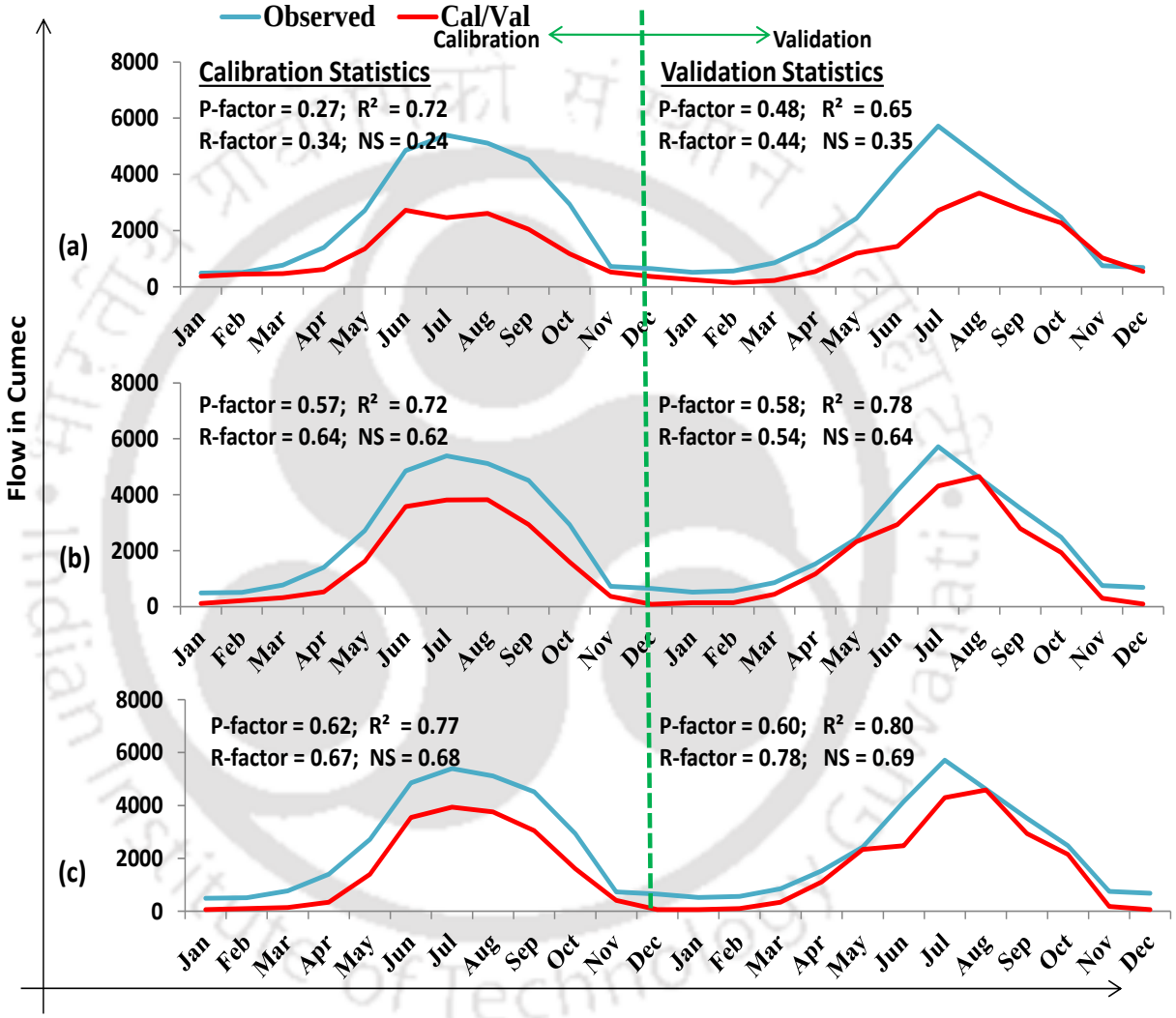

Fig. 5.3 Calibration (1993-2001) and Validation (2002-2005) results at Chowldhoaghat (Subansiri Basin): (a) *Case-I*: From multi-outlet calibration/validation results of the **Brahmaputra Basin model** using nine sensitive parameters; (b) *Case-II*: Single-outlet calibration/validation of the **Subansiri Basin model** using the same set of parameters and same magnitudes as Case-I; (c) *Case-III*: Single-outlet calibration/validation of the **Subansiri Basin model** using the different set of parameters than Case-I.

5.2.3 Discussions on Model results

It is observed from the result (*Fig. 5.2*, *Fig 5.3*) that the calibration/ validation statistics as obtained in Case-III were found fair as compared to the other two cases (Case-I/II). This is probably due to the fact the SWAT model tries to adjust more either on the main stem outlets or for the larger sub-watersheds during calibration. So, the outputs at smaller basins' outlets are compensated to a greater extent as compared to the large basins' outlets. However, the sub-watershed can be modeled to obtain good calibration as well as validation statistics as Case-III. This can be achieved by using different input datasets during the model simulation and calibration/validation. A small watershed possesses a relatively homogeneous characteristic as compared to a large watershed. As such, the hydrologic processes for the small watersheds are defined little differently than the large ones. For example, the snowmelt base temperature (*Table 5.1*) which was an important factor for calibrating the Brahmaputra basin model is not found suitable for the Dhansiri and Subansiri basin models.

5.3 Conclusion

The SWAT hydrologic model provides acceptable outputs at the drainage outlet of small and medium watersheds. Even it is capable of providing reasonably balanced outputs at various drainage outlets considered across a large basin. However, the model for large watershed provides an inferior output at outlets of sub-basins. This is because a small watershed possesses merely homogeneous characteristics, whereas a large watershed possesses heterogeneous characteristics. A hydrologic model for large watershed needed spatial calibration and validation to capture the spatial variability. On the other hand, one set of observed data is sufficient during the calibration and validation of a hydrologic model for a small watershed.

The model for large watershed becomes unable to accurately capture the hydrology of each sub-basin. However, a balanced output is provided by such model satisfying the spatial variability of all the sub-basins' characteristics. Therefore, a sub-basin needs to be modeled independently rather than deriving outputs at its outlets from the comprehensive large river basin model. However, the comprehensive basin model can be used as a tool for deriving

outputs at tributary outlets if modeling of the later is hard to exercise due to data scarcity situations.

The Brahmaputra River consists of as many as 278 numbers of tributaries and sub-tributaries within the Indian boundary (as per Central Ground Water Board) along with numerous streams along the China and Bangladesh portions. A hydrologic model established for the entire Brahmaputra basin comprehensively is not expected to provide acceptable results at all the tributary outlets. It is better to model the tributary basins independently if adequate and reliable input data are available. This information would help derive the parameters required for water resources management schemes.

######## ########

Chapter 6

Transboundary Effects

6.0 Introduction

The Brahmaputra is a transboundary river that flows through China, India, and Bangladesh. The Brahmaputra poses a huge challenge to the researchers, engineers, environmentalists, and policymakers to culminate the effective benefits while managing the water resources, due to its complexity in watershed characteristics. Another issue of having limited researches about this mighty basin is its transboundary nature. It is, therefore, the need of time to develop a comprehensive water management cooperation mechanism for water sharing between the basin sharing co-nations namely India, China, Bhutan, and Bangladesh. The status of water resources available from the Yarlung Tsangpo/Brahmaputra in the coming decades should be technically justified in a safe, equitable and sustainable manner without generating any sense of deprivation or unfairness in a win-win situation for the co-basin nations. Unfortunately, this basin has no comprehensive policy till date towards managing the water resources. It is, therefore, the results of the present SWAT model are analyzed to quantify the transboundary effects that may likely result from certain human induced reasons.

6.1 Transboundary issues

The Brahmaputra flows through three different countries (China, India, and Bangladesh), but its basin covers 'Bhutan' as the fourth nation. Interestingly, China occupies the majority (≈ 50%) of the basin area, followed by India (≈ 36%). This mighty river basin is characterized by wide spatial variations in topography, land cover, soil types, and weather components, etc. Hydrology changed upstream would surely impact along with the downstream. The Himalayan range is fed by glaciers which can melt at increased temperatures. The magnitudes of rainfall over the China portion of the basin are relatively

lower as compared to the other areas. So, an increased amount of precipitation there may lead to more chances of flood along with the downstream areas. The information on such kinds of natural events should be made available to the basin sharing co-nations so that they can undertake adequate measures against the probable seriousness caused by the upstream water.

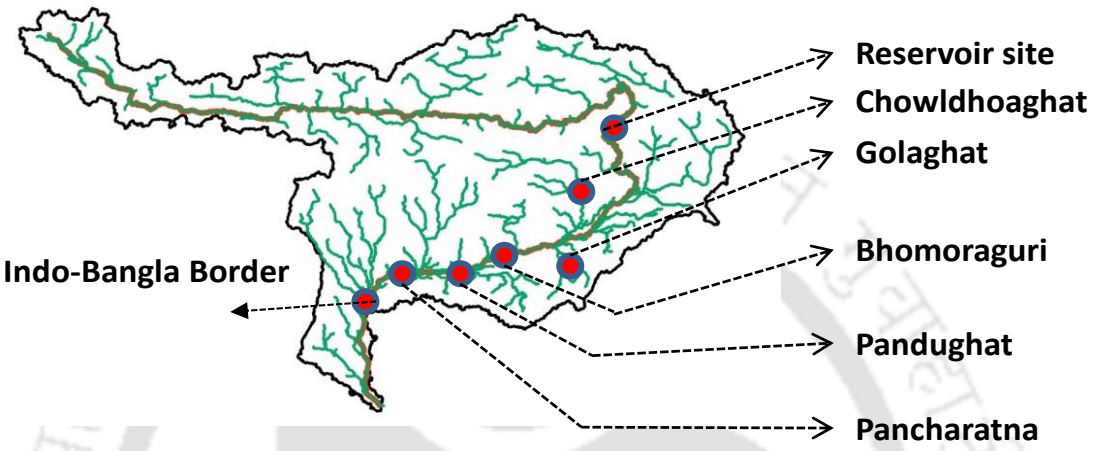

Fig. 6.1 Brahmaputra basin showing the salient locations for transboundary effect studies

The intensity of natural events if aided by certain man-made causes upstream would escalate the casualties along with the downstream areas. China has constructed several hydroelectric dam at the tributaries of the Brahmaputra. Besides, they have planned to construct four major hydroelectric dams including water diversion dam at the mainstem of the Brahmaputra (Alam et al., 2016). These structures would be utilized for deriving their own benefits only. For this, they may need to store a large amount of water, which would lead to scarcity of water along downstream. On the contrary, releasing water more than the natural flows of the river would cause floods at the downstream locations. India being the immediate downstream country is more vulnerable to these transboundary effects. As such, all the information relating to the natural and man-made events beyond the national boundary, if not obtained, India would surely face the problems by Brahmaputra water. Unfortunately, we are ignorant about any mutual understanding between India and China for hydro-climatological data exchange. However, hydrologic modelling can serve the purpose to some extent. The present analysis is forwarded as an attempt towards estimating

the transboundary effects of the mighty Brahmaputra river basin, in terms of impact of hypothetically assumed reservoir coupled with water diversion scenarios.

Table 6.1 Specifications of Reservoir

Sl No	Items	Specifications	Remarks
1	DAM height	116 m	*Assumed*
2	Elevation of bed level of Dam	1896 m above MSL	*Obtained from DEM*
3	Elevation of top-level of Dam	2012 m above MSL	----
4	Reservoir surface area	579 ha	*Estimated using DEM and for reservoir full condition*
5	Maximum water level	Same as Dam height	*Assumed*
6	Reservoir volume	291 Mm^3	*Obtained using Google earth*
7	Maximum water depth at reservoir site (without reservoir)	30 m during June month	*Obtained from SWAT model output*
8	Provision of Principal spillway	30 m below the Principal spillway (i.e. ht. of emergency spillway =81m)	*Assumed*
9	Provision of the Emergency spillway	5 m below the maximum water level (i.e. ht. of principal spillway =111m)	*Assumed*

6.2 Methodology

The hydrologic model established (*chapter 4*) in SWAT platform is re-run for different hypothetical scenarios of water diversion from a reservoir assumed at a location before the Brahmaputra just entering into India. Assuming reservoir height as 116 m above the base, the parameters like surface area (579 ha) and volume (291 Mm^3) corresponding to the reservoir full condition are estimated using the DEM. Water withdrawn from the reservoir will be diverted beyond the basin boundary and would no longer contribute to the stream again. This reservoir at 1896 m elevation is expected to significantly impact on the river discharges along with the downstream. *Table 6.1* describes the specifications of the hypothetical reservoir whereas *Table 6.2* describes the water diversion scenarios adopted in the present study.

Initially, the flow values at the selected reservoir location are ascertained from the final run of the SWAT model. Then, the SWAT model is run for each of the hypothetical withdrawal scenarios created, to assess the hydrological alterations along with the downstream locations. This enables us to have changed values of flows, at different locations of the lower riparian country (India) due to water withdrawal from the upper riparian country (China). The hydrologic alterations due to the impact of reservoir with considerations of certain water diversion scenarios are assessed in this chapter. Here, the changes in values of discharges, sediments etc. are assessed concerning the original condition (i.e. without reservoir), and they are presented in the following sections.

Table 6.2 Different scenarios for water diversion

Scenarios	Diversion	Reservoir specifications
Scenario-1	10% water diversion	*Same as Table 6.1*
Scenario-2	25% water diversion	
Scenario-3	50% water diversion	
Scenario-4	80% water diversion	

6.3 Results and discussions

6.3.1 Impacts on river flows

This section discusses the consequent impacts of reservoir on monthly as well as annual flow values along the downstream, at four main stem locations i.e. Bhomoraguri, Pandughat, Pancharatna and Indo-Bangla Border (*Fig. 6.1*), all within Indian boundary The reservoir impact is analyzed based on certain scenarios of water diverted from the hypothetical reservoir at the upper riparian country (China). The reservoir site is selected at a location just before the Brahmaputra river entering into India and its specifications are already listed in *Table 6.1*.

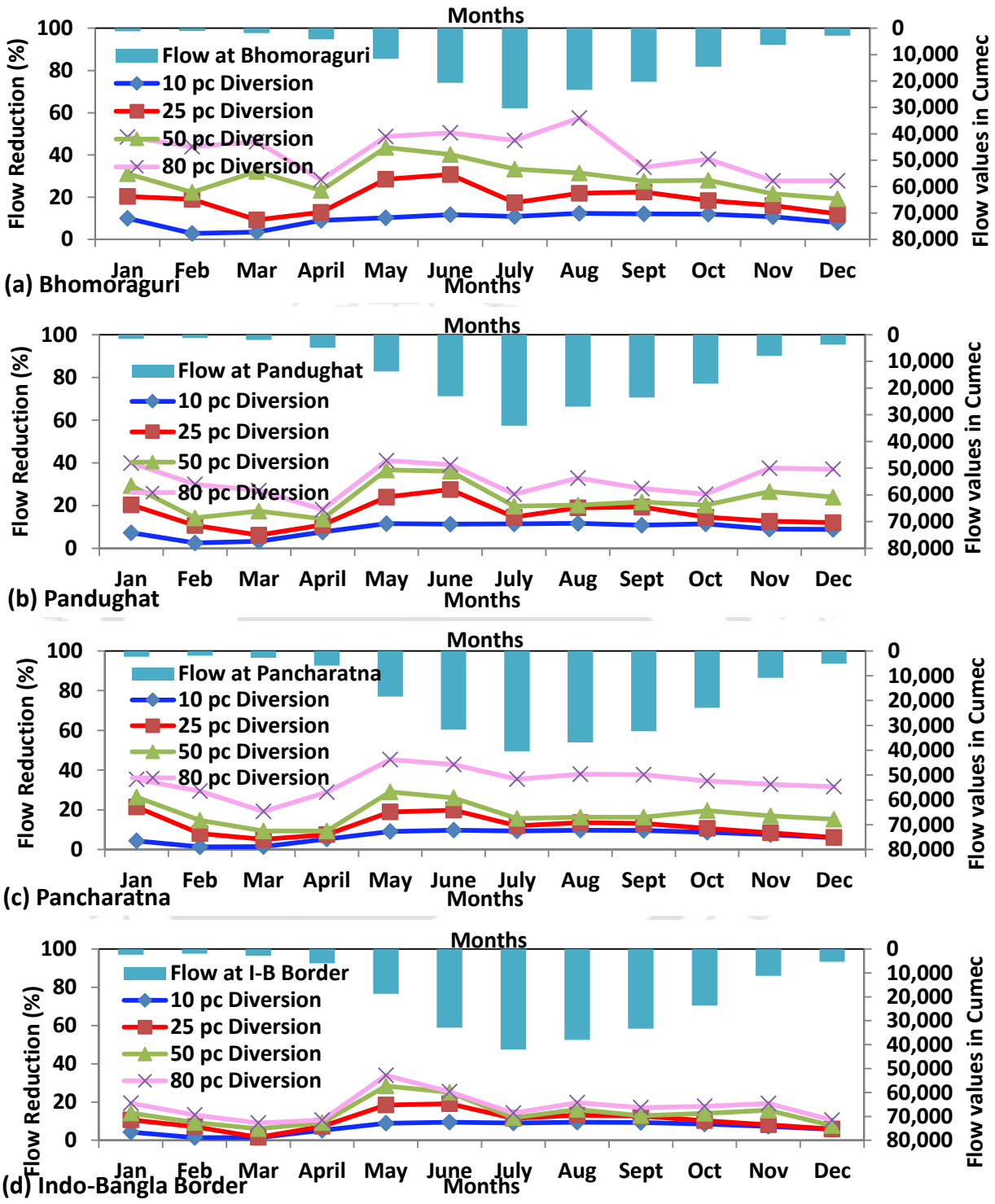

Fig. 6.2 Impact of reservoir showing flow reduction [%] at lower riparian country (India) from the reservoir at upper riparian country (China) for different diversion rates [10% (blue), 25% (red), 50% (green) and 80% (pink)]. The simulated flow values are shown in the secondary vertical axis for four downstream locations: (a) Bhomoraguri, (b) Pandughat, (c) Pancharatna and (d) Indo-Bangla border.

The SWAT model is run by using the weather data on a daily basis only, but it has a provision to have outputs based on daily, monthly and/or annually. Initially, the model established in *chapter 4* is re-run on a monthly basis, for both the conditions (i) without considering the reservoir and (ii) considering the reservoir. The changes in monthly flow values are presented in Sec.6.3.1.1. Similar conceptions were applied for assessing the impacts on the annual flows, and are presented in Sec.6.3.1.2.

6.3.1.1 Impact on monthly discharges

The month-wise percent reduction in flow values at the downstream locations of the reservoir site is shown in *Fig. 6.2*. This reduction is obtained from the hydrologic model (SWAT) run results with respect to water withdrawal at the rates of 10%, 25%, 50% and 80% of the values of simulated discharges (*Table 6.3*) at the reservoir site. The amount of the monthly flow values at all the four downstream locations are also shown in *Fig. 6.2*. The magnitude of reservoir impact is not constant throughout the year corresponding to a particular scenario of diversion. For example, flow at Bhomoraguri (*Fig. 6.2a*) reduces in the range between 2.89 – 12.35% corresponding to the 10% diversion scenario. Here, the minimum value (2.89%) stands during February whereas the maximum value (12.35%) stands during August month. Similarly, this reduction in flow values at the same location lies in the ranges like 3.80–30.72%, 16.09–43.50% and 18.79–60.00%, corresponding to 25%, 50% and 80% diversions respectively. It is obvious from the figure (*Fig. 6.2*) that the reservoir impact with higher rates of water withdrawal, in general, lead to higher rates of flow reduction at all the downstream points, with a little deviations. The results of the SWAT hydrologic model showed base flow taking longer duration (>31 days) to contribute to the main stem discharge. This contribution, especially during the lean period (December-April) is significant, thus the flow reduction happens at a lower rate during April in particular. However, the flow reduction during March at Bhomoraguri is quite significant (32.24% and 51.69%) corresponding to 50% and 80% water diversions respectively. This is due to the higher intensity of rainfall [*Fig. 6.3a*] surrounding the water withdrawal site (i.e. Indo-China Border). The higher amount of rainfall (>200mm) produces more runoff at this site. The amount of water withdrawal depends upon the runoff at the reservoir site.

Therefore, more amount of withdrawal from the reservoir leads to more reduction at the subsequent downstream locations.

Table 6.3 Flow values (simulated) at the reservoir site i.e. Indo-China Border. Here, figures represent the mean values of the SWAT model simulation results (1991-2005) on monthly basis.

Month	Flow in m^3/s
Jan	100.4
Feb	28.0
Mar	44.1
Apr	711.2
May	6878.2
Jun	8364.8
Jul	4920.1
Aug	4994.2
Sep	4266.0
Oct	2439.8
Nov	910.0
Dec	312.3

The flow reduction in April happens only 16.09% and 18.79% corresponding to 50% and 80% water withdrawal respectively. This is because the spatial variations in rainfall values across the basin impact the reduction percentages. During March-April, the areas starting from the immediate upstream location of the diversion site to the Bhomoraguri site experience more rainfall (101-200 mm) (*Fig. 6.3b,c*) than the other areas of the basin. As such, the actual flow production by the hydrologic model at the diversion site becomes relatively low. However, the flow production at Bhomoraguri is much higher since several tributaries that contribute to the mainstem discharges join the mainstem between this point and the reservoir site near Indo-China border. Therefore, the flow reductions at Bhomoraguri during that period are relatively less significant despite water withdrawal at the significant rates.

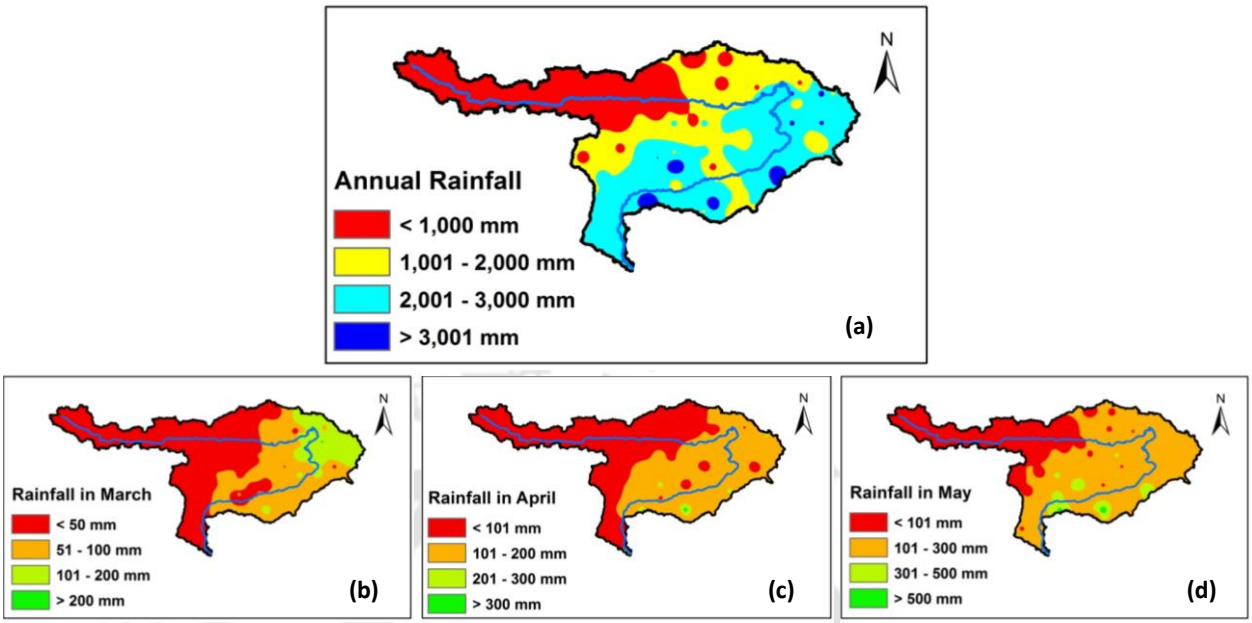

Fig. 6.3 Total rainfall over the Brahmaputra basin during (i) Annual [(a)] and (ii) Monthly [(b) March; (c) April; (d) May] basis. Here, annual (or monthly) rainfall values of one year are obtained by summing up the daily rainfall values during that particular year (or month). The final values for rainfall as shown in the above plots represent the average of all such values during the entire study period (1991-2012).

The monsoon season of the Brahmaputra basin starts in late April and continues till early July [*Fig. 6.3c,d*] in majority northern part of the basin which, however, starts a little late and continues upto August for other areas. As such, the flow reduction becomes maximum during May-June at all the downstream locations. Surprisingly, this reduction, in general, gets decreased during July-August (*Fig. 6.2*), due to the higher amount of rainfall causing more water contribution from the tributaries to the mainstem discharges. Moreover, the magnitudes of water reduction along the downstream locations decrease, due to several tributaries joining the mainstem and contributing to mainstem flow. The groundwater contribution may also be another aspect of having low values of reduction percentage along with the downstream points. Out of the four salient locations considered within the lower riparian country (India) for transboundary effect, Bhomoraguri, the nearest point from the diversion site is likely to experience the highest impact. On the other hand, Indo-Bangla (I-B) border, the farthest point from the diversion site is likely to have the least impact of reservoir. Here, the maximum monthly reduction in flow values stands only at 34%

corresponding to 80% diversion. Whereas the respective values at the other locations stand higher as 60% (Bhomoraguri), 42% (Pandughat) and 43% (Pancharatna). It is because several tributaries join the main stem between the diversion site and I-B border that contributes to the Brahmaputra discharges.

6.3.1.2 Impacts on annual discharges

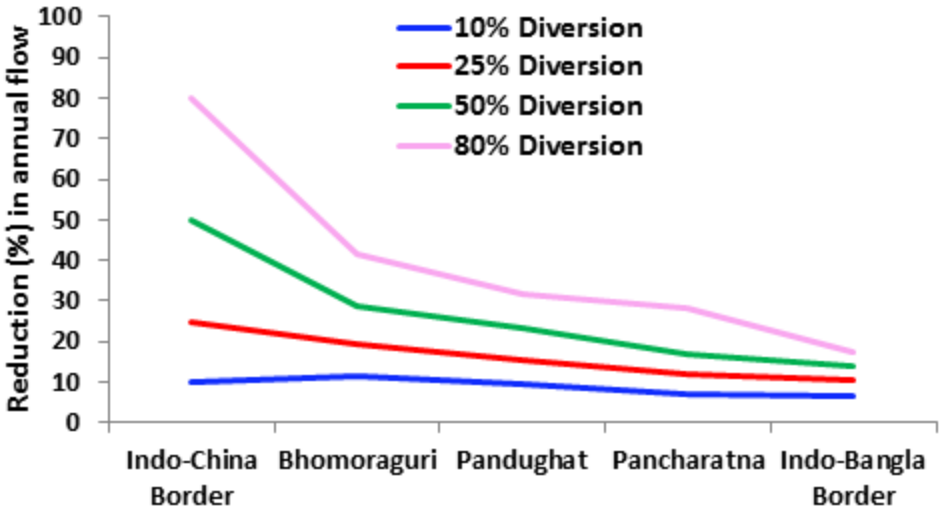

Fig. 6.4 Reduction [%] in annual flow values at (a) Bhomoraguri, (b) Pandughat, (c) Pancharatna and (d) Indo-Bangla border, due to reservoir with flow diversions at the rates of 10%, 25%, 50% and 80% from the reservoir site at Indo-China border.

Fig. 6.4 shows the trend of annual impact on the Brahmaputra river discharges at four downstream locations. The water reservoir impacts on the annual flows, for all kinds of scenarios of water diversion which describe decrease in flow values than the normal conditions of flow without reservoir. It is observed from *Fig. 6.4*, reservoir operations with 10% diversion leads to the flow reductions as 11.52% (Bhomoraguri), 9.65% (Pandughat), 6.85% (Pancharatna) and 6.66% (Indo-Bangla Border). A similar phenomenon is observed for the other rates of diversion. The immediate downstream location i.e. Bhomoraguri is likely to experience the highest decrease in annual discharge as 12%, 19%, 29%, and 42%,

resulting from 10%, 25%, 50%, and 80% withdrawal respectively. Whereas the respective values stand lower at the successive downstream locations. This is because several tributaries join the Brahmaputra river within India. The rainfall magnitudes in these tributary basins are relatively higher than the upstream locations. As such, flow production from these sub-basins significantly contributes to the river flows of the mainstem Brahmaputra. Moreover, the amount of groundwater contribution can't also be ignored to have greater flow values at the downstream locations, despite water withdrawal from the upstream points. It thus, the impact of reservoir with water diverted from a far upstream would have relatively less effect on the extreme downstream. Among all, the most downstream location i.e. I-B border is likely to suffer the least impact. This indicates that the impact of reservoir coupled with flow diversion reduces along the downstream.

6.3.2 Impact on water quality

A hydrologic model can provide location-specific hydrologic information across a river basin which may be utilized by the water resource managers for planning and designing of hydraulic structures. In the event of data scarcity situations like the Brahmaputra basin, these models only serve the purposes of obtaining the information regarding quantitative and qualitative assessment of river flows. Even, any made-made structure which would alter the hydrologic parameters along the downstream can promptly be ascertained by the application of hydrologic models. Following the quantitative assessment in the previous section (*Sec. 6.3.1*), the qualitative assessment on the lower riparian country due to water withdrawal at the upper riparian country has been addressed in this section, with special emphasis on sediment concentration.

Fig. 6.5 shows the alteration of sediment concentration at certain selected locations, due to consideration of reservoir. It is clear from this figure that the impact on sediment concentration is significant only during the high values of river flows (April-Oct). For example, the original values of sediment concentration in mg/L at Bhomoraguri during January, June, and December are 68.8, 219.8 and 99.9 respectively. While considered the effect of water reservoir, the respective values stand as 65.9, 171.4 and 95.3 mg/L corresponding to 80% water withdrawal. This means the reservoir has little impacts during the lean period (Nov-Mar). Infact, the river flow carries lesser amount of sediment during

the lean period. This is because the low water flow is incapable of producing much sediment from the watershed. Moreover, bank erosion during the high flood season is much significant adding more sediment to the river flows.

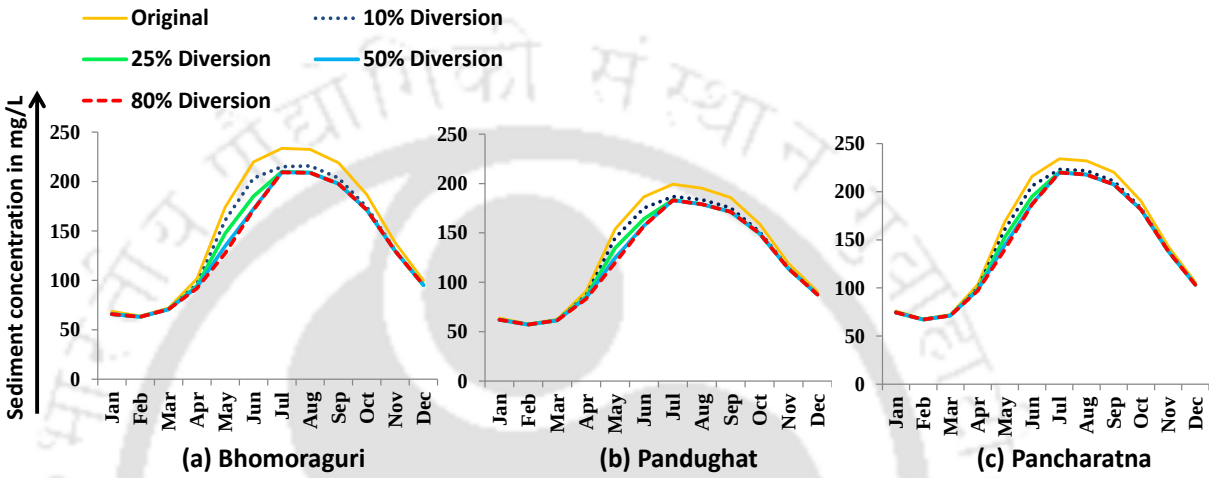

Fig. 6.5 Changes in sediment concentration at: (a) Bhomoraguri; (b) Pandughat; (c) Pancharatna due to water diversion at Indo-China border. Here, the average values of sediment concentration in mg/L are shown against each month of the year.

The maximum sediment concentration at Bhomoraguri and Pancharatna happens during July and the value is 234 mg/L, for both the locations. 'Bhomoraguri' is the nearest point from the reservoir site. As such, sediments would either be trapped or carried by the diverted-water leading to a decrease in sediment concentration at this point. However, this decrease is not significant at Pancharatna, the farthest point considered in this analysis. This is because the alluvial characteristics of the basin between Bhomoraguri and Pancharatna have greater sediment losses that contribute to the river flow at later point. Whereas, high values of sediment concentration may lead to loss of aquatic habitats, wetlands, and recreation attributes. Moreover, it becomes a concern for human health and erosion hazards. Some other water-quality parameters like nitrogen, phosphorous, nitrates, ammonium, dissolved oxygen, etc. can be assessed by the hydrologic models, even with due consideration of man-made structures. Based on the qualitative analyses for those

parameters, the processes and cost of treatment of water, if derived for water supply projects, can be ascertained.

6.4 Strategies for transboundary issues

The Brahmaputra basin lacks adequate hydro-climatological information required for developing a management plan of water resources. Especially the weather records and measured discharges are found insufficient to decide an action plan for management of the basin. As such, strategies to improve the data network system should be initiated to facilitate the water resource planners with adequate data in the forthcoming days.

The Brahmaputra River is the life line for many people living along its bank, especially India and Bangladesh. It has enormous potential towards water resources and hydropower generation. Although it is probably the least exploited basin and there is no comprehensive management policy for this basin till date, in context to India. Whereas developing management policy is based on rigorous analyses of the basin in terms of hydrology and hydraulics perspectives. These analyses for the transboundary Brahmaputra basin are quite challenging due to non-obtaining of required hydro-climatic data beyond the nation border. Even, we too faced lot of data challenges while establishing the hydrological model (*chapter 4*) in SWAT platform, which ultimately we could overcome by utilizing several global dataset and observed dataset from India and Tibet and could get reasonably acceptable outputs.

It is evident from the present analysis that there happens hydrological alteration at the downstream of inter-basin transfer project site. A water diversion dam if built at the land of upper riparian country (China) would impact on the hydrological behaviour of the lower riparian country (India). For example, 'Bhomoraguri', a location within India is likely to experience the decrease in annual discharge up to 42%, if a water storage cum diversion reservoir is considered at Indo-China border, a location before the Brahmaputra just enters into India. If China continues building large dams like the assumed one as in the present study, India would face huge deprivation of the natural resources. Therefore, the stake holders should initiate certain strategies of developing mutual cooperation among the basin sharing nations, for sharing information regarding physical, meteorological, and

hydrological characteristics of the basin. Especially, cooperation with the upper riparian country i.e. China which occupies the largest area (>50%) of the Brahmaputra basin is essentially needed for water resource management policy making in Indian context. The model can also be utilized by inserting reservoirs in different tributaries within one country (say India) to check the best possible cobminations that can help mitigating water problem of that country, in case upper repairian countries go for huge diversion for their need. Possible impacts on flow due to such reservoir insertion on downstream repairian country can also be investigated utilizing the model presented.

6.5 Conclusion

The Brahmaputra river possesses severe disasters in India resulting from floods and bank erosion. These natural phenomena are even likely to get escalated if the natural course is disturbed by constructing some barriers or reservoirs, especially along the upstream. The present study provides a sample example wherein India is likely to experience a water crisis due to the hypothetical diversion act by China. The Brahmaputra would flow at lower rates along the downstream if our assumption becomes into reality. Even the monthly, as well as annual flows, would significantly decrease at the Indo-Bangla border which is around 915 km downstream of the reservoir site. The impact of reservoir at this location stands up to -9.44%, -19.09%, -28.43% and -34% on monthly flow, corresponding to diversion at the rates of 10%, 25%, 50%, and 80% respectively. Water transfer from a single reservoir leads to such huge impacts which however may even become severe if diverted from multiple sites upstream. This information would provide a basis for management of the water resources. However, the scale of reservoir impact would vary if the assumptions were made differently. The structural parameters like reservoir volume, dam height, spillway height etc. if assumed different than the magnitudes taken in the present study would result in varying impacts. As such, an extensive study considering all possible pros and coins along with adoptations of reservoir operation policies are needed to accurately quantify the transboundary effects of the mighty Brahmaputra.

######### ########

Chapter 7

Climate Change Impact Analysis

7.0 Introduction

The variability of hydrological variables is being driven by changes in climate variables. The study of the impact of climate change on hydrological variables depends on projections of future climate provided by General Circulation Models (GCM). However, we hardly use GCM outputs directly because they produce error/biases due to their limited spatial resolution and various thermodynamic and climate system processes. Even in cases of Regional Climate Models (RCMs), where the climate is simulated by taking into account the regional characteristics of the area under investigation, there are observed biases between the simulation and the in-situ measurements (Lazoglou et al., 2019). Hence they cannot be used directly as input to any semi-distributed or lumped hydrological model. Otherwise, the error between the GCM output with respect to historical observations is often observed to be large (Ramirez-Villegas et al., 2013). Therefore, often these GCM models have to be downscaled to an appropriate, but higher resolution (Von Storch et al., 1993).

The issues of uncertainties of future climate data of various downscaled GCM outputs are not avoidable (Chen et al., 2011). Taking that into account along with other factors such as time constraints, human resources, and computational constraints, downscaling of GCM models is not a straight forward or simple task especially for the Brahmaputra basin with 69 gauge stations available in our hands. To tackle this problem, one approach may be to use the bias-correction and spatial interpolation methods in order to bring the GCM outputs close towards the observed climate variables of the Brahmaputra river basin.

There are a lot of uncertainties in atmosphere–ocean general circulation models (AOGCM). Different GCMs can simulate quite different regional changes, even under the same anthropogenic forcing scenario (Mukherjee et al., 2011) and it is very difficult to

ascertain which one of the AOGCMs are most reliable. As such, IPCC encourages ensemble of the GCMs for a comprehensive assessment of regional change projections. However, it is not guaranteed to have the best results of climate change analyses using ensemble of the GCMs which are poorly simulated for a specific region. Therefore, we selected certain GCMs based on their suitability for the Brahmaputra basin or its sub-basins, as identified in some previous researches (Mukherjee et al., 2011; Sarthi et al., 2016; Saharia and Sarma, 2018), and the availability of data for both the present and future periods. In this study, three GCMs namely GFDL_ESM2M, IPSL-CM5 and HadGEM-2CC were considered for the climate change analysis.

This chapter of the report describes in detail, about the climate change impact analysis over the Brahmaputra basin. The step-wise procedures for this analysis are:

Step1: Downloading GCM data

Step2: Interpolation of GCM data

Step3: Bias correction of GCM data

Step4: Evaluation of all GCMs

Step5: Trend analysis.

7.1 Methodology

Three GCMs of CMIP5 archive, viz. GFDL-ESM2M, HadGEM2-CC, and IPSL-CM5-1R are used in the present study. The grid size of each GCM is presented in *Table 7.1*. These GCMs were selected based on the availability of data for the present and the future period**.** These GCM data are freely available at https:// cmip-pcmdi.llnl.gov/cmip5/.

The historical data of GCM were downloaded for 15 years (1991-2005). Indeed, we used historical data upto 2005, because one of the weather datasets used in MODEL_6 (*Chapter 4*) is available upto that year only. On the contrary, GCM data for the future periods (2006-2099) were downloaded concerning two RCP (representative concentration pathways) scenarios namely RCP4.5 and RCP8.5. These two RCPs were chosen as they represent the complete range of impact, with RCP4.5, denotes the agreement of the community to lower the greenhouse gas emission, while RCP8.5 represents the business scenario with the highest possible emission.

Table 7.1 GCMs used in the present study

GCM	Grid	Archive
GFDL-ESM2M	$(2.02 \times 1.25)^0$	**Coupled Model Inter-comparison Project Phase -V (CMIP5)**
HadGEM2-CC	$(1.25 \times 1.875)^0$	
IPSL-CM5-LR	$(1.89 \times 3.75)^0$	

Initially, GCM data (for daily values of PCP, TMax, TMin) were downloaded for historical (1991-2005) and future (2006-2099) periods, and then interpolated to the nearest weather station. Thenafter, bias correction analyses are carried out by applying an appropriate method to obtain the bias correction factors. These factors were obtained by comparing the interpolated GCM data with the corresponding observed data during 1991-2005. Finally, the bias factors were applied to the interpolated values of GCM, for both the historical and future periods, to generate the bias-corrected GCM data (during 1991-2099) for the Brahmaputra basin.

Based on the bias-corrected values during 1991-2005, the performance of each GCM considered in this study is evaluated and compared to identify the best suitable GCM for the basin. Indeed, the GCM identified as the best would be forwarded for the climate studies during the future periods (2006-2099). This is done because climate change impact analysis for a large river basin with numerous gauge weather stations becomes computationally expensive. Moreover, the GCM replicating best for the present period is expected to represent the same even during the future periods too.

We considered 1991-2005 as historical and 2006-2099 as the future period. Since the period 2006-2019 has already been over, we carried out Man-Kendall and Sen's slope trend analysis for the remaining future period (i.e. 2020-2099) only. However, the bias-corrected data during the period 2006-2019 is used in certain analyses of climate change impact of the Brahmaputra basin. The detailed analyses of interpolation, bias correction, evaluation along with the climate change impacts on weather variables are described in the following sections of the current chapter. As well, the streamflow prediction of the Brahmaputra river is presented in the next chapter.

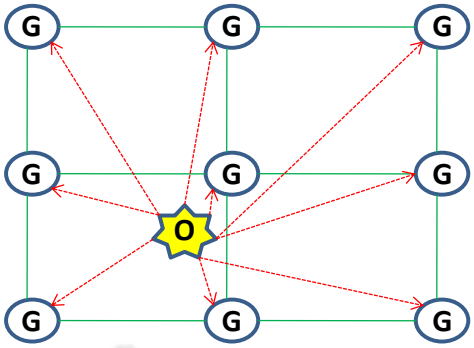

Fig. 7.1 Framework of Weather stations needed for Interpolation. Here, "G' refers to GCM station and 'O' refers to observed stations. GCM data at an observed station is derived by interpolating the data from 9 GCM stations surrounding to the observed station.

7.2 Interpolation of GCM data

Interpolation of climate data using different methods from the neighboring points to a required point has been carried by many people in the past. For instance, Yussouf & Stensrud (2006) employed Cressman scheme interpolating method to interpolate the 12 day mean bias value from neighboring points to a given station. Mohammadi et al. (2017) used inverse distance squared weighting and gradient inverse distance method to interpolate the data from the neighboring observations to any desired location. Using a similar concept, the climate variables viz. precipitation (PCP), maximum temperatures (TMax), and minimum temperatures (TMin) are interpolated from the neighboring available data points (*Fig. 7.1*) to the desired location and then corrected for bias. The biased corrected outputs are then used for future climate change impact studies.

The interpolated PCP, TMax, and TMin were obtained for all the three GCMs for the period 1991-2005. Out of 69 stations' observed dataset available with us, only 36 (*Table 7.2*) stations were found to remain at close proximity with the GCM coordinates. Hence, we adopted interpolation and subsequently bias correction corresponding to these 36 stations only. Knowing the coordinates of 36 stations (*Fig. 7.2b*) and that of different grids (*Fig. 7.2a*), the GCMs outputs were interpolated in order to obtain the GCMs' PCP, TMax, and TMin at each weather stations location. Although there are many sophisticated techniques for interpolating climate data such as Kriging (Hudson & Wackernagel, 1994; Hinge et al.,

2018), Thiessen polygons (Thiessen, 1911), Neural networks (Antonić et al., 2001), etc., all of these methods exhibit certain limitations too.

Table 7.2 Stations considered for Climate change study. These stations are among the 69 raingauges (as used in MODEL_6 in *Chapter 4*) having observed weather data.

Station Code	North Latitude	East Longitude		Station Code	North Latitude	East Longitude
S-1	30.44	82.81		S-19	29.09	87.6
S-2	30.44	83.44		S-20	29.66	91.11
S-3	29.82	84.38		S-21	29.03	91.67
S-4	29.41	85.84		S-22	29.87	95.76
S-5	29.82	89.06		S-23	26.5	91.5
S-6	29.82	93.13		S-24	26.5	92.5
S-7	28.3	91.06		S-25	26.5	93.5
S-8	26.7	95		S-26	27.5	90.5
S-9	25.76	92.81		S-27	27.5	91.92
S-10	25.76	90.63		S-28	27.5	93.5
S-11	24.82	88.75		S-29	27.5	95.5
S-12	24.82	89.38		S-30	28.5	94.5
S-13	27.32	88.44		S-31	28.5	96.5
S-14	26.8	89.36		S-32	30.75	92.19
S-15	27.01	92.81		S-33	30.44	94.69
S-16	28.57	89.69		S-34	29.51	96.88
S-17	28.88	88.75		S-35	28.5	92.5
S-18	29.82	82.81		S-36	28.5	95.5

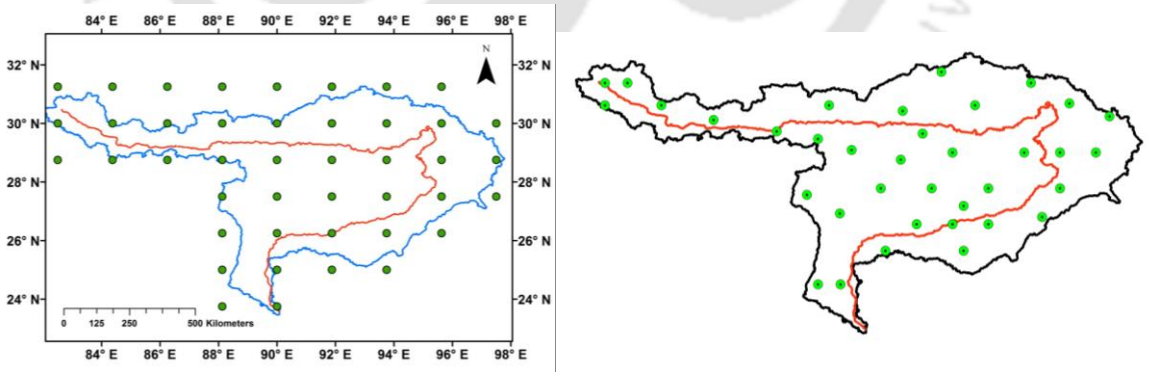

Fig. 7.2 Weather stations: (a) GCM coordinates (HadGEM2-CC); (b) Observed weather stations considered for climate change studies. These 36 stations remain at close proximity to the GCM coordinates. Interpolation and Bias correction of GCM outputs are done corresponding to these 36 stations only.

In the present study, we used the Inverse Distance Weighted Average interpolation (IDWA), the most widely adopted method, which assumes that the effect of neighboring points on the desired interpolated point solely depends on the inverse of the distance between the neighboring points and the desired location. The IDWA method is given by the equation (*Eq 7.1*) as follows:

$$V_f = \frac{\sum_{i=1}^{n} \frac{1}{d_i^2} V_i}{\sum_{i=1}^{n} 1/{d_i}^2} \qquad \text{(Eq. 7.1)}$$

Where, V_f is the interpolated value required at the station, V_i is the data at grid point i, d_i is the distance of i from the station, n is the number of points. Here, for each weather station we choose 9 neighboring GCM points (*Fig. 7.1*), each with a weight depends on its linear distance to the weather station in inverse proportions.

7.3 Bias correction

Climate projections are run at coarse spatial resolution. These models are based on physical laws such as conservation of energy, mass and momentum, thermodynamic and radiation laws. However, these models will neither resolve nor represent all relevant processes from planetary waves down to turbulence. Sub-grid processes are simplified by parameterizations. As a consequence, many relevant atmospheric, oceanic and coupled processes are not realistically represented, with knock-on effects on other processes even far away from where the primary biases occur. In short, climate model biases are severe enough to justify the use of bias correction techniques to render model output more useful for impact studies. GCM outputs should therefore be bias corrected and downscaled to local scales. In the present analysis, Bias correction was carried out, whereas no Downscaling was adopted because of:

- Large number of GCM points fall within the Brahmaputra basin (~25 nos.).
- As many as 9 GCM points are almost concentric to Observed station.
- Every GCM point remains at close proximity (~10-50 km) to a certain Observed station.
- Spatial variability is considered by applying IDW (Inverse Distance Weighing) method.

- Downscaling approach would be computationally expensive for 69 weather stations.

7.3.1 Bias Correction Methods

There are various methods for bias correction. Some of them are:

1. Linear scaling method
2. Delta change method
3. Quantile mapping method.

In the present analysis, we have adopted the Linear scaling approach.

7.3.1.1 Linear Scaling Method

Linear scaling method (Teutschbein & Seibert, 2013; Shrestha et al., 2017) was employed for bias correction of interpolated GCM outputs (i.e. PCP, TMax, and TMin). This method is based on the difference between monthly observed and raw GCM values. These differences are then applied to simulated climate data to obtain bias corrected climate variables.

Bias correction factor = $M_O - M_G$ (Eq. 7.2)

Where, M_O = Monthly mean observed for a particular month

M_G = Monthly mean raw GCM data for the same month as M_O

Additive correction is used for temperature and *multiplicative correction* is used for precipitation as defined by Hempel et al. (2013). Additive correction is used for temperature so as to ensure that absolute changes (whether positive or negative) are not modified, however precipitation being a non-negative parameter, a multiplicative correction is applied so as to make sure that the corrected data are non-negative in nature. The following equation as defined by Shrestha et al., (2017) were used for Linear scaling correction:

$$P_h(d)^b = P_h(d) * [\mu_m * P_{obs}(d) / \mu_m * P_h(d)] \quad \text{(Eq. 7.3)}$$

$$P_{rwf}(d)^b = P_{rwf}(d) * [\mu_m * P_{obs}(d) / \mu_m * P_h(d)] \quad \text{(Eq. 7.4)}$$

$$T_h(d)^b = T_h(d) + [\mu_m * T_{obs}(d) - \mu_m * T_h(d)] \quad \text{(Eq. 7.5)}$$

$$T_{rwf}(d)^b = T_{rwf}(d) + [\mu_m * T_{obs}(d) - \mu_m * T_h(d)] \quad \text{(Eq. 7.6)}$$

Here 'P' refers to precipitation, 'T' for temperature, 'd' refers to daily, 'μ'$_m$ refers to the long term monthly mean, superscript letter 'b' refers to bias-corrected, 'h' refers to historical raw GCM data, 'obs' refers to observed data and 'rwf' is the raw GCM future data.

7.3.2 Bias Correction results and discussion

7.3.2.1 Results on Bias correction factors

Initially, the bias correction factors on monthly basis are calculated using *Eq. 7.2*. These factors are different for different GCMs, and for different stations. An example is shown in the *Table 7.3*, indicating the values of bias correction factors. Similar factors are obtained for the weather variables at all other stations, and corresponding to all three GCMs. Here, the correction factors on monthly basis are assumed to remain constant over the present as well as the future periods. Later, these factor are applied to the raw GCM outputs by using the respective Equations (*Eqs. 7.3-7.6*), in order to obtain the bias-corrected daily outputs at a station. Finally these corrected data are utilized in climate change studies of the basin.

Table 7.3 Month-wise Bias correction factors for GCM variables at Station S1

For: Station Code: S1									
	GFDL-ESM2M			HadGEM2-CC			IPSL-CM5-LR		
Mon	PCP	Tmx	Tmn	PCP	Tmx	Tmn	PCP	Tmx	Tmn
1	1.26	-3.84	-9.53	4.74	-5.50	-10.01	0.45	-3.31	-6.17
2	1.06	-3.98	-9.02	5.06	-6.21	-9.59	1.14	-2.99	-3.44
3	0.92	-3.58	-8.20	2.44	-6.83	-10.22	0.74	-1.31	-1.76
4	0.66	-5.65	-9.87	0.97	-8.79	-12.30	0.69	-1.32	-1.28
5	0.70	-5.91	-6.73	0.37	-8.53	-11.20	0.63	0.05	0.77
6	0.50	-4.08	-4.02	0.25	-6.49	-9.06	1.30	2.18	3.53
7	0.44	-0.65	-3.29	0.33	-2.39	-6.37	4.73	-0.90	0.99
8	0.45	-0.82	-2.95	0.49	-4.02	-5.88	0.99	-3.37	-2.38
9	0.22	-1.41	-3.99	0.83	-5.83	-6.25	0.35	-2.18	-2.73
10	0.15	-3.27	-7.67	0.38	-5.62	-10.09	0.14	-1.82	-3.88
11	0.32	-2.21	-7.78	0.63	-5.40	-10.70	0.11	-0.50	-3.98
12	0.62	-1.35	-6.86	1.61	-3.95	-9.04	0.15	-0.97	-4.49

The raw as well as bias corrected GCM daily data are compared with the observed daily data and their differences can be observed from the figure (*Fig. 7.3*). This figure is shown for only two variables (PCP, TMax) corresponding to a particular weather station (S1) and for one year (1991) only, as for example. Similar observations can be viewed for the other stations' datasets and for all other variables pertaining to the entire period (1991-2005) of bias correction studies

7.3.2.2 Results on daily outputs

.

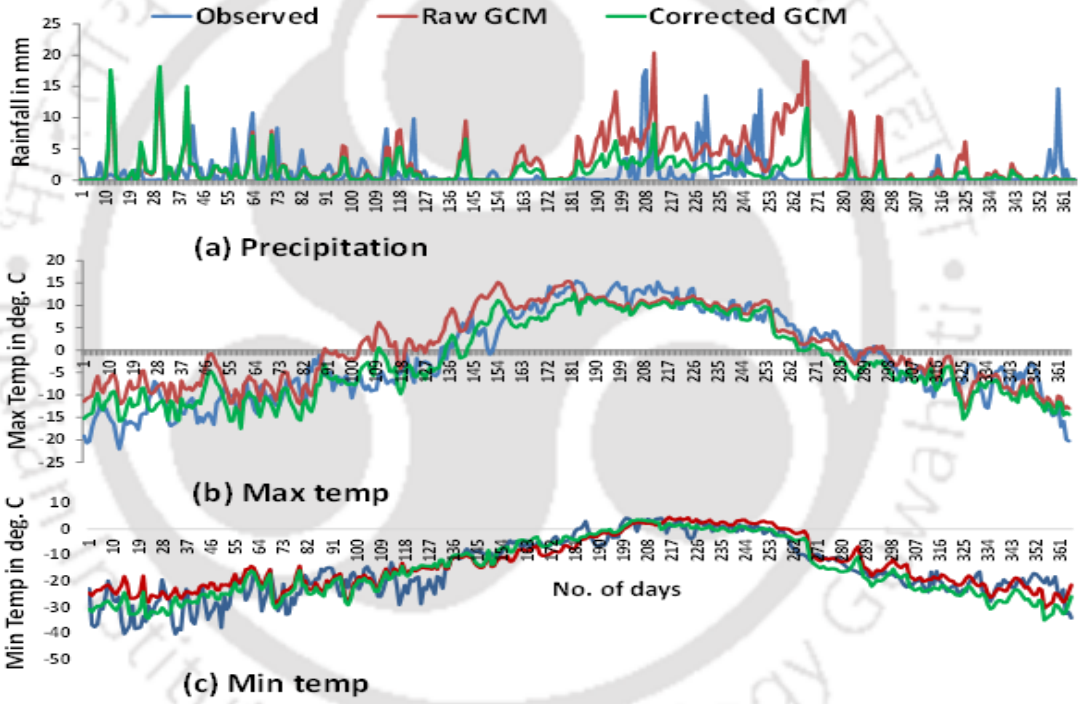

Fig. 7.3 Values of Bias corrected GCMs [for IPSL-CM5-LR] with respect to Observed data for one year (1991) only, at a station (S1) for (a) Precipitation (top) and (b) Maximum temperature (bottom) and (c) Minimum temperature (bottom).

It is well understood that the bias correction methods can't completely remove the model biases. However, the raw data are brought close towards the actual observations, after correcting them for biases. This is evident from the *Fig. 7.3* that while correcting for bias, the raw GCM data points which showed wide disagreement with the observed ones became

closer to the later. Even few points, especially during 90-150 days of the year, the bias-corrected values are almost concentric to the observed values. So, bias correction provides the reasonably acceptable outputs of the GCM, similar to the observed values and they might further be utilized for climate change studies of an area.

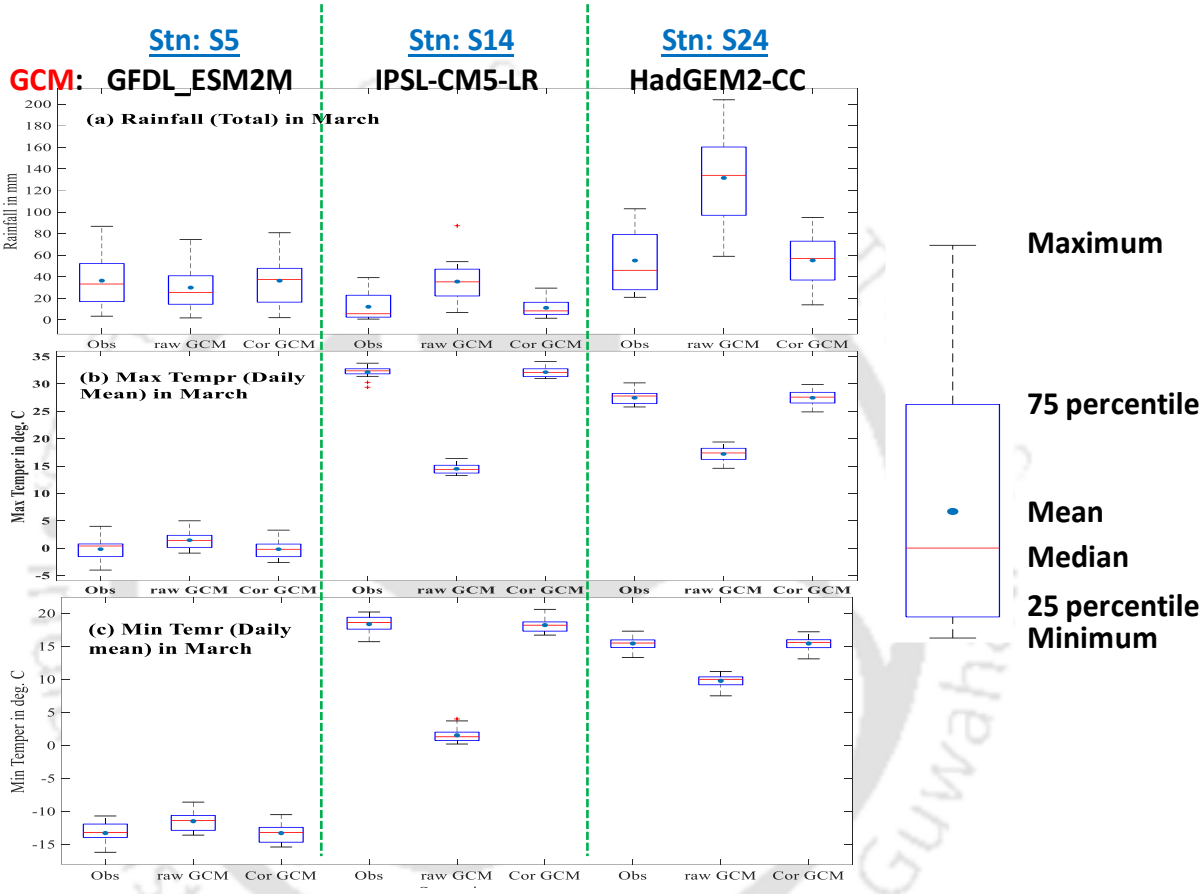

Fig. 7.4 Box plot for monthly mean values of Rainfall (top row), maximum temperature (middle row) and minimum temperature (bottom row) at certain salient stations selected on random basis. Here, the GCM outputs are shown at stations: S5 (for GFDL-ESM2M). S14 (for IPSL-CM5-LR) and S24 (for HadGEM2-CC) for the month of March only.

7.3.2.3 Results on monthly outputs

Linear scaling method of bias correction is based on the long monthly average values of the weather data series. This means bias correction factors are calculated on the basis of long monthly average of both raw GCM and observed data. Subsequently, they are applied to the daily outputs (raw) of GCM, in order to obtain the corrected daily values. As such,

the daily values of corrected GCM are not expected to remain at very close magnitudes of the actual observations on point to point basis, but the monthly mean values of the corrected GCM coincides exactly the observed datasets. And this is evident from the figure (*Fig. 7.4*) as for example. Rainfall being non-negative parameter, multiplicative correction is applied to them. On the other hand, additive correction were applied to the temperature data to ensuring absolute changes are not modified. Therefore, the total rainfall in a month remains exactly same for both the corrected GCM and the observed data sets. For example, the total rainfall corresponding to the corrected GCM (GFDL-ESM2M) during March at station S5 is 36 mm that is exactly same in magnitudes as the observed rainfall during the same month. Similar results at the same locations are observed for TMax ($+0.48^0$C) and TMin (-12.9^0C) of GFDL-ESM2M, during the same month.

The daily mean maximum temperature at station S24 is 27^0 Celsius pertaining to bias corrected HadGEM-2CC data that is exactly same in magnitudes to the value of observed maximum temperature during March. A similar observation can be noticed for other months at all other stations, and for all the GCMs. It therefore becomes more judicious to adopt the climate change studies on monthly basis rather than on the daily basis.

7.3.3 Remarks on Bias correction analysis

In this analysis, we adopted Linear scaling method for correcting the GCM biases. Although each approach has its advantages and limitations over the other, we found this method more suitable for simplicity. It is clear that none of the bias correction methods completely remove the model biases. However, the raw GCM outputs are brought to closer in magnitudes of the actually observed values at ground. Moreover, the corrected GCM outputs are not possible to match the observed ones at point to point scale. This is because Linear scaling method is based on the long term monthly mean values. As such, the monthly mean values of the corrected GCM values become exactly same as the corresponding observed values. It is therefore, the monthly values provide better results for climate change studies as compared to the daily values.

7.4 Uncertainty analysis: Evaluation of GCMs

Climate change studies are generally forwarded by taking the outputs from several GCMs. The present study considers three GCMs for computation of interpolation followed by the bias correction based on their historical (1991-2005) records. However, managing the GCM data and it's processing to make them use for both the present and future climate change studies are computationally very expensive. It becomes more tedious for the large Brahmaputra river basin considering numerous gauge weather stations. Therefore, the present climate change study for the future periods (2006-2099) is intended to forward by utilizing the outputs of a GCM identified as the best among the selected GCMs. This section describes the evaluations of the performances of all GCMs based on the historical (corrected) records, and to identify one GCM that best replicates the observed weather records. It is assumed that the GCM identified best suitable for the historical records would reflect the same for the future periods too. The most suitable GCM so selected would be considered for the future climate change studies. The most suitable GCM so selected would be considered for the future climate change studies including likely impact on the Brahmaputra basin.

7.4.1 Methods of evaluation

The ability of the GCMs to simulate the historical PCP, TMax and TMin values can be assessed using a different type of evaluation measure. However, no individual measure is considered superior to the other, instead combined use of different measures can provide a comprehensive assessment of the model performance (Flato et al., 2014). For this study, the output of the three GCMs model is compared with the observed data using statistical measures defined by World Meteorological Organization (WMO) and by comparing SWAT application with the GCMs model output and with the observed data. These statistical measures include root mean square error (RMSE) [*Eq. 7.7*] and Nash-Sutcliff efficiency (NSE) [*Eq. 7.8*] and correlation coefficient [*Eq. 7.9*].

$$RMSE = \sqrt{\frac{1}{N}\sum_{i=1}^{N}(S_i - O_i)^2} \qquad \text{(Eq. 7.7)}$$

$$NSE = 1 - \left(\frac{\sum_{i=1}^{n} (O_i - S_i)^2}{\sum_{i=1}^{n} (O_i - \bar{O})^2} \right) \quad \text{(Eq. 7.8)}$$

$$R^2 = \left(\frac{\sum_{i=1}^{n} (O_i - \bar{O})(S_i - \bar{S})}{\sqrt{\sum_{i=1}^{n} (O_i - \bar{O})^2} \sqrt{\sum_{i=1}^{n} (S_i - \bar{S})^2}} \right)^2 \quad \text{(Eq. 7.9)}$$

Here 'S' and 'O' refers to the simulated (i.e. model generated) and observed values, $\bar{O}$ and $\bar{S}$ are the mean of observed and model-generated data series, 'i' denotes the simulated and observed pairs and 'N' refers to the total number of such pairs.

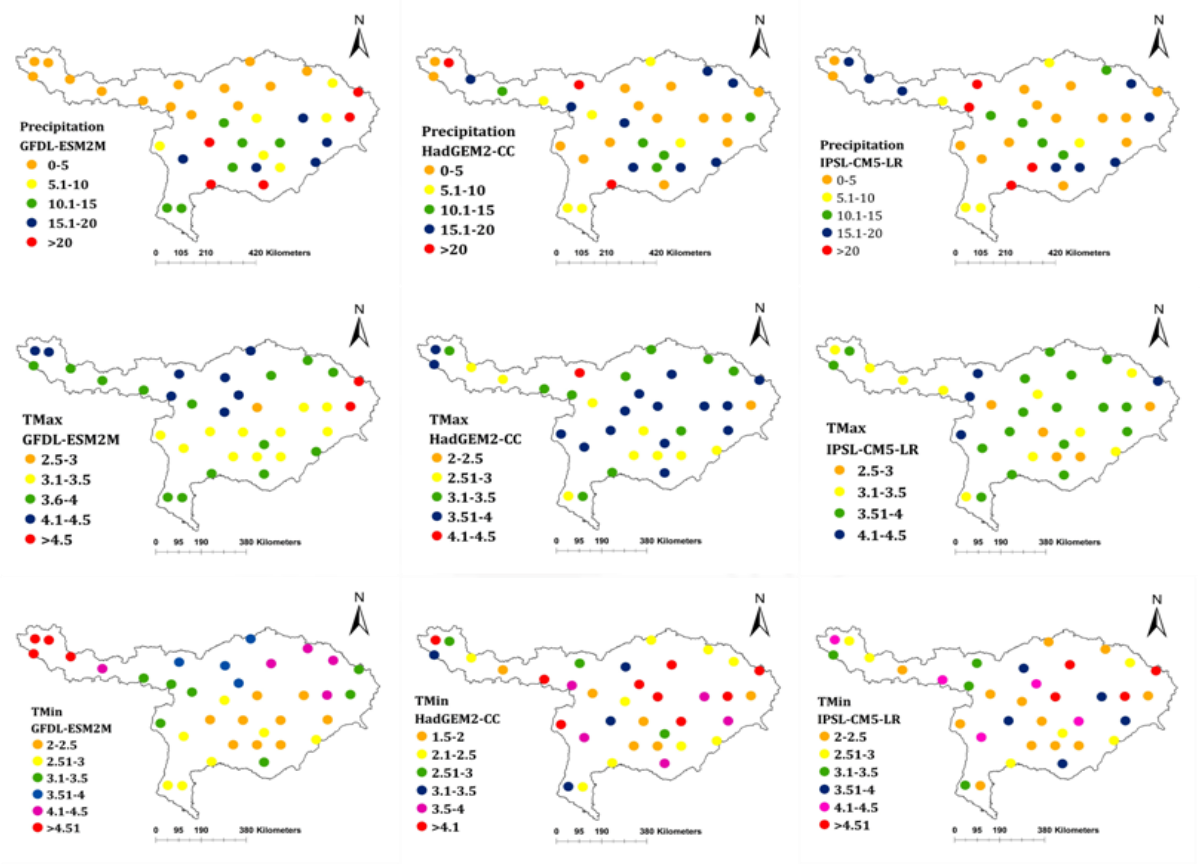

Fig. 7.5 RMSE of the GCMs in simulating precipitation (mm/day) [first row], maximum temperature (°C) [second row] and minimum temperature (°C) [third row] at different stations of the Brahmaputra Basin. Different columns refer to different GCMs.

7.4.2 GCM evaluation results and discussions

In the present study, the comparison of the bias corrected GCM outputs are presented by applying two statistical measures like RMSE and NSE as well as SWAT model run results. The data series of all GCMs and the observed records on daily basis corresponding to each weather station are utilized for calculation of the RMSE and NSE. These computations for each weather variables, and at each station, and even for all the three GCMs are found difficult for presentation. As such, they are shown in GIS plot (*Fig. 7.5*) and Tabular form (*Table 7.4*) in order to add more clarity and simplicity in presentation.

7.4.2.1 Spatial distribution of RMSE

The root mean square error obtained using *Eq 7.7* is used to evaluate how well the three GCMs can simulate the long term (1991-2005) daily PCP, TMax, and TMin over the 36 stations of the basin. The first, the second, and the third rows of *Fig. 7.5* present the RMSE in PCP, TMax, and TMin respectively, at 36 stations.

Fig. 7.5 shows that GFDL-ESM2M, HadGEM2-CC, and IPSL-CM5-1R simulate rainfall with error in the range of 1-20 mm/day or even more in some stations. The GFDL-ESM2M simulations had errors up to 5 mm/day in the northern region. In the southern and eastern regions, five stations had maximum errors (RMSE>20). The HadGEM2-CC had error values ranging from 0 to 20, but as compared to GFDL-ESM2M, there were lesser number of stations falling under RMSE > 20 mm/day. It can be seen from *Fig. 7.5* that most of the stations had errors within 0 to 5 mm/day range. In the case of IPSL-CM5-1R, the error rates were higher in the northern and southeastern regions (>15 mm/day). On the other hand, the central region had errors within 0 to 15 mm/day.

The GCMs were tested for their ability to replicate historical records of temperatures and maximum and minimum temperatures. The RMSE produced by GFDL-ESM2M ranges from 3.6 to 4.5 in the northern region, whereas the errors are comparatively less in the central region. This error was found maximum in two stations located at the extreme east. In the case of HadGEM2-CC, more errors were prevalent in the central region with the RMSE range of 3.1 to 4. The IPSL-CM5-1R performs well in simulating TMax with a lesser number of stations showing 4.1 – 4.5 range of RMSE. Most of the stations show RMSE under a value of 4. In the simulation of TMin, the GFDL-ESM2M shows the highest

error in the most upstream part of the basin (>4.5). The central region was able to capture the observed values within RMSE values of 2 to 3 whereas the RMSE was higher in the northeast region of the basin. For HadGEM2-CC model, many stations have RMSE > 4.1 as compared to the other two GCMs. The stations located in the central regions show higher error rates. In the case of IPSL-CM5-1R, only four stations were found with RMSE > 4.5. The majority of the stations have RMSE within 2 to 3 and few stations scattered in the RMSE range of 4.5-4.5. Thus, the spatial variability of the RMSE at each weather station considered across the large Brahmaputra river basin is much significant, thereby leads to difficulty in culminating the performance of GCMs. Therefore, the results of RMSE as well as the NSE values are summarized in *Table 7.4*.

Table 7.4 Root mean square error (RMSE) and Nash-Sutcliff efficiency (NSE) of precipitation (mm/day), maximum temperature (°C) and minimum temperature (°C) evaluated on three GCMs. **The best-fitted GCM values are displayed in bold.**

Variable	GCM	Indices	Mean	Standard Deviation	Max.	Min.	Median	1st Quartile	3rd Quartile
Precipitation	GFDL-ESM2M	RMSE	10.08	7.19	23.38	1.44	7.45	3.83	15.26
		NSE	-0.16	0.21	0.04	-0.87	-0.11	-0.20	-0.02
	HadGEM2-CC	RMSE	**9.81**	**7.17**	24.29	1.39	7.26	3.28	15.37
		NSE	**-0.04**	**0.11**	0.17	-0.34	0	-0.09	0.02
	IPSL-CM5-LR	RMSE	10.64	7.52	26.15	1.49	7.48	4.01	15.96
		NSE	-0.27	0.24	0.09	-0.89	-0.21	-0.40	-0.09
Max. Temp. (TMax)	GFDL-ESM2M	RMSE	3.75	0.47	4.65	2.78	3.81	3.39	4.07
		NSE	0.48	0.25	0.80	0.05	0.49	0.25	0.70
	HadGEM2-CC	RMSE	**3.33**	**0.39**	4.05	2.47	3.41	2.97	3.81
		NSE	**0.46**	**0.16**	0.83	0.29	0.58	0.46	0.74
	IPSL-CM5-LR	RMSE	3.54	0.39	4.11	2.84	3.63	3.22	3.85
		NSE	0.55	0.22	0.81	0.15	0.56	0.34	0.75
Min. Temp. (TMin)	GFDL-ESM2M	RMSE	3.38	**0.99**	5.80	2.28	3.17	2.55	3.96
		NSE	0.78	0.06	0.86	0.51	0.80	0.77	0.82
	HadGEM2-CC	RMSE	**3.36**	1.08	5.32	1.84	2.93	2.23	4.06
		NSE	**0.75**	**0.04**	0.88	0.69	0.83	0.81	0.85
	IPSL-CM5-LR	RMSE	3.26	1.06	6.03	2.07	3.08	2.45	3.93
		NSE	0.78	0.17	0.86	-0.19	0.81	0.80	0.83

7.4.2.2 Analysis of RMSE and NSE

While the analysis of RMSE gives an idea about the performance of each GCM compared to the recorded climate data in a particular station, the information needs to be further scrutinized to select the most accurate GCM. The average RMSE and NSE were calculated for each GCM for PCP, TMax, and TMin to determine the GCM which gives the best performance. The spatial distribution of RMSE has been shown in *Fig. 7.5* which clearly indicates a wide variation in the RMSE values. A similar variation was observed in NSE values of bias corrected GCM variables with respect to space. The results of the analysis are given in *Table 7.4* with the best results highlighted in bold letters. It can be seen from this table that the HadGEM2-CC performed better than the other two models in simulating mean PCP with RMSE of 9.81 and NSE of -0.04. These values stand minimum than the corresponding mean values of the other two GCMs, thus signifying better resemblance with the observed data. Likewise, in TMax and TMin as well, the HadGEM2-CC outperformed GFDL-ESM2M and IPSL-CM5-LR. Thus, the outputs (i.e. interpolated and bias-corrected values) of HadGEM2-CC are found to best replicate the observed weather records across the Brahmaputra basin. Therefore this GCM (HadGEM2-CC) only would be forwarded for the climate impact studies of the present study area.

Table 7.5 Coefficient of correlation (R^2) values between the SWAT model outputs using the bias corrected GCM variables and the observed discharge values at three outlet locations where observed data are available. **The best-fitted GCM values are display in bold.**

Location	R^2 Values for the outputs of bias corrected GCM-fed SWAT model run			R^2 values during multi-site calibration of the default SWAT model
	GCM			
	GFDL-ESM2M	**HadGEM2-CC**	IPSL-CM5-LR	
Bhomoraguri	0.81	**0.85**	0.61	0.86
Pandughat	**0.86**	0.84	0.61	0.84
Pancharatna	0.79	**0.80**	0.46	0.91

7.4.2.3 Analysis of SWAT model outputs

To evaluate the performance of each GCM in hydrological simulations, the SWAT model was set up for the study area using ArcSWAT under ArcGIS 10.4 software interface and run using the bias-corrected historical climate forcing data of the three GCMs. The climate variables used were the PCP, TMax, and TMin, which are essential for running the SWAT model. The output hydrograph (*Fig. 7.6*) obtained at Bhomoraguri, Pandughat, and Pancharatna using the bias-corrected GCM variables were compared to the measured monthly average discharge (*Table 7.5*) using the coefficient of determination for performance evaluation.

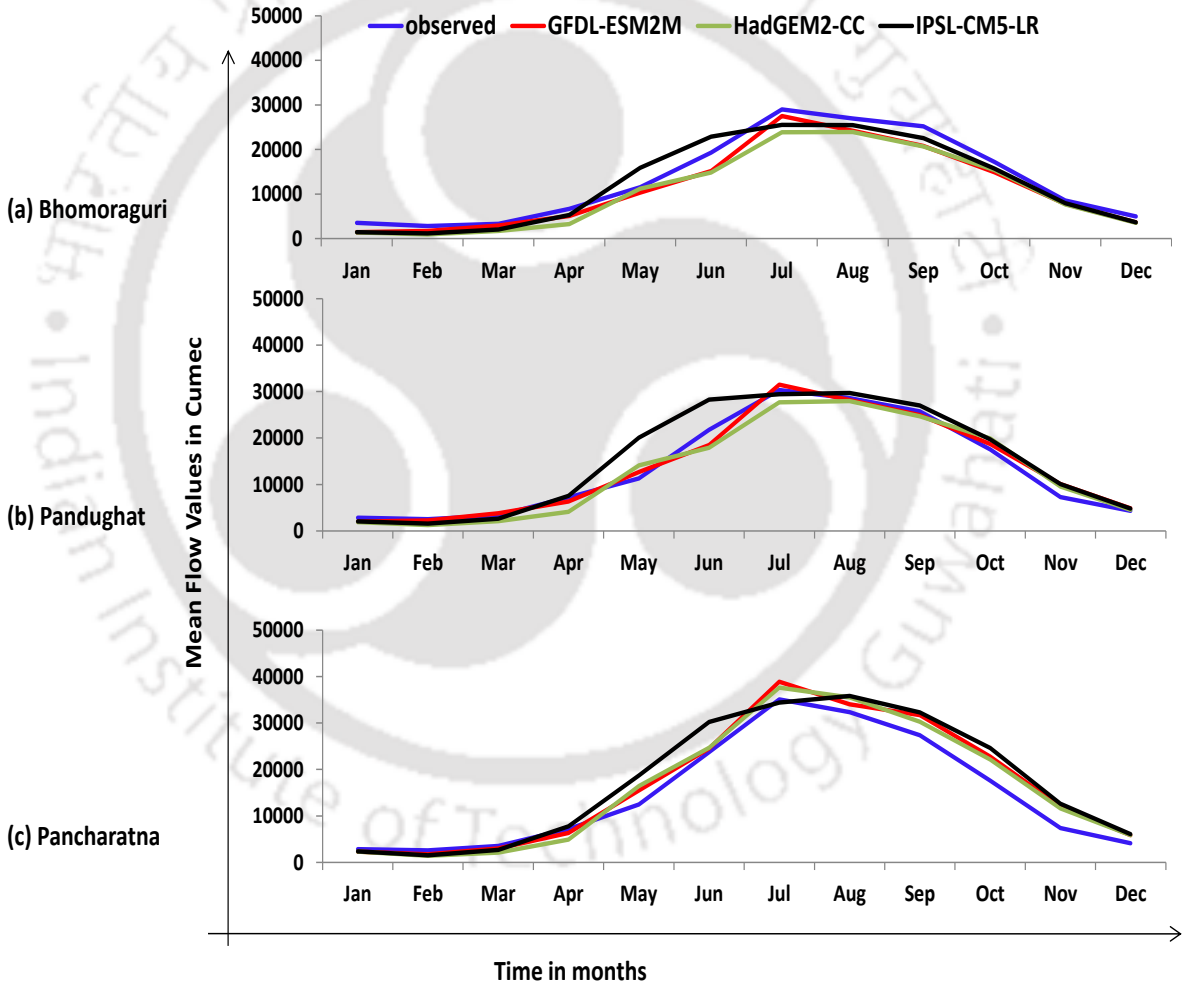

Fig. 7.6 Comparison of SWAT model simulation (1991-2005) results using observed and bias-corrected GCM data at three outlets: (a) Bhomoraguri; (b) Pandughat; (c) Pancharatna. Here, the monthly observed discharges averaged over the simulation period are plotted against the corresponding SWAT model outputs run using GCM (corrected) data.

The performance of the SWAT models using different GCMs is not same at all the outlets. The GFDL-ESM2M performed best at Pandughat with an R^2 value of 0.861 whereas HadGEM2-CC and IPSL-CM5-LR performed best at Bhomoraguri with an R^2 value of 0.85 and 0.612 respectively. However, when the overall performance of the three GCMs in all three stations was considered, the HadGEM2-CC was found to be the best with 0.851 and 0.8 values of R^2 in Bhomoraguri and Pancharatna stations. So, it can be concluded from this analysis that HadGEM2-CC model data provided the best performance in simulating the hydrology of the Brahmaputra basin, as compared to the other GCMs.

7.4.3 Remarks on GCMs evaluation

The evaluations of the bias-corrected GCMs are carried out in terms of statistical as well as SWAT model run results. Each GCM possesses certain uncertainties. It becomes evident from the above analyses that the outputs of the bias-corrected HadGEM2-CC provide better agreement to the observed data, than that of the other GCMs. Moreover, the same GCM provides the best performance in simulating the hydrology of the Brahmaputra basin. Hence, this GCM i.e. **HadGEM2-CC** may be termed as the most suitable for the present study area. As such, this GCM would be utilized for the future climate change studies and its subsequent impacts on the Brahmaputra basin.

7.5 Impact analysis due to climate change

Climate change due to the increase of greenhouse gas emissions is considered to be one of the major challenges to human beings in the 21st century (Schipper and Pelling, 2006). According to the Fourth Assessment Report (AR4) of the Intergovernmental Panel on Climate Change (IPCC, 2007), by the end of the 21st century, the average global surface temperature is likely to increase by 1.1 to 6.4°C and global average sea level rise of between 0.18 m and 0.59 m relative to 1980–1999. It will lead to changes in precipitation, atmospheric moisture, increase in evaporation and probably raise the frequency of extreme events. The consequences of these phenomena will influence many aspects of human society, such as the reduction of agriculture production, increase the risk to animals, destruction of infrastructure, damage to socio-economic, enhanced water conflicts,

poverty, and war. Sterrnan (2008) showed that if we do not act, the overall costs and risks of climate change will be equivalent to losing at least 5% of global GDP each year, starting from now and keep losing. If a wider range of risks and impacts is taken into account, the estimated damage could rise up to 20% of GDP or more. So there is a need to have a robust and accurate estimation of variation of natural factors due to climate change, at least in the hydrological cycle and flooding events, to provide a strong basis for mitigating the impacts of climate change and adapt to these challenges. This section of the report describes the trend in changes of the climatic variables during 1991-2099.

7.5.1 Trend analysis: Methods

In order to quantify the temporal trends of climate variables (Temperature/precipitation) across the study area till the year 2099, present study first used the nonparametric Mann-Kendall test to detect the existence of increasing or decreasing trend (Kendall, 1975), then followed by nonparametric Sen's method to estimate the magnitude of the trend (Sen, 1968). The Mann-Kendall test statistic (S) is calculated using *Eq. 7.10*.

$$S = \sum_{i=1}^{n-1} \sum_{j=k+1}^{n} sgn(X_j - X_k) \qquad \text{(Eq. 7.10)}$$

where x_j and x_k denote the annual Temperature/precipitation values in years' j and k respectively, and j >k. The indicator function "sgn" is given as follows:

$$sgn(X_j - X_k) = \begin{cases} 1, & if\ (X_j - X_k) > 0 \\ 0, & if\ (X_j - X_k) = 0 \\ -1, & if\ (X_j - X_k) < 0 \end{cases} \qquad \text{(Eq. 7.11)}$$

The statistic S is approximately normally distributed having the mean, E(S) = 0, when n ≥ 8. The variance statistic is computed as:

$$Var(S) = \frac{n(n-1)(2n+5) - \sum_{i=1}^{m} t_i(i)(i-1)(2i+5)}{18} \qquad \text{(Eq. 7.12)}$$

Where, t_i is the number of ties. The test statistics Z_C is computed as:

$$Z_c = \begin{Bmatrix} \frac{S-1}{\sqrt{Var(S)}} \\ 0, S = 0 \\ \frac{S+1}{\sqrt{Var(S)}}, S < 0 \end{Bmatrix} \quad \text{(Eq. 7.13)}$$

Z_C follows a standard normal distribution. A two-tail test is performed using a significance level α to evaluate its significance.

Non-parametric Sen's slope estimator is then estimated considering a linear trend as expressed in the following equations.

$$f(t) = Q(t) + B \quad \text{(Eq. 7.14)}$$

Here, B is a constant, whereas Q represents the slope which is calculated as per *Eq. 7.15*.

$$Q_i = \frac{X_j - X_k}{j-k} \quad \text{(Eq. 7.15)}$$

In case if there are *n* values of x_j in the Temperature/precipitation time series, we get as many as *N = n(n-1)/2* slope estimates *Qi*. The *N* values of *Qi* are then ranked from the smallest to the largest and the Sen's slope estimator is the median of these *N* values of *Qi* (*Eq. 7.16 or 7.17*).

if N is odd, $$Q_m = \frac{1}{2}\left(Q_{\left[\frac{N}{2}\right]} + Q_{\left[\left(\frac{N}{2}\right)/2\right]}\right) \quad \text{(Eq. 7.16)}$$

if N is even, $$Q_m = Q_{\left[\frac{N+1}{2}\right]} \quad \text{(Eq. 7.17)}$$

Finally, a two-sided 100(1-α) confidence interval is computed about the slope estimate using a Non-parametric test. Positive (or negative) values of Q_m denote upward (or downward) trends in the datasets.

The trend analysis is applied to the bias-corrected HadGEM2-CC data during 2020-2099, for both the RCP4.5 and RCP8.5 scenarios. To identify the local trend existing in the long time series, analyses were carried out by dividing the data into smaller timescales i.e. 2020-2040 (Future1 i.e. "F1"), 2041-2070 (Future2 i.e. "F2") and 2071-2099 (Future3 i.e. F3). As stated earlier in Sec. 7.1, the trend analysis by Man-Kendall and Sen's slope was done for the bias-corrected future data during 2020-2099 only, whereas the period 2006-2019

was not considered for this analysis. We carried out the climate change analysis to show the impacts through the annual and seasonal variations of the weather variables of the Brahmaputra basin

7.5.2 Annual trend analysis: Results and discussions

Fig. 7.7 describes the trend pattern of changes in maximum temperature at a certain station (i.e. S26) for RCP4.5 and during F1 (2020-2040) period, as for example. Here, the value in y-axis, for a year is obtained by averaging all days' maximum temperature values during that particular year. In this figure, Z (or Zc) is the Mann Kendall statistics, and the trend is said to be 'Significant' (S) if its value is more than 1.96. Otherwise, the trend is 'Non-significant' (NS). Moreover, Sen's slope value signifies that the maximum temperature at S26 station during 2040 increases by 4.7% with respect to the base year (2020) corresponding to the RCP4.5 scenario.

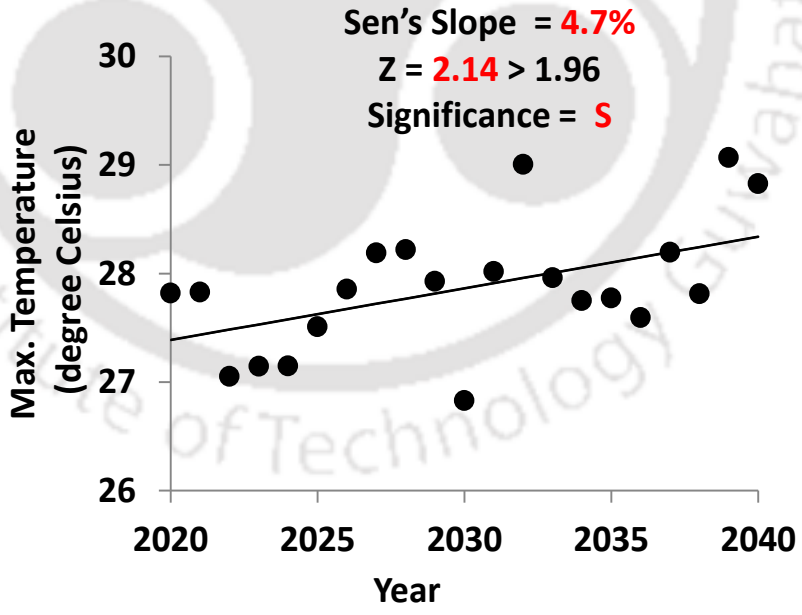

Fig. 7.7 Trend of annual Maximum temperature at a Station (S26) for RCP4.5, and during F1 (2020-2040) period. Here, the value for a particular year represents the basin average value of daily maximum temperatures during that year.

Likewise, the trends of all the variables (PCP, TMax, TMin) at all the 36 stations (S1-S36) corresponding to both the scenarios (RCP4.5 and RCP8.5) during all the time scales (F1, F2, F3) are obtained by applying Mann-Kendall and Sen's slope method. Moreover, trend plots are made for the annual and the seasonal (i.e. four seasons) changes of climatic parameters. Thus, we have several hundreds of such trend plots for the entire study area. And, we underwent difficulties in presenting such a huge numbers of trend plots in our report. Therefore, they are presented in the GIS plot as shown in the subsequent figures, for space constraint and to simplify the presentation. And, the relevant discussions regarding the future climate change of the Brahmaputra basin is forwarded on the basis of the respective figures.

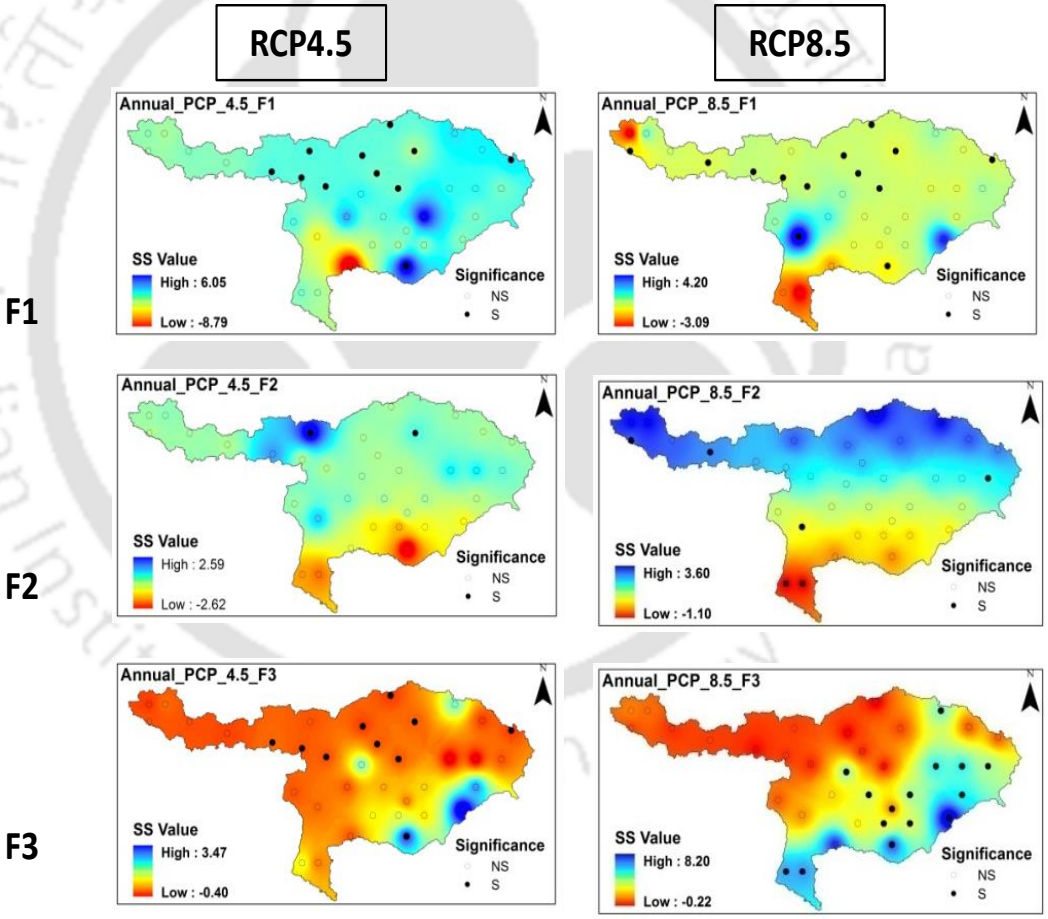

Fig. 7.8 Simulated (i.e. Bias corrected GCM) annual rainfall (PCP) under RCP4.5 (first column) and RCP8.5 (second column) for F1 (2020-2040), F2 (2041-2070) and F3 (2071-2099). Here, the sum of all values of daily rainfall during a particular year over F1 (or F2 or F3) was used for calculation of the Sen's slope (SS) value. Dark circles represent significant (S) whereas hollow circles represent non-significant (NS) trend.

7.5.2.1 Trends in annual PCP

7.5.2.1.1 Trends under RCP4.5

For the F1 period (*Fig. 7.8*) Under RCP4.5, 10 out of 36 stations located in the northern part of the basin are found to have significant trends with a moderately high value of Sen's slope. The areas in the southeast of the basin show a significantly increasing trend whereas the non-significant decreasing trend is seen on the southwestern side. In the F2 period, only two stations in the northern area show a significantly increasing trend. Down the southern areas, a non-significant decreasing trend of PCP is seen. In the late century F3 scenario, the majority of the stations exhibit decreasing trends and only in the southern areas, one station is found to have an increasing trend.

7.5.2.1.2 Trends under RCP8.5

For F1 period (*Fig. 7.8*) Under RCP8.5, only one station shows a significantly increasing trend and the majority of the stations show a decreasing trend. In F2 period, the upper half of the basin shows an increasing trend while the lower half shows a decreasing trend. The highest positive values of Sen's slope lie in the upper Indo-China region and the lowest Sen's slope value lie towards the southern side. Under the F3 period, the areas in the northern side of the basin show non-significantly decreasing trend, whereas the southern side of the basin shows increasing trends. The increasing trends were significant in the southern areas of Assam Meghalaya borders.

7.5.2.1.3 Future annual Rainfall of Brahmaputra basin

The annual rainfall during 2020-2040 is likely to increase over majority of the basin areas upto 6.05% (RCP4.5) and 4.2% (RCP8.5). Significant increasing trend in annual rainfall has been observed over the China portion of the basin. This portion is basically the Himalayan range, and would undergo changes in hydrological cycle due to the increase in rainfall. However, the plain areas over India would experience relatively low impact in the annual rainfall, than the hilly areas. The annual rainfall over Bangladesh during 2040 is likely to decrease upto 3.09% with respect to the base year (2020), and corresponding to RCP 8.5. This area of the basin would even undergo shortfall in annual rainfall during 2041-2070. The Himalayan range would experience a continuous increase in the annual

rainfall till 2070, with respect to the base year (2020). Interestingly, this area would suffer a little shortfall in annual rainfall till the end of 2099, but the southern part of the basin is likely to have more impact with increase in rainfall. During 2071-2099, this change would stand upto + 3.47% (RCP4.5) and +8.2% (RCP 8.5). While Akhtar et al. (2011) reported an increase of over 5% in annual rainfall in the southern part of the basin. So, the annual rainfall in the Brahmaputra basin would change in the near future following an increasing trend over majority of the basin areas. However, the snow-fed areas of the Himalayan range and the river mouth portion near the Bay of Bengal would be more susceptible to the future rainfall changes as compared to the plain areas.

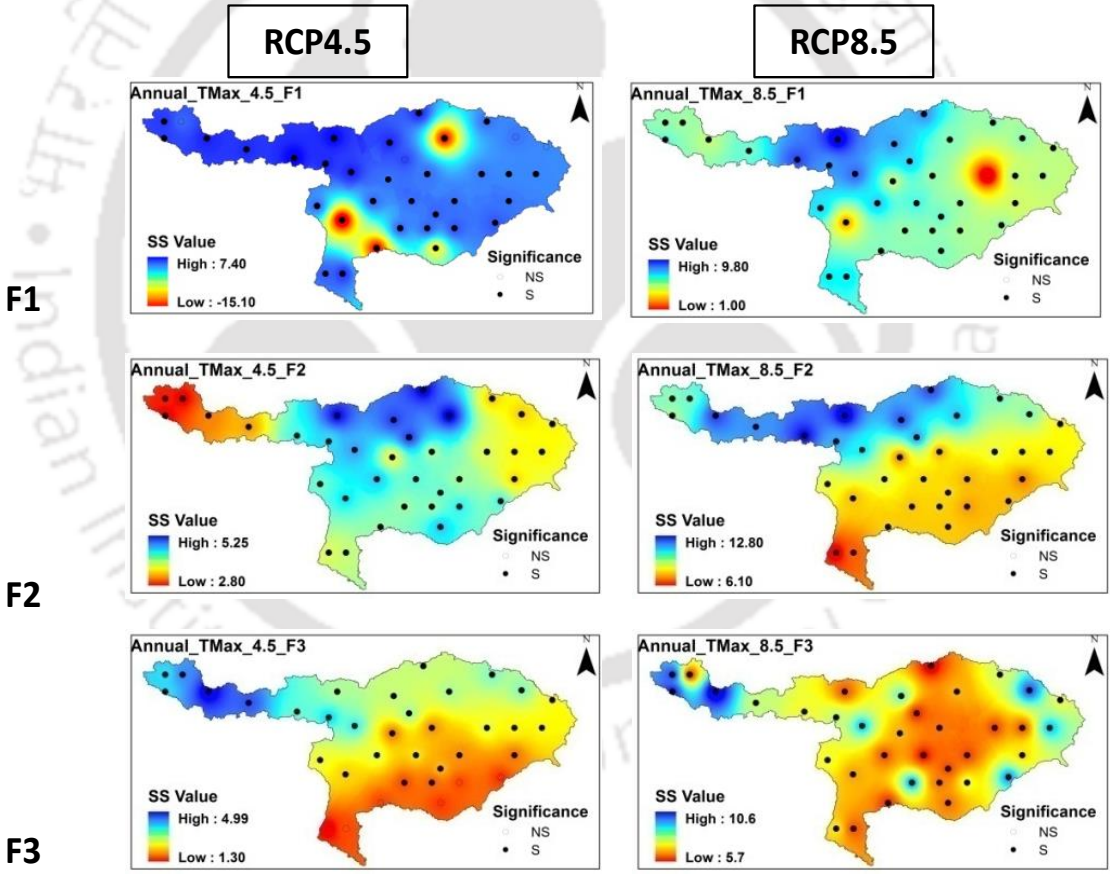

Fig. 7.9 Simulated (i.e. Bias corrected GCM) annual maximum temperature (TMax) under RCP4.5 (first column) and RCP8.5 (second column) for F1 (2020-2040), F2 (2041-2070) and F3 (2071-2099). Here, the average of all values of daily maximum temperature during a particular year over F1 (or F2 or F3) was used for calculation of the Sen's slope (SS) value. Dark circles represent significant (S) whereas hollow circles represent non-significant (NS) trend.

7.5.2.2 Trends in annual TMax

7.5.2.2.1 Trends under RCP4.5

The trend analysis of annual TMax for F1 under RCP4.5 (*Fig.7.9*) shows a significantly increasing trend over most parts of the basin with few pockets showing a significantly decreasing trend. The annual maximum temperature may increase upto 7.4% during 2020-2040 which would even escalate upto 8.25% during the next time duration (2041-2070). Of course, the rate of this increase would occur at relatively slower pitch with a maximum value as 4.99% till the end of the century. The plain areas of India and Bangladesh would have lesser impacts due to change in maximum temperature till 2099.

7.5.2.2.2 Trends under RCP8.5

Trend analysis of annual TMax under RCP 8.5 (*Fig. 7.9*), the F1 period shows increasing trend all over the basin with Sen's slope ranging from 9.8 to 1. The higher values of Sen's slope are attributed to the northern areas. In F2 period, the increase in TMax is higher (upto 12.8%) in the northern areas whereas increase in the southern areas would happen upto 6.1%. Moreover, the TMax would increase all over the basin during 2071-2099, with a minimum value of 8.7%.

7.5.2.2.3 Future annual TMax of Brahmaputra basin

Comparing RCP4.5 and RCP8.5, it can be seen from *Fig.7.9* that most of the stations were showing a significantly increasing trend in RCP4.5 with little deviations at a few stations over the study area. Under RCP8.5, TMax follows increasing trend at all the stations, with minimum Sen's slope of 1 among all the future periods. Under F2, there is a rise in both upper and lower values of increasing trend in Tmax for both the RCP scenarios. However, TMax during 2071-2099 would increase at relatively lower rate, than 2041-2070. Overall, the Brahmaputra basin's annual maximum temperature would increase by the end of the current century.

7.5.2.3 Trends in annual TMin

7.5.2.3.1 Trends under RCP4.5

For F1 period under RCP4.5 (*Fig. 7.10*), the trend analysis of the annual minimum temperature shows the overall increasing trend in the basin with little deviations as

decreasing trends at only few stations. This deviation perhaps is due to either the incorrect assessment in the GCM outputs or the bias has not been properly removed. The bias factors calculated using the Linear Scaling method (*Sec. 7.3.1.1*) is correctly reflected provided the observed records are merely correct that results in correct relationship between these data and the GCM outputs. Moreover, the TMin would increase throughout the basin upto 4.25% for F2 (2041-2070) and 5.12% during F3 (2071-2099). However, the plain areas of India and Bangladesh would have relatively less impact as compared to the hilly areas.

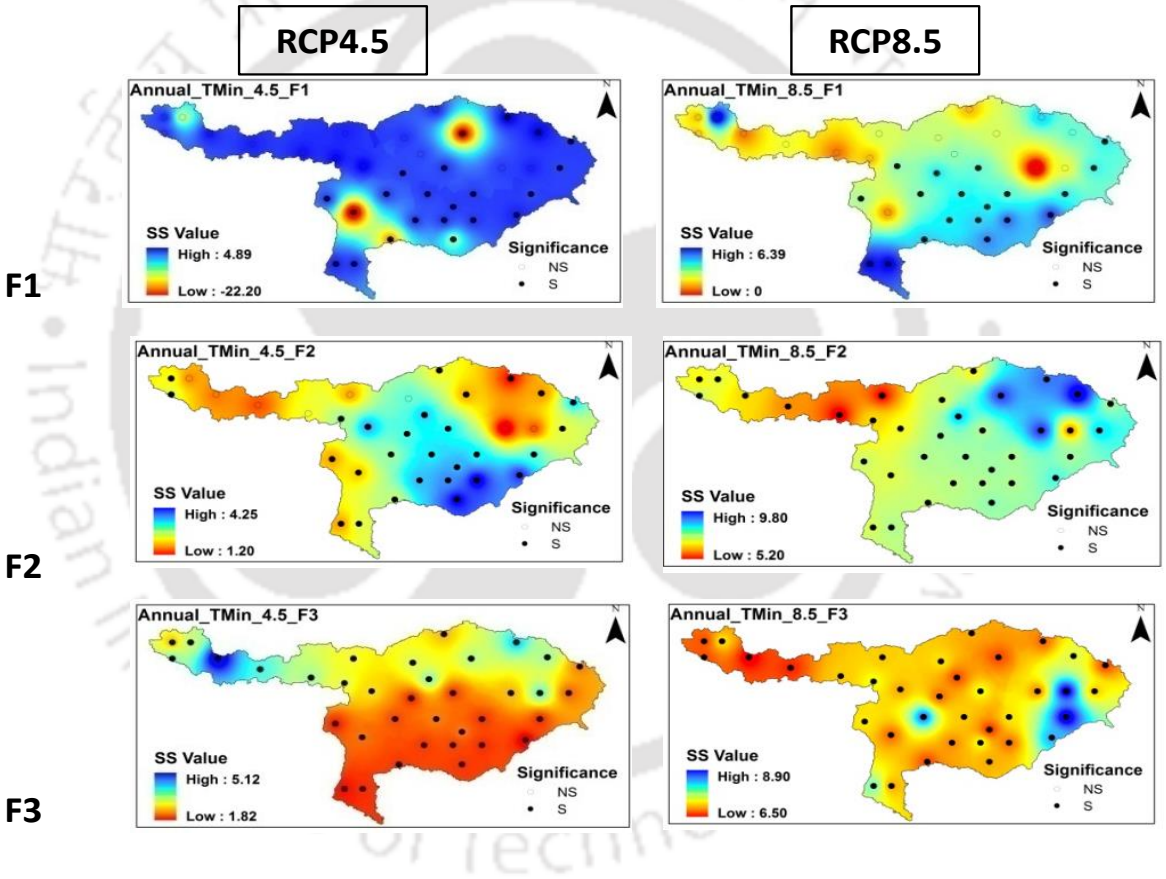

Fig. 7.10 Simulated (i.e. Bias corrected GCM) annual minimum temperature (TMin) under RCP4.5 (first column) and RCP8.5 (second column) for F1 (2020-2040), F2 (2041-2070) and F3 (2071-2099). Here, the average of all values of daily minimum temperature during a particular year over F1 (or F2 or F3) was used for calculation of the Sen's slope (SS) value. Dark circles represent significant (S) whereas hollow circles represent non-significant (NS) trend.

7.5.2.3.2 Trends under RCP8.5

During 2020-2040, the TMin under RCP8.5 (*Fig. 7.10*) shows a significantly increasing trend over the plain areas of India and Bangladesh at higher rates than over the northern (China) part of the basin. Here, the maximum increase in TMin would stand upto 6.29%, but the TMin would even increase at higher rates, over the entire basin during the F2 (2041-2070) period and the value lies in between 5.2 - 9.8%. A similar increasing trend would prevail even during the F3 (2071-2099) period. The TMin would increase upto 8.5% during 2099 from the base year (2071). Overall, the TMin would significantly increase till the end of the current century.

7.5.2.3.3 Future annual TMin of Brahmaputra basin

The annual minimum temperature of the Brahmaputra basin would increase during all the future periods and under both the RCP scenarios. TMin is likely to decrease at a few stations during 2020-2041 (RCP4.5). This is perhaps not the fair estimates so far the trend values are concerned. Because only two stations, out of 36 total stations considered for climate change analysis is not expected to exhibit the opposite trend, than the others, even by a huge margin. Generally speaking, the annual TMin would increase over the entire Brahmaputra basin till 2099, and for both the RCP scenarios.

7.5.2.4 Annual Climate of Brahmaputra basin during 2006-2099.

The values of annual rainfall, maximum temperature and minimum temperature during 2006-2099 have been plotted (*Fig. 7.11*) to estimate the pattern of climate change. This plot shows the basin average values, for each variable, and during the entire period. For precipitation, the daily values in the records of bias-corrected GCM (i.e. HadGEM2-CC) database are added to obtain the total annual rainfall during a particular year. On the other hand, for temperature, the daily values are averaged over a particular year, in order to obtain the annual temperature value. As per the trend line, the maximum temperature is likely to increase by 3.2 ^{0}C (RCP4.5) and 6.8 ^{0}C (RCP8.5) starting from the year 2006 to the year 2099. So, the Brahmaputra basin is likely to experience an increase in maximum temperature at the rate of 0.029 ^{0}C/year and 0.062 ^{0}C/year, for RCP 4.5 and RCP8.5 respectively. At the end of the century, the minimum temperature of the Brahmaputra basin

is likely to increase at the rate of 0.009 ^{0}C/year (RCP 4.5) and 0.052 ^{0}C/year (RCP8.5), with respect to the base year 2006. Moreover, the annual rainfall of the basin would increase by 2.29 mm/year for RCP4.5, starting from 2006 till 2099. This value stands even higher for RCP8.5, and the value is 2.56 mm/year. So, it is obvious that the climatic variables would increase at higher rates for RCP 8.5, as compared to RCP4.5. It can be concluded from this analysis that the Brahmaputra river basin would experience the impacts of global climate change.

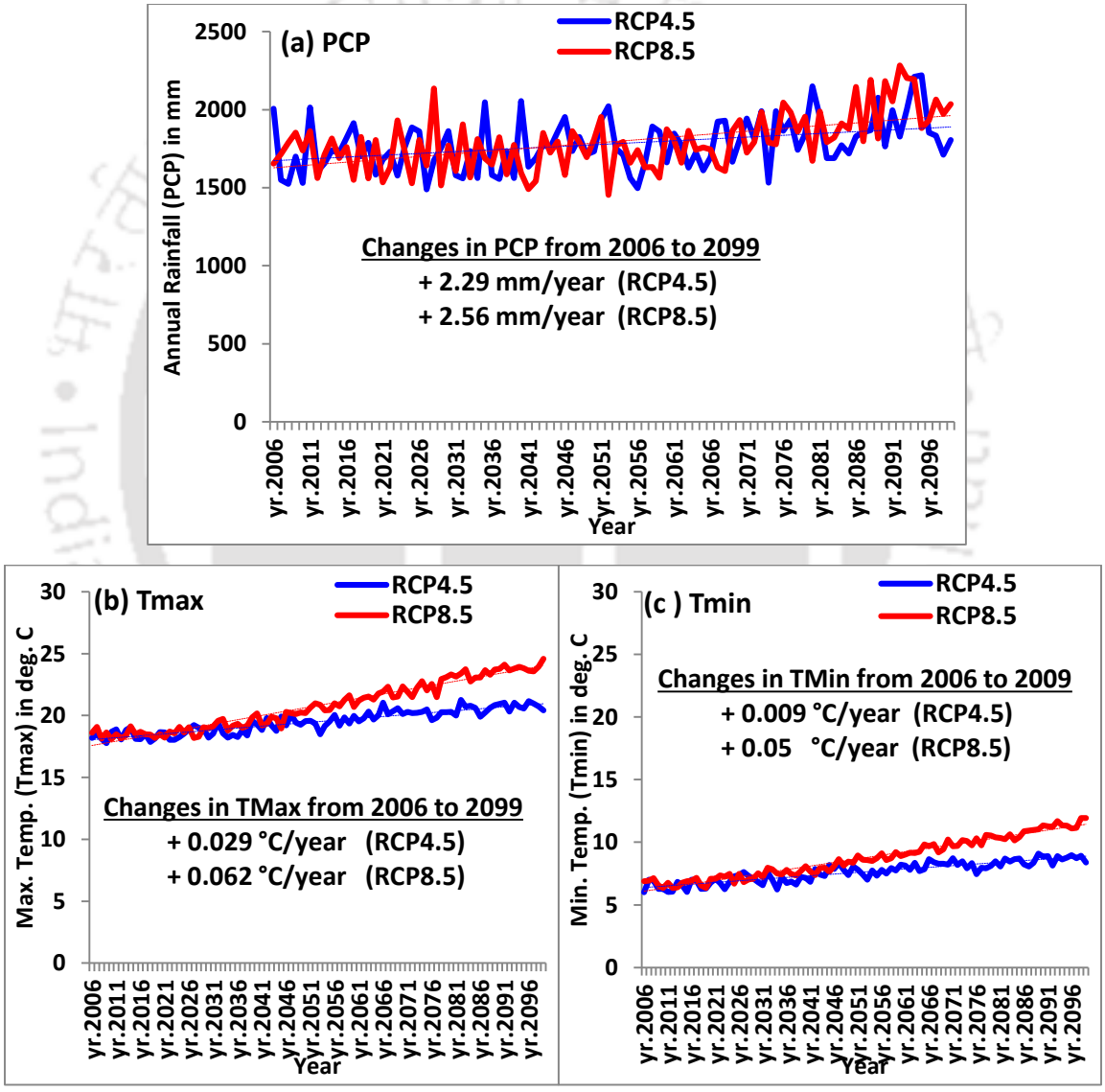

Fig. 7.11 Pattern of Climate changes of the Brahmaputra river basin during 2006-2099: (a) Rainfall (PCP); (b) Maximum temperature (Tmax); (c) Minimum temperature (Tmin). Here, blue line corresponds to RCP4.5 and the red line corresponds to RCP8.5.

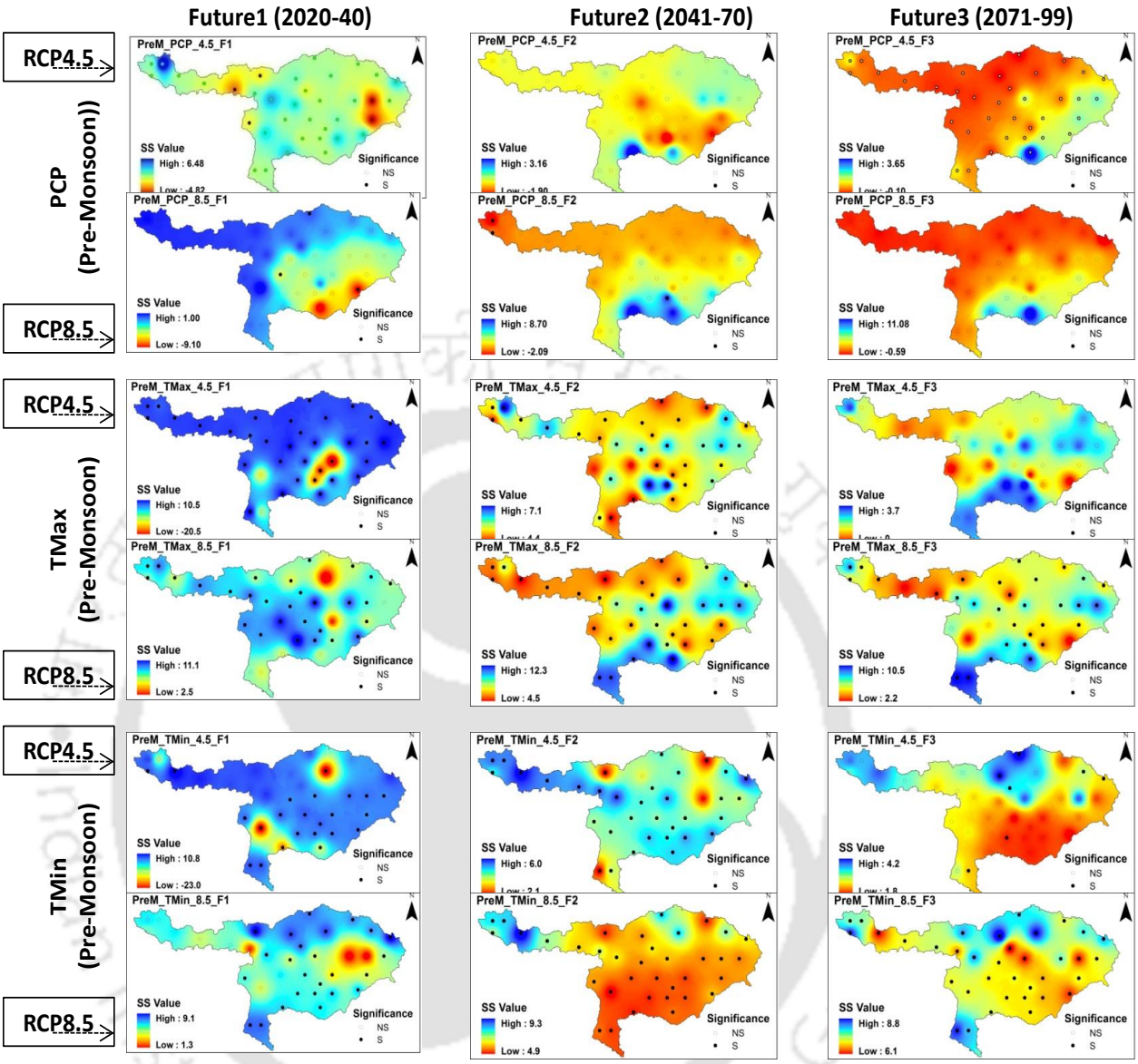

Fig. 7.12 Climate change during **Pre-Monsoon** season for PCP, TMax and TMin under RCP4.5 and RCP8.5 scenarios, corresponding to F1, F2 and F3 periods. Dark circles represent significant (S) whereas hollow circles represent non-significant (NS) trend.

7.5.3 Seasonal trends: Results and discussions

This section of the report describes the pattern of seasonal climate change during the present and future periods, over the entire Brahmaputra basin. A year is divided into four different seasons like (a) pre-monsoon [Mar-May]; (b) monsoon [Jun-Aug]; (c) post-monsoon [Sept-Nov]; and (d) winter [Dec-Feb] season. For each season, the station-wise

bias corrected values of the GCM (i.e. HadGEM2-CC) are grouped according to the respective timescales (BP, F1, F2. F3).

Initially, trend values during a particular timescale were determined by using Sen's Slope method, followed by the significance level of each trend by using Man-Kendall Test. Like the annual climate change (*Sec. 7.5.2*), the seasonal climate changes are also represented in GIS plots, for simplicity and clarity of presentation.

7.5.3.1 Pre-Monsoon season

The pre-monsoon rainfall during 2020-99, corresponding to RCP4.5 does not significantly vary w.r.t. the respective base years (*Fig. 7.12*). However, a significant decreasing trend upto 4.82% (F1) and 1.9% (F2) at certain locations are observed. As well, decreasing, but insignificant trends were observed for RCP8.5 scenario over majority of the basin, and during all future timescales.

On the contrary, the max temperature (TMax) during pre-monsoon periods would increase significantly. A sharp increase in TMax would happen during F1 (upto 10.5%) and F2 (upto 7.1%) periods, corresponding to RCP4.5 scenario. As well, this increase during F3 period would pace at relatively slower rate, and the value stands upto 3.7%. However, for RCP8.5, the pre-monsoon TMax is likely to increase significantly high with a minimum value of 10.5%, during all future time periods. The minimum temperature (TMin) of the basin would also increase during pre-monsoon periods till the end of the century, with relatively higher rates for RCP8.5.

7.5.3.2 Monsoon season

The monsoon rainfall during 2020-99 would increase, but not very significant for both the scenarios (*Fig. 7.13*). Of course, the rate of increase in the coming two decades (i.e. 2020-40) would pace at relatively high values, than the later periods (F2 and F3) of the current century. The monsoon rainfall during F1 period can rise upto 10.8% and 21.95%, for RCP4.5 and RCP8.5 respectively. This increase, however, is not very significant at majority of the locations over the basin, although, the monsoon rainfall would increase over the entire basin till the end of the century.

The Brahmaputra basin would experience a rise in TMax and TMin, during 2020-99, the rate of increase being higher for RCP8.5 than for the RCP4.5. Interestingly, the TMax would increase at higher pace (upto 5.4%) during the coming two decades, as compared to F2 and F3 timescales of RCP4.5. For RCP8.5, the temperature would rise upto 10.8% (TMax) during the F2 period and upto 7.4% (TMin) during F1 timescales. It is observed that the Himalayan range of the basin is likely to have more impacts in the monsoon temperature.

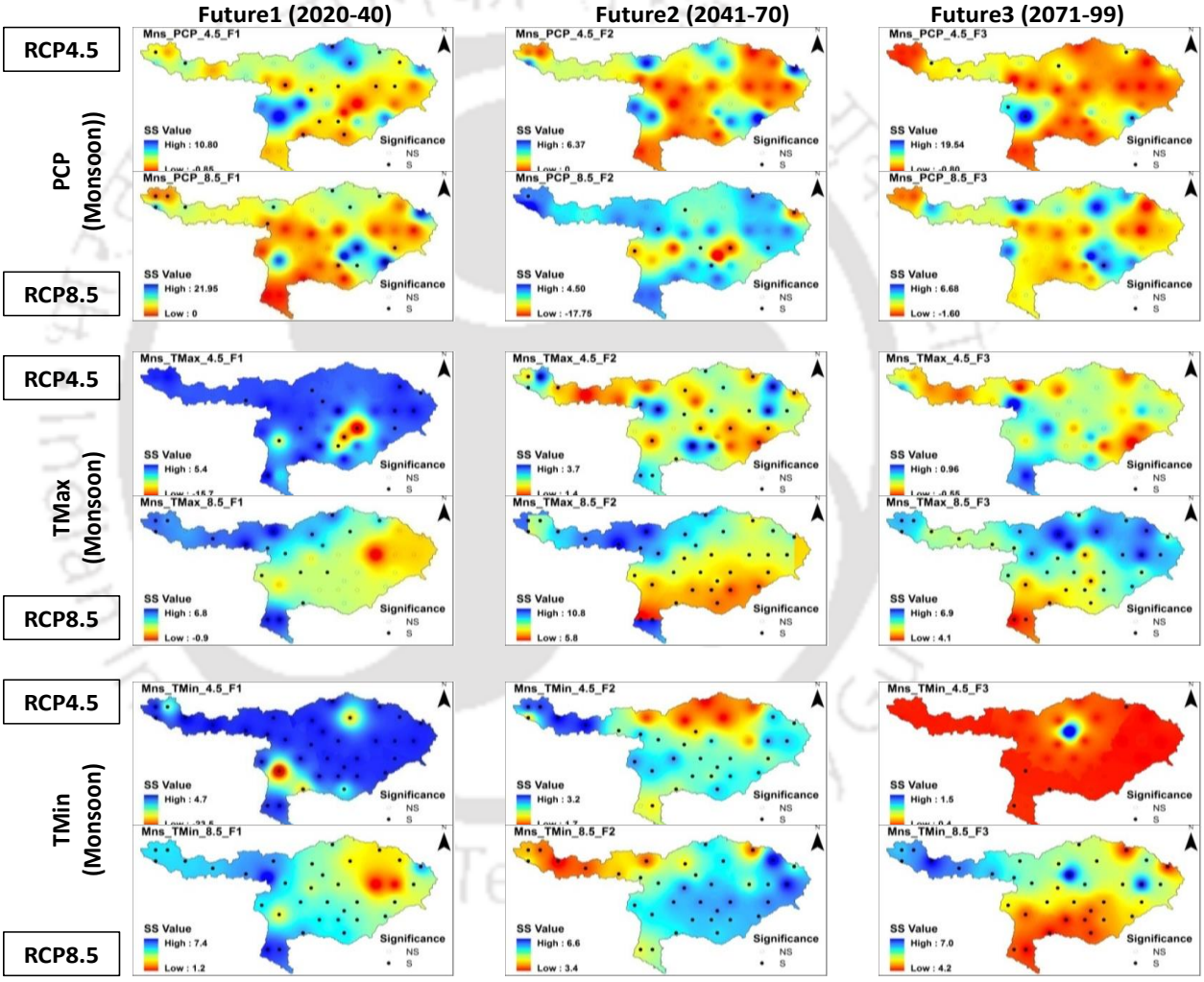

Fig. 7.13 Climate change during **Monsoon** season for PCP, TMax and TMin under RCP4.5 and RCP8.5 scenarios, corresponding to F1, F2 and F3 periods. Dark circles represent significant (S) whereas hollow circles represent non-significant (NS) trend.

7.5.3.3 Post-Monsoon season

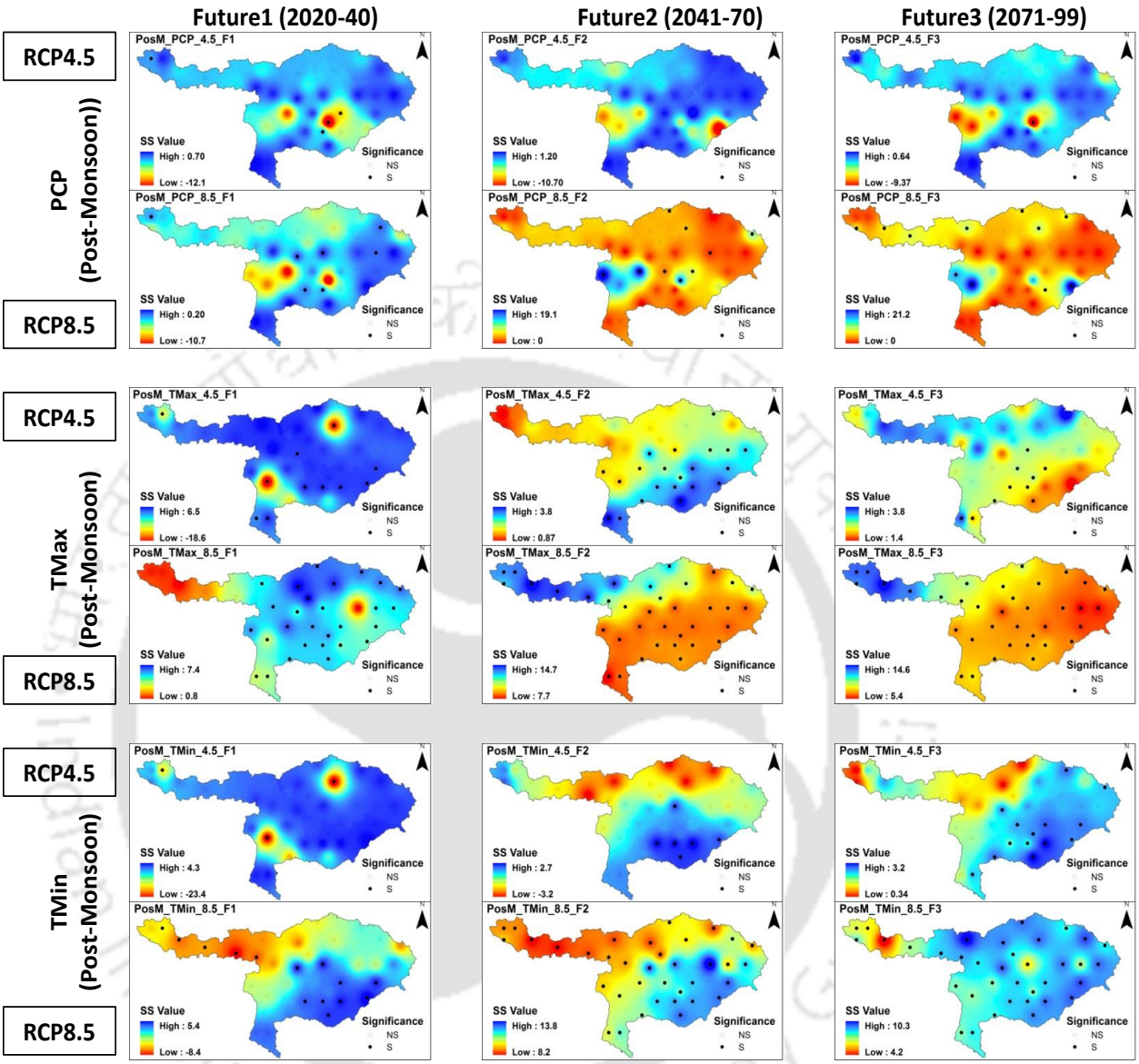

Fig. 7.14 Climate change during **Post-Monsoon** season for PCP, TMax and TMin under RCP4.5 and RCP8.5 scenarios, corresponding to F1, F2 and F3 periods. Dark circles represent significant (S) whereas hollow circles represent non-significant (NS) trend.

The rainfall magnitudes during the forthcoming post-monsoon seasons (*Fig. 7.14*) are likely to rise insignificantly w.r.t. the year 2020, but the maximum temperature would increase to the greater extent. A rise upto 14.6% in TMax during F3 period of RCP8.5 is expected over the majority locations of the basin, especially, the Himalayan range. The corresponding rise in TMin would occur upto only 3.2%. The rise in post-monsoon

temperature would lead to melting of glaciers over the Himalayas, resulting in increased future discharges of the Brahmaputra.

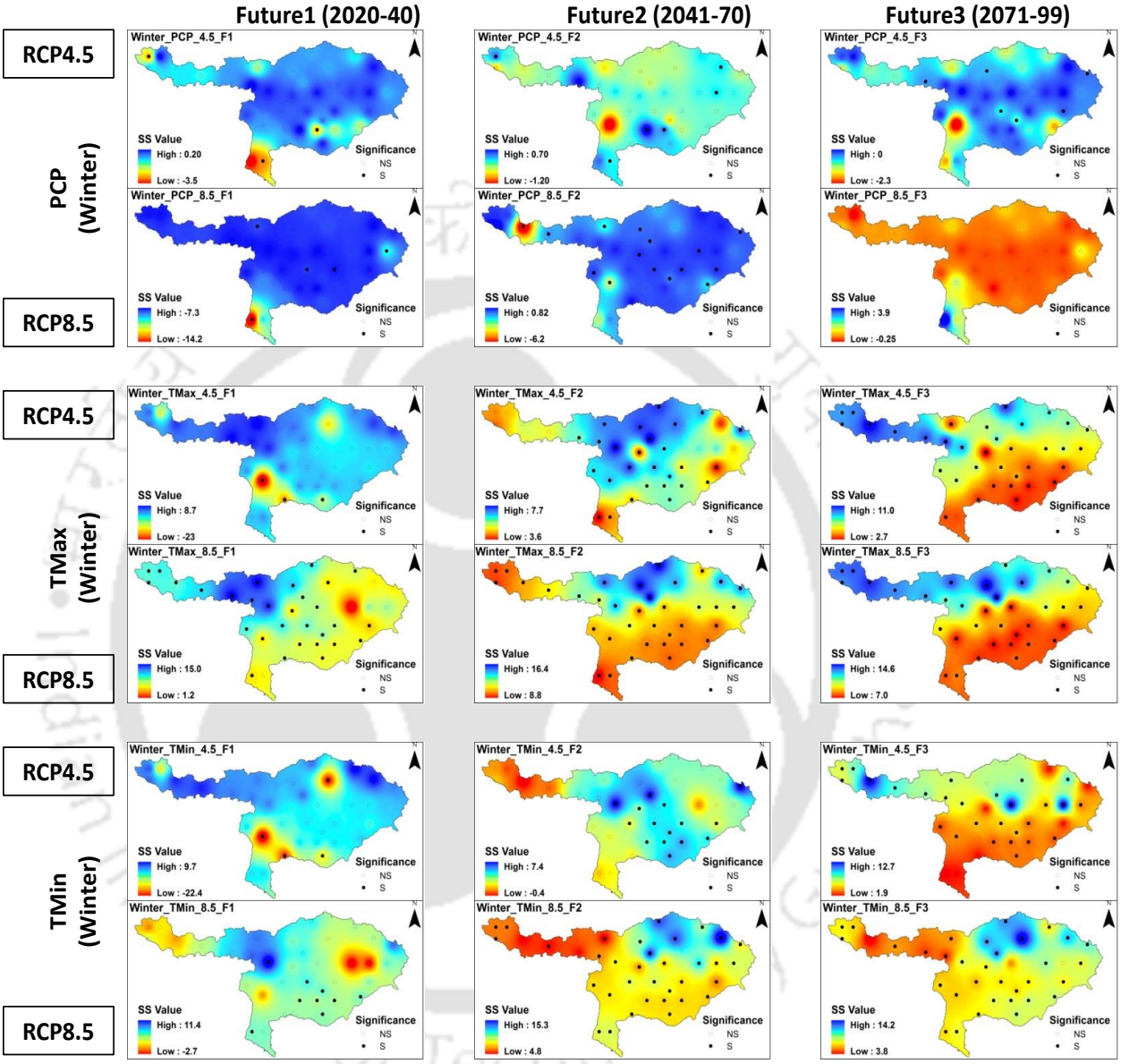

Fig. 7.15 Climate change during **Winter** season for PCP, TMax and TMin under RCP4.5 and RCP8.5 scenarios, corresponding to F1, F2 and F3 periods. Dark circles represent significant (S) whereas hollow circles represent non-significant (NS) trend.

7.5.3.4 Winter season

During winter season, the rainfall over the present basin is likely to decrease till 2099 (*Fig. 7.15*), for both the two scenarios, although not very significant, but the future temperature over the basin would increase till the end of the current century. The highest increase in

maximum temperature would occur during 2041—70, and the value is 16.4%. On the other hand, the corresponding value for minimum temperature lies at only 11.0%. As such, the global climate change would definitely impact on the Brahmaputra basin's winter season.

7.5.4 Remarks on CC studies

Anthropogenic emission of greenhouse gases has resulted in global climate change, which with unabated emissions is projected to continue into the future (IPCC 2013). Climate change is not only associated with the rise in temperature, but also with the change in the global precipitation cycle, leading to variation in spatial and temporal precipitation patterns. Such a variation would affect the quantity and quality of available water resources of the Brahmaputra basin, thereby increasing the competition among agriculture, ecosystems, settlements, industry, and energy sectors. Due to the global climate change, the values of climatic variables across the Brahmaputra basin would change till 2099. According to the results of the highest possible emission scenario (RCP8.5), the annual rainfall may increase upto 2.56 mm per year till the end of the current century. As such, the increased precipitation variability would lead to floods. On the other hand, the increase in temperature may also affect the basin hydrology in the forthcoming decades. The basin average TMax may rise up to 0.062 ^{o}C/year till the year 2099. This would result in melting of glaciers over the Himalayan range of the basin area. Subsequently, the Brahmaputra basin would undergo changes in the basin behaviour, due to change in the basin hydrology.

7.6 Strategic management for CC impacts

The global climate change is likely to impact on the weather variables of the Brahmaputra river basin, during both the present and future periods. It is evident from the present analysis that the annual rainfall will increase upto 2.56 mm per year till the end of the current century. Besides, the basin average temperature will rise up to 0.062 ^{0}C/year (TMax) and 0.05 ^{0}C/year (TMin) till the year 2099. Therefore, the Brahmaputra would experience changes in its basin hydrology due to the increase in rainfall and temperature. Indeed increase in rainfall may result in flood whereas decrease in rainfall may results in

drought in the non-monsoon season. On the other hand, increase in temperature will lead to melting of glaciers over the Himalayan range of the Brahmaputra basin. Consequently, the ecology of the Brahmaputra basin would undergo alterations due to the impact of climate change. As such, it is the need of time to develop strategies to tackle the probable impacts of climate change so as to restore the natural features like wetlands, forest areas etc. that will lead to enhance habitat preservation. The ecologically sensitive areas having high diversity of species and undergoing a significant change are to be identified for protection under climate change scenarios. The structural complexity and bio-diversity of vegetation of the Brahmaputra basin needs to be preserved as adaption strategy for climate change.

7.7 Conclusion

In the present analysis, we considered only three GCMs selected based on the availability of records for present and future periods. The results presented in this analysis may little vary if we could consider more than three numbers, and even using GCMs other than CMIP5 database. As downscaling techniques for a huge area like the Brahmaputra basin would computationally be very expensive, we applied interpolation followed by bias correction of the GCM data. Another reason is that there are several grid points of each GCM, falling within the present basin. Even, many of them were almost concentric to the observed weather stations. Finally, we could identify HadGEM2-CC, as the most suitable one, among all GCMs selected for the present study. While comparing the performances of all the GCMs, it was observed the data of this particular GCM to replicate merely the ground observations. Therefore, the trend analysis using the well-established Mann-Kendall and Sen's slope methods is expected to provide a valid result for the climate change impact over the Brahmaputra basin.

########## ##########

Chapter 8

Streamflow Projections

8.0 Introduction

Anthropogenic emission of greenhouse gases has resulted in global climate change, which with unabated emissions is projected to continue into the future (IPCC 2013). Climate change is not only associated with the rise in temperature, but also with the change in the global precipitation cycle, leading to variation in spatial and temporal precipitation patterns of the Brahmaputra basin. Such a variation would affect the quantity and quality of available water resources, thereby increasing the competition among agriculture, ecosystems, settlements, industry, and energy sectors. Increased precipitation variability and the competition among various sectors could limit the amount of water available for agricultural production. Rainfed agricultural systems in developing countries are particularly vulnerable to climate variability because the output of the systems is dictated by the prevalent climate and precipitation patterns. Thus, climate-change-associated warming, drought, flooding, and precipitation variability pose a threat to food security, especially to the poor populations in developing countries (IPCC 2014).

The evaluation of climate change over the Brahmaputra river basin has been discussed in the previous chapter (i.e. *Chapter 7*). This section of the report describes the impact of such climate change on the future discharge of the Brahmaputra river.

8.1 Climate change impacts on streamflow

8.1.1 Impacts on annual discharges

The projected annual discharge time series are divided into three smaller time scale, i.e. from 2020-2040 (F1), 2041-2070 (F2) and 2071-2099 (F3). The discharge values are obtained from the SWAT model run using the bias-corrected GCM (HadGEM2-CC) data

for the present as well as for all the future timescales. The annual discharge variability of these three timescales is analyzed and compared with respect to the annual discharge during the base period (2006-2019) of the SWAT model output. The SWAT model is simulated by using the daily values of input variables, and to provide outputs on annual basis.

The annual discharge values obtained from the SWAT model simulation for each time scales are shown in *Fig. 8.1*, as box plot. Here, the SWAT model is run using the input variables obtained from the bias corrected HadGEM2-CC database. The simulation was done for the respective periods (i.e. BP, F1, F2 & F3) individually, and for both the RCP scenarios. Then, the outputs corresponding to three locations (Bhomoraguri, Pandughat & Pancharatna) are derived from the simulation results for this analysis.

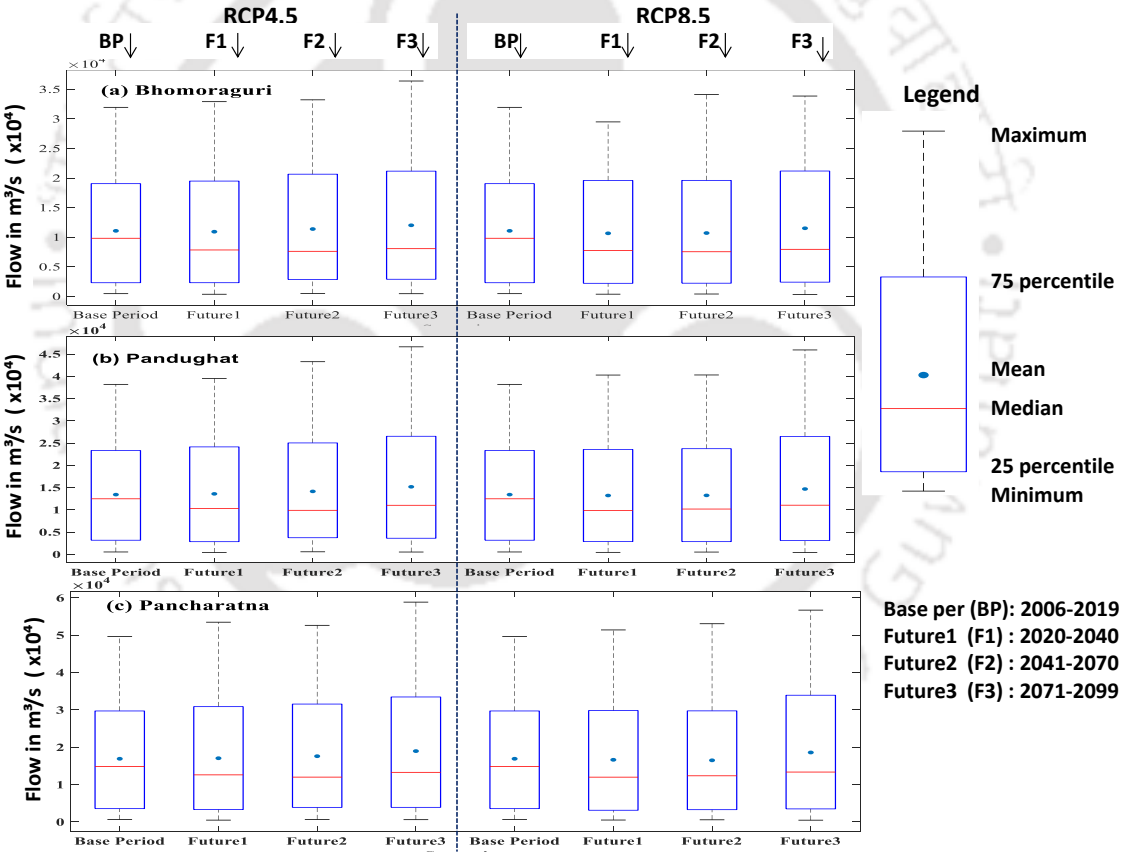

Fig. 8.1 Impact of future climate change on the annual discharges of the Brahmaputra basin at the three locations: a) Bhomoraguri, b) Pandughat and c) Pancharatna. Here, the results of SWAT model run using bias-corrected HadGEM2-CC corresponding to RCP4.5 (Left column) and RCP8.5 (Right column) are shown as Box plot.

The box-plot result indicates that the mean values of the projected discharge are higher than the base time period, for the majority of the timescales under both the RCP4.5 and

RCP8.5 scenarios, at all the three locations. From the figure (*Fig. 8.1*), it is also evident that there is a wide variation in the maximum discharge values of all the three-time scales at each location with respect to the base period.

Table 8.1 Percentage (%) changes in annual discharge due to climate change w.r.t base period (2006-2019).

Location	Future 1 (2020-2040)		Future 2 (2041-2070)		Future 3 (2071-2099)	
	RCP 4.5	RCP 8.5	RCP 4.5	RCP 8.5	RCP 4.5	RCP 8.5
Bhomoraguri	-1.32	-3.78	+2.75	-3.36	+8.47	+3.93
Pandughat	+1.25	-1.50	+1.26	-1.31	+9.34	+13.06
Pancharatna	+0.84	-1.63	+4.05	-1.63	+9.93	+12.13

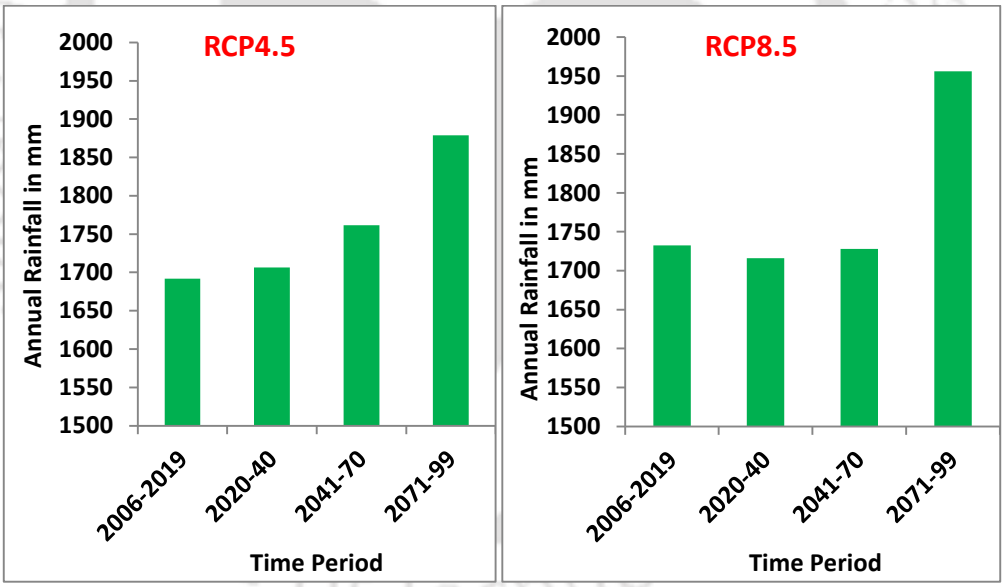

Fig. 8.2 Annual rainfall over the Brahmaputra basin during different timescales, and for both RCP4.5 and RCP8.5 scenarios. Here, the values in y-axes represent the basin average annual (total) rainfall during BP (2006-2019), F1 (2020-40), F2 (2041-70) and F3 (2071-2099).

Referring to the *Table 8.1*, which denotes the percentage changes in annual mean discharges w.r.t. the base period (2006-2019), it has been observed that there is a positive increment, for all scenarios at majority time scales, except few deviations. The basin

average annual rainfall (*Fig. 8.2*) value during the base period is 1690 mm, for RCP4.5. This value insignificantly changes during the F1 (2020-40) period. As such, the changes in annual discharge values at all three locations are found to be insignificant. The annual rainfall during F2 period would increase to 1760 mm, thereby the annual discharge value during this period is likely to increase w.r.t. the base period discharge values. Indeed, this is clear from the *Table 8.1* that this increase would happen to 4.05% at Pancharatna. However, the annual discharge during F3 period would increase at higher rates, and the values are 8.47% (Bhomoraguri), 9.34% (Pandughat) and 9.93% (Pancharatna). This is due to increase in annual rainfall to the greater extent (*Fig. 8.2*), as a consequence of global climate change. As well, for RCP4.5, the temperature (TMax/TMin) of the Brahmaputra basin during F3 period would increase by 2-3 ^{0}C (*Fig. 8.3*) from the base period. This would aid to increase in the future annual discharge at the end of the century.

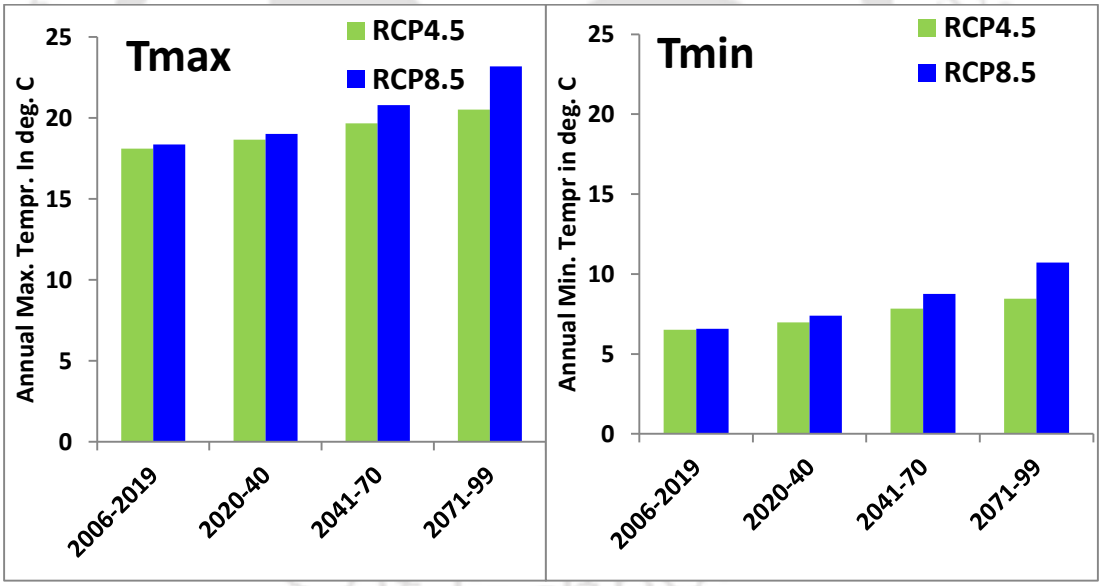

Fig. 8.3 Annual Temperature (a) TMax; (b) TMin, over the Brahmaputra basin during different timescales, and for both RCP4.5 and RCP8.5 scenarios. Here, the values in y-axes represent the basin average values during BP (2006-2019), F1 (2020-40), F2 (2041-70) and F3 (2071-2099).

For RCP8.5, the annual discharge during both the F1 and F2 periods would decrease, as compared to the base period. It is evident from *Table 8.1*, this decrease may happen upto 3.78%. Of course, the Brahmaputra basin would experience deficit in annual discharges during F1 and F2 periods, due to the impact of climate change. The annual rainfall values

(*Fig. 8.2*) during these periods would decrease, as compared to the base period. However, there is a sharp increase in annual rainfall (*Fig. 8.2*) over the basin, during F3 periods, w.r.t. the base period. This value during F1 period is 1730 mm, which would rise upto 1955 mm, thereby increasing by 225 mm. As a result, the Brahmaputra discharge would increase to large extent. The upstream location i.e. Bhomoraguri is likely to have the least impact, whereas the downstream locations (i.e. Pandughat and Pancharatna) are likely to experience the impact to greater extent. This is because annual rainfall during that period are relatively higher at the plain areas than the hilly areas. The highest increase in annual discharge under RCP8.5 would occur at Pandughat (13.06 %), followed by Pancharatna (12.13 %), during 2071-2099, and with respect to the base periods.

8.1.2 Impacts on seasonal discharges

The impact of climate change on the seasonal discharges of the Brahmaputra River at certain locations is shown in *Table 8.2*. For this analysis, a year is divided in to four seasons as:

- Pre-monsoon [Mar-May];
- Monsoon [Jun-Aug];
- Post-monsoon [Sep-Nov] and
- Winter [Dec-Feb].

The SWAT model simulated flow values obtained by using the bias corrected GCM variables are shown in graphical forms (*Fig. 8.4--8.6*). These figures show the season-wise flow values at all the three locations during 2006-2099. Based on the mean values, the percentage changes of the future seasonal discharges w.r.t the base period (2006-2019) are calculated and presented in *Table 8.2*. It is evident from the *Table 8.2*, that the future change in climate of the basin greatly impacts on the seasonal discharges at all locations. During pre-monsoon, the river discharges at Bhomoraguri would decrease, during all the timescales (F1, F2, F3), and for both the RCP scenarios. This discharges would even decrease at the other two locations (Pandughat, Pancharatna) during 2020-2040 (F1) and 2041-2070 (F2). However, the Pre-Monsoon discharges at the later two locations would increase during 2071-2099 (F3) under both the RCP scenarios. The maximum increase in

this discharge would happen up to 10.33% (Pandughat) and 10.4% (Pancharatna) under RCP4.5 and RCP8.5 respectively.

The river flows during monsoon period at all locations would increase for RCP 4.5 scenario. The highest increase in monsoon discharges under RCP4.5 would occur during F3 timescale, and their values are +14.31% (Bhomoraguri), +16.17% (Pandughat) and +15.17% (Pancharatna).

Table 8.2 Impact of climate change on seasonal discharges of the Brahmaputra River at three outlets (i.e. Bhomoraguri, Pandughat, Pancharatna).

Outlet	Season	%ge change in Seasonal discharges due to climate change w.r.t. Base period (2006-2019)					
		F1 (2020-40)		F2 (2041-70)		F3 (2071-99)	
		RCP4.5	RCP8.5	RCP4.5	RCP8.5	RCP4.5	RCP8.5
1	Pre-Monsoon	-12.85	-15.30	-13.10	-13.07	-7.72	-13.19
	Monsoon	+3.37	-1.91	+5,28	+0.24	+14.31	+5.89
	Post-Monsoon	-1.99	-1.23	+5.46	-3.42	+7.07	+8.86
	Winter	-16.00	-11.67	-1.39	-15.70	-0.55	-6.95
2	Pre-Monsoon	-2.07	-8.29	-4.37	-4.03	+10.33	+7.55
	Monsoon	+4.84	-1.03	+5.27	-0.03	+16.17	+7.15
	Post-Monsoon	+0.14	+1.66	+9.96	-0.13	+11.38	+15.22
	Winter	-17.39	-10.32	+0.31	-14.90	+1.45	-5.27
3	Pre-Monsoon	-0.50	-8.08	-6.46	-4.60	+8.90	+10.40
	Monsoon	+3.93	-1.13	+3.69	-1.34	+15.17	+8.26
	Post-Monsoon	-0.66	+1.21	+9.04	-1.38	+10.58	+14.49
	Winter	-17.49	-10.80	-1.10	-16.23	-0.57	-5.93

Outlets: 1. Bhomoraguri, 2. Pandughat, 3. Pancharatna

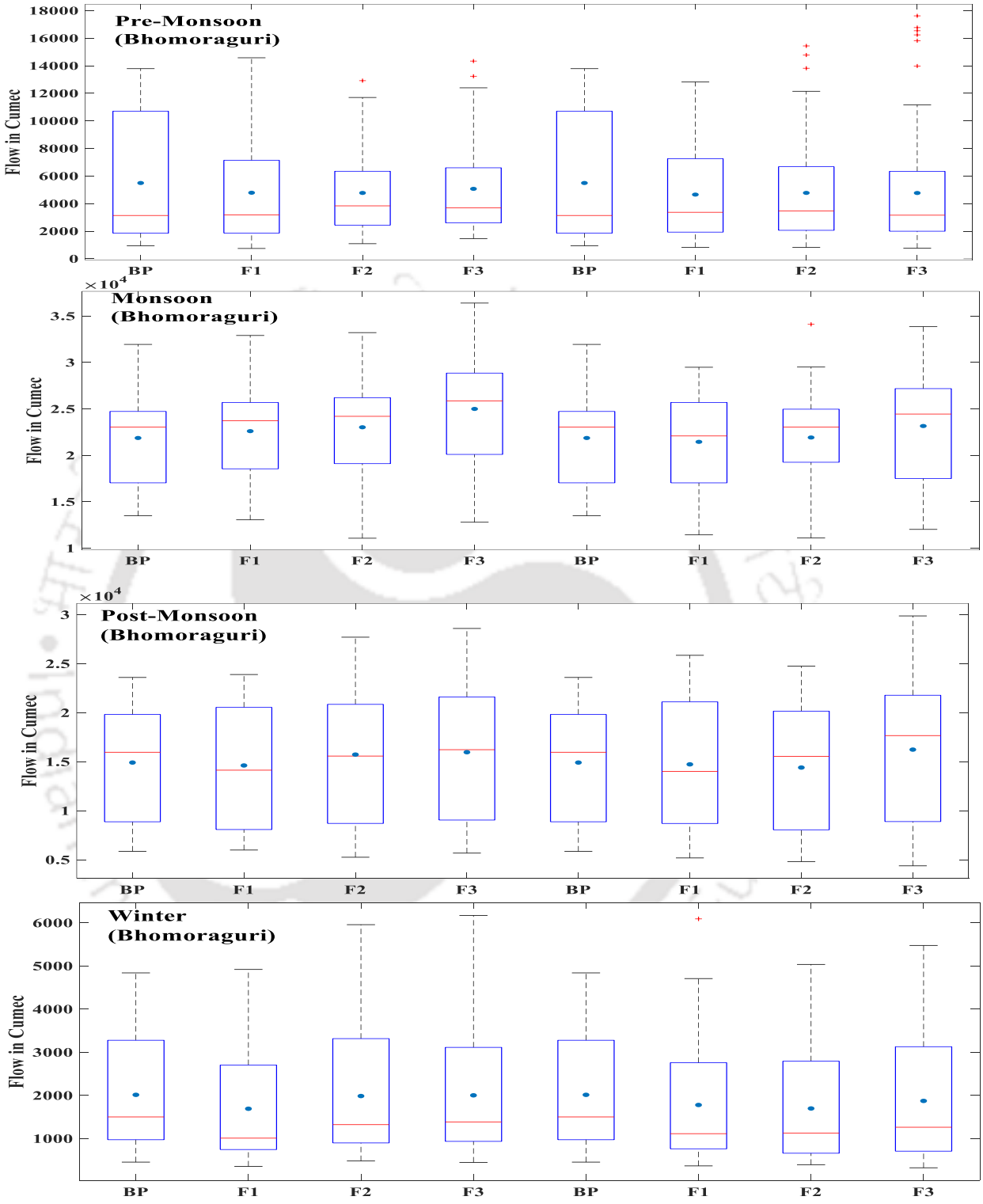

Fig. 8.4 Box plot for seasonal discharges at **Bhomoraguri**. Here, first four plots correspond to RCP4.5, and the rest four belongs to RCP8.5.

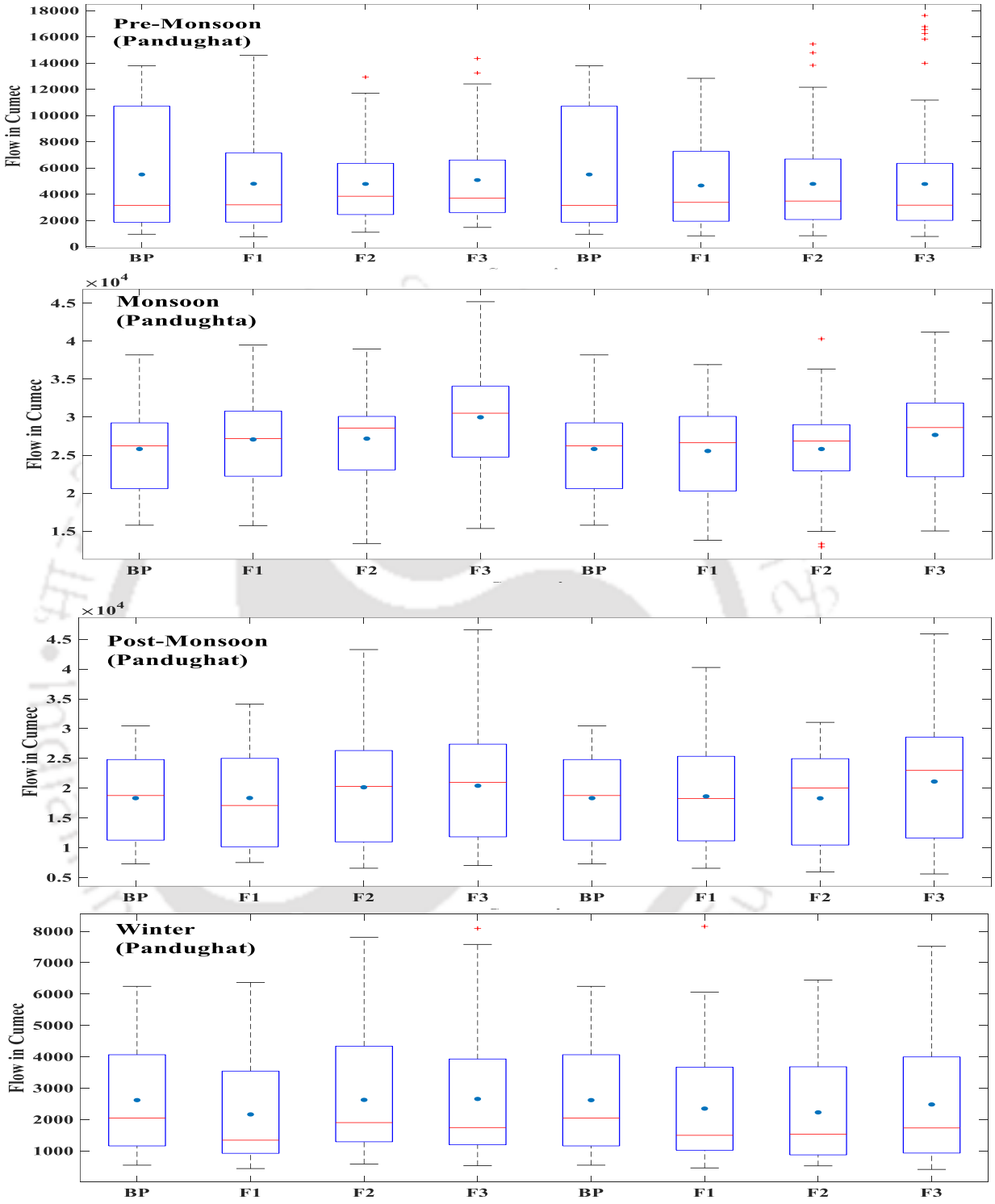

Fig. 8.5 Box plot for seasonal discharges at **Pandughat**. Here, first four plots correspond to RCP4.5, and the rest four belongs to RCP8.5.

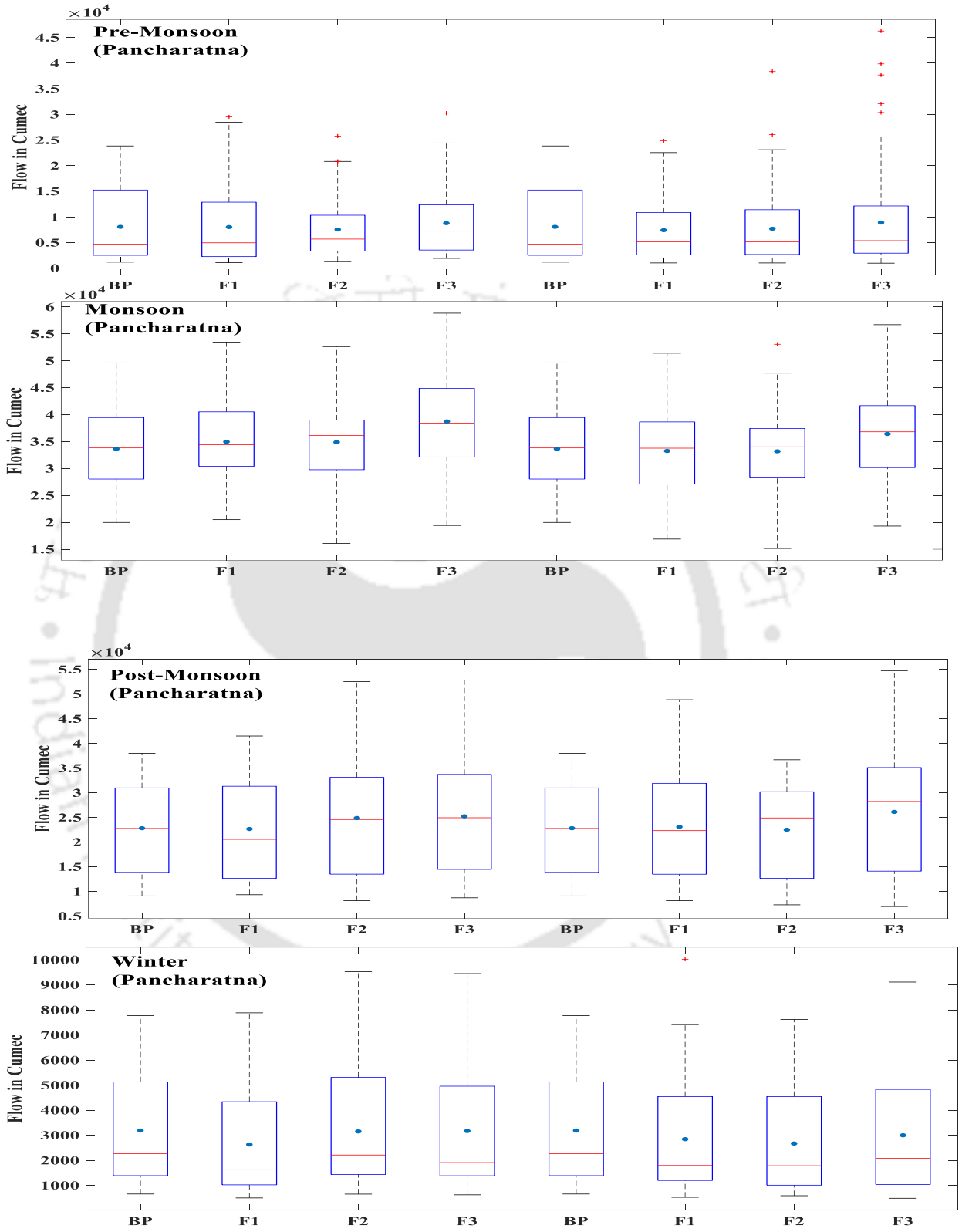

Fig. 8.6 Box plot for seasonal discharges at **Pancharatna**. Here, first four plots correspond to RCP4.5, and the rest belongs to RCP8.5.

The discharges during pre-monsoon and winter season would likely to decrease at majority of the locations, and under both the RCP scenarios. This is due to decrease in future annual rainfall values during the pre-monsoon as well as the winter seasons. Normally, the monsoon discharges during the present and future periods are higher than the other seasons. The Brahmaputra discharge during the monsoon season would rise upto 16.17% (Pandughat) under RCP4.5 and during F3 period. However, under RCP8.5, the rate of increase in discharges during post-monsoon season stands even higher than that of the monsoon season, particularly during F3 period. This may be due to shifting of the monsoon season towards the post-monsoon season. So, the global climate change would impact on the Brahmaputra basin hydrology in the forthcoming years.

8.2 Scope of strategic management for Brahmaputra basin

Climate change impact analyses show that the Brahmaputra would flow at higher rates than the present condition for majority of time periods, especially during 2071-2099. Here, the projected annual discharge will occur up to a maximum value of +13.06% at Pandughat, with respect to the base period. On the other hand, the seasonal discharges will even be greatly impacted due to climate change, and stands up to +15.22% during the post-monsoon period. Therefore, the concerned agencies need to develop certain strategies to combat the probable flood havoc during the future periods. These strategies may include redesigning the existing structures of flood protection viz. embankment, spurs, dikes etc. to make them capable to resist the flood pressure. A related strategy is flood proofing, which involves elevating critical places or equipment or placing it within waterproof containers or foundation systems. Another strategy may be implementing watershed management practices over selected locations of the Brahmaputra basin. This will preserve and restore the vegetated land cover in the watershed and thereby help managing the stormwater runoff. Watershed management at tributary catchment level will also reduce sediment yield to help maintaining carrying capacity of the channels downstream. Thus natural watershed hydrology will be maintained along with other benefits like increasing groundwater recharge, reducing runoff as well as sediment yield and improving the quality of runoff.

The discharge of the Brahmaputra river would significantly decrease during the winter as well as pre-monsoon seasons of the future periods. The maximum reduction in seasonal discharge will occur up to 17.49% as compared to the present condition. So, it becomes clear that the Brahmaputra basin would experience drought like situations in the pre-monsoon and winter seasons of the forthcoming decades. As such, adaptions strategies development is the need of time to combat the probable worse scenarios due to drought. Some strategies may include

- Constructing adequate infrastructure to enhance water storage capacity.
- Adopting Ecological Management Practices for ballancing water in different seasons.
- Creating awareness among the basin inhabitants to make habit of optimal use of water.
- Generating systems to minimize water loss and emphasize on recycle of water.
- Modifying water demand such as growing crops that require less water.

8.3 Conclusion

The Brahmaputra River basin is likely to get influenced by the global climate change. Due to the changes in future climatic variables, the basin hydrology would surely get altered. The annual precipitation, maximum temperature and minimum temperature are likely to increase during the next 79 years (2020-2099). As a result, there is likely to have impacts on the future river discharges. For RCP8.5 scenario, the annual flow of the Brahmpautra river at Pandughat may rise upto 13.06% during 2071-2099, than that of the base period (2006-2019). On the other hand, the post-monsoon discharges during the same period at the same location would even increase (upto 15.22%), for the same RCP scenario. As well, the future river flows, especially during the pre-monsoon and winter seasons at large, would decrease with respect to the base period. Therefore, increase in river flows would lead to severe flood and bank erosion, causing loss of property and life. On the other hand, decrease in river flows would lead to water deficit which may ultimately impact on agricultural and industrial production, navigation, power generation projects etc. of the Brahmaputra basin.

########## ##########

Chapter 9

Summary and Future Scope

9.1 Summary

The present study has been carried out to investigate the Brahmaputra river basin hydrologically. For this, a hydrologic model on SWAT platform was established to fulfill the various objectives planned herein this study. Besides, the impact of climate change on the Brahmaputra basin is evaluated for the present and future periods. Based on the selected objectives, following are the concluding remarks on the of the study.

9.1.1 Hydrologic modelling

- The Brahmaputra river basin encompasses four different nations viz. China, India, Bangkadesh and Bhutan. As such, hydrological modelling is a challenge, due to the hurdles in obtaining the hydro-climatic information beyond the national boundary. Therefore, development of mechanism for sharing data among the basin sharing co-nations is the need of time.
- Satellite estimations of weather data may suffer certain systematic errors, and therefore, their reliability should be checked prior to application in any water resource schemes. While evaluating the CFSR precipitation data, we found to have under-estimations in their estimates, than the gauge observations of the Brahmaputra basin. This information would be helpful to research community. It is obvious that the hydrologic models based on only the CFSR data, would lead to underestimated simulation results. Therefore, we used several sets of weather data, in combinations with this dataset to obtain satisfactory outputs during the model simulation.
- Choosing a hydrologic model for a complex and large river basin like the Brahmaputra is important. The Brahmputra basin is characterized by snow at its

source and ocean at its mouth, and has wide spatial variations in topography, landuse, soil properties and weather components. The present modelling study in SWAT platform provided us satisfactory replica of the basin hydrology. This is probably due to the capability of SWAT model to simulate basin hydrology by the way of considering several input data at fine resolution, even at the level of first order stream.

- The hydrologic model developed using the CFSR, IMD grid and China stations weather data provided the best satisfactory simulation results for the present basin. This model is found to be capable of providing reasonably balanced outputs at various drainage outlets considered across the Brahmaputra basin. The model simulated for the entire basin, and calibrated for discharge, at locations only within Indian boundary could be helpful to derive the outputs at any desired locations across the basin. Moreover, it can provide various information like sediment discharge, water quality parameters, ground water components etc., that would be helpful to the stake holders for Brahmaputra basin water resourves management.

9.1.2 Basin scale impact studies

- The SWAT hydrologic model for the transboundary Brahmaputra basin is capable to provide necessary outputs at the desired locations whether at the mainstem or at tributary. In fact, it is difficult to accurately capture the hydrology of each sub-basin, due to heteorogeneous characteristics of such as large river basin. However, a balanced output is provided by such a model satisfying the spatial variability of all the sub-basins' characteristics. For the data-scarced Brahmaputra basin, the present modelling approach would be helpful to derive desired outputs at any specified stream outlet that are necessary for basin planning and management. However, the basin impact causes of the present model are found to produce relatively inferior outputs at the tributary outlets, than the mainstem outlets. Therefore, a sub-basin needs to be modeled independently rather than deriving outputs at its outlets from the comprehensive large basin model. However, the comprehensive basin model can be a tool for deriving outputs at tributary outlets if modeling of the later is hard to exercise due to data scarcity situations.

9.1.3 Transboundary effects

- The Brahmaputra basin is quite susceptible to transboundary effects. China shares the largest part of the basin (≈ 51%), and therefore human induced activities thereon, would impact the basin hydrology at nations downstream. A reduction in the monthly discharges may occur upto 34% if 80% water is withdrawn from a reservoir constructed at a point before the Brahmaputra enters India. Here, the reduction corresponds to Indo-Bangla border, which is 915 km from the diversion site. This impact becomes very significant at the immediate downstream locations of the diversion site. Therefore, the present modelling approach could provide a science based element on the impacts due to transboundary conflicts, and they would be helpful in managing the water resources.

9.1.4 Climate change impact studies

- For analyzing the climate change impact assessment on the Brahmaputra basin, we utilized three GCMs of CMIP5 archive, viz. GFDL-ESM2M, HadGEM2-CC, and IPSL-CM5-1R. They were selected based on their data availability for both the present and future periods. We found computationally expensive to consider more than three GCMs for the large Brahmaputra river basin.
- Lest downscaling at 69 observed weather stations, we applied interpolation followed by bias correction of the GCM outputs. This was done because, as many as 25 GCM stations fall within the basin boundary, out of which 9 were found merely concentric to the gauge stations. Besides, downscaling techniques are not always guaranteed to provide the error-free results. Interestingly, the present approach resulted in satisfactory estimations of the GCM outputs after applying the interpolation as well as bias correction techniques. The bias corrected outputs, in many cases, were found to remain very close to the observed values of the Brahmaputra basin.
- The performances of GCMs were evaluated based on their ability to represent the weather data, at par the gauge observations during the present period. Here, we identified HadGEM2-CC as the most suitable, for the Brahmaputra basin, among all the GCMs selected in the present study. This particular GCM only is forwarded

for impacts of climate change study during the present and future periods. We divided the future periods (2020-2099) into three time scales as i) upto 2040, ii) upto 2070, and iii) upto 2099. Here, we could not consider the year 2100, because of data unavailability for the GCMs concerned.

- The global climate change is likely to impact the Brahmaputra basin in the coming days. The annual rainfall of the basin would increase upto 2.56 mm per year at the end of the current century, for RCP8.5 scenario. As such, the increased precipitation variability would lead to floods. On the other hand, the increase in temperature may also affect the basin hydrology in the forthcoming decades. Average maximum temperature of the basin may rise up to 0.062 ^{o}C/year till the year 2099. This would result in melting of glaciers over the Himalayan range of the basin area.
- The changes in rainfall and temperature due to climate change impacts would alter the basin hydrology in the forthcoming years, thereby affecting the quantity and quality of available water resources of the Brahmaputra. In case adequate measures against these impacts are not adopted, there is a possibility of increased competitions among various sectors like agriculture, ecosystems, settlements, industry, and energy.

9.1.5 Ptrojection of streamflow

- The streamflow of the Brahmaputra river at certain locations are predicted based on the simulation results of the SWAT hydrologic model. The bias corrected weather variables of HadGEM2-CC were utilized as input to the default model, to provide the outputs, both for the present and future time scales. For climate change impact analysis on river discharges, the model simulated values were utilized, corresponding to three important locations namely Bhomoraguri, Pandughat and Pancharatna.
- The river discharges are projected till 2099, and compared with respect to the base period (2006-2019) values. For RCP4.5 scenario, the climate change is not expected to impact largely, on annual discharge of the Brahmaputra river during F1 (2020-2040), F2 (2041-2070). However, this impact will be very significant till the

end of the current century. the annual discharge during F3 period would increase at higher rates, and the values are 8.47% (Bhomoraguri), 9.34% (Pandughat) and 9.93% (Pancharatna), all corresponding to RCP4.5.

- For RCP8.5, the Brahmaputra basin would experience deficit in annual discharges during F1 and F2 periods, due to the impact of climate change. This is due to decrease in annual rainfall values during these periods, as compared to the base period. The highest increase in annual discharge under RCP8.5 would occur at Pandughat (13.06 %), followed by Pancharatna (12.13 %), during 2071-2099, and with respect to the base periods. Whereas 'Bhomoraguri' is likely to have the least impact (3.93%) during that period.
- Climate change impact analysis showed a deficit in Brahmaputra basin rainfall values during the pre-monsoon and winter seasons of the future periods. As such, the discharges during those seasons would likely to decrease at majority of the locations, and corresponding to both the RCP scenarios almost throughout the running century.
- The river flows during monsoon period at all locations would increase under both RCP4.5 and RCP8.5 scenarios, with relatively lower rates of increase for the later. The highest increase in monsoon discharges may rise upto 16.17% at Pandughat during F3 period and under RCP4.5. The corresponding values at the other two outlets are +14.31% (Bhomoraguri) and +15.17% (Pancharatna).
- The post-monsoon discharges of the Brahmaputra will be impacted by the probable climate change during the forthcoming years. The rate of increase in discharges during post-monsoon season stands even higher than that of the monsoon season, particularly under RCP8.5 scenario of F3 timescale. This may be due to shifting of the monsoon season towards the post-monsoon season.
- Deficit in future river discharges during the pre-monsoon and winter seasons would lead to water deficit that may ultimately impact on agricultural and industrial production, navigation and power generation projects of the Brahmaputra basin. On the contrary, increase in the future river discharge, especially during monsoon and post-monsoon periods, would cause flood and bank erosion, thereby leading to loss of life and property.

- The findings of the climate change impact analysis would be helpful for policy making, planning and mitigation strategies to fight against the possible flood or drought scenarios of the Brahmaputra river basin.

9.2 Future scope

The scopes of future study may be recommended as follows:

- The CFSR rainfall values were found to be under-estimated than the actual gauge observations at the Brahmaputra basin. Therefore, we added few observed datsets to them, and used as input in the hydrological models that ultimately resulted in satisfactory replica of the basin hydrology. The model simulation could produce even better results provided we could have considered so many observed stations dataset at finer spatial resolution. Therefore, utilization of as many as observed weather stations datasets may lead to even better estimations of basin hydrology including transboundary and climate change effects. This may be undertaken as scope in future study.
- The hydrologic model established in the present study was calibrated for discharge at five locations only, that too within Indian boundary. This spatial calibration if done at several outlets uniformly distributed across the basin, would provide more judicious results, and this may be forwarded as a scope of future work.
- Basin impact study of the present SWAT model was done corresponding to only two tributary basins. The result may change if more tributary basins are considered across the entire basin, and may be undertaken as a future course of actions.
- It is heard from the media that China is constructing several dams and reservoirs on the Brahmaputra. Instead of a hypothetical reservoir, if we could consider a real case, the estimations of transboundary effects could have been more realistic. This may be considered as a path of future study.
- The structural parameters like reservoir volume, dam height, spillway height etc. if assumed different than the magnitudes taken in the present study would result in varying impacts. Therefore, the scope of future study lie in considering all possible

pros and coins along with adoptations of reservoir operation policies to accurately quantify the transboundary effects of the mighty Brahmaputra.

- In this study, we selected only three GCMs, for climate change impact analysis, out of which only one was identified as the best suitable for the present area. Then this particular GCM was forwarded for the CC impact analysis on the present and future hydro-climatic variables. Moreover, we adopted interpolation followed by bias correction of the raw GCM outputs. There is a scope of selecting several GCMs or its ensemble, and to adopt downscaling techniques while analyzing the climate change impacts of the Brahmaputra basin.

######## ########

References

Abbaspour KC, Rouholahnejad E, Vaghefi S, Srinivasan R, Yang H and Klove B (2015) A continental-scale hydrology and water quality model for Europe: Calibration and uncertainty of a high-resolution large-scale SWAT model. Journal of Hydrology 524 (2015) 733–752.

Abbaspour KC, Yang J, Maximov I, Siber R, Bogner K, Mieleitner J, Zobrist J, Srinivasan R (2007) Modelling hydrology and water quality in the pre-alpine/alpine Thur watershed using SWAT.Journal of Hydrology (2007) 333, 413– 430.

Adhikari U, Pouyan A, Herman MR, Messina JP (2017) Multiscale assessment of the impact of climate change on water resources in Tanzania. J. of Hydrol. Eng., ASCE. ISSN 1084-0699.

Akhtar MP, Sharma N, Ojha CSP (2011) Braiding process and bank erosion in the Brahmaputra River. Int J Sediment Res 26:431–444.

Aktar MN, Al Hossain BMT, Ahmed T (2015) Climate change impacts on water availability in the Brahmaputra basin. *5th International Conference on Water and Flood Management*.

Alam S, Ali MM, Islam Z (2016) Future streamflow of Brahmaputra River Basin under synthetic climate change scenarios. J. of Hydrol. Eng. 21(11):05016027.

Antonić O, Križan J, Marki A, Bukovec D (2001) Spatio-temporal interpolation of climatic variables over large region of complex terrain using neural networks. Ecol Modell 138:255–263.

Apurv T., Mehrotra R., Sharma A., Goyal M.K., Dutta S. (2015) Impact of climate change on floods in the Brahmaputra basin using CMIP5 decadal predictions. J. of Hydrolo. 527 (2015) 281–291.

Arnold JG, Moriasi DN, Gassman PW, Abbaspour KC, White MJ, Srinivasan R, Santhi C, Harmel R D, Griensven AV, Van Liew MW, Kannan N, Jha MK (2012) SWAT: model use, calibration, and validation, Journal of ASABE ---ISSN 2151-0032.

Barman S and Bhattacharjya RK (2015) Change in snow cover area of Brahmaputra river basin and its sensitivity to temperature, Environmental Systems Research 4 (1), 1-10.

Barnston AG, Thomas JL (1983) Rainfall measurement accuracy in FACE: A comparison of gauge and radar rainfall. J of Climate and applied meteorology, Volume 22, 2038-2052.

Bekiaris IG, Panagopoulos IN, Mimikou MA (2005) Application of the SWAT (SOIL AND WATER ASSESSMENT TOOL) model in the Ronnea catchment of Sweden. J. Global NEST, Vol 7, No 3, pp 252-257.

Bezbaruah D, Kotoky P, Baruah J, Sarma JN (2003). Geomorphological explanation of swamps along the Brahmaputra river channel, ASSAM. J. Geological Society of India, Vol. 62, pp. 605-613, Nov. 2003.

Bhatt CM, Rao GS, Begum A, Manjusree P, Sharma SVSP, Prasanna L, Bhanumurthy V (2013) Satellite images for extraction of flood disaster footprints and assessing the disaster impact: Brahmaputra floods of june-july 2012, ASSAM. J. Current Science, Vol. 104, No. 12.

Biemans H, Haddeland I, Kobat P, Ludwig F, Hutjes RWA, Heinke J, Bloh W, Gerten D (2011) Impact of reservoirs on river discharge and irrigation water supply during the 20th century. J. Water resources research, Vol. 47, W03509, doi:10.1029/ 2009WR008929.

Blackmore D (2006). "Management structures to lead the Brahmaputra basin into the 21 century." (This paper was commissioned as an input to the study on Natural Resources, Water and the Environment Nexus for Development and Growth in Northeast India).

Blacutt LA, Herdies DL, Goncalves LG, Vila DA, Andrade M (2015) Precipitation comparison for the CFSR, MERRA, TRMM3B42 and Combined Scheme datasets in Bolivia. Journal of Atmospheric Research 163 (2015) 117–131.

Bora M, Goswami DC (2015) A study on seasonal and temporal variation in physico-chemical and hydrological characteristics of river kolong at nagaon town, Assam, India. Scholars Research Library, Archives of Applied Science Research, 2015, 7(5): 110-117. ISSN 0975-508X.

Borah DK, Bera M (2004) Watershed-scale hydrologic and nonpoint-source pollution models: Review of applications. Trans. ASAE 47(3): 789-803.

Borah J, Ahmed MF, Sarma PK (2010) Brahmaputra river islands as potential corridors for dispersing tigers: a case study from Assam, India. International Journal of Biodiversity and Conservation Vol.2(11),pp 350-358, November 2010..

Borah T, Mahanta C (2006) Modelling Approach to Sediment Concentration and Key Parameters in a Part of the Brahmaputra River. Thesis, M.Tech in Water Resources, IITG.

Bou AE, Velazquez MP, Velazquez DP (2017) Economic value of CC adaptation strategies for WR mangt in Spain's Jucar basin. J. of Hydrolo. Eng. ASCE. ISSN 0733-9496.

Brath A, Montanari A, Toth E (2004) Analysis of the effects of different scenarios of historical data availability on the calibration of a spatially-distributed hydrological model. Journal of Hydrology 291 (2004) 232–253.

Chen J, Brissette FP, Leconte R (2011) Uncertainty of downscaling method in quantifying the impact of climate change on hydrology. J Hydrol. 401:190–202.

Chen L, Xu J, Wang G, Liu H, Zhai L, Li S, Sun C, Shen Z (2018) Influence of rainfall data scarcity on non-point source pollution prediction: Implications for physically based models. Journal of Hydrology 562 (2018) 1–16.

Chetry R (2014) The dynamics in channel shift of the Brahmputra along the agyathuri-sualkuchi area of Kamrup district, ASSAM. J. European Scientific, Vol.10, No.35, 2014 ISSN:1857-7881.

Chowdhury R, Ward N (2004) Hydro-meteorological variability in the greater Ganges–Brahmaputra–Meghna basins. J. of Climatology, Vol.24, Issue.12 pp.1495-1508, 2004.

Daggupati P, Yen H, White MJ, Srinivasan R, Arnold JG, Keitzer CS, Sowa SP (2015) Impact of model development, calibration, and validation decisions on hydrological simulations in West lake Erie basin. J. of Hyd. Processes. DOI: 10.1002/hyp.10536.

Dahal V, Shakya NM, Bhattarai R (2016) Estimating the impact of climate change on water availability in Bagmati Basin, Nepal. Environ. Process.3: 1. https://doi.org/10.1007/s40710-016-0127-5.

Das J, Umamahesh NV (2017) Uncertainty and nonstaionarity in streamflow extremes under climate change scenario over a river basin. J. of Hydrolo. Eng., ASCE. ISSN 1084-0699.

Das TK, Haldar SK, Gupta ID, Sen S (2014) IMPACT OF RIVER BANK EROSION." Living Reviews of Landscape Research, 8(2014),3.

Deka SK, Sarma AK (2011) Impact of climate change on precipitation characteristics of Brahmaputra basin. Technical Report submitted to the Ministry of Water Resources, July'2011.

Deori DJ, Abujam S (2015) Fish Diversity and Habitat Ecology of Dihing River- a Tributary of Brahmaputra River. Journal of Fisheries and Aquatic Studies, 2015, ISSN:2347-5129.

Derry LA, Stedinger JR, Duncan CC (2007) A Simple Predictive Tool for Lower Brahmaputra River Basin Monsoon Flooding. Earth Interactions, Volume 11, No. 21, pp-1, 2007.

Dinku T, Connor S, Ceccato P (2011) Evaluation of satellite rainfall estimates and gridded gauge products over the Upper Blue Nile region. In: Melesse A.M. (eds) Nile River Basin. Springer, Dordrecht,109–127, DOI: 10.1007/978-94-007-0689-7.

Draper S, Kundell J (2007) Impact of CC on transboundary water sharing. J. WR Plan & Mangt. ASCE, ISSN 0733-9496.

Dutta MK, Barman S, Aggarwal SP (2010) A study of erosion-deposition processes around Majuli island, Assam. J. of Earth Science India, Vol.3(IV), Oct'2010, pp. 206-216, ISSN: 0974 – 8350.

Dutta P, Sarma AK (2020) Hydrological modelling as a tool for water resources management of the data-scarced Brahmaputra basin. Journal of Water and climate change, doi/10.2166/ wcc.2020.186/ 670198/jwc2020186.

Espinosa B, Hromadka TV, Perez R (2015) Comparison of radar data versus rainfall data. Journal of MethodsX 2 (2015) 423–431. DOI.org/10.1016/j.mex.2015.10.007.

Eum H, Sredojevic D, Slobodan P (2011) Engineering procedure for the climate change flood risk assessment in the upper Thames river basin. J. of Hydrolo. Eng., ASCE, ISSN 1084-0699/2011/7-608–612.

Finsen F, Milzow C, Smith R, Berry P, Gottwein PB (2014) Using Radar Altimetry to Update a Large-Scale Hydrological Model of the Brahmaputra River Basin. Hydrology Research, 45.1, 2014.

Fischer S (2015) Sensitivity of Sediment Transport on River Characteristics in the Large, Braided Brahmaputra River. Thesis for M.Tech, Stockholm University, 2015.

Flato G, Marotzke J, Abiodun B, et al. (2014) Evaluation of climate models. In: Climate change 2013: the physical science basis. Contribution of Working Group I to the Fifth Assessment Report of the Intergovernmental Panel on Climate Change. Cambridge Univ. Press, pp 741–866.

Fohrer N, Haverkamp S, Eckhardt K, Frede HG (2001) Hydrologic Response to Land Use Changes on the Catchment Scale. J. of Phys. Chem.Earth (B),Vol. 26, No. 7-8, pg. 577-582.

Forsee WJ, Ahmed S (2011) Evaluating urban storm water infracture design in response to projected climate change. J. of Hydrolo. Eng., ASCE. ISSN 1084-0699/2011/11-865–873.

Gain AK, Giupponi C (2015) A Dynamic Assessment of Watre scarcity risk in the Lower Brahmaputra river basin:An integrated approach. J. of Eclogical Indicator, 2015.

Garimella B, Sarma AK (2007) 1 -D & 2 -D River Modelling Using Mike 11 and Mike 21 C. BTP, IITG.

Gassman P, Reyes M, Green C, Arnold JG (2007) The Soil and Water Assessment Tool: Historical development, applications, and future research directions. J of ASABE 50(4):1211–1250.

Ghosh S, Dutta S (2012) Impact of Climate Change on Flood Characteristics in Brahmaputra Basin Using a Macro-Scale Distributed Hydrological model. J. Earth Syst. Sci, 121, No. 3, pg. 637-657.

Girija TR, Mahanta C, Chandramouli V (2007) Water Quality Assessment of an Untreated EffluentImpacted Urban Stream: The Bharalu Tributary of the Brahmaputra River, India. J. Environ Monit Assess (2007) 130:221–236.

Gogoi C, Goswami DC (2013) A study on bank erosion and bank line migration pattern of the Subansiri river in Assam using remote sensing and GIS technology. The international Journal of Engineering And Science (IJES), Vol 2, Issue 9, pp-1-6, 2013. ISSN(e):2319-1813 ISSN(p): 2319-1805.

Gogoi MP, Gogoi B, Hazarika S, Borgohain P (2012) GIS based study on fluvio-morphology of the river Brahmaputra in part of upper Assam, NE India. J of Frontline Research, Vol.: 02 (2012), 114-121, ISSN: 2249-9903.

Goswami DC (1985) Brahmaputra River, Assam, India: Physiography, Basin Denudation and Channel Aggradation. Water Resources Research, VOL. 21, NO. 7, Pg 959-978, JULY 1985.

Goyal M. (2014) Statistical Analysis of Long Term Trends of Rainfall During 1901–2002 at Assam, India; J. of Water Resource Mngt (2014) 28: 1501-1515.

Grimes DIF, Diop M (2003) Satellite-based rainfall estimation for river flow forecasting in Africa .I: Rainfall estimates and hydrological forecasts. J. Hydrological Sciences 48(4) August 2003.

Grizzetti B, Bouraoui F, Granlund K, Rekolainen S, Bidoglio G (2003) Modelling diffuse emission and retention of nutrients in the Vantaanjoki watershed (Finland) using the SWAT model. Ecological Modelling 169 (2003) 25–38. doi:10.1016/S0304-3800(03)00198-4.

Gruber A, Levizzani V (2008) Assessment of Global Precipitation Products: A project of the World Climate Research Programme. Report No. 128, WMO T.D no. 1430, available at: www.researchgate.net.

Guo R, Liu Y (2016) Evaluation of Satellite Precipitation Products withRain Gauge Data at Different Scales: Implications for Hydrological Applications. Journal: Water, DOI:10.3390/ w8070281. www.mdpi.com/journal/water.

Gupta HV, S Sorooshian and Yapo PO (1999) Status of automatic calibration for hydrologic models: comparison with multi-level expert calibration. J of Hydrologic Engg 4(2):135-142.
Gupta PK, Panigrahy S, Parihar JS (2011) Impact of Climate Change on Runoff of the Major River Basins of India Using Global Circulation Model (HadCM3) Projected Data. Journal: Indian Society of Remote Sensing, 39(3):337–344, 2011.
Guse B, Pfannerstill M, Fohrer N (2015) Dynamic modeling of land use change impacts on Nitrate loads in rivers. Environ. Process.2: 575. https://doi.org/10.1007/s40710-015-0099-x.
Hanumagutti SR (2006) Water quality modelling of river Brahmaputra using multivariate statistical technique." BTP,IITG.
Hazarika J, Sarma AK (2013) Identifying homogeneous climatic regions in Brahmaputra -barak basin using fuzzy clustering concept and analysing impact of climate change on Barak basin. Technical Report submitted to the Ministry of Water Resources, October'2013.
Hazarika N, Das AK (2014) Process Dynamics and Controls in Two Partially-Confined Rivers of Upper Brahmaputra Plain. Journal of Geomatics and Geosciences, Vol. 5, No.1, 2014.
Hazarika S (2012) In Assam, Brahmaputra River remains uncontrollable." Article in "The New York Times, July 9, 2012.
Hempel S, Frieler K, Warszawski L, Schewe J, Piontek F (2013) A trend-preserving bias correction – The ISI-MIP approach. Earth System Dynamics Discussions. 4. 49. 10.5194/esdd-4-49-2013.
Hinge G, Surampalli RY, Goyal MK (2018) Prediction of soil organic carbon stock using digital mapping approach in humid India. Environ Earth Sci 77:. doi: 10.1007/s12665-018-7374-x.
Hudson G, Wackernagel H (1994) Mapping temperature using kriging with external drift: theory and an example from Scotland. Int J Climatol 14:77–91.
Hughes DA (2006) Comparison of satellite rainfall data with observations from gauging station networks. Journal of Hydrology (2006) 327, 399– 410.
Jain A, Sarma AK (2003) Developing a GIS Depicting Erosion Pattern of Majuli River Island Using Remote Sensing Imageries. BTP, IITG.
Jang T, Kim H, Kim S, Seong C, Park S (2012) Assessing Irrigation Water Capacity of Land Use Change in a Data-Scarce Watershed of Korea. J. of Irrig. Drain Eng., 2012, 138(5): 445-454.
Javanmard S, Yatagai A, Nodzu MI, Jamali JB, Kawamoto H (2010) Comparing high-resolution gridded precipitation data with satellite rainfall estimates of TRMM 3B42 over Iran. Advances of Geo-science, 25, 119–125, 2010. DOI:10.5194/adgeo-25-119-2010.
Jha M (2009) Hydrologic Simulations of the Maquoketa River Watershed Using SWAT. www.card.iastate.edu.
Jha MK, Gassman PW (2014) Changes in hydrology and stream flow as predicted by modeling experiment forced with climate model. Hydrological Processes 28: 2772-2781.
Johnson T, Butcher J, Parkar A, Weaver CP (2012) Invest. The sensitivity of U.S. streamflow and water quality to CC. J. WR Plan & Mangt. ASCE, ISSN 0733-9496.
Kalita HM, Sarma AK (2014) Optimal Protection Measures For Controlling River Bank Erosion. Phd thesis, IITG.
Kamal Y, Sarma AK (2008) Numerical Simulation of River Flow. BTP, IITG.
Kannan N, Santhi C, Di Luzio M, Potter S, Arnlod JG (2005) Measuring environmental benefits of conservation practices: the conservation effects assessment project (CEPA)- A model calibration approach at the national level 2005. ASAE Annual International Meeting.
Katkar M, Sarma AK (2009) GIS based Geomorphological Study of River Brahmaputra, Assam. Thesis for M.Tech in Water Resources, IITG.
Kendall MG (1975) Rank Correlation Methods, 4th edn. Charles Griffin, London.
Kerim A, Sarma AK (2017) Impact of spatial data availability on climate change prediction in the Weyib river basin in Ethiopia". Water Res. Management (Springer).
Kotoky P, Sarma JN (2001) Hydrogeomorphological studies of the brahmaputra river channel from Majuli to Kaziranga- -an apprisal of its bank erosion and flood problem. Project Sponsored by Dept. of Science & Technology, Govt. of India, 2001.

Kotoky P, Bezbaruah D, Baruah J, Sarma JN (2003) Erosion activity on Majuli-the largest river island of the world. J. Current Science, Vol. 84, No. 7, 10 April, 2003.
Kotoky P, Bezbaruah D, Baruah J, Borah GC, Sarma JN (2006) Characterization of clay minerals in the Brahmaputra river sediments, ASSAM, INDIA. J. Current Science, Vol. 91, No.9.
Koutsouris AJ, Chen D, Lyon SW (2016) Comparing global precipitation data sets in eastern Africa: a case study of Kilombero Valley, Tanzania. Int. J. Climatol.36: 2000–2014.
Kumar AK, Dutta S (2008) Identification of Climatic Change Sensitive Land Use and Land Cover in the Brahmaputra basin using Vegetation Indices and Topography Dataset. BTP, IITG.
Kumar R, Chatterjee C (2005) Regional Flood Frequency Analysis Using L-Moments for North Brahmaputra Region of India. J. of Hydrolo. Eng., (ASCE) ,Vol..10, No.1, pp.1-7, 2005.
Lahiri, SK, Sinha R (2012) Tectonic Controls on the Morphodynamics of the Brahmaputra River System in the Upper Assam Valley, India. ELSEVIER, Geomorphology.
Latif A (1969) Investigation of Brahmaputra River. Journal of Hydraulic Engg. (ASCE) Vol.95 No.5, pp.1687-1698, 1969.
Lazoglou G, Anagnostopoulou C, Skoulikaris C, Tolika K (2019) Bias Correction of Climate Model's Precipitation Using the Copula Method and Its Application in River Basin Simulation.Water 2019, 11, 600.
Lee A, Cho S, Kang D, Kim S (2014) Analysis of the effect of climate change on Nakdong river streamflow using indicators of hydrologic alterations. J. of Hydro-environment Research. doi.org/10.1016/j.jher.2013.09.003
Lee T, Srinivasan R, Moon J, Omani N (2011) Estimation of fresh water inflow to bays from gaged and ungaged watershed. ASABE, Vol. 27(6): 917-923. ISSN 0883-8542.
Lempert M, Ostrowski M (2002) A hydrologic model to bridge the gap between conceptual and physically based approaches. https://www.researchgate.net/publication/ 250929031.
Li Li, Hao ZC, Wang JH, Yu ZB (2008) Impact of future climate change on runoff in the head region of Yellow river. J. of Hydrolo. Eng., ASCE. ISSN 1084-0699/2008/5-347–354.
Li BS, Zhou PJ, Wang XY et al. (2013) Opportunities and Eco-environmental Influence of Cascade Hydropower Development and Water Diversion Projects in Hanjiang River Basin.J. Geol. Society of India. 82: 692. https://doi.org/10.1007/ s12594-013-0207-3.
Liechti CT, Matos JP, Boillat JL, Schleiss AJ (2012) Comparison and evaluation of satellite derived precipitation products for hydrological modeling of the Zambezi River Basin. Hydrol. Earth Syst. Sci. 16: 489–500, doi: 10.5194/hess-16-489-2012.
Madadgar S.and Moradkhani S (2013) Drought analysis under climate change using COPULA. J. of Hydrolo. Eng,, ASCE, ISSN1084-0699/2013/7-746-759.
Mahanta C, Sarma AK, Sarma B (2011) Water Quality Degradation in the Tributaries of the Brahmaputra-Barak Basin and Their Environmental Management Strategies. World Environmental and Water Resources Congress, pg:4636-4648.
Maheshwari R, Sarma AK (2005) Streamflow Forecasting For Brahmaputra River: A Time Series and Neural Network Approach. BTP, IITG.
Mandal KL, Bhattacharjee T, Dasgupta R (2006) Environment Friendly Seismic Surveys in Logistically Difficult Areas within Brahmaputra River Bed—A Case Study. 6th International Conference & Exposition on Petroleum Geophysics, Kolkata.
Mandal S (2005) Water quality evaluation in an urban stretch of Brahmaputra river using WQI and Regression analysis. Thesis for M.Tech in Water Resources, IITG, 2005.
Mann HB (1945) Nonparametric Tests Against Trend. Econometrica 13:245–259.
Masunga H, Iguchi T, Oki R, Kashi M (2002) Comparison of Rainfall Products Derived from TRMM Microwave Imager and Precipitation Radar. Journal of applied meteorology, American Meteorological society, Volume 41, pg 849-862.
Mikhailov VN, Dotsenko MA (2006) Peculiarities of the Hydrological Regime of the Ganges and Brahmaputra River Mouth Area. Water Resources, 2006, Vol. 33, No. 4, 2006 ISSN 0097-8078.

Miller W, Butler R, Piechota T, Praire J, Grantz K, Derosa G (2012) Water mangt decisions using multiple hyd. Model within S.J. river basin under CC conditions. J. WR Plan & Mangt. ASCE, ISSN 0733-9496.

Mitchell TD, Jones PD (2005) An improved method of constructing a database of monthly climate observations and associated high-resolution grids, Int. Journal of. Climatol., 23, 693–712.

Mohammadi SA, Azadi M, Rahmani M (2017) Comparison of spatial interpolation methods for gridded bias removal in surface temperature forecasts. J Meteorol Res 31:791–799.

Mohammed K, Saiful IAKM, Tarekul IGM, Alfieri L, Bala SK, Uddin KMJ (2017) Impact of high-end climate change on floods and low flows of the Brahmaputra River. *J. of Hydrolo. Eng.*, ASCE, 22(10), 4017041.

Moriasi DN, Rossi CG, Arnold JG, Tomer MD (2012) Evaluating hydrology of SWAT with new tile drain equations. J. Soil Water Cons. 67(6), 513-524. DOI.10.2489/jswc.67.6.513.

Moriasi DN, Arnold JG, Van LM, Bingner R, Harmel RD, Veith T (2007) Model Evaluation Guidelines for Systematic Quantification of Accuracy in Watershed Simulations. Transactions of the ASABE. 50. 10.13031/2013.23153.

Mukherjee A, Sarma AK (2006) 2D Flow Simulation In Alluvial River Using MIKE Software. MTP, IITG.

Mukherjee N, Khan MFA, Hossain BMTA, Islam AKMS, Aktar MN, Rahman S (2011) A Hybrid approach for climate change scenario generation for Bangladesh using GCM model results. 3rd International Conference on Water & Flood Management (ICWFM-2011**).**

Nandi A, Mahanta C (2014) Sediment Budget, Local Transport Capacity Estimates and 1D Sediment Transport Modelling in a Large Alluvial River. Thesis of M.Tech.,IITG, 2014.

Neitsch SL, Williams J, Arnold JG, Kiniry J (2011) Soil and water assessment tool documentation version 2009. Technical report, Texas water resources institute.

New M, Hulme M, Jones P (2000) Representing twentieth-century space-time climate variability, Part II: Development of 1901–96 monthly grids of terrestrial surface climate, J. Climate, 1(3),2217–2238, 2000.

Nyatuame M, Gyimah VO, Ampiaw F (2014) Statistical Analysis of Rainfall Trend for Volta Region in Ghana. Int. Journal of Atmospheric Sciences. DOI:org/10.1155/2014/203245.

Nyeko M (2015) Hydrologic Modelling of Data Scarce Basin with SWAT Model: Capabilities and limitations. J. of Water Resour Manage (2015)29:81–94DOI 10.1007/s11269-014-0828-3.

Pande S, Savenije H, Bastidas LA, Gosain AK (2012) A Parsimonious Hydrological Model for a Data Scarce Dryland Region. J. of Water Resour Manage (2012) 26:909–926. DOI 10.1007/s11269-011-9816

Patil M (2013) Impact of climate change on stream flow of Ranganadi hydropower project." MTP,IITG.

Perambudoor S (2005) Reservoir Operation Policy Considering the Environmental Aspects. MTP, IITG.

Pervez S, Henebry GM (2015) Assessing the impact of climate and land use land cover change on fresh water availability in the Brahmaputra basin. J. of Hydrol. doi.org/10.1016/j.ejrh.2014.09.003

Phan DB, Wu CC, Hsieh SC (2011) Impact of CC on stream discharge and sediment yield at N.Vietnam. J. of W. Resources. ISSN 00978078.

Phukan A,Goswami R, Borah D, Nath A, Mahanta C (2012) River Bank Erosion and Restoration in the Brahmaputra River in India. The Clarion: Multidisciplinary International Journal, Vol.1 , NO. 1, PP:1-7, 2012, ISSN:2277-1697.

Ploeg MJVD, Haldorsen S, Leijnse A, Heim M (2012) **Sub permafrost groundwater systems: dealing with virtual reality while having virtually no data.** J. Hydrol., 475 (2012), pp. 42-52, 10.1016/j.jhydrol. 2012.08. 046.

Prasad YR, Dutta S (2009) Bank Erosion Prediction in an Alluvial River Bed. MTP, IITG.

Prudhomme C, Giuntoli I, Robinson E, Clark D, et al. (2014) Hydrological droughts in the 21st century, hotspots and uncertainties from a global multimodel ensemble experiment. Proceedings of the National Academy of Sciences, https://doi.org/10.1073/pnas.1222473110.

Pumo D, Arnone E, Francipane A Carracilo D and Noto L (2017) Potential implications of CC and urban. on w/s hydrology. J. of Hydr.ology.

Qi C, Grunwald S (2005) GIS-based hydrologic modeling in the Sandusky watershed using SWAT. American Society of Agricultural Engineers Vol. 48(1): 169−180, ISSN 0001-2351.

Ramirez-Villegas J, Challinor AJ, Thornton PK, Jarvis A (2013) Implications of regional improvement in global climate models for agricultural impact research. Environ Res Lett 8:24018

Rao KHVD, Bhanumurthy V, Roy PS (2009) Application of Satellite - based Rainfall Products and SRTM DEM in Hydrological Modelling of Brahmaputra Basin. J. Indian Soc. Remote Sens. (December 2009) 37:587–600.

Ravindra K, Dutta S (2011) Mapping and Modelling of Braided River Morphology. MTP,IITG.

Reddy KRP (2005) Water quality evaluation in an urban stretch of Brahmaputra river using QUAL2K. BTP, IITG, 2005.

Reddy NN, Sreeja P (2011) Streamflow Forecasting For Brahmaputra River. BTP,IITG.

Richardson WR, Thorne CR (1998) Secondary Currents around Braid Bars in Brahmaputra River, Bangladesh. Journal of Hydraulic Engineering, (ASCE) Vol.124, No.3.

Romilly TG, Gebremichael M (2011) Evaluation of satellite rainfall estimates over Ethiopian river basins. Hydrol. Earth Syst. Sci.15:1505–1514, doi: 10.5194/ hess-15-1505-2011.

Rosenberg NJ, Epstein DJ, Wang D, Vail L, Srinivasan R, Arnold JG (1999) Possible impacts of global warming on the hydrology of the Ogallala aquifer region. J of Climate Change 42(4): 677-692.

Rossi M, Kirschbaum D, Valigi D, Mondini AC, Guzzetti F (2017) Comparison of Satellite Rainfall Estimates and Rain Gauge Measurements in Italy, and Impact on Landslide Modeling. Journal of Climate, doi:10.3390/cli5040090. www.mdpi.com/ journal/ climate, 2017.

Roy D, Barr J, Venema HD (2011) Ecosystem approaches in integrated water resources management (IWRM): A review of transboundary river basins. UNEP and IISD. Retrieved from http://www.iisd.org/publications/ecosystem-approaches-integrated-water-resources-anagement- iwrm-review-transboundary

Roy P, Hussain Z (2014) Magnitude of floods and its consequences in Puthimari river basin of Assam, India. European Academic Research Vol. II, Issue 2, May 2014. ISSN 2286-4822.

Saharia AM; Sarma AK (2018) Future climate change impact evaluation on hydrologic processes in the Bharalu and Basistha basins using SWAT model. J. Nat Hazards, 92:1463–1488, https://doi.org/10.1007/s11069-018-3259-2.

Sankhua R (2005) ANN Based Spatio-Temporal Morphological Model of River Brahmaputra. Phd Thesis, IITRoorkee, 2005.

Sankhua RN, Sharma N, Pandey AD (2006) Application of artificial neural network for daily river stage forecast in the river Brahmaputra. J. of Water and Energy, Vol : 63, Issue : 3,pp: 55-62.

Sapiona MRP, Arkin PA (2008) An Intercomparison and Validation of High-Resolution Satellite Precipitation Estimates with 3-Hourly Gauge Data. American Meteorological Society. DOI: 10.1175/2008JHM1052.1.

Sarkar A, Garg RD, Sharma N (2012) RS-GIS Based Assessment of River Dynamics of Brahmaputra River in India. Journal of Water Resource and Protection, 2012, 4, 63-72.

Sarma AK, Singh VP (2017) "Chapter 105-Brahmaputra river basin", In Singh VP (editor), Handbook of Applied hydrology, 2nd ed., McGraw-Hill Education, New York, 2017.

Sarma D, Sarma AK (2010) Analysis of Extreme Stream Flow Condition in Brahmaputra River. MTP, IITG.

Sarma JN, Acharjee S (2012) A GIS based study on bank erosion by the river Brahmaputra around Kaziranga National Park, Assam, India. J. Earth System Dynamics.. DOI: 10.5194/esdd-3-1085-2012.

Sarma JN (2005) Fluvial Process & morphology of the Brahmaputra River in Assam, India. J. Geomorphology 70(2005) 226-256.

Sarma JN, Borah D, Goswami U (2007) Change of River Channel and Bank Erosion of the Burhidihing River, Assessed using Remote Sensing and GIS. Journal of Indian Society of Remote Sensing, Vol.35, No.1, 2007.

Sarma JN, Phukan M (2006) Bank erosion and bankline migration of the Brahmaputra River in Assam during the twentieth century. Journal of the Geological Society of India. 68. 1023-1036.

Sarthi PP, Kumar P, Ghosh S (2016) Possible future rainfall over Gangetic Plains (GP), India,in multi-model simulations of CMIP3 and CMIP5. J. Theor Appl Climatol (2016) 124:691–701. DOI 10.1007/ s00704-015-1447-5.

Saxena U, Mahanta C (2006) Heavy Metal Distribution Studies in Brahmaputra Floodplains adjoining Guwahati City. BTP, IITG.

Schipper L, Pelling M (2006) Disaster risk, climate change and international development: scope for, and challenges to, integration. Disasters, 2006, 30(1): 19−38. https//doi.org/10.1111/j.1467-9523.2006.00304.x.

Schulz J, Albert P, Behr H D, Caprion D, et al. (2009) Operational climate monitoring from space: the EUMETSAT Satellite Application Facility on Climate Monitoring (CM-SAF), Atmos. Chem. Phys., 9, 1687–1709, DOI:10.5194/acp-9-1687-2009.

Seibert J, McDonnell J (2002) On the dialogue between experimentalist and modeler in catchment hydrology: use of soft data for multicriteria model calibration. W R Research 38: 23-1-23-14. DOI.10.1029/2001WR000978.

Sen PK (1968) Estimates of the Regression Coefficient Based on Kendall's Tau. J Am Stat Assoc 63:1379–1389. doi: 10.1080/01621459.1968.10480934.

Sharma N, Ashargie A (2012) Simulation Study for Channelization of the Brahmaputra river in Assam. J. Water and Energy International, Vol.69,Issue 6, 2012.

Sharma N, Pandey AD, Venkatesh K (2004) ANN Model Development for Bank-Line Migration of River Brahmaputra Using Remote Sensing Data. ISH J. of Hydraulic Engineering, Vol.10, No. 1.

Sharma N, Akhtar M, Zeleke B (2011) Satellite Data Based Impact Assessment of Basin Characteristics for Brahmaputra River System of India. World environmental and water resource congress 2011, ASCE.

Shepherd B, Harper D, and Millington A (1999) Modeling catchment-scale nutrient transport to watercourses in the U.K.Hydrobiologia395-396: 227-237.

Shil P (2010) Water Quality Evaluation in a Part of the Ghorajan Stream, A Tributary to the Brahmaputra River. Thesis for M.Tech in Water Resources, IITG.

Shivam, Goyal MK, Sarma AK (2016) Analysis of the change in temperature trend in Subansiri river basin for RCP scenario using CMIP5 datasets. J. Theor Appl Climatology, 129, 1175–1187 (2017). https://doi.org/10.1007/s00704-016-1842-6

Shrestha M, Acharya SC, Shrestha PK (2017) Bias correction of climate models for hydrological modelling–are simple methods still useful? Meteorol Appl 24:531–539.

Siddiqui SA, Hossain MA (2015) Development of a Sequential Artificial Neural Network for Predicting River Water Levels Based on Brahmaputra and Ganges Water Levels. J. Neural Computing and applications, Vol. 26, issue 8, 2015.

Sikder S, Chen X, Hossain F (2016) Are General Circulation Models Ready for Operational Streamflow Forecasting for Water Management in the Ganges and Brahmaputra River Basins? American Meteorological Society Journal: Vol. 17 Issue 1.

Simonovic S, Li L (2003) Met for assessment CC impacts on large scale flood protection system. J. WR Plan & Mangt. ASCE, ISSN 0733-9496.

Singh S, Sarma AK (2014) A Study on Scouring around Bridge Piers. M.Tech Thesis.,IITG, 2014.

Singh SK, Reisberg L, Lanord ZF (2003) Re-Os isotope systematic of sediments of the Brahmaputra River system. Geochimica et Cosmochica Acta, Vol. 67, No.21, pg.4101-4111, 2003.

Singh V, Goyal MK (2017) Unsteady high velocity flood flows and the dev. of rating curves in a Himalayan basin under CC scenarios. J. of Hydrolo. Eng., ASCE. ISSN 1084-0699.

Singh VP, Frevert DK (2006) (editors) Watershed Models. CRC Press, Boca Raton, Florida, 2006.

Singh VP, Sharma N, Ojha CSP (2004) (editors) The Brahmaputra Basin Water Resources. Kluwer Academic Publishers, Dordrecht, Netherlands, 2004.

Srinivasan MS, Gerald-Marchant P, Veith TL, Gburek WJ, Steenhuis TS (2005) Watershed-scale modeling of critical source areas of runoff generation and phosphorus transport. J. of American Water Resour. Assoc. 41(2): 361-375.

Srinivasan MS, Gerald-Marchant P, Veith TL, Gburek WJ, Steenhuis TS (2005) Watershed-scale modeling of critical source areas of runoff generation and phosphorus transport. J. of American Water Resour. Assoc. 41(2): 361-375.

Stephen HG, Sinokrot BA (1993) Proj. global CC impact on water tempr. in five North Central U.S. streams. J. Climate Change, 24, pages 353–381(1993)

Sterman JD (2008) Risk communication on climate: mental models and mass balance. Science, Vol. 322, Issue 5901, pp. 532-533. DOI: 10.1126/science.1162574.

Stone MC, Hotchkiss RH, Hubbard CM, Fontaine TA, Mearns LO, Arnold JG (2001) Impacts of climate change on Missouri river basin water yield. J. American Water Resour. Assoc. 37(5): 1119-1130.

Surfleet C, Tullos D (2013) Variability in Effect of Climate Change on Rain-on-Snow Peak Flow Events in a Temperate Climate. J. of Hydrology. 479. 24–34. 10.1016/j.jhydrol.2012.11.021.

Swamee PK, Sharma N, Dwivedi A (2008) Lacey Regime Equations for River Brahmaputra. Journal of Hydraulic Research, Vol. 46, No. 5, pp. 707-710, 2008.

Tabari H, Kisi O, Ezani A, Talaee PH (2012) SVM, ANFIS, regression and climate based models for reference evapotranspiration modeling using limited climatic data in a semi-arid highland environment. Journal of Hydrology, 444 (2012), pp. 78-89.

Talukdar DK (2013) Statistical Study of Some Engineering properties of the Brahmaputra River Sand. J. of Emerging Technology and Advanced Engineering, Vol.3, Issue 3, March'2013.

Talukdar S, Pal S (2017) Impact of dam on inundation regime of flood plain wetland of punarbhaba river basin of barind tract of Indo-Bangladesh. J. International Soil and Water Conservation Research. Vol.5, Issue 2, pg 109-121, https://doi.org/10.1016/ j.iswcr.2017.05.003.

Tavakoli M, Smedt F (2012) Impact of climate change on streamflow and soil moisture in the Vermilion basin, Illinois. J. of Hydrolo. Eng., ASCE. ISSN 1084-0699/2012/10-1059-1070.

Teutschbein C, Seibert J (2013) Is bias correction of regional climate model (RCM) simulations possible for non-stationary conditions? Hydrol Earth Syst Sci 17:5061–5077.

Thiessen AH (1911) Precipitations averages for large areas: Monthly Weather Rev.

Thorne V, Coakley P, Grimes D, Dugdale G (2001) Comparsion of TAMSAT and CPC rainfall estimates with rainfall, for southern Africa. Int. J. Remote Sens. 22 (10), 1951–1974.

Thu HN, Wehn U (2016) Data sharing in international transboundary contexts: The Vietnamese perspective on data sharing in the Lower Mekong Basin. J. of Hydrology 536 (2016) 351–364.

Todd MC, Barret EC, Beaumont MJ, Bellerby TT (1999) Estimation of daily rainfall over the upper Nile River basin using a continuously calibrated satellite infrared technique. Meteorol. Appl. 6 (3), 201–210.

Trefry et.al. (2015) Regional Rainfall Frequency Analysisfor the State of Michigan" J. of Hydrologic Engineers, ASCE, 2005, 10(6): 437-449.
Tuppad P, Santhi C, Srinivasan R (2010) Assessing BMP effectiveness: Multi-procedure analysis of observed water quality data. Environmental Monitoring and Assessment 170: 315-329. DOI.10/1007/s10061-009-1235-8.
Valdivieso FO, Sendra JB (2014) Semi-distributed Hydrological Model with Scarce Information: Application to a Large South American Binational Basin. J. Hydrol. Eng., 2014, 19(5): 1006-1014.
VanLiew MW, Garbrecht J (2003) Hydrologic simulation of the little Washita river experimental watershed using SWAT. J. of the American Water Resources Association 39: 413-426.
Von SH, Zorita E, Cubasch U (1993) Downscaling of global climate change estimates to regional scales: an application to Iberian rainfall in winter time. J Clim 6:1161–1171.
Wakid A (2009) Protection of endangered Ganges river dolphin in Brahmaputra river, Assam, India. J. Current Science, vol. 97, No. 8, October 25, 2009.
Wang W, Lu H, Leung LR, Li HY, Zhao J, Tian F , Yang K, Sothea K, (2017) Dam Construction in Lancang-Mekong River Basin Could Mitigate Future Flood Risk From Warming-Induced Intensified Rainfall. J. Geophysical Research Letter, https://doi.org/10.1002/ 2017GL075037.
Wilk J, Kniveton D, Andersson L, Layberry R, et al. (2006) Estimating rainfall and water balance over the Okavango River Basin for hydrological applications. J. Hydrology (2006) 331, 18– 29.
Wurbs RA, Muttiah RS, Felden F (2005) Incorporation of climate change in water availability modelling. J. of Hydrologic Engineering, ASCE. ISSN 1084-0699/2005/5-375–385.
Xie P, Arkin PA (1995) Analyses of global monthly precipitation using gauge observation, satellite estimates, and numerical model predictions. Journal of Climate, volume 9, pg 840-858.
Yang YC, Wi S, Ray PA, Brown M, Khalil A (2016) The future Nexus of the Brahmaputra river basin- climate, water, energy and food trajectory". J. of Global Environment Changes.
Yatagai A, Xie P, Alpert P (2008) Development of a daily gridded precipitation data for the middle east, Adv. Geosci., 12, 165–170, 2008,http://www.adv-geosci.net/12/165/2008/.
Yatagai A, Arakawa O, Kamiguchi K, Kawamoto H, Nodzu MI, Hamada A (2009) A 44-year daily gridded precipitation dataset for Asia based on a dense network of rain gauges, SOLA, 5, 137–140.
Yates DN, Strzepek KM (1998) Modeling the Nile basin under climate change. J. of Hydrolo. Eng., ASCE. ISSN 1084-0699/98/0002-0098-0108.
Yen H, Bailey RT, Arabi M, Ahmadi M, White MJ and Arnold JG (2014) The role of interior watershed processes in improving parameter estimation and performance of watershed models. J. of Environmental Quality 43: 1601. DOI: 10.2134/jeq2013.03.0110.
Yu MY, Chen XL, Li LH, Bao AM, Paix MZ (2011) Streamflow simulation by SWAT using different precipitation sources in large arid basins with scarce raingauges. Water Resour Manage 25:2669–2681.
Yussouf N, Stensrud DJ (2006) Prediction of near-surface variables at independent locations from a bias-corrected ensemble forecasting system. Mon Weather Rev 134:3415–3424.
Zhang X, Srinivasan R, Zhao K, Van LM (2008) Evaluation of global optimization algorithms for parameter calibration of a computationally intensive hydrologic model. J. of Hydrologic Process.(2008), DOI: 10.1002/hyp.7152.
Zhang Y, Xia J, Liang T, Shao Q (2010) Impact of Water Projects on River Flow Regimes and Water Quality in Huai River Basin. J. *Water Resour Manage* 24, 889–908 (2010). https://doi.org/10.1007/s11269-009-9477-3.
Zhu X, Zhang C, Yin J, Zhou H, Jiang Y (2014) Optimization of water diversion based on reservoir operating rules: analysis of the Biliu River Reservoir, China. J. Hydrol. Eng., 19 (2), pg. 411-421.

######### #########

LIST OF PUBLICATIONS

[J] Dutta P., Sarma A.K. (2020) "Hydrological modelling as a tool for water resources management of data-scarce Brahmaputra basin." Journal of water and climate change, ISSN: 2040-2244, DOI: 10.2166/wcc.2020.186/670198/jwc2020186.

[J] Dutta P., Sarma A.K. (2020) "Modelling based approach of analyzing diversion impacts: A case study of the Brahmaputra basin." Journal of Current Science, Vol. 119 No. 6, ISSN: 0011-3891.

[J] Dutta P, Hinge G, Marak JDK, Sarma A.K. (2020) "Future climate and its impact on streamflow: A case study of the Brahmaputra river." Journal of Modeling earth science and environment, ISSN (print): 2363-6203. DOI:10.1007/s40808-020-01022-2. (in Press)

[C] Dutta P., Hinge G., Sarma A.K. (2019) "Deriving Flow scenarios for a tributary from a large watershed model in SWAT." 16th Annual meeting of the Asia Oceania Geosciences Society (AOGS) held at SUNTEC, Singapore.

[C] Dutta P. Sarma A.K. (2018) "Hydrological assessment of the transboundary Brahmaputra river using SWAT." International conference on Infrastructure development (ICID2018) held at JEC, Jorhat, India.

[C] Dutta P., Devi D., Sarma A.K. (2018) "Comparing global high resolution precipitation data with rain gauge data in Assam, India." International conference on Hydraulics, water resources and coastal engineering (HYDRO-2018) held at NIT Patna, India.

*Note: [J] Journal; [C] International Conference

######## ########

APPENDIX A: Bias Correction Factors

Station-wise bias correction factors for PCP, TMax, TMin concerning all GCMs

[GFDL-ESM2M, HadGEM2-CC, IPSL-CM5-LR]

Station Code: S1

	GFDL-ESM2M			HadGEM2-CC			IPSL-CM5-LR		
Mon	PCP	Tmx	Tmn	PCP	Tmx	Tmn	PCP	Tmx	Tmn
1	1.26	-3.84	-9.53	4.74	-5.50	-10.01	0.45	-3.31	-6.17
2	1.06	-3.98	-9.02	5.06	-6.21	-9.59	1.14	-2.99	-3.44
3	0.92	-3.58	-8.20	2.44	-6.83	-10.22	0.74	-1.31	-1.76
4	0.66	-5.65	-9.87	0.97	-8.79	-12.30	0.69	-1.32	-1.28
5	0.70	-5.91	-6.73	0.37	-8.53	-11.20	0.63	0.05	0.77
6	0.50	-4.08	-4.02	0.25	-6.49	-9.06	1.30	2.18	3.53
7	0.44	-0.65	-3.29	0.33	-2.39	-6.37	4.73	-0.90	0.99
8	0.45	-0.82	-2.95	0.49	-4.02	-5.88	0.99	-3.37	-2.38
9	0.22	-1.41	-3.99	0.83	-5.83	-6.25	0.35	-2.18	-2.73
10	0.15	-3.27	-7.67	0.38	-5.62	-10.09	0.14	-1.82	-3.88
11	0.32	-2.21	-7.78	0.63	-5.40	-10.70	0.11	-0.50	-3.98
12	0.62	-1.35	-6.86	1.61	-3.95	-9.04	0.15	-0.97	-4.49

Station Code: S2

	GFDL-ESM2M			HadGEM2-CC			IPSL-CM5-LR		
Mon	PCP	Tmx	Tmn	PCP	Tmx	Tmn	PCP	Tmx	Tmn
1	0.84	-3.56	-9.09	1.67	-5.14	-9.71	0.31	-3.14	-6.08
2	0.63	-3.55	-8.86	1.64	-5.75	-9.61	0.69	-2.76	-3.77
3	0.48	-2.77	-7.15	0.81	-6.04	-9.26	0.40	-0.79	-1.11
4	0.43	-4.53	-8.52	0.47	-7.72	-10.91	0.48	-0.54	-0.43
5	0.48	-4.52	-5.39	0.25	-7.12	-9.97	0.45	1.26	1.72
6	0.61	-3.14	-3.41	0.32	-5.36	-8.51	1.59	3.14	3.75
7	0.71	-0.46	-3.06	0.52	-1.82	-5.99	7.36	-0.60	1.06
8	0.67	-0.50	-2.69	0.71	-3.45	-5.49	1.53	-2.98	-2.13
9	0.26	-0.68	-3.23	0.92	-4.87	-5.52	0.44	-1.56	-2.08
10	0.12	-2.78	-6.82	0.29	-4.83	-9.45	0.11	-1.41	-3.29
11	0.21	-2.05	-6.97	0.32	-4.92	-9.92	0.07	-0.38	-3.34
12	0.37	-1.17	-5.73	0.50	-3.63	-7.98	0.09	-0.87	-3.62

Station Code: S3

	GFDL-ESM2M			HadGEM2-CC			IPSL-CM5-LR		
Mon	PCP	Tmx	Tmn	PCP	Tmx	Tmn	PCP	Tmx	Tmn
1	0.54	-8.55	-13.90	0.71	1.21	-3.39	0.23	-8.94	-13.03
2	0.44	-8.93	-13.76	0.66	0.54	-3.57	0.54	-9.29	-11.94
3	0.28	-7.51	-11.23	0.27	1.26	-2.61	0.25	-6.89	-8.63
4	0.22	-9.68	-12.36	0.13	-0.89	-4.37	0.24	-7.02	-7.94
5	0.09	-9.77	-9.72	0.04	-1.54	-4.88	0.12	-5.26	-5.51
6	0.09	-6.92	-7.70	0.10	-1.65	-4.11	0.62	-3.97	-3.36
7	0.14	-2.64	-7.03	0.17	1.87	-1.88	0.71	-6.10	-5.16
8	0.14	-2.76	-7.10	0.21	0.30	-1.85	0.24	-6.31	-7.32
9	0.06	-3.84	-7.21	0.22	-1.03	-1.05	0.10	-6.36	-7.28
10	0.08	-6.57	-8.47	0.25	0.82	-2.46	0.09	-7.15	-7.34
11	0.20	-6.97	-10.43	0.21	0.84	-4.15	0.07	-6.66	-9.51
12	0.37	-6.70	-10.69	0.33	1.83	-2.26	0.11	-7.38	-10.83

Station Code: S4

	GFDL-ESM2M			HadGEM2-CC			IPSL-CM5-LR		
Mon	PCP	Tmx	Tmn	PCP	Tmx	Tmn	PCP	Tmx	Tmn
1	1.04	-7.73	-12.08	1.06	0.27	-3.56	0.54	-4.64	-7.99
2	0.85	-8.01	-12.09	0.98	-0.32	-4.37	1.12	-4.48	-6.86
3	0.65	-6.70	-10.34	0.48	0.00	-4.47	0.60	-2.25	-4.29
4	0.48	-8.87	-10.86	0.23	-2.15	-5.41	0.53	-2.32	-2.88
5	0.18	-9.19	-8.59	0.08	-2.31	-5.36	0.25	-0.61	-0.61
6	0.09	-6.46	-6.79	0.09	-1.91	-4.48	0.49	0.35	1.16
7	0.08	-2.05	-6.19	0.10	1.41	-2.28	0.33	-2.02	-1.38
8	0.11	-2.29	-6.59	0.15	-0.23	-2.61	0.18	-2.45	-4.05
9	0.06	-3.40	-6.54	0.19	-1.86	-1.80	0.09	-2.75	-3.97
10	0.11	-6.01	-7.19	0.33	-0.36	-2.36	0.13	-3.04	-2.87
11	0.42	-6.45	-8.79	0.41	-0.25	-3.86	0.14	-2.44	-4.54
12	0.64	-6.28	-9.77	0.49	0.63	-3.14	0.26	-3.42	-6.58

Station Code: S5

	GFDL-ESM2M			HadGEM2-CC			IPSL-CM5-LR		
Mon	PCP	Tmx	Tmn	PCP	Tmx	Tmn	PCP	Tmx	Tmn
1	1.32	-3.48	-4.12	1.90	4.02	4.77	0.70	-0.91	-1.90
2	1.03	-3.00	-3.02	1.33	4.56	5.03	0.82	0.35	0.35
3	1.08	-1.67	-1.81	0.78	4.80	3.90	0.88	2.13	2.12
4	0.98	-2.84	-2.81	0.51	2.14	-0.18	1.49	2.10	2.26
5	0.50	-3.27	-1.96	0.30	1.65	-1.38	1.04	2.65	2.17
6	0.28	-0.26	-2.30	0.34	1.33	-1.20	1.61	2.38	2.23
7	0.24	2.43	-2.07	0.35	2.30	0.33	0.85	-0.52	-0.26
8	0.33	1.77	-2.18	0.44	1.18	0.11	0.59	-0.29	-1.49
9	0.31	1.43	-1.66	0.68	0.31	0.80	0.52	-0.82	-1.46
10	0.21	-1.03	-1.34	0.43	3.28	1.94	0.27	-0.51	0.66
11	0.36	-2.40	-2.46	0.26	3.91	1.14	0.15	0.62	-0.04
12	0.44	-2.66	-3.95	0.70	4.20	3.47	0.27	-0.56	-2.20

Station Code: S6

	GFDL-ESM2M			HadGEM2-CC			IPSL-CM5-LR		
Mon	PCP	Tmx	Tmn	PCP	Tmx	Tmn	PCP	Tmx	Tmn
1	0.00	-3.67	-5.97	0.64	1.71	-0.12	0.52	-2.90	-5.38
2	0.00	-3.77	-6.32	0.61	1.41	-1.31	0.51	-2.02	-4.85
3	0.00	-3.89	-5.40	0.63	-0.50	-3.93	1.05	-1.90	-3.53
4	0.00	-6.23	-3.89	0.42	-4.60	-5.82	1.66	-3.03	-1.15
5	0.00	-7.36	-1.42	0.50	-5.49	-4.59	1.30	-3.74	-0.59
6	0.00	-5.27	-2.16	0.34	-5.07	-3.95	0.94	-4.97	-1.42
7	0.00	-0.87	-2.76	0.35	-3.45	-3.07	0.46	-4.54	-3.19
8	0.00	-1.08	-2.62	0.37	-4.20	-3.08	0.36	-4.25	-3.42
9	0.00	-1.24	-1.48	0.54	-4.88	-2.48	0.42	-5.25	-3.50
10	0.00	-2.35	0.12	1.00	-2.24	-0.41	0.66	-4.22	-1.03
11	0.00	-2.73	-2.00	0.55	-0.85	-3.17	0.34	-1.78	-2.11
12	0.00	-2.15	-3.41	0.40	1.50	-0.22	0.35	-1.84	-3.39

Station Code: S7

Mon	GFDL-ESM2M			HadGEM2-CC			IPSL-CM5-LR		
	PCP	Tmx	Tmn	PCP	Tmx	Tmn	PCP	Tmx	Tmn
1	0.31	13.84	7.47	0.28	11.78	5.48	0.58	12.79	9.67
2	0.70	12.65	7.12	0.32	12.28	4.66	0.71	13.57	10.06
3	1.58	10.64	7.59	0.30	12.60	4.68	1.65	13.54	11.13
4	0.83	10.41	6.79	0.34	11.85	3.94	3.50	12.45	10.87
5	1.14	10.35	6.19	0.80	10.12	3.99	2.92	10.77	9.93
6	1.36	12.88	7.58	0.89	10.44	4.52	3.16	8.97	9.53
7	1.59	11.49	7.76	1.25	8.12	4.34	1.78	8.16	7.96
8	1.43	12.34	7.98	1.12	8.43	4.15	1.41	9.59	7.85
9	1.35	14.28	9.30	0.93	8.90	4.16	1.21	10.08	7.64
10	1.06	15.27	9.12	2.27	10.35	7.43	1.03	11.80	8.61
11	0.45	15.79	9.76	1.00	11.56	7.50	0.46	13.78	9.71
12	0.28	16.77	9.45	0.36	12.70	6.32	0.55	14.40	9.90

Station Code: S8

Mon	GFDL-ESM2M			HadGEM2-CC			IPSL-CM5-LR		
	PCP	Tmx	Tmn	PCP	Tmx	Tmn	PCP	Tmx	Tmn
1	0.53	8.69	5.94	0.53	5.15	1.55	0.93	7.47	7.36
2	1.33	7.42	5.30	0.70	5.19	0.67	1.30	8.12	7.48
3	2.61	5.70	5.38	0.58	5.27	0.08	2.51	8.37	8.20
4	1.79	4.51	4.08	0.72	3.98	-0.97	6.91	6.51	7.87
5	2.17	3.59	2.98	1.34	1.68	-1.39	5.33	4.01	6.53
6	2.66	6.80	4.66	1.28	2.80	-0.49	6.52	2.50	6.35
7	3.19	6.00	5.01	2.35	0.93	-0.40	3.86	2.26	5.06
8	3.35	6.31	5.08	2.32	0.88	-0.68	3.35	3.31	4.79
9	3.66	8.21	6.61	2.42	1.02	-0.54	3.45	3.79	4.86
10	2.54	9.52	6.24	5.52	2.71	1.74	2.49	5.73	5.44
11	1.53	10.55	7.60	3.65	5.01	2.60	1.55	8.15	6.96
12	0.59	11.39	7.99	0.96	6.17	2.55	1.15	8.78	7.54

Station Code: S9

Mon	GFDL-ESM2M			HadGEM2-CC			IPSL-CM5-LR		
	PCP	Tmx	Tmn	PCP	Tmx	Tmn	PCP	Tmx	Tmn
1	1.37	3.19	0.67	1.05	8.48	1.86	2.23	1.74	0.08
2	5.27	2.16	0.59	1.61	9.43	2.23	3.80	2.75	1.25
3	12.05	1.28	0.35	1.64	9.91	1.82	6.02	3.70	2.24
4	5.24	-0.82	-0.28	1.34	7.63	1.61	11.85	1.37	3.28
5	4.42	-1.50	-0.61	2.02	4.68	1.43	8.17	-0.61	3.10
6	2.10	4.44	1.64	0.84	5.78	1.52	5.96	-0.56	3.19
7	1.71	5.56	2.26	1.18	5.09	1.71	2.66	0.95	2.51
8	1.93	5.80	2.54	1.27	5.13	1.50	2.34	1.99	2.44
9	2.99	6.26	3.33	2.25	4.66	1.52	3.77	1.61	2.23
10	3.74	6.39	2.21	7.81	6.26	3.23	4.12	1.91	0.92
11	1.95	6.22	1.60	3.68	8.51	2.14	1.92	2.91	-0.63
12	1.20	6.12	0.81	1.55	9.11	0.81	2.10	2.87	-1.68

Station Code: S10

Mon	GFDL-ESM2M			HadGEM2-CC			IPSL-CM5-LR		
	PCP	Tmx	Tmn	PCP	Tmx	Tmn	PCP	Tmx	Tmn
1	1.06	4.47	2.07	0.61	11.29	3.98	1.57	2.31	-0.64
2	2.28	3.70	1.29	0.47	12.84	4.15	1.46	3.48	0.30
3	7.35	2.84	1.63	0.95	13.02	4.72	2.63	4.54	2.26
4	5.12	0.51	0.42	1.11	10.85	4.10	7.51	2.62	2.96
5	4.59	-1.10	-0.89	2.22	7.22	2.85	9.71	-0.50	1.79
6	2.44	2.52	0.78	1.27	5.17	2.19	8.91	-3.25	1.43
7	2.34	2.58	1.31	1.62	3.56	2.28	3.91	-2.76	0.75
8	2.80	2.90	1.78	1.77	3.50	2.17	3.42	-1.46	0.74
9	3.19	4.02	2.61	2.57	3.90	2.52	3.92	-1.07	0.44
10	2.65	6.28	2.60	5.68	7.48	5.08	3.71	0.88	-0.10
11	1.14	7.25	4.54	1.55	10.38	5.60	1.19	2.75	0.20
12	0.76	7.58	4.81	0.70	11.50	5.17	1.21	3.09	-0.13

Station Code: S11

Mon	GFDL-ESM2M			HadGEM2-CC			IPSL-CM5-LR		
	PCP	Tmx	Tmn	PCP	Tmx	Tmn	PCP	Tmx	Tmn
1	0.70	5.61	3.30	0.24	11.83	3.17	0.68	5.47	2.46
2	1.79	5.55	2.68	0.23	13.72	4.23	0.81	7.24	3.88
3	3.51	5.69	2.06	0.39	14.03	4.28	0.86	9.42	5.13
4	1.68	5.31	0.73	0.25	13.39	3.18	1.14	10.42	6.01
5	1.32	4.19	1.12	0.60	10.13	3.12	1.94	8.20	6.42
6	1.39	6.34	2.54	1.12	4.85	0.95	5.65	2.81	5.02
7	1.69	4.80	2.46	1.21	3.98	1.15	3.33	0.59	3.33
8	1.96	4.47	2.88	1.26	3.05	0.88	2.48	1.33	3.33
9	2.43	5.32	3.66	1.85	3.27	1.65	3.42	1.50	3.25
10	1.49	7.64	3.99	3.09	7.41	4.38	2.52	3.63	3.08
11	0.52	8.64	5.97	0.40	10.77	4.39	0.38	5.59	3.17
12	0.30	9.13	6.44	0.18	12.02	3.76	0.37	6.18	2.72

Station Code: S12

Mon	GFDL-ESM2M			HadGEM2-CC			IPSL-CM5-LR		
	PCP	Tmx	Tmn	PCP	Tmx	Tmn	PCP	Tmx	Tmn
1	0.62	5.60	3.91	0.25	11.30	3.84	0.70	4.45	2.28
2	1.43	5.43	3.37	0.23	13.06	4.83	0.74	6.10	3.69
3	3.75	5.45	2.33	0.40	13.24	4.07	1.01	8.07	4.43
4	1.97	4.91	1.49	0.23	12.77	3.26	1.52	8.81	5.72
5	1.74	3.71	1.43	0.59	9.89	2.97	2.65	6.64	5.70
6	1.49	6.04	2.55	0.84	5.41	1.17	5.75	1.84	4.35
7	1.56	4.95	2.77	1.08	3.88	1.35	3.02	0.23	3.05
8	1.72	4.93	3.31	1.09	3.28	1.18	2.32	1.06	3.08
9	2.18	5.87	4.14	1.72	3.52	1.86	3.14	1.31	2.97
10	1.57	7.73	4.68	3.26	7.03	4.58	2.58	2.92	2.91
11	0.51	8.52	6.70	0.49	10.23	4.95	0.42	4.59	3.05
12	0.40	8.81	6.82	0.29	11.39	4.36	0.55	5.03	2.40

Station Code: S13

Mon	GFDL-ESM2M			HadGEM2-CC			IPSL-CM5-LR		
	PCP	Tmx	Tmn	PCP	Tmx	Tmn	PCP	Tmx	Tmn
1	0.73	-0.16	2.84	0.38	4.43	5.04	0.55	0.28	3.74
2	0.47	-1.38	1.77	0.17	4.69	3.89	0.40	0.56	3.64
3	0.40	-0.78	2.23	0.09	5.24	2.98	0.27	2.17	4.22
4	0.19	-1.45	0.76	0.06	5.55	1.72	0.28	2.57	4.05
5	0.12	-2.00	-1.39	0.11	4.68	0.06	0.37	1.56	2.31
6	0.20	2.31	-1.79	0.25	4.15	-0.05	1.49	-0.46	2.11
7	0.40	2.37	-1.72	0.66	2.53	0.07	1.28	-2.31	-0.34
8	0.49	2.39	-0.40	0.67	2.33	1.18	0.87	-0.78	0.11
9	0.38	3.54	-0.17	0.76	2.35	0.87	0.67	-0.07	-0.40
10	0.21	3.79	1.79	0.71	4.64	4.93	0.40	1.49	2.31
11	0.25	3.31	5.38	0.26	4.93	5.40	0.17	2.55	4.20
12	0.21	3.20	5.19	0.18	5.52	5.88	0.23	2.08	4.21

Station Code: S14

Mon	GFDL-ESM2M			HadGEM2-CC			IPSL-CM5-LR		
	PCP	Tmx	Tmn	PCP	Tmx	Tmn	PCP	Tmx	Tmn
1	0.32	13.58	11.20	0.16	13.49	6.74	0.24	13.94	11.24
2	0.28	13.74	13.03	0.08	15.16	8.67	0.21	15.67	14.29
3	0.40	14.47	14.98	0.09	15.95	9.80	0.23	17.67	16.84
4	0.49	12.61	13.31	0.14	15.20	8.75	0.65	16.88	16.70
5	0.43	10.36	10.14	0.32	13.06	6.51	1.10	14.13	13.96
6	0.95	12.52	8.29	0.81	10.74	4.80	5.30	9.93	11.67
7	1.29	11.31	8.10	1.44	7.58	4.87	3.29	7.05	9.27
8	1.35	11.22	8.36	1.29	7.12	4.78	2.09	8.31	8.72
9	1.12	12.96	9.12	1.42	7.79	4.74	1.67	9.55	8.63
10	0.57	14.88	10.26	1.59	10.85	7.32	0.88	12.43	10.19
11	0.13	15.94	13.40	0.13	12.98	7.78	0.08	14.86	11.70
12	0.07	16.59	13.27	0.05	14.14	7.43	0.07	15.15	11.40

Station Code: S15									
	GFDL-ESM2M			HadGEM2-CC			IPSL-CM5-LR		
Mon	PCP	Tmx	Tmn	PCP	Tmx	Tmn	PCP	Tmx	Tmn
1	0.14	11.54	8.94	0.11	14.39	9.88	0.21	10.33	9.17
2	0.34	10.44	9.53	0.12	15.23	10.44	0.30	11.18	10.78
3	0.39	9.71	9.93	0.07	15.79	9.71	0.31	12.06	11.76
4	0.34	8.47	8.13	0.14	14.20	8.10	1.10	10.66	11.17
5	0.35	7.73	5.89	0.28	11.64	6.56	0.90	8.52	8.98
6	0.38	11.20	6.18	0.30	11.19	6.08	1.18	6.60	7.92
7	0.41	10.60	6.21	0.42	9.50	5.86	0.62	6.25	6.23
8	0.34	11.06	6.58	0.31	9.74	5.90	0.37	7.73	6.16
9	0.28	13.00	8.01	0.27	10.44	6.33	0.32	8.42	6.34
10	0.33	14.11	8.48	0.74	12.90	9.72	0.41	10.09	7.60
11	0.12	14.26	10.01	0.19	14.07	10.06	0.13	11.71	8.79
12	0.08	14.76	9.98	0.09	15.13	9.72	0.15	11.90	8.51

Station Code: S16									
	GFDL-ESM2M			HadGEM2-CC			IPSL-CM5-LR		
Mon	PCP	Tmx	Tmn	PCP	Tmx	Tmn	PCP	Tmx	Tmn
1	0.36	-5.66	-4.68	0.28	-0.76	0.45	0.22	-2.91	-2.04
2	0.31	-6.15	-5.16	0.18	-0.45	-0.27	0.23	-2.30	-1.35
3	0.47	-5.64	-4.68	0.17	-0.67	-1.94	0.35	-1.19	-0.48
4	0.31	-7.42	-5.88	0.11	-2.99	-5.30	0.51	-1.98	-0.69
5	0.12	-7.08	-3.96	0.09	-2.76	-4.12	0.33	-1.23	0.60
6	0.10	-2.77	-5.31	0.14	-1.59	-4.56	0.65	-1.05	-0.29
7	0.19	-0.47	-4.67	0.34	-0.93	-2.87	0.66	-3.21	-2.36
8	0.27	-1.09	-4.36	0.41	-1.89	-2.71	0.49	-2.73	-3.08
9	0.18	-0.85	-3.90	0.39	-2.75	-2.70	0.30	-2.81	-3.27
10	0.12	-3.28	-2.73	0.29	-1.33	-0.05	0.17	-2.80	-0.37
11	0.13	-3.89	-2.44	0.11	-0.83	-1.41	0.07	-1.06	-0.11
12	0.12	-3.81	-3.90	0.12	-0.20	-0.20	0.09	-1.79	-2.00

Station Code: S17									
	GFDL-ESM2M			HadGEM2-CC			IPSL-CM5-LR		
Mon	PCP	Tmx	Tmn	PCP	Tmx	Tmn	PCP	Tmx	Tmn
1	0.40	-0.53	-0.42	0.27	3.50	3.15	0.17	1.53	1.11
2	0.26	0.06	-0.01	0.16	4.36	2.93	0.22	2.79	2.60
3	0.36	1.26	1.08	0.16	4.76	2.38	0.29	4.56	4.23
4	0.41	-0.66	0.74	0.16	2.43	0.47	0.60	3.71	5.12
5	0.24	-0.98	1.13	0.15	2.39	-0.40	0.58	4.41	5.09
6	0.12	2.47	0.46	0.14	3.09	-0.25	0.91	4.41	5.37
7	0.16	5.20	1.08	0.23	4.04	1.67	0.60	1.34	2.77
8	0.22	4.39	1.03	0.29	2.76	1.44	0.36	1.55	1.11
9	0.20	4.35	1.43	0.41	1.69	1.68	0.29	1.81	1.30
10	0.15	2.16	2.16	0.36	3.47	3.56	0.18	2.29	3.83
11	0.19	0.75	3.38	0.14	3.31	3.72	0.07	3.13	4.89
12	0.15	0.66	0.69	0.12	3.67	3.06	0.07	2.13	1.43

Station Code: S18									
	GFDL-ESM2M			HadGEM2-CC			IPSL-CM5-LR		
Mon	PCP	Tmx	Tmn	PCP	Tmx	Tmn	PCP	Tmx	Tmn
1	1.73	-9.26	-14.75	1.31	-3.37	-8.49	0.48	-8.46	-12.82
2	1.44	-10.07	-16.30	1.32	-4.63	-10.67	1.27	-9.02	-13.24
3	1.16	-10.22	-15.91	0.67	-5.63	-11.95	0.70	-7.86	-12.20
4	0.71	-12.78	-15.44	0.27	-7.63	-11.99	0.57	-8.12	-9.90
5	0.31	-13.42	-10.19	0.13	-7.61	-8.02	0.30	-7.66	-5.54
6	0.18	-10.43	-8.05	0.16	-6.61	-6.81	1.09	-7.00	-3.49
7	0.15	-5.30	-7.28	0.16	-2.80	-4.87	0.99	-8.02	-4.67
8	0.16	-4.98	-7.09	0.20	-3.83	-4.56	0.25	-7.59	-6.43
9	0.14	-5.94	-7.40	0.43	-5.44	-3.85	0.18	-7.09	-6.66
10	0.13	-8.17	-8.99	0.40	-4.58	-5.28	0.11	-7.73	-7.39
11	0.39	-7.53	-10.07	0.39	-4.00	-6.91	0.09	-6.22	-8.83
12	0.69	-6.98	-10.46	0.36	-2.41	-6.22	0.14	-5.81	-9.96

Station Code: S19									
	GFDL-ESM2M			HadGEM2-CC			IPSL-CM5-LR		
Mon	PCP	Tmx	Tmn	PCP	Tmx	Tmn	PCP	Tmx	Tmn
1	0.01	-1.19	-3.43	0.01	2.95	0.57	0.01	1.10	-1.12
2	0.00	-1.11	-3.11	0.00	3.32	0.16	0.00	1.91	0.33
3	0.01	0.03	-1.73	0.00	3.64	-0.05	0.01	3.75	2.40
4	0.04	-1.26	-2.93	0.02	1.96	-2.66	0.05	3.68	2.67
5	0.14	-1.75	-2.39	0.09	1.72	-3.38	0.37	4.51	3.27
6	0.20	1.13	-1.92	0.23	2.18	-2.37	1.67	4.49	4.58
7	0.29	3.62	-0.96	0.42	3.21	0.08	1.17	0.76	1.79
8	0.40	2.72	-1.30	0.53	1.62	-0.41	0.65	0.43	-0.64
9	0.19	2.67	-1.37	0.42	0.46	-0.59	0.29	0.88	-0.67
10	0.02	0.64	-1.65	0.06	2.34	0.26	0.03	1.58	1.27
11	0.01	0.11	-1.07	0.01	2.85	-0.29	0.00	2.89	1.27
12	0.00	0.27	-2.37	0.00	3.48	0.47	0.00	2.05	-0.84

Station Code: S20									
	GFDL-ESM2M			HadGEM2-CC			IPSL-CM5-LR		
Mon	PCP	Tmx	Tmn	PCP	Tmx	Tmn	PCP	Tmx	Tmn
1	0.06	-1.22	-3.74	0.07	7.47	6.26	0.04	2.18	-0.65
2	0.06	-0.99	-2.88	0.06	8.15	7.13	0.05	3.58	1.80
3	0.11	-0.18	-0.59	0.06	7.81	6.42	0.10	5.10	4.65
4	0.12	-1.88	-1.23	0.06	4.30	1.55	0.24	4.59	4.92
5	0.31	-1.60	-0.62	0.21	4.06	0.67	0.78	5.23	4.69
6	0.33	2.98	-1.01	0.43	4.01	1.18	1.95	4.46	4.47
7	0.37	4.71	-0.24	0.59	4.40	2.41	1.16	2.12	2.06
8	0.45	3.82	-0.17	0.61	3.49	2.31	0.74	2.53	1.19
9	0.40	3.48	-0.07	0.69	2.44	2.21	0.61	1.63	0.68
10	0.05	1.87	-0.55	0.10	5.55	3.04	0.08	2.57	2.36
11	0.02	-0.06	-1.38	0.02	5.86	2.19	0.01	3.41	2.09
12	0.02	-0.05	-2.86	0.03	7.21	4.89	0.02	2.67	-0.25

Station Code: S21									
	GFDL-ESM2M			HadGEM2-CC			IPSL-CM5-LR		
Mon	PCP	Tmx	Tmn	PCP	Tmx	Tmn	PCP	Tmx	Tmn
1	0.08	-0.38	-3.13	0.08	4.23	1.28	0.06	2.30	-0.44
2	0.06	-0.60	-3.11	0.04	4.80	1.50	0.04	3.37	1.08
3	0.09	-0.14	-1.74	0.04	4.28	-0.30	0.08	4.63	2.99
4	0.12	-1.90	-2.17	0.06	1.50	-3.28	0.25	3.90	3.46
5	0.09	-0.83	-1.33	0.07	2.37	-2.54	0.23	5.07	3.60
6	0.07	3.94	-1.43	0.10	3.68	-1.41	0.39	4.59	3.56
7	0.10	5.29	-0.30	0.16	3.72	0.20	0.27	2.39	1.65
8	0.10	4.45	-0.19	0.14	2.78	0.08	0.15	2.81	0.85
9	0.09	4.42	0.02	0.16	1.59	-0.44	0.13	2.13	0.35
10	0.09	3.08	-0.74	0.18	3.24	0.45	0.13	3.11	1.64
11	0.07	1.14	-0.52	0.06	2.58	-0.72	0.04	3.76	2.26
12	0.02	1.01	-2.15	0.03	3.68	0.43	0.02	2.90	-0.08

Station Code: S22									
	GFDL-ESM2M			HadGEM2-CC			IPSL-CM5-LR		
Mon	PCP	Tmx	Tmn	PCP	Tmx	Tmn	PCP	Tmx	Tmn
1	0.08	-0.38	-3.13	0.22	1.70	-0.16	0.28	-1.89	-3.97
2	0.06	-0.60	-3.11	0.56	0.64	-0.04	0.66	-1.68	-1.71
3	0.09	-0.14	-1.74	0.86	-1.85	-1.35	2.04	-2.29	0.98
4	0.12	-1.90	-2.17	0.61	-5.30	-3.94	2.78	-2.94	1.34
5	0.09	-0.83	-1.33	0.62	-5.65	-4.05	1.44	-3.00	0.14
6	0.07	3.94	-1.43	0.56	-3.41	-2.96	1.33	-2.90	-0.20
7	0.10	5.29	-0.30	0.49	-2.08	-2.05	0.54	-2.26	-1.71
8	0.10	4.45	-0.19	0.46	-2.41	-1.70	0.40	-1.68	-1.50
9	0.09	4.42	0.02	0.70	-3.39	-1.48	0.46	-2.94	-2.00
10	0.09	3.08	-0.74	1.39	-2.83	0.46	0.78	-3.31	0.12
11	0.07	1.14	-0.52	0.46	-2.05	-3.01	0.31	-1.34	-0.43
12	0.02	1.01	-2.15	0.18	1.20	-0.93	0.21	-0.70	-2.43

Station Code: S23									
	GFDL-ESM2M			HadGEM2-CC			IPSL-CM5-LR		
Mon	PCP	Tmx	Tmn	PCP	Tmx	Tmn	PCP	Tmx	Tmn
1	0.53	10.66	10.30	0.35	10.14	6.20	0.57	11.05	10.97
2	1.16	9.70	10.24	0.36	11.01	6.25	0.86	12.02	12.27
3	2.73	8.41	10.45	0.46	10.62	5.75	1.61	12.42	13.42
4	2.63	5.69	9.14	0.77	8.44	4.80	5.76	9.97	13.50
5	1.64	4.79	7.38	1.03	6.53	4.07	4.77	7.64	11.93
6	1.06	9.43	7.50	0.64	7.03	3.83	4.79	6.17	10.84
7	0.84	9.76	7.43	0.79	5.64	3.65	1.71	5.81	8.61
8	0.87	10.28	7.82	0.75	5.93	3.68	1.13	7.67	8.30
9	0.69	11.67	9.49	0.67	6.14	4.44	0.90	8.25	9.02
10	1.00	13.30	11.06	2.68	8.66	8.25	1.48	10.63	11.48
11	0.38	13.95	12.78	0.63	10.75	8.50	0.35	12.77	12.27
12	0.15	14.24	12.17	0.17	11.36	7.21	0.21	12.64	11.15

Station Code: S24									
	GFDL-ESM2M			HadGEM2-CC			IPSL-CM5-LR		
Mon	PCP	Tmx	Tmn	PCP	Tmx	Tmn	PCP	Tmx	Tmn
1	0.54	10.96	10.63	0.36	10.18	6.31	0.62	10.55	10.88
2	1.03	10.03	10.67	0.33	10.94	6.43	0.81	11.48	12.20
3	2.47	8.44	10.67	0.41	10.28	5.67	1.59	11.53	13.06
4	2.11	5.75	8.99	0.61	8.15	4.48	5.01	9.11	12.84
5	1.64	4.97	7.35	0.93	6.35	3.80	4.25	7.03	11.29
6	1.03	9.66	7.64	0.55	7.03	3.63	4.24	5.75	10.27
7	0.91	10.01	7.63	0.81	5.69	3.51	1.80	5.55	8.27
8	1.30	10.46	8.04	1.07	5.89	3.55	1.62	7.32	8.06
9	0.83	11.99	9.80	0.75	6.20	4.36	1.10	7.90	8.86
10	1.06	13.57	11.52	2.71	8.66	8.37	1.55	10.15	11.38
11	0.49	14.25	13.10	0.83	10.86	8.67	0.46	12.33	12.16
12	0.16	14.47	12.52	0.18	11.45	7.31	0.23	12.20	11.04

Station Code: S25									
	GFDL-ESM2M			HadGEM2-CC			IPSL-CM5-LR		
Mon	PCP	Tmx	Tmn	PCP	Tmx	Tmn	PCP	Tmx	Tmn
1	0.54	13.03	10.78	0.47	10.79	6.16	0.87	11.19	10.76
2	1.29	11.80	11.27	0.55	11.03	6.59	1.19	11.89	12.19
3	2.67	9.67	11.20	0.49	10.17	5.57	2.20	11.41	12.70
4	1.26	7.27	9.52	0.43	8.08	4.32	4.12	8.82	12.34
5	1.10	7.14	8.17	0.63	6.54	3.82	2.59	7.40	11.02
6	0.82	11.52	8.83	0.38	7.66	3.78	2.37	6.42	10.12
7	0.90	11.38	8.82	0.72	6.16	3.53	1.35	6.67	8.56
8	1.25	11.92	9.21	0.90	6.46	3.57	1.40	8.18	8.60
9	1.13	13.60	11.17	0.87	6.61	4.45	1.31	8.56	9.35
10	0.91	15.29	12.53	2.40	9.06	8.40	1.14	10.68	11.32
11	0.43	16.20	13.43	0.98	11.63	8.57	0.47	12.93	11.85
12	0.22	16.43	12.59	0.32	12.25	7.04	0.42	12.95	10.77

Station Code: S26									
	GFDL-ESM2M			HadGEM2-CC			IPSL-CM5-LR		
Mon	PCP	Tmx	Tmn	PCP	Tmx	Tmn	PCP	Tmx	Tmn
1	0.45	11.91	11.28	0.31	17.55	14.60	0.36	13.21	12.30
2	0.79	10.82	11.19	0.27	18.30	14.78	0.52	13.93	13.56
3	2.14	9.86	11.52	0.43	17.94	13.91	1.21	14.47	14.57
4	2.57	7.36	10.47	0.98	15.39	12.64	5.36	12.28	14.73
5	1.84	5.85	8.38	1.80	12.55	11.09	5.83	9.65	13.16
6	1.48	9.60	7.43	1.70	11.69	9.82	7.43	7.58	11.78
7	1.65	10.02	7.41	2.29	10.71	9.68	3.63	6.68	9.27
8	1.26	10.49	7.78	1.48	11.08	9.80	1.71	8.50	8.80
9	1.23	12.04	9.49	1.79	11.55	10.77	1.52	9.46	9.51
10	0.90	14.03	11.23	2.38	15.54	14.96	1.16	12.48	12.23
11	0.37	15.04	13.47	0.46	17.52	15.20	0.26	14.99	13.35
12	0.19	15.52	13.19	0.20	18.53	15.24	0.21	14.97	12.62

Station Code: S27									
	GFDL-ESM2M			HadGEM2-CC			IPSL-CM5-LR		
Mon	PCP	Tmx	Tmn	PCP	Tmx	Tmn	PCP	Tmx	Tmn
1	0.46	13.96	12.26	0.34	17.34	13.68	0.62	13.09	12.65
2	1.08	12.95	12.59	0.38	18.26	14.02	1.00	13.95	14.19
3	1.94	11.37	12.73	0.36	17.78	12.91	1.55	14.05	15.10
4	1.55	8.95	11.41	0.63	14.96	11.65	4.88	11.54	14.96
5	1.42	8.19	9.71	1.22	12.50	10.72	4.59	9.30	13.39
6	1.13	12.18	9.72	1.00	12.55	10.17	4.71	7.88	12.24
7	1.04	12.06	9.60	1.15	11.35	9.82	1.92	7.51	9.98
8	1.21	12.52	9.95	1.19	11.61	9.86	1.38	9.34	9.68
9	1.01	14.26	11.90	1.02	12.14	10.81	1.24	9.88	10.49
10	1.07	15.91	13.38	2.38	15.27	15.15	1.53	12.29	13.12
11	0.41	16.85	14.71	0.61	17.08	15.15	0.43	14.75	13.96
12	0.17	17.17	13.93	0.19	18.00	14.17	0.28	14.64	12.69

Station Code: S28									
	GFDL-ESM2M			HadGEM2-CC			IPSL-CM5-LR		
Mon	PCP	Tmx	Tmn	PCP	Tmx	Tmn	PCP	Tmx	Tmn
1	0.64	14.97	11.91	0.50	14.91	10.90	1.28	10.48	9.56
2	1.67	13.43	12.75	0.61	15.28	11.07	2.03	10.80	11.14
3	2.81	11.40	13.01	0.44	14.97	10.16	2.91	10.24	11.65
4	1.05	9.15	11.32	0.43	12.43	9.12	5.23	7.55	11.28
5	1.27	9.19	9.84	1.00	10.63	8.57	4.14	6.38	10.38
6	1.23	12.98	10.10	0.94	11.19	8.26	3.90	5.52	9.56
7	1.20	12.49	9.97	1.16	9.74	7.77	1.58	6.05	7.94
8	1.52	13.18	10.32	1.37	10.11	7.77	1.32	8.02	7.82
9	1.39	14.88	12.33	1.16	10.56	8.64	1.50	8.15	8.42
10	0.92	16.69	13.45	2.19	13.22	13.05	1.37	10.10	10.12
11	0.35	17.82	14.47	0.67	15.06	13.14	0.50	12.32	10.38
12	0.24	18.16	13.69	0.28	15.69	11.46	0.61	12.12	9.38

Station Code: S29									
	GFDL-ESM2M			HadGEM2-CC			IPSL-CM5-LR		
Mon	PCP	Tmx	Tmn	PCP	Tmx	Tmn	PCP	Tmx	Tmn
1	0.63	15.62	11.57	0.56	13.20	9.10	1.13	14.55	13.59
2	1.85	14.21	12.31	0.82	13.46	9.36	1.83	15.09	15.11
3	3.31	11.70	12.22	0.62	13.30	8.85	3.41	14.53	15.62
4	1.16	10.06	11.07	0.47	11.25	7.85	4.81	12.10	15.08
5	1.18	9.96	9.80	0.81	9.53	7.29	3.05	10.40	13.47
6	1.39	12.82	10.18	0.92	10.17	6.85	3.28	8.88	12.08
7	2.00	11.74	9.83	1.55	8.15	6.14	2.26	8.35	9.96
8	1.58	12.37	10.12	1.24	8.22	6.01	1.55	9.59	9.92
9	1.74	14.55	12.34	1.18	8.95	6.92	1.55	10.32	10.60
10	1.18	16.58	13.92	2.51	11.39	12.00	1.15	13.08	13.35
11	0.29	18.13	14.59	0.64	13.58	12.09	0.29	16.10	14.48
12	0.23	18.50	13.29	0.30	14.11	9.74	0.45	16.13	13.60

Station Code: S30									
	GFDL-ESM2M			HadGEM2-CC			IPSL-CM5-LR		
Mon	PCP	Tmx	Tmn	PCP	Tmx	Tmn	PCP	Tmx	Tmn
1	0.83	22.92	19.98	0.58	23.19	19.99	0.98	23.86	22.90
2	1.89	22.07	20.55	0.85	23.23	20.17	1.54	24.67	24.80
3	2.66	20.79	20.80	0.68	22.12	18.44	2.50	24.46	25.48
4	1.39	17.81	19.49	0.63	18.30	16.13	4.49	21.76	24.67
5	1.49	15.70	17.52	1.22	15.62	14.79	4.04	18.72	21.72
6	1.62	17.92	16.27	1.60	15.46	13.96	5.11	16.22	19.25
7	2.16	17.33	15.72	2.43	14.04	13.45	3.31	14.54	16.41
8	1.71	18.18	16.01	1.86	14.48	13.47	1.90	16.24	16.35
9	1.85	20.34	18.17	1.84	15.50	14.67	1.89	17.15	17.26
10	1.11	22.80	20.40	2.20	19.42	19.59	1.35	21.07	21.55
11	0.35	24.60	21.33	0.47	21.67	19.36	0.30	25.19	23.73
12	0.27	25.23	20.93	0.26	23.27	19.43	0.41	25.22	23.02

Station Code: S31									
	GFDL-ESM2M			HadGEM2-CC			IPSL-CM5-LR		
Mon	PCP	Tmx	Tmn	PCP	Tmx	Tmn	PCP	Tmx	Tmn
1	0.68	20.36	15.98	0.57	20.69	17.31	0.86	21.81	20.29
2	1.90	20.67	16.50	1.03	21.89	17.50	1.54	23.96	22.04
3	2.73	20.71	17.62	0.83	22.58	16.90	2.75	25.15	23.38
4	1.22	22.12	18.25	0.69	22.66	16.08	3.78	26.13	23.90
5	1.26	21.91	17.75	1.21	21.51	16.00	2.61	25.13	22.44
6	1.77	21.93	16.95	1.68	19.74	14.98	3.29	21.14	19.71
7	2.88	18.72	16.10	2.81	16.20	14.22	2.91	17.65	16.92
8	1.78	18.78	15.96	1.80	15.64	13.82	1.71	17.70	16.59
9	2.08	21.23	17.25	1.86	16.80	13.99	1.41	19.25	16.41
10	1.26	23.66	17.16	2.54	20.67	16.99	1.00	22.76	18.42
11	0.30	24.26	17.15	0.51	21.53	16.24	0.24	25.32	20.34
12	0.27	23.28	16.74	0.32	21.45	16.54	0.37	23.90	20.34

Station Code: S32									
	GFDL-ESM2M			HadGEM2-CC			IPSL-CM5-LR		
Mon	PCP	Tmx	Tmn	PCP	Tmx	Tmn	PCP	Tmx	Tmn
1	0.07	-1.22	-2.14	0.07	7.47	6.26	0.04	2.18	-0.65
2	0.06	-0.89	-2.88	0.06	8.15	7.13	0.05	3.58	1.80
3	0.41	-0.18	-0.59	0.04	7.81	6.42	0.10	5.10	4.65
4	0.12	-1.88	-1.23	0.06	4.30	1.55	0.24	4.59	4.63
5	0.37	-1.60	-0.62	0.21	4.06	0.67	0.78	5.23	4.69
6	0.33	2.98	-1.01	0.43	4.01	1.18	1.95	4.46	4.47
7	0.37	4.71	-0.24	0.59	4.40	2.41	1.16	2.12	2.06
8	0.50	3.82	-0.17	0.67	3.49	2.31	0.74	2.53	1.19
9	0.40	3.48	-0.07	0.69	2.44	2.21	0.61	1.63	0.68
10	0.05	1.87	-0.55	0.10	5.55	3.04	0.08	2.57	2.36
11	0.19	-0.06	-1.38	0.02	5.86	2.16	0.01	2.41	2.09
12	0.02	-0.05	-2.86	0.12	6.21	4.89	0.02	2.67	-0.25

Station Code: S33									
	GFDL-ESM2M			HadGEM2-CC			IPSL-CM5-LR		
Mon	PCP	Tmx	Tmn	PCP	Tmx	Tmn	PCP	Tmx	Tmn
1	0.81	20.36	18.02	0.49	20.69	17.31	0.62	21.81	22.03
2	1.90	15.67	16.50	1.63	21.89	17.50	1.54	23.96	19.04
3	2.34	20.71	17.62	0.83	22.58	16.90	2.75	25.15	23.38
4	1.22	22.12	18.25	0.69	22.66	16.08	3.78	26.13	23.05
5	1.55	21.91	17.75	1.21	21.51	16.00	2.61	25.13	22.44
6	1.77	21.93	16.95	1.76	19.74	14.98	3.29	21.14	19.71
7	2.88	18.72	16.10	2.81	16.20	14.22	2.91	17.65	16.92
8	1.78	18.68	15.96	1.80	15.64	13.82	1.71	17.70	16.59
9	2.08	21.23	17.25	1.86	16.80	13.99	1.14	19.25	16.41
10	1.26	23.66	17.16	2.54	20.67	16.99	1.00	20.76	18.42
11	0.30	24.26	17.15	0.51	21.53	16.24	0.24	25.32	20.34
12	1.27	23.28	16.74	1.23	21.45	16.54	0.37	23.90	20.34

Station Code: S34									
	GFDL-ESM2M			HadGEM2-CC			IPSL-CM5-LR		
Mon	PCP	Tmx	Tmn	PCP	Tmx	Tmn	PCP	Tmx	Tmn
1	0.11	-7.18	-13.90	0.71	1.87	-3.19	0.23	-9.99	-10.07
2	0.38	-8.93	-13.76	0.66	0.54	-3.57	0.54	-9.29	-9.09
3	0.28	-7.00	-11.23	0.27	1.26	-2.61	0.25	-6.89	-8.63
4	0.22	-9.68	-12.36	0.13	-0.89	-4.37	0.24	-7.02	-7.94
5	0.89	-9.77	-9.72	0.64	-1.54	-4.88	0.12	-5.26	-5.57
6	0.09	-6.92	-7.86	0.10	-1.65	-4.11	0.62	-3.97	-3.36
7	0.11	-2.64	-7.03	0.17	1.87	-1.88	0.71	-6.10	-5.16
8	0.14	-2.76	-7.10	0.51	0.30	-1.85	0.24	-6.31	-7.32
9	0.61	-3.84	-7.21	0.22	-1.03	-1.05	0.10	-6.36	-7.28
10	0.08	-6.57	-8.22	0.25	0.82	-2.46	0.09	-7.15	-7.34
11	0.20	-6.97	-10.88	0.21	0.84	-4.15	0.07	-6.66	-9.51
12	0.37	-6.70	-10.69	0.33	1.83	-2.26	0.11	-7.38	-10.83

Station Code: S35									
	GFDL-ESM2M			HadGEM2-CC			IPSL-CM5-LR		
Mon	PCP	Tmx	Tmn	PCP	Tmx	Tmn	PCP	Tmx	Tmn
1	0.01	-2.91	-3.67	0.09	2.95	0.70	0.05	2.04	-1.77
2	0.20	-1.18	-3.18	0.00	3.32	0.61	0.00	1.91	0.33
3	0.81	0.25	-1.73	0.00	3.64	-0.05	0.01	3.75	2.40
4	0.04	-1.26	-2.93	0.02	1.96	-2.66	0.05	2.84	2.67
5	0.14	-1.75	-2.39	0.09	1.72	-3.38	0.37	4.51	3.27
6	0.21	1.13	-1.92	0.23	2.18	-2.37	1.67	4.49	4.58
7	0.29	3.25	-0.96	0.42	3.21	0.08	1.17	0.76	1.79
8	0.33	2.72	-1.30	0.53	1.62	-0.41	0.65	0.43	-0.24
9	0.27	2.67	-1.37	0.42	0.46	-0.59	0.29	0.88	-0.67
10	0.02	0.36	-1.65	0.06	2.34	0.26	0.03	1.58	1.27
11	0.01	0.11	-1.07	0.01	2.85	-0.29	0.05	2.89	1.27
12	0.03	0.27	-2.37	0.00	3.48	0.47	0.00	2.05	-0.15

Station Code: S36									
	GFDL-ESM2M			HadGEM2-CC			IPSL-CM5-LR		
Mon	PCP	Tmx	Tmn	PCP	Tmx	Tmn	PCP	Tmx	Tmn
1	0.97	13.05	11.28	0.10	15.61	14.02	0.64	3.14	10.24
2	0.94	14.17	13.68	0.27	18.97	10.78	0.20	10.34	11.63
3	2.11	9.86	11.52	0.30	12.39	13.91	1.21	15.73	14.74
4	0.56	7.61	10.68	0.80	15.39	10.06	5.63	12.28	13.07
5	1.37	5.85	6.85	2.98	10.55	11.09	7.28	9.65	13.16
6	3.29	4.60	3.69	3.59	8.07	9.82	7.43	7.06	12.18
7	1.65	7.02	7.41	2.29	10.71	12.17	3.63	5.27	7.27
8	1.03	10.92	7.18	1.48	11.08	9.80	3.14	8.50	9.38
9	4.76	12.04	9.05	1.95	11.55	10.77	1.52	9.25	9.51
10	0.23	12.68	13.23	2.79	13.41	12.40	1.16	12.48	10.32
11	0.37	13.36	13.07	0.46	17.52	15.20	1.53	14.99	14.03
12	2.12	15.25	11.94	0.97	15.53	14.92	0.13	13.68	11.16

APPENDIX B: Trends in PCP

Table B1: **Precipitation** trend analysis results on **Annual** basis of future data (2020-2099) using Mann-Kendall Test and Sen' slope method:

(Z= Mann-Kendall Z; S= Significance level; SS=Sen's Slope in %ge; *= Statistically significant; N= Not-significant)

***Note*: Z is the statistical parameter. Trend value corresponding to Z value more than +1.96 (-1.96) represents statistically significant.**

Station	RCP4.5									RCP8.5								
	2020-2040			2041-2070			2071-2099			2020-2040			2041-2070			2071-2099		
	Z	S	SS	Z	S	SS	Z	S	SS	Z	S	SS	Z	S	SS	Z	S	SS
S1	-1.0	-	-0.1	0.14	-	0.20	-	-	-	-	-	-3.1	-	-	-0.4	0.96	-	0.9
S2	-	-	-0.5	1.14	-	0.30	0.21	-	0.10	-	-	0.8	0.25	-	0.1	1.41	-	0.7
S3	1.12	-	0.1	1.61	-	0.18	-	-	-	-	-	-0.1	0.75	-	0	0.92	-	0.1
S4	-	-	0	0.50	-	0.08	-	-	-	-	-	-0.3	-	-	0	1.56	-	0.2
S5	1.72	-	0.7	2.11	-	2.59	0.17	-	0	-	-	-0.2	0.11	-	0	0.84	-	0.2
S6	-	-	-0.6	2.11	-	0.59	0.09	-	0.05	-	-	-0.4	-	-	-0.1	1.14	-	0.30
S7	0.69	-	1.05	0.07	-	0.19	0.84	-	1.60	0.27	-	0.5	0.39	-	0.7	2.95	-	4.0
S8	-	-	0	-	-	-	0.77	-	3.48	0.57	-	3.10	0.25	-	1.20	2.49	-	8.20
S9	2.00	-	6.06	-	-	-	0.36	-	2.73	-	-	-0.9	0.5	-	2.60	1.98	-	6.50
S10	-	-	-	-	-	-	0	-	0	-	-	-	0.75	-	2.0	1.22	-	6.90
S11	0.15	-	0.23	-	-	-	0.39	-	0.9	-	-	-	2.14	-	3.6	1.97	-	5.60
S12	-	-	-	-	-	-	0.06	-	0.2	-	-	-3.1	2.46	-	3.6	1.98	-	5.70
S13	1.84	-	0.75	0.50	-	0.21	0.09	-	0	0.39	-	0.5	-	-	-0.5	0.92	-	0.5
S14	-	-	-	0.64	-	1.02	0.09	-	0.1	1.96	-	4.20	-	-	-0.9	0.62	-	1.10
S15	0.33	-	0.12	0	-	0	0.54	-	0.2	-	-	-0.1	-	-	-0.1	2.61	-	0.9
S16	2.57	-	0.65	0.71	-	0.05	-	-	-	-	-	-0.1	-	-	0	-	-	0
S17	2.39	-	0.55	0.57	-	0.09	-	-	0	-1.3	-	-0.2	0.14	-	0	0.17	-	0.1
S18	-	-	-	0.36	-	0.10	-	-	0	-	-	-0.8	-	-	-0.1	1.14	-	0.3
S19	2.26	-	0.69	0.71	-	1.30	0.47	-	0.1	-	-	0	1.14	-	0.2	-	-	-0.1
S20	2.08	-	0.56	0.50	-	0.14	-	-	-0.1	-	-	-0.1	-	-	0	-	-	-0.2
S21	2.26	-	0.23	0.79	-	0.07	-	-	0	-	-	0	-	-	0	-	-	0
S22	1.90	-	1.25	0.39	-	0.10	-	-	-0.1	-	-	-0.2	-	-	0	0.96	-	0.50
S23	-	-	-	-	-	-	0.62	-	0.8	-	-	-0.4	0.5	-	0.7	1.37	-	2.20
S24	-	-	-	-	-	-	0.43	-	1.0	-	-	-0.4	0.03	-	0	1.98	-	2.40
S25	-	-	-	-	-	-	0.36	-	0.7	0	-	0	-	-	-0.2	2.23	-	2.9
S26	0.57	-	2.40	0.36	-	0.41	0	-	0	0.75	-	1.10	-	-	-1.1	1.22	-	1.90
S27	0.75	-	0.57	0.39	-	0.17	0.36	-	0.4	-	-	-0.2	-	-	-0.2	2.87	-	3.00
S28	0.45	-	5.47	0.14	-	0.14	0.73	-	0.6	-	-	-0.2	0.04	-	0	3.21	-	3.80
S29	0.09	-	0.19	0	-	0	1.03	-	2.3	-0.3	-	-0.2	0.36	-	0.3	3.36	-	4.70
S30	0.69	-	0.99	0.57	-	0.77	-	-	-0.4	-	-	-0.3	-	-	-0.5	3.36	-	4.71
S31	0.21	-	0.25	0.57	-	0.53	0	-	0	0.27	-	0.4	2.72	-	3.7	2.72	-	3.70
S32	2.08	-	0.58	0.50	-	0.14	-	-	-0.1	-	-	-0.1	-	-	0	-	-	-
S33	0.69	-	1.45	0.07	-	0.19	0.94	-	1.60	0.27	-	0.5	0.39	-	0.7	2.95	-	4.2
S34	1.96	-	1.45	0.39	-	0.15	-	-	-0.1	-	-	-0.2	-	-	0	0.96	-	0.55
S35	2.27	-	0.25	0.79	-	0.07	-	-	0	-	-	0	-	-	0	-	-	-
S36	0.79	-	0.99	0.57	-	0.77	-	-	-0.4	-	-	-	-	-	-0.5	3.36	-	4.74

Table B2: **Precipitation** trend analyses values on **Seasonal** basis of future data (2020-2040) using Mann-Kendall Test and Sen' slope method

(Z= Mann-Kendall Z; SS=Sen's Slope in %ge;)

***Note*: Z is the statistical parameter. Trend value corresponding to Z value more than +1.96 (-1.96) represents statistically significant.**

Station	RCP4.5 (2020-2040)								RCP8.5 (2020-2040)							
	Pre-Monsoon		Monsoon		Post-Monsoon		Winter		Pre-Monsoon		Monsoon		Post-Monsoon		Winter	
	Z	SS	Z	SS	Z	SS	Z	SS	Z	SS	Z	SS	Z	SS	Z	SS
S1	-	-3.1	1.81	2.1	1.12	0.7	-	-3.5	0.15	0.4	0.03	0	-0.3	0	-	-
S2	-	-1.5	1.15	2.5	-	0	-	-2.7	0.57	0.1	0.09	0.2	-	-0.6	-	-4.0
S3	0.36	0.07	2.18	1.13	-	0.03	-	-	0.21	0	0	0	0.21	0.1	-	-
S4	-	-	2.24	0.82	-	-0.02	-	-	-	0	0.15	0	0.57	0.2	-	-2.0
S5	0.97	0.95	2.05	2.52	-	-0.60	0.51	0.14	0.09	0	0.75	1.20	-	-	-	-0.2
S6	-	-	3.81	3.41	-	-2.81	-	-	-	-1.2	1.96	1.30	-	-	-	0
S7	0.12	1.15	0.54	6.29	-	-7.35	-	-	-	-4.4	3.35	10.80	-	-	-1	-0.7
S8	0.12	1.15	0.54	8.19	-	-7.35	-	-	-	-8.5	1.99	20.1	0	0	-	-0.8
S9	0.91	6.49	1.03	10.8	-	-7.12	-	-	-	-9.1	0.75	17.60	-	-	-	-
S10	0.12	3.28	-	-0.4	-	-21.1	-	-	-	-	1.0	22.0	-	-	-	-0.8
S11	0.24	0.47	0.85	8.18	-	-4.90	-	-	-	-0.8	0.09	0.7	-	-9.0	-1	-0.2
S12	0.18	0.42	0.97	9.84	-	-	-	-	-	-	0.27	4.60	-	-	-	-0.2
S13	0.48	0.07	1.93	5.70	-	-0.55	-	-	-	-0.2	1.41	4.1	-1	-2.1	-	-0.7
S14	-	-	-	-	-	-	-	-	0.69	1.0	1.98	19.3	-	-3.1	-	-0.2
S15	0.91	0.63	0.60	1.12	-	-0.80	-	-	-	-	2.20	3.30	-	-	-	-0.2
S16	0.79	0.12	2.96	2.26	0.15	0.07	-	-	-	-0.2	1.18	0.08	-	-	-	-0.1
S17	0.54	0.11	2.78	2.05	0.15	0.01	-	-	-	-0.3	1.42	0.7	-	-0.9	-	-0.8
S18	-	-	1.63	1.04	0.94	0.34	-	-	0	0	0.21	0.1	0.09	0	-	-4.4
S19	0.66	0.07	2.05	2.90	-	-0.43	0.03	0	-	-0.1	0.51	0.5	-	-0.6	-	0
S20	1.03	0.32	2.36	3.17	-	-0.46	0.27	0	-	-0.5	1.36	2.30	-	-	0.21	0
S21	0.79	0.16	2.30	0.71	0.03	0	0.27	0.01	-	-0.2	1.78	0.4	-	-0.4	-	0
S22	1.39	2.23	1.57	2.07	0.21	0.02	0.51	0.16	-	-	2.02	2.40	-1.6	-3.0	-	-0.1
S23	0.36	0.34	0.54	4.21	-	-4.85	-	-	-	-4.2	1	9.7	-	-5.9	-	-0.7
S24	0.06	0	0.42	5.30	-	-4.12	-	-	-	-4.9	0.82	7.4	-	-5.4	-	-
S25	0	0	0.79	2.07	-	-3.35	-	-	-	-5.7	1.06	7.30	-	-3.4	-	-1.0
S26	0.85	2.53	0.91	8.15	-	-3.60	-	-	-	-	1.78	19.5	-	-6.8	-	-0.5
S27	0.66	2.53	1.09	5.59	-	-2.93	-	-	-	-4.4	1.90	8.0	-	-4.7	-	-0.6
S28	1.42	2.16	2.21	5.34	-	-4.13	-	-	-1.3	-3.2	2.75	9.4	-	-4.8	-	-0.9
S29	0.24	1.00	1.03	4.90	-	-4.69	-	-	-	-5.2	3.17	11.2	-	-5.3	-6.3	-1.0
S30	0	0	1.99	8.78	-	-3.29	-	-	-	-4.2	3.29	10.80	-	-6.8	-1.3	-1.1
S31	-	-	1.33	5.79	-	-2.93	-	-	-	-3.7	3.96	14.9	-	-	-	-0.8
S32	1.03	0.32	2.36	3.17	-	-0.46	0.27	0	-	-0.5	1.36	2.30	-	-	0.21	0
S33	-	-	3.83	3.41	-	-2.81	-	-	-	-1.2	1.96	1.35	-	-	-	-
S34	1.45	2.28	1.57	2.07	0.29	0.02	0.51	0.16	-	-	2.02	2.40	-	-	-	-
S35	1.35	2.25	2.21	5.32	-	-4.13	-	-	-1.3	-3.2	2.72	9.44	-	-	-	-
S36	0	0	1.99	8.77	-	-3.29	-	-	-	-4.2	3.29	10.87	-	-6.8	-	-

Table B3: **Precipitation** trend analyses values on **Seasonal** basis of future data (2041-2070) using Mann-Kendall Test and Sen' slope method

(Z= Mann-Kendall Z; SS=Sen's Slope in %ge;)

***Note*: Z is the statistical parameter. Trend value corresponding to Z value more than +1.96 (-1.96) represents statistically significant..**

Station	RCP4.5 (2041-2070)								RCP8.5 (2041-2070)							
	Pre-Monsoon		Monsoon		Post-Monsoon		Winter		Pre-Monsoon		Monsoon		Post-Monsoon		Winter	
	Z	SS	Z	SS	Z	SS	Z	SS	Z	SS	Z	SS	Z	SS	Z	SS
S1	0	0	0.86	0.30	0.21	0.20	0.14	0.30	-	-2.1	0.04	0	1	0.8	-	-2.6
S2	0.54	0.20	0.96	0.90	-	-	0	0	-	-0.5	0.21	0.2	1.21	2.1	-	-0.9
S3	1.11	0.13	0.79	0.23	0	0	0.50	0.13	0.32	0	0.64	0.1	1.36	0.3	-	-0.3
S4	0.36	0.12	1.07	0.26	0	0	-	-	-	-0.1	-	0	-	0	1.07	0.1
S5	0.71	0.47	1.43	0.89	0	0	2.0	0.66	0.18	0.1	-	-0.5	1.53	1.3	-	-0.4
S6	0.79	0.54	1.50	0.84	-	-	2.18	0.31	-	-0.1	-	-0.9	0.54	0.2	-	-0.1
S7	-	-	1.78	5.14	-	-	-	-	0.64	2.6	-	-2.1	1.50	4.90	-	-0.7
S8	-	-	1.03	6.38	-	-	-	-	0.54	4.3	-	-5.7	0.82	7.2	-	-1.5
S9	0.11	1.66	1.07	5.39	-	-	-	-	0.7	7.2	-	-8.7	1.14	14.3	-	-2.7
S10	0.64	3.16	0.68	4.40	-	-	-	-	1.07	8.7	-	-	2.64	15.5	-	-0.7
S11	0.46	0.44	0.89	5.39	-	-	-	-	0.96	1.1	-	-9.4	2.82	19.1	-	-0.2
S12	0.18	0.31	0	0	-	-	-	-	1.25	1.90	-	-	2.43	18.4	-	-0.2
S13	0.43	.06	0.86	1.30	0.21	0.12	-	-	-	0	-	-4.6	3.46	2.4	-	-0.2
S14	0.61	0.16	0.57	2.81	0.50	1.28	-	-	1.18	0.6	-	-	2.96	7.0	-	-0.1
S15	-	-	1.11	0.58	-	-	-	-	0.75	0.4	-	-1.4	1.36	1.2	-	-0.1
S16	0.07	0.02	0.57	0.34	-	-	0.36	0.02	-0.5	0	-	-0.5	1.57	0.7	-	-0.1
S17	0.71	0.13	0.82	0.30	-	-	0.04	0	-	0	-	-0.4	2.03	0.8	-2.0	-0.1
S18	0.04	0.07	0.71	0.21	0.71	0.18	0	0	-	-0.6	-	-0.1	0.86	0.3	-0.5	-0.7
S19	0.68	0.03	1.18	0.53	-	-	0.54	0	0	0	0	0	1.75	0.8	-	0
S20	0.57	0.12	0.71	0.46	-	-	2.03	0.04	-	0	-	-1.1	1.78	1.1	-	0
S21	0.46	0.05	0.89	0.13	-	-	1.71	0.03	-	0	-	-0.3	0.96	0.1	0.43	0
S22	0.61	0.68	1.43	0.38	-	-	-	-	-	-0.6	-	-0.8	1.03	1.0	-	-0.2
S23	-	-	1.03	2.60	-	-	-	-	1	3.8	-	-5.1	1.07	4.3	-	-0.5
S24	-	-	0.39	2.08	-	-	1.18	0.54	2.12	6.8	-	-	0.27	3.8	-	-0.3
S25	-	-	1.25	2.70	-	-	-	-	0.75	2.0	-	-3.4	0.86	4.8	-	-0.9
S26	0	0	2.36	6.07	-	-	-	-	0.71	1.5	-	-	2.57	9.5	-	-0.4
S27	0	0	0.86	1.85	-	-	-	-	0.75	1.9	-	-4.2	1.46	4.2	-	-0.6
S28	-	-	1.43	2.82	-	-	-	-	0.54	1.2	-	-2.9	1.57	5.3	-	-6.2
S29	-	-	1.68	5.89	-	-	-	-	0.39	1.1	-	-1.5	1.46	5.5	-	-1.8
S30	0.82	1.12	1.14	4.57	-	-	-	-	0.14	0.4	-1.5	-4.1	2.14	4.4	-	-1.1
S31	0.46	0.56	1.50	5.21	-	-	-	-	0.92	2.3	1.03	4.5	1.86	5.9	0.77	0.83
S32	0.57	0.12	0.71	0.46	-	-	2.03	0.04	-	0	-	-1.1	1.78	1.1	-	0
S33	0.79	0.52	1.55	0.84	-	-	2.18	0.31	-	-0.1	-	-0.9	0.54	0.24	-	-
S34	0.61	0.68	1.40	0.38	-	-	-	-	-	-0.6	-	-0.8	1.03	1.0	-	-
S35	0.46	0.15	0.89	0.13	-	-	1.75	0.03	-	0	-	-0.3	0.98	0.1	0.43	0
S36	0.85	1.12	1.14	4.59	-	-	-	-	0.14	0.43	-1.5	-4.1	2.14	4.42	-	-

Table B4: **Precipitation** trend analyses values on **Seasonal** basis of future data (2071-2099) using Mann-Kendall Test and Sen' slope method

(Z= Mann-Kendall Z; SS=Sen's Slope in %ge;)

***Note*: Z is the statistical parameter. Trend value corresponding to Z value more than +1.96 (-1.96) represents statistically significant.**

Station	RCP4.5 (2071-2099)								RCP8.5 (2071-2099)							
	Pre-Monsoon		Monsoon		Post-Monsoon		Winter		Pre-Monsoon		Monsoon		Post-Monsoon		Winter	
	Z	SS	Z	SS	Z	SS	Z	SS	Z	SS	Z	SS	Z	SS	Z	SS
S1	0.77	0.99	0.24	0.31	0.02	0.14	-	-	0.06	0.1	0.77	0.8	0.62	0.4	0.96	3.9
S2	0.58	0.20	0.54	0.48	0.28	0.45	-	-	0.88	0.3	0.84	1.38	0.62	0.6	0.99	1.3
S3	1.11	0.15	0.13	0.06	0.28	0.08	-	-	0.47	0	0.24	0.1	0.24	0.1	1.11	0.47
S4	0.88	0.18	0.54	0.16	0	0	-	-	0.77	0.2	0.36	0.1	0.06	0	1.33	0.7
S5	0.36	0.19	0.47	0.23	0.54	0.50	-	-	1.88	0.9	-	-0.7	0.88	0.6	-	-
S6	0.06	0.01	0.39	0.25	0.39	0.35	-	-	0.66	0.30	-	-	1.56	1.0	0.54	0.30
S7	0.06	0.19	1.93	6.59	-	-	-	-	0.54	1.20	1.98	5.30	2.01	7.30	0.77	0.20
S8	0.13	1.28	1.98	13.86	-	-	-	-	0.47	3.50	0.58	4.50	2.27	21.20	0.54	0.4
S9	0.24	3.66	1.96	19.55	-	-	-	-	1.92	11.1	0.06	0.80	2.11	20.5	1.18	1.50
S10	-	0	1.41	9.92	-	-9.4	-	-	0.69	7.10	0.58	6.70	1.88	14.60	0.58	0.2
S11	0.62	0.9	2.61	11.2	-	-6.5	-	-0.1	0.96	1.10	0.88	4.90	2.44	15.0	0.66	0.1
S12	0.13	0.4	1.22	9.3	-	-5.1	-	-0.2	0.66	1.50	1.07	0.98	1.18	11.1	0.92	0.1
S13	0.47	0.1	1.14	1.80	-	-	-	-0.7	1.18	0.20	0.28	1.0	0.66	1.10	0.69	0.24
S14	0.36	0.2	1.29	5.6	-	-3.8	-	-0.1	0.81	0.7	0.43	3.90	0.96	3.60	1.18	0.1
S15	0.13	0.1	1.74	1.60	-	-0.5	-	-0.2	0.81	0.60	0.66	0.7	1.41	1.30	0.81	0.1
S16	0.24	0	-	0	-	-0.1	-	-0.1	1.26	0.2	-	-0.6	0.73	0.3	0.62	0.1
S17	0.24	0	0.28	0.1	0.02	0	-	-0.1	1.29	0.4	-	-0.4	1.11	0.4	0.43	0.1
S18	0.81	0.3	0.43	0.2	-	-0.2	-	-0.4	0.02	0.3	0.84	0.3	0.62	0.2	0.92	1.20
S19	-	0	0.69	0.3	0.73	0.3	-	0	0.66	0.1	-	-0.7	0.24	0.1	0.58	0
S20	-	-0.1	-	-0.2	-	-0.1	-	0	0.77	0.1	-	-	0.81	0.4	0.32	0
S21	-	0	-	0	0	0	0.36	0	0.66	0	-	-0.3	0.81	0.1	-	0
S22	0.47	0.5	-	-0.8	-	-0.1	-	-0.1	0.36	0.3	-	-0.2	1.52	1.70	0.81	0.30
S23	0.21	0.7	1.78	7.40	-	-	-	-0.4	1.03	4.80	0.32	0.9	1.52	6.10	1.26	0.31
S24	0.17	0.6	1.86	7.3	-	-	-	-0.4	0.92	4.0	0.24	1.50	1.59	6.20	1.18	0.3
S25	0.32	1.30	2.04	6.0	-	-0.5	1.52	-0.8	0.81	3.9	0.47	1.40	1.96	7.70	1.29	0.6
S26	0.09	0.3	1.11	6.3	-	-3.8	-	-0.3	0.62	1.50	0.21	1.80	0.92	2.30	1.03	0.12
S27	0.09	0.4	2.04	6.20	-	-	-	-0.5	0.69	2.0	0.88	2.90	1.41	4.40	0.81	0.3
S28	0.28	1.0	2.46	5.90	-	-	-	-0.9	1.14	2.90	1.26	4.20	2.16	6.0	0.81	0.6
S29	0.39	1.60	1.71	6.70	-	-	-	-	1.22	3.90	1.99	5.90	1.97	8.50	0.99	0.9
S30	0.21	0.3	0.73	2.60	-	-	-	-0.8	1.20	0.48	1.59	5.80	1.99	8.6	0.97	0.7
S31	0.43	1.70	0.02	0.1	-	-	-	-	0.92	2.30	1.03	0.45	1.96	5.90	0.77	0.8
S32	-	-0.1	-	-0.2	-	-0.1	-	0	0.77	0.1	-	-	0.81	0.4	0.32	0
S33	0.08	0.04	0.39	0.25	0.39	0.65	-	-	0.66	0.30	-	-	1.56	1.0	0.54	0.36
S34	0.61	0.78	1.43	0.38	-	-	-	-	-	-0.6	-	-0.8	1.09	1.0	-	-
S35	0.25	1.3	2.46	5.96	-	-	-	-	1.14	2.98	1.26	4.20	2.16	6.70	0.81	0.68
S36	0.43	1.45	0.02	0.17	-	-	-	-	0.92	2.38	1.03	0.45	1.96	5.98	0.77	0.86

APPENDIX C: Trends in TMax

Table C1: **Temperature (Max.)** trend analysis results on **Annual** basis of future data (2020-2099) using Mann-Kendall Test and Sen's slope method:

(Z= Mann-Kendall Z; S= Significance level; SS=Sen's Slope in %ge; *= Statistically significant; N= Not-significant)

***Note*: Z is the statistical parameter. Trend value corresponding to Z value more than +1.96 (-1.96) represents statistically significant.**

Station	RCP4.5									RCP8.5								
	2020-2040			2041-2070			2071-2099			2020-2040			2041-2070			2071-2099		
	Z	S	SS	Z	S	SS	Z	S	SS	Z	S	SS	Z	S	SS	Z	S	SS
S1	2.45	xxx	6.0	2.18	xxx	2.85	3.43	xxx	3.71	3.53	xxx	6.10	5.28	xxx	9.80	4.63	xxx	10.00
S2	-	xxx	4.6	2.36	xxx	2.79	3.58	xxx	4.14	3.41	xxx	6.0	5.46	xxx	10.00	4.71	xxx	9.80
S3	2.02	xxx	6.6	2.11	xxx	3.16	3.56	xxx	4.91	2.99	xxx	5.60	5.32	xxx	12.00	4.56	xxx	10.60
S4	2.20	xxx	6.3	2.50	xxx	3.28	3.58	xxx	4.41	3.11	xxx	6.50	5.78	xxx	11.30	4.75	xxx	9.00
S5	2.33	xxx	7.1	2.93	xxx	5.18	2.23	xxx	3.10	3.84	xxx	9.80	5.50	xxx	12.80	5.05	xxx	7.90
S6	-	xxx	-	2.93	xxx	5.25	2.34	xxx	3.11	2.99	xxx	6.30	5.60	xxx	10.90	5.20	xxx	8.50
S7	2.69	xxx	4.3	4.32	xxx	3.57	2.42	xxx	1.85	3.11	xxx	5.60	6.10	xxx	7.30	5.50	xxx	5.90
S8	3.23	xxx	5.1	4.46	xxx	4.32	1.74	xxx	1.52	3.41	xxx	6.01	5.96	xxx	7.80	5.46	xxx	5.70
S9	-	xxx	-	4.50	xxx	4.55	1.82	xxx	1.55	3.59	xxx	6.30	6.17	xxx	7.90	5.61	xxx	6.00
S10	-	xxx	-	3.89	xxx	4.10	1.78	xxx	1.61	3.77	xxx	6.30	6.07	xxx	8.00	5.31	xxx	6.20
S11	3.11	xxx	5.0	2.96	xxx	3.77	1.11	xxx	1.32	3.71	xxx	7.00	5.57	xxx	6.10	4.18	xxx	7.40
S12	3.17	xxx	6.2	3.28	xxx	3.90	1.48	xxx	1.63	3.96	xxx	7.10	5.71	xxx	6.90	4.26	xxx	7.20
S13	2.08	xxx	4.4	3.64	xxx	4.23	3.21	xxx	2.60	3.59	xxx	7.30	5.78	xxx	8.50	4.97	xxx	6.80
S14	-	xxx	-	3.71	xxx	4.41	3.06	xxx	2.32	2.63	xxx	3.60	6.07	xxx	7.80	5.16	xxx	6.20
S15	2.33	xxx	4.80	4.21	xxx	4.24	2.79	xxx	2.21	3.29	xxx	6.60	6.10	xxx	8.10	5.16	xxx	6.20
S16	2.08	xxx	6.70	3.00	xxx	4.66	2.72	xxx	3.64	3.77	xxx	8.50	5.32	xxx	10.50	5.46	xxx	7.80
S17	2.33	xxx	6.50	2.82	xxx	4.46	2.91	xxx	3.75	3.90	xxx	8.00	5.39	xxx	11.10	4.78	xxx	7.40
S18	2.45	xxx	5.80	2.43	xxx	2.79	3.47	xxx	3.74	3.35	xxx	6.60	5.10	xxx	9.50	4.60	xxx	9.70
S19	2.51	xxx	7.40	2.71	xxx	4.31	2.91	xxx	3.46	3.59	xxx	8.80	5.50	xxx	12.50	4.82	xxx	7.70
S20	2.33	xxx	6.40	2.89	xxx	5.00	2.46	xxx	2.98	3.59	xxx	7.90	5.39	xxx	11.90	5.42	xxx	9.30
S21	1.90	xxx	5.60	3.21	xxx	5.02	2.76	xxx	3.20	3.29	xxx	7.40	5.39	xxx	11.20	5.38	xxx	9.00
S22	1.54	xxx	4.30	2.85	xxx	3.45	2.83	xxx	3.35	2.45	xxx	6.20	5.78	xxx	9.90	4.82	xxx	7.50
S23	3.05	xxx	4.80	4.25	xxx	4.08	2.19	xxx	1.64	3.41	xxx	6.10	6.17	xxx	7.90	5.46	xxx	6.20
S24	3.17	xxx	5.00	4.32	xxx	4.12	2.12	xxx	1.72	3.41	xxx	6.10	6.28	xxx	8.00	5.50	xxx	6.10
S25	3.17	xxx	5.30	4.71	xxx	4.38	1.86	xxx	1.61	3.59	xxx	5.90	6.20	xxx	7.50	5.68	xxx	6.00
S26	2.14	xxx	4.70	3.78	xxx	4.55	3.17	xxx	2.70	3.35	xxx	7.50	5.74	xxx	8.70	5.27	xxx	6.70
S27	2.20	xxx	4.50	410	xxx	4.29	2.76	xxx	2.43	3.23	xxx	6.80	6.10	xxx	8.10	5.35	xxx	6.80
S28	2.54	xxx	4.40	4.21	xxx	4.05	2.95	xxx	1.98	3.05	xxx	6.10	6.32	xxx	7.70	5.42	xxx	6.10
S29	2.69	xxx	4.30	4.35	xxx	3.48	2.42	xxx	1.84	3.11	xxx	5.40	6.14	xxx	7.30	5.57	xxx	5.80
S30	1.90	xxx	4.10	3.64	xxx	3.77	2.98	xxx	2.68	0.51	xxx	1.00	6.03	xxx	8.60	5.20	xxx	7.10
S31	1.72	xxx	3.70	3.64	xxx	3.58	2.64	xxx	2.52	2.75	xxx	5.70	5.99	xxx	8.30	5.16	xxx	6.40
S32	2.33	xxx	6.42	2.89	xxx	5.20	2.46	xxx	2.96	3.59	xxx	7.98	5.39	xxx	11.90	5.42	xxx	9.32
S33	1.54	xxx	4.30	2.85	xxx	3.45	2.83	xxx	3.35	2.45	xxx	6.20	5.78	xxx	9.90	4.82	xxx	7.50
S34	1.72	xxx	3.70	3.64	xxx	3.58	2.64	xxx	2.52	2.75	xxx	5.70	5.99	xxx	8.30	5.16	xxx	6.40
S35	2.54	xxx	4.40	4.21	xxx	4.05	2.95	xxx	1.98	3.05	xxx	6.10	6.32	xxx	7.70	5.42	xxx	6.10
S36	1.72	xxx	3.70	3.64	xxx	3.58	2.64	xxx	2.52	2.75	xxx	5.70	5.99	xxx	8.30	5.16	xxx	6.40

Table C2: **Temperature (Max.)** trend analyses values on **Seasonal** basis of future data (2020-2040) using Mann-Kendall Test and Sen's slope method

(Z= Mann-Kendall Z; SS=Sen's Slope in %ge;)

***Note*: Z is the statistical parameter. Trend value corresponding to Z value more than +1.96 (-1.96) represents statistically significant..**

Station	RCP4.5 (2020-2040)								RCP8.5 (2020-2040)							
	Pre-Monsoon		Monsoon		Post-Monsoon		Winter		Pre-Monsoon		Monsoon		Post-Monsoon		Winter	
	Z	SS	Z	SS	Z	SS	Z	SS	Z	SS	Z	SS	Z	SS	Z	SS
S1	2.45	10.5	2.57	5.4	0.75	2	0.75	4.6	1.78	7.4	2.51	5.8	0.27	1.20	2.26	10.1
S2	-	-1.8	-	-1.9	-	-8.7	-	-7.3	1.72	6.30	2.20	5.20	0.45	1.20	2.20	10.5
S3	2.26	9.9	1.54	4.9	1.42	3.1	0.57	6.5	1.42	6.70	1.66	5.10	0.51	1.0	2.14	10.1
S4	2.51	10.3	2.20	5	1.18	3.8	0.63	4.2	1.60	6.50	1.96	5.80	0.82	2.00	2.20	11.20
S5	2.33	7.8	2.45	5.2	1.66	5.9	1.36	8.7	2.33	11.10	2.75	6.80	1.98	5.10	2.63	15.0
S6	-	-	-	-9.2	-	-	-	-9.6	2.20	9.40	2.14	3.60	2.26	7.00	1.96	6.50
S7	3.47	8.5	1.30	2.6	2.08	4.4	0.03	0	2.26	7.30	1.24	2.30	3.29	4.80	2.63	6.20
S8	3.05	9.2	1.48	3	2.45	4.6	1.30	1.6	2.45	9.70	1.36	2.80	3.65	4.70	2.63	7.10
S9	-	-4.9	-	-7	-	-3.3	-	-5.6	2.14	9.00	1.72	3.10	3.53	5.50	2.81	7.10
S10	-	-	-	-15	-	-9.3	-	-13	2.33	9.00	2.02	3.70	3.29	5.50	2.93	8.20
S11	2.45	8.9	1.78	4.1	2.39	1.7	0.94	1.6	2.39	9.20	2.87	6.50	3.17	3.80	2.51	6.30
S12	2.63	9.1	2.02	3.7	2.69	4.9	1.12	2.8	2.45	10.40	2.99	6.60	2.87	4.10	2.63	6.70
S13	2.93	9.1	1.66	2.5	1.60	4.7	0.45	2.5	2.51	8.70	1.96	2.60	2.33	6.0	2.87	10.3
S14	-	-	-	-	-	-	-	-23	1.66	3.60	1.00	1.80	2.39	3.90	2.51	6.40
S15	3.29	9.0	2.02	2.7	1.78	4.8	0.51	1.7	2.33	6.60	1.78	3.00	2.81	5.90	2.57	9.70
S16	2.75	10.2	1.72	4.1	1.36	6.5	1.00	7.2	2.02	8.90	3.17	4.20	2.26	5.70	2.57	14.50
S17	2.63	10.2	1.90	4.1	1.30	4.7	1.00	7.7	2.26	9.80	2.75	4.90	1.24	5.20	2.39	13.40
S18	2.51	10.5	2.26	4.7	0.75	1.8	0.75	4.1	1.72	7.40	2.39	5.60	0.57	1.50	2.45	10.20
S19	2.45	9.6	1.96	5.4	1.30	5	1.12	8.3	2.14	10.40	2.69	6.60	1.06	3.90	2.26	15.0
S20	2.93	7.4	2.14	4.4	1.54	5.7	0.63	4.3	2.14	7.90	2.93	5.30	2.08	7.40	2.26	11.70
S21	2.87	8.5	1.78	4.3	1.36	5.2	0.45	3.4	2.14	8.20	2.81	4.40	2.26	7.30	2.14	9.00
S22	2.33	7.3	1.54	4.7	1.30	4.5	1.06	6.4	2.45	9.40	1.30	1.70	2.26	6.30	1.60	6.70
S23	3.28	8.5	2.08	3	2.26	5.1	1.18	2.7	2.08	8.30	1.48	3.00	3.47	5.50	2.81	7.40
S24	3.23	8.8	1.96	3	2.45	5.2	1.18	2.5	2.14	8.30	1.60	2.90	3.47	5.50	2.81	7.10
S25	3.17	8.9	1.54	2.7	2.33	4.8	1.66	2.2	2.33	9.10	1.36	2.80	3.41	4.70	2.81	6.90
S26	3.11	9.4	2.08	2.4	1.54	4.7	0.45	3.8	2.45	7.10	2.33	3.0	2.57	6.60	2.87	10.70
S27	3.29	8.9	2.08	2.8	1.78	4.7	0.51	1.8	2.26	6.20	1.96	2.90	2.81	5.90	2.51	10.20
S28	3.41	8.6	1.84	2.6	1.84	4.6	0.03	0	2.14	6.70	1.66	2.90	2.99	5.10	2.51	8.70
S29	3.47	8.4	1.30	2.7	2.08	4.3	-	-0.1	2.26	7.10	1.30	2.30	3.35	4.80	2.69	5.80
S30	3.17	8.5	1.72	2.5	1.66	4.2	-	-0.1	0.69	2.50	-	-0.9	0.45	0.8	0.21	1.20
S31	3.23	8.2	1.60	2.5	1.60	2.7	0.21	0.6	2.08	7.50	1.24	1.60	2.45	5.20	1.90	9.10
S32	2.93	7.8	2.14	4.4	1.54	5.9	0.63	3.3	2.14	7.96	2.93	5.68	2.08	6.40	2.26	10.70
S33	2.87	8.6	1.78	4.3	1.36	5.2	0.45	3.4	2.14	8.20	2.81	4.40	2.26	6.30	2.14	8.00
S34	2.33	7.3	1.54	4.7	1.30	4.5	1.06	6.4	2.45	9.40	1.30	1.70	2.26	6.30	1.60	6.70
S35	3.41	8.6	1.84	2.6	1.84	4.6	0.03	0	2.14	6.70	1.66	2.90	2.99	5.10	2.51	8.70
S36	3.23	8.2	1.60	2.5	1.60	2.7	0.21	0.6	2.08	7.50	1.24	1.60	2.45	5.20	1.90	9.10

Table C3: **Temperature (Max.)** trend analyses values on **Seasonal** basis of future data (2041-2070) using Mann-Kendall Test and Sen's slope method

(Z= Mann-Kendall Z; SS=Sen's Slope in %ge;)

***Note*: Z is the statistical parameter. Trend value corresponding to Z value more than +1.96 (-1.96) represents statistically significant..**

Station	RCP4.5 (2041-2070)								RCP8.5 (2041-2070)							
	Pre-Monsoon		Monsoon		Post-Monsoon		Winter		Pre-Monsoon		Monsoon		Post-Monsoon		Winter	
	Z	SS	Z	SS	Z	SS	Z	SS	Z	SS	Z	SS	Z	SS	Z	SS
S1	2.45	5.5	2.65	3.1	0.57	0.87	1.39	4.4	3.85	10.90	5.50	8.30	5.74	13.20	2.64	9.40
S2	2.32	4.5	2.28	2.8	0.96	1.3	1.61	4.7	3.93	10.90	5.57	8.60	5.67	13.40	2.82	9.80
S3	2.18	4.9	1.71	2.5	1.39	1.9	1.61	5.4	3.85	12.30	5.32	9.50	5.57	14.70	2.85	10.50
S4	2.50	4.4	2.14	2.4	1.11	1.6	1.75	5.1	4.03	10.80	5.50	10.00	5.64	14.20	2.93	11.30
S5	3.00	7.0	3.93	3.7	1.64	2.3	2.28	6.8	4.14	11.60	5.25	10.60	5.14	14.00	3.53	15.10
S6	3.03	7.1	3.96	3.7	1.63	2.2	2.18	6.9	3.60	7.80	5.21	8.80	5.32	11.00	3.64	14.50
S7	2.78	5.2	1.82	1.6	3.68	3	2.07	3.9	2.60	4.60	4.89	7.80	5.85	8.50	4.78	9.80
S8	2.78	5.8	2.21	1.5	4.21	3.4	3.60	5	2.43	6.20	5.00	6.60	5.85	8.90	5.25	9.90
S9	2.78	6.0	2.21	1.7	4.82	3.8	4.17	5.9	3.30	6.20	5.14	6.70	5.96	9.20	5.03	9.70
S10	2.43	4.7	1.75	1.9	4.35	2.9	3.00	4.8	3.00	6.00	4.92	7.20	5.60	8.90	4.96	10.40
S11	1.50	4.6	1.21	2.3	3.89	3.7	2.64	3.6	2.03	5.30	3.07	5.80	5.82	7.70	4.78	8.80
S12	1.78	4.5	1.18	2.3	4.14	3.3	3.03	4.4	2.60	5.90	3.46	6.30	5.85	8.60	5.07	9.70
S13	2.78	4.6	2.64	1.8	2.21	1.7	2.39	6.3	3.82	7.60	5.39	7.70	4.96	8.40	3.89	10.60
S14	2.89	5.1	2.43	1.7	2.46	1.6	2.53	6.5	3.21	6.20	5.10	7.10	5.39	8.40	4.89	10.50
S15	2.85	5.3	2.57	1.9	3.28	2.4	2.57	6.3	3.35	5.20	5.35	7.70	5.42	8.60	4.64	10.40
S16	2.85	6.1	3.25	2.5	1.32	1.6	2.39	7.5	3.60	9.30	5.39	9.80	4.82	10.10	3.10	14.30
S17	2.96	5.9	2.64	2.4	1.25	1.3	2.36	6.6	4.10	10.10	5.32	9.90	4.96	11.40	3.53	11.90
S18	2.64	5.9	2.75	2.6	0.79	0.98	1.53	4.2	3.96	10.40	5.53	8.00	5.50	12.60	2.78	9.30
S19	2.64	6.3	2.28	2.8	1.50	1.8	2.36	5.9	4.10	12.0	5.39	10.80	5.14	14.20	3.25	12.90
S20	2.89	6.3	4.00	3.6	1.32	1.8	2.03	7.2	3.60	9.80	5.32	9.50	5.07	12.50	3.64	16.20
S21	2.78	5.9	4.10	3.6	1.43	1.8	2.14	7.7	3.53	8.50	5.35	9.10	5.17	10.80	3.60	16.40
S22	3.14	5.0	2.96	3.4	1.18	1.6	1.07	3.9	3.32	6.70	5.21	8.60	5.46	10.40	3.93	14.60
S23	2.68	5.1	1.82	1.6	4.21	3	3.28	5.7	2.96	6.10	5.35	7.00	5.67	9.10	4.96	10.00
S24	2.68	5.3	1.93	1.6	4.25	3.1	3.35	5.8	3.03	5.90	5.39	7.00	5.78	9.10	5.03	9.90
S25	2.85	6.3	1.68	1.4	4.21	3.5	3.86	5.7	3.03	5.80	5.21	6.40	5.78	9.00	5.03	9.90
S26	2.85	5.1	2.71	1.9	2.18	1.9	2.71	7.2	3.75	7.40	5.42	8.10	5.00	8.40	4.07	11.60
S27	3.00	5.2	2.71	2.0	3.10	2.3	2.50	6.6	3.50	5.40	5.46	7.80	5.39	8.50	4.57	10.80
S28	2.85	5.4	2.32	1.9	3.64	3.3	2.00	5.0	2.96	4.60	5.32	7.40	5.67	8.50	4.60	10.00
S29	2.78	5.2	1.68	1.6	3.53	3.0	2.07	3.7	2.57	4.50	4.89	7.40	5.85	8.40	4.67	9.70
S30	3.21	5.1	2.50	2.7	2.21	2.4	1.82	6	3.28	5.20	5.64	8.00	5.50	8.90	4.32	12.00
S31	3.00	4.6	2.64	2.8	2.64	2.9	1.68	4.8	3.14	5.10	5.64	8.20	5.35	8.40	4.25	11.80
S32	2.89	6.3	4.00	3.6	1.32	1.8	2.03	7.2	3.60	9.80	5.32	9.50	5.07	12.50	3.64	16.20
S33	3.00	5.2	2.71	2.0	3.10	2.3	2.50	6.6	3.50	5.40	5.46	7.80	5.39	8.50	4.57	10.80
S34	3.03	7.1	3.96	3.7	1.63	2.2	2.18	6.9	3.60	7.80	5.21	8.80	5.32	11.00	3.64	14.50
S35	2.78	4.6	2.64	1.8	2.21	1.7	2.39	6.3	3.82	7.60	5.39	7.70	4.96	8.40	3.89	10.60
S36	3.21	4.6	2.50	2.7	2.21	2.4	1.82	6	3.28	5.20	5.64	8.00	5.50	8.90	4.32	11.80

Table C4: **Temperature (Max.)** trend analyses values on **Seasonal** basis of future data (2071-2099) using Mann-Kendall Test and Sen's slope method

(Z= Mann-Kendall Z; SS=Sen's Slope in %ge;)

***Note*: Z is the statistical parameter. Trend value corresponding to Z value more than +1.96 (-1.96) represents statistically significant.**

Station	RCP4.5 (2071-2099)								RCP8.5 (2071-2099)							
	Pre-Monsoon		Monsoon		Post-Monsoon		Winter		Pre-Monsoon		Monsoon		Post-Monsoon		Winter	
	Z	SS	Z	SS	Z	SS	Z	SS	Z	SS	Z	SS	Z	SS	Z	SS
S1	1.14	2.7	2.9	0.43	1.44	2.2	3.58	9.1	3.51	10.50	2.80	6.20	4.71	13.20	2.87	13.00
S2	1.41	2.9	0.36	0.71	1.37	3.0	3.43	9.4	3.53	10.40	2.91	6.10	4.71	13.20	3.06	13.20
S3	1.18	3.3	0.28	0.47	1.44	3.6	3.4	11.0	3.26	10.00	2.61	5.40	4.63	14.60	2.95	13.70
S4	1.22	3.1	0.32	0.35	1.37	3.4	3.51	9.6	3.32	9.10	2.98	5.40	4.48	12.90	3.02	12.70
S5	1.48	3.5	0	0	1.11	3.2	2.23	3.7	4.03	8.00	3.40	6.20	3.06	9.90	3.96	13.30
S6	1.56	3.7	-	-	0.96	3.3	2.42	8.4	3.62	8.40	3.85	6.70	3.55	7.80	4.30	13.30
S7	1.43	0.82	-	-	1.52	1.8	2.49	2.7	2.42	3.50	3.77	5.60	4.45	5.90	3.85	7.00
S8	0	0	-	-	1.43	1.4	2.42	3.5	1.26	2.20	3.43	5.90	4.78	6.80	4.03	7.40
S9	0.43	0.89	-	-	2.01	1.8	2.38	3.4	1.78	2.40	3.06	5.10	5.08	7.70	3.96	7.80
S10	0.28	0.05	0.36	0.45	2.31	2.5	2.43	3.7	2.46	4.00	2.76	4.60	5.05	7.50	4.00	7.30
S11	0.06	0.02	0.54	0.13	2.64	3.5	2.04	3.9	1.86	7.00	2.31	4.10	4.97	7.70	4.71	7.60
S12	0.09	0.36	0.47	0.61	2.61	2.1	1.86	3.9	1.56	4.80	2.12	4.30	5.42	8.20	4.82	8.10
S13	1.07	1.4	-	-	1.52	2.5	3.17	6.7	3.13	5.40	3.92	5.70	4.03	7.00	2.98	9.20
S14	1.14	1.5	0.13	0.25	1.78	2.7	3.02	6.7	2.79	4.80	2.98	4.70	4.82	7.30	3.62	7.10
S15	0.81	1.3	-	-	2.08	2.6	2.64	5.1	2.79	4.80	2.98	4.70	4.40	7.10	3.52	7.00
S16	1.44	2.5	0.09	0.14	1.41	3.5	2.68	9.1	4.26	6.70	4.03	6.40	3.36	8.60	3.17	11.60
S17	1.29	2.6	-	-	1.26	2.1	2.68	10.3	3.62	6.90	3.66	5.60	3.43	9.20	2.68	11.20
S18	1.14	2.4	0.13	0.20	1.44	2.3	3.77	9.2	3.28	9.50	3.13	6.10	4.78	12.60	2.79	12.70
S19	1.44	3.1	0.13	0.17	0.99	3.4	2.79	10.0	3.66	7.70	3.13	5.40	3.25	10.20	3.02	12.50
S20	1.29	2.9	0.28	0.40	1.07	3.3	1.97	6.9	3.92	8.80	3.73	6.90	2.95	8.60	4.60	14.60
S21	1.22	2.2	0.28	0.27	1.37	3.0	2.46	7.9	3.96	8.10	3.92	6.90	3.17	8.10	4.56	14.20
S22	1.03	1.8	0.66	0.96	1.11	2.5	2.27	7.6	3.66	7.50	3.96	6.60	3.43	6.30	3.32	10.70
S23	0.43	0.77	0.02	0.16	2.19	2.3	2.42	3.9	2.64	2.80	2.98	5.00	4.90	7.20	3.77	7.10
S24	0.47	0.57	-	-	2.04	2.3	2.46	3.8	2.53	2.60	3.10	5.20	4.97	7.30	3.85	7.20
S25	0.32	0.42	-	-	1.76	1.7	2.38	3.4	1.89	2.50	3.25	5.70	4.93	7.80	4.22	7.70
S26	1.22	1.6	-	-	1.56	2.5	2.98	6.7	3.58	5.10	3.88	5.80	4.07	7.20	3.13	9.20
S27	0.92	1.3	-	-	2.14	2.6	2.64	5.4	3.70	4.80	3.92	5.70	4.52	6.80	3.36	8.50
S28	0.81	1.2	-	-	1.97	2.3	2.72	3.9	3.25	4.00	3.81	5.60	4.48	6.20	3.40	7.30
S29	0.51	0.71	-	-	1.52	1.8	2.49	3.7	2.42	3.50	3.70	5.60	4.45	5.80	3.88	7.00
S30	1.07	1.3	0.06	0.15	1.56	2.6	2.57	6.0	3.66	5.90	4.00	6.20	4.15	6.40	3.77	10.00
S31	1.08	1.2	0.24	0.43	1.48	2.2	2.49	5.6	3.36	5.40	4.03	6.20	3.92	5.50	3.17	8.70
S32	1.29	2.6	0.09	0.13	1.26	2.1	2.68	10.3	3.62	6.90	3.66	5.60	3.43	9.20	2.68	11.20
S33	1.56	3.1	-	-	0.96	3.9	2.42	8.0	3.62	8.90	3.85	6.10	3.55	7.20	4.30	11.30
S34	1.07	1.4	-	-	1.52	2.5	3.17	6.7	3.13	5.40	3.92	5.70	4.03	7.00	2.98	9.20
S35	0.81	1.3	-	-	2.08	2.6	2.64	5.1	2.79	4.80	2.98	4.70	4.40	7.10	3.52	7.00
S36	1.07	1.6	0.06	0.20	1.56	2.80	2.57	6.6	3.66	5.92	4.00	6.80	4.15	5.40	3.77	9.20

APPENDIX D: Trends in TMin

Table D1: **Temperature (Min.)** trend analyses values on **Annual** basis of future data (2020-2099) using Mann-Kendall Test and Sen's slope method:

(Z= Mann-Kendall Z; S= Significance level; SS=Sen's Slope in %ge; *= Statistically significant; N= Not-significant)

***Note*: Z is the statistical parameter. Trend value corresponding to Z value more than +1.96 (-1.96) represents statistically significant.**

Station	RCP4.5									RCP8.5								
	2020-2040			2041-2070			2071-2099			2020-2040			2041-2070			2071-2099		
	Z	S	SS	Z	S	SS	Z	S	SS	Z	S	SS	Z	S	SS	Z	S	SS
S1	1.66	xxx	3.78	2.07	xxx	2.38	2.61	xxx	2.56	1.48	xxx	2.00	4.75	xxx	6.70	5.06	xxx	7.10
S2	-	xxx	-7.79	1.28	xxx	1.89	2.76	xxx	3.18	1.30	xxx	6.4	4.64	xxx	6.90	5.08	xxx	7.10
S3	1.72	xxx	4.21	1.32	xxx	1.80	3.13	xxx	5.12	0.75	xxx	1.50	4.10	xxx	6.50	3.58	xxx	6.50
S4	1.90	xxx	3.96	1.36	xxx	1.65	2.53	xxx	3.73	0.82	xxx	2.70	4.14	xxx	6.00	5.16	xxx	6.60
S5	1.60	xxx	3.97	1.32	xxx	1.98	2.23	xxx	2.90	1.72	xxx	3.00	3.93	xxx	5.30	4.78	xxx	6.90
S6	-	xxx	-20.3	1.03	xxx	2.03	2.53	xxx	3.30	1.12	xxx	3.00	5.25	xxx	9.10	5.31	xxx	8.80
S7	2.63	xxx	2.89	3.82	xxx	3.11	2.49	xxx	1.91	3.41	xxx	4.20	6.46	xxx	7.50	6.13	xxx	7.20
S8	3.65	xxx	3.97	4.64	xxx	3.93	2.68	xxx	1.82	3.90	xxx	5.40	6.21	xxx	7.90	6.10	xxx	7.30
S9	-	xxx	-6.22	4.64	xxx	4.13	2.64	xxx	1.99	3.96	xxx	4.90	6.28	xxx	7.60	5.98	xxx	7.20
S10	-	xxx	-	3.25	xxx	2.69	2.23	xxx	2.00	3.53	xxx	4.40	6.32	xxx	7.20	5.68	xxx	7.00
S11	3.41	xxx	3.85	2.28	xxx	1.96	2.38	xxx	1.89	3.47	xxx	5.80	6.14	xxx	7.10	5.46	xxx	6.70
S12	3.29	xxx	3.59	3.07	xxx	2.51	2.31	xxx	1.96	3.84	xxx	5.90	6.24	xxx	7.40	5.76	xxx	7.00
S13	2.26	xxx	2.94	2.75	xxx	1.98	2.61	xxx	1.91	2.33	xxx	3.40	5.78	xxx	7.20	5.65	xxx	6.70
S14	-	xxx	-22.2	2.85	xxx	2.13	2.91	xxx	2.22	1.66	xxx	1.70	6.35	xxx	7.00	5.65	xxx	6.70
S15	2.45	xxx	3.25	3.75	xxx	3.45	2.98	xxx	2.26	3.41	xxx	4.10	6.46	xxx	7.50	5.65	xxx	6.70
S16	1.78	xxx	4.80	2.36	xxx	3.49	2.61	xxx	2.71	2.45	xxx	3.70	4.64	xxx	6.80	5.08	xxx	7.40
S17	1.78	xxx	4.51	2.28	xxx	2.82	2.57	xxx	3.00	1.60	xxx	2.00	4.53	xxx	6.50	5.20	xxx	6.80
S18	1.66	xxx	3.42	2.43	xxx	2.53	2.46	xxx	3.54	1.78	xxx	2.10	5.07	xxx	7.10	5.20	xxx	7.20
S19	1.54	xxx	4.19	1.78	xxx	2.40	2.34	xxx	3.40	0.94	xxx	1.50	3.85	xxx	5.20	4.86	xxx	7.10
S20	1.36	xxx	3.51	1.46	xxx	3.05	2.23	xxx	3.05	1.24	xxx	3.10	4.42	xxx	7.10	5.16	xxx	8.40
S21	1.18	xxx	2.88	1.96	xxx	3.35	2.57	xxx	3.59	1.78	xxx	3.60	5.07	xxx	8.30	5.16	xxx	7.80
S22	2.02	xxx	4.63	1.78	xxx	1.95	2.27	xxx	3.42	1.18	xxx	3.90	5.28	xxx	9.80	5.27	xxx	8.20
S23	3.29	xxx	3.23	4.00	xxx	3.43	2.64	xxx	2.00	3.59	xxx	4.20	6.39	xxx	7.30	5.87	xxx	7.00
S24	3.41	xxx	3.43	4.10	xxx	3.59	2.72	xxx	2.03	3.84	xxx	4.40	6.28	xxx	7.40	5.95	xxx	7.00
S25	3.41	xxx	3.43	4.67	xxx	4.25	2.64	xxx	1.95	3.90	xxx	5.10	6.28	xxx	7.40	6.13	xxx	7.30
S26	2.45	xxx	2.97	3.00	xxx	2.86	2.91	xxx	2.05	2.81	xxx	3.70	6.10	xxx	7.40	5.61	xxx	6.80
S27	2.08	xxx	3.18	3.50	xxx	3.24	3.02	xxx	2.30	3.47	xxx	4.10	6.39	xxx	7.50	5.65	xxx	6.70
S28	2.81	xxx	3.20	3.85	xxx	3.20	2.53	xxx	1.98	3.59	xxx	3.90	6.36	xxx	7.40	5.76	xxx	6.80
S29	2.63	xxx	2.75	3.93	xxx	3.12	2.49	xxx	1.95	3.41	xxx	4.10	6.39	xxx	7.50	6.13	xxx	7.20
S30	1.78	xxx	3.14	0.63	xxx	1.18	2.53	xxx	2.54	0	xxx	0	4.14	xxx	9.20	5.57	xxx	7.30
S31	2.02	xxx	2.84	2.43	xxx	2.51	2.12	xxx	2.16	2.33	xxx	4.10	5.92	xxx	8.20	5.42	xxx	6.90
S32	1.66	xxx	3.78	2.07	xxx	2.38	2.61	xxx	2.56	1.48	xxx	2.00	4.75	xxx	6.70	5.06	xxx	7.10
S33	2.02	xxx	4.90	1.78	xxx	1.45	2.27	xxx	3.92	1.18	xxx	4.40	5.28	xxx	8.80	5.27	xxx	8.90
S34	2.08	xxx	3.18	3.50	xxx	3.24	3.02	xxx	2.30	3.47	xxx	4.10	6.39	xxx	7.50	5.65	xxx	6.70
S35	2.81	xxx	3.20	3.85	xxx	3.20	2.53	xxx	1.98	3.59	xxx	3.90	6.36	xxx	7.40	5.76	xxx	6.80
S36	1.90	xxx	3.96	1.36	xxx	1.65	2.53	xxx	3.73	0.82	xxx	2.70	4.14	xxx	6.00	5.16	xxx	6.60

Table D2: **Temperature (Min.)** trend analyses values on **Seasonal** basis of future data (2020-2040) using Mann-Kendall Test and Sen's slope method

(Z= Mann-Kendall Z; SS=Sen's Slope in %ge;)

***Note*: Z is the statistical parameter. Trend value corresponding to Z value more than +1.96 (-1.96) represents statistically significant.**

Station	RCP4.5 (2020-2040)								RCP8.5 (2020-2040)							
	Pre-Monsoon		Monsoon		Post-Monsoon		Winter		Pre-Monsoon		Monsoon		Post-Monsoon		Winter	
	Z	SS	Z	SS	Z	SS	Z	SS	Z	SS	Z	SS	Z	SS	Z	SS
S1	1.6	7.2	2.51	4.1	-	-1.4	1.18	6	1.90	6.70	3.11	5.30	-	-	0.57	0.22
S2	-	-4.7	-	-6.2	-	-13	-	-8.6	1.72	6.40	3.23	5.30	-	-	0.39	2.00
S3	1.96	10.8	2.33	4.7	-	-	0.88	8	1.18	6.50	2.81	5.40	-	-	0.09	0.60
S4	1.78	8.6	2.45	4.3	0.03	0.13	0.34	8.1	1.12	5.00	3.17	5.50	-	-	0.69	4.00
S5	1.24	7.8	2.93	3.7	0.51	1.04	0.75	4	2.39	9.20	3.96	5.90	-	-	1.24	8.30
S6	-	-23	-	-	-	-	-	-	2.14	8.30	3.53	3.30	-	-	0.45	3.70
S7	2.69	4.1	3.90	3.4	1.36	3.2	-	-	2.02	4.90	3.96	4.10	2.20	4.70	1.48	4.70
S8	3.11	5.2	3.71	3.5	1.78	4.2	0.63	1	2.33	6.80	4.38	4.60	2.51	5.40	1.96	5.20
S9	-	-6.6	-	-5.1	-	-5.8	-	-9.9	2.39	6.60	4.56	5.30	2.33	4.30	2.20	4.80
S10	-	-	-	-	-	-	-	-	2.45	6.80	4.62	5.70	1.36	2.70	1.60	4.70
S11	3.41	6.5	3.66	3.3	1.54	3.3	0.27	0.52	2.45	8.00	4.26	6.90	1.72	3.30	1.98	5.20
S12	3.23	6.6	3.65	4.1	1.60	3.7	0.39	0.69	2.63	8.00	4.44	6.70	1.90	3.50	1.72	5.20
S13	2.57	5.8	4.08	3.6	0.75	1.7	-	-	1.96	6.20	4.02	5.20	-	-	1.42	4.10
S14	-	-22	-	-	-	-	-	-	1.66	4.80	3.47	3.50	-	-	0.15	0.60
S15	2.63	6.1	3.90	3.7	1.06	2.8	0.21	0.31	2.51	5.90	4.44	4.90	1.36	2.70	2.14	5.60
S16	1.72	7.8	3.47	3.8	0.75	2.4	0.69	4.0	2.08	6.90	3.96	5.20	-	-	2.02	11.40
S17	1.54	6.9	3.29	3.9	0.88	2.5	0.94	4.3	1.54	2.00	1.54	7.50	-	-	1.66	8.70
S18	2.02	6.5	2.63	3.9	-	-	1.48	5.3	1.48	5.90	3.11	5.40	-	-	0.69	3.00
S19	1.18	7.0	2.99	4	0.09	0.36	1.12	4.6	1.18	6.10	4.02	5.90	-	-	1.06	6.90
S20	1.54	5.6	3.36	3.9	1.18	2.8	0.51	2.7	2.63	8.30	3.71	4.60	-	-	1.06	5.10
S21	1.42	6.0	3.59	4.1	0.75	1.7	0.51	4.6	2.63	7.80	3.65	4.60	-	-	1.36	6.00
S22	1.24	3.5	1.90	3	1.12	3.4	1.54	9.7	2.14	7.50	2.75	3.20	0	0	0.69	4.20
S23	3.05	5.3	3.84	3.6	1.54	3.4	0.03	0.12	2.45	6.40	4.50	5.20	1.96	3.60	1.96	4.50
S24	3.17	5.3	3.84	3.6	1.42	4.3	0.15	0.35	2.33	6.30	4.50	5.20	2.33	3.70	2.08	4.10
S25	3.17	5.3	3.84	3.6	1.42	4	0.15	0.34	2.51	6.90	4.38	4.80	2.39	4.80	1.98	4.40
S26	2.39	6.3	3.84	3.7	1.06	2.2	-	-	1.90	6.50	4.32	5.10	-	-	1.75	5.60
S27	2.69	6.4	3.96	3.7	1.00	1.8	0.15	0.35	2.51	6.30	4.32	4.90	1.06	2.10	2.14	5.90
S28	2.93	4.7	3.90	3.8	1.18	2.4	0.21	0.43	2.39	3.90	4.32	4.50	1.96	3.80	1.30	4.0
S29	2.69	4.0	3.84	3.4	1.30	3.2	-	-1.1	2.08	4.80	3.90	4.10	2.08	4.70	1.54	4.70
S30	2.26	5.7	3.65	3.8	0.75	1.8	0.03	0.14	0.57	1.30	1.36	1.20	-	-	-	-2.70
S31	2.33	4.6	3.29	3.8	1.12	3	0.63	1.5	2.26	5.50	3.53	4.10	1.18	2.50	1.18	5.40
S32	1.42	6.0	3.59	4.1	0.75	1.7	0.51	4.6	2.63	7.80	3.65	4.60	-	-	1.36	6.00
S33	1.24	3.8	1.90	3.4	1.12	3.20	1.54	9.7	2.62	7.50	2.70	3.20	0	0	0.69	4.30
S34	1.24	7.8	2.93	3.7	0.51	1.04	0.75	4	2.39	9.20	3.96	5.90	-	-	1.24	8.30
S35	2.69	4.1	3.90	3.4	1.36	3.2	-	-	2.02	4.90	3.96	4.10	2.20	4.70	1.48	4.70
S36	2.26	5.5	3.65	3.6	0.75	2.4	0.03	0.14	0.57	1.35	1.36	1.50	-	-1.9	-	-2.30

Table D3: **Temperature (Min.)** trend analyses values on **Seasonal** basis of future data (2041-2070) using Mann-Kendall Test and Sen's slope method

(Z= Mann-Kendall Z; SS=Sen's Slope in %ge;)

***Note*: Z is the statistical parameter. Trend value corresponding to Z value more than +1.96 (-1.96) represents statistically significant.**

Station	RCP4.5 (2041-2070)								RCP8.5 (2041-2070)							
	Pre-Monsoon		Monsoon		Post-Monsoon		Winter		Pre-Monsoon		Monsoon		Post-Monsoon		Winter	
	Z	SS	Z	SS	Z	SS	Z	SS	Z	SS	Z	SS	Z	SS	Z	SS
S1	2.64	5.3	4.14	3.1	0.64	1.5	0.50	1.3	3.39	7.80	5.10	4.20	4.00	9.10	2.68	6.30
S2	2.07	5.2	3.85	3.1	-	-	0.21	0.45	3.43	7.90	4.85	3.80	4.10	9.10	2.68	6.30
S3	2.36	6.0	3.82	3.2	-	-	-	-	2.96	9.40	3.82	3.40	3.21	8.20	1.78	5.00
S4	2.36	5.2	3.93	3.2	-	-1.3	0.36	0.67	2.89	7.10	4.28	3.70	3.25	8.30	1.96	5.10
S5	2.00	2.1	2.50	1.8	-	-3	1.07	4.0	2.60	5.10	3.78	3.70	4.00	8.60	1.96	4.80
S6	2.00	4.4	2.43	1.7	-	-3.1	0.89	3.8	3.57	7.80	4.89	5.50	5.60	9.80	3.60	13.20
S7	3.96	4.5	4.00	2.5	1.07	1.0	2.71	3.8	4.42	5.70	5.99	5.90	4.56	12.60	4.21	6.50
S8	3.85	5.1	4.50	2.7	2.14	2.0	3.46	4.7	4.75	6.00	5.85	5.70	5.28	12.40	4.50	7.40
S9	4.00	4.8	4.71	2.8	2.64	2.2	3.60	5.5	4.35	5.50	5.85	5.50	5.67	12.50	4.14	7.70
S10	3.68	4.3	3.68	2.4	1.36	1.3	1.61	2.4	3.71	5.10	5.74	5.40	5.82	10.80	3.96	7.90
S11	2.89	2.1	2.53	2.3	1.07	1.35	0.86	1.8	3.89	5.50	4.35	4.60	5.64	10.20	4.21	8.70
S12	3.35	3.9	2.78	2.2	1.39	1.5	1.53	2.3	3.82	5.20	4.60	4.90	5.64	11.20	4.28	8.90
S13	3.21	4.1	4.53	2.9	-	-	1.43	3.0	3.82	5.80	6.07	5.50	5.53	9.60	3.46	7.70
S14	3.64	4.2	4.21	2.8	0.29	0.45	1.61	2.7	3.68	4.90	5.89	5.50	5.74	10.30	3.89	7.80
S15	4.03	4.4	4.71	2.6	1.28	1.5	2.89	5.1	3.85	5.40	5.92	5.80	5.99	11.10	4.10	8.30
S16	2.89	5.6	3.89	2.6	0.07	0.23	2.32	7.4	3.28	6.30	5.21	5.20	4.53	9.20	2.50	8.10
S17	2.68	5.4	4.17	2.8	-	-1.4	1.71	5.1	3.07	6.70	5.03	4.90	3.78	9.30	2.36	6.50
S18	2.89	4.6	4.14	2.1	0.79	1.8	0.86	1.8	3.50	7.10	5.25	4.50	4.14	9.60	2.75	6.20
S19	2.21	5.3	3.50	2.5	-	-3.2	1.43	4.4	2.39	6.10	4.28	4.20	3.21	8.60	1.78	5.10
S20	1.71	3.6	2.53	1.7	-	-1.2	1.53	5.8	3.00	5.70	4.53	4.40	4.67	8.50	2.82	9.80
S21	2.32	4.3	3.35	2.1	-	-	1.93	7.2	3.46	6.30	4.96	5.10	5.25	8.70	3.82	13.60
S22	2.85	4.6	4.00	2.8	-	-	1.03	3.8	4.35	7.30	5.17	6.60	5.57	10.60	3.53	15.30
S23	4.14	4.9	4.17	2.6	2.11	2.5	3.03	4.3	4.25	5.10	5.78	5.60	5.78	11.80	3.82	7.50
S24	4.32	4.6	4.28	2.5	2.14	2.5	3.14	4.7	4.50	5.30	5.85	5.60	5.71	12.10	3.93	7.40
S25	4.10	5.1	4.50	2.7	2.78	2.7	3.78	5.6	4.50	5.30	5.85	5.60	5.71	12.10	3.93	7.40
S26	3.75	4.3	4.53	2.9	0.79	0.99	2.14	2.6	3.71	5.30	5.89	5.70	5.89	10.10	3.93	8.60
S27	3.75	4.2	4.57	2.6	1.07	1.2	2.71	4.9	3.71	5.30	5.78	5.80	6.03	10.90	4.36	8.90
S28	3.75	4.2	4.35	2.6	0.96	1.0	2.93	4.4	4.17	5.20	6.03	5.90	5.71	11.80	4.00	7.60
S29	3.93	4.4	3.93	2.5	1.14	1.1	2.64	2.8	4.39	5.60	5.89	5.90	5.42	12.60	4.17	6.30
S30	1.24	2.2	2.20	2.0	-	-	0.33	1.2	2.20	5.60	3.47	5.00	4.44	13.80	2.39	11.20
S31	3.25	3.9	4.39	2.8	-	-	1.61	3.7	3.85	5.60	5.89	6.40	5.60	11.80	3.96	8.80
S32	2.00	4.4	2.43	1.7	-	-3.1	0.89	3.8	3.57	7.80	4.89	5.50	5.60	9.80	3.60	13.20
S33	2.00	2.1	2.50	1.8	-	-3	1.07	4.0	2.60	5.10	3.78	3.70	4.00	8.60	1.96	9.80
S34	2.89	5.6	3.89	2.6	0.07	0.23	2.32	7.4	3.28	6.30	5.21	5.20	4.53	9.20	2.50	8.10
S35	3.85	5.1	4.50	2.7	2.14	2.0	3.46	4.7	4.75	6.00	5.85	5.70	5.28	12.40	4.50	7.40
S36	3.21	4.1	4.53	2.9	-	-	1.43	3.0	3.82	5.80	6.07	5.50	5.53	9.60	3.46	7.70

Table D4: **Temperature (Min.)** trend analyses values on **Seasonal** basis of future data (2071-2099) using Mann-Kendall Test and Sen's slope method

(Z= Mann-Kendall Z; SS=Sen's Slope in %ge;)

***Note*: Z is the statistical parameter. Trend value corresponding to Z value more than +1.96 (-1.96) represents statistically significant.**

Station	RCP4.5 (2071-2099)								RCP8.5 (2071-2099)							
	Pre-Monsoon		Monsoon		Post-Monsoon		Winter		Pre-Monsoon		Monsoon		Post-Monsoon		Winter	
	Z	SS	Z	SS	Z	SS	Z	SS	Z	SS	Z	SS	Z	SS	Z	SS
S1	1.86	3.7	1.41	0.97	0.47	0.34	1.97	5.9	3.51	7.50	5.76	6.00	3.70	6.80	3.21	7.30
S2	1.63	3.5	1.48	1.0	1.18	2.2	2.19	8.0	3.47	7.50	5.91	6.20	3.47	6.50	2.98	6.80
S3	1.59	3.8	1.18	0.75	1.33	2.6	2.87	12.7	2.27	6.30	5.72	6.70	1.67	4.20	1.44	3.80
S4	1.59	3.2	1.56	1.01	1.18	2.1	2.49	8.3	3.13	7.10	5.61	6.30	2.91	7.50	2.49	5.90
S5	1.48	3.1	1.22	0.61	0.69	1.4	2.16	6.7	4.00	8.00	4.75	5.60	3.92	10.30	2.83	5.70
S6	1.78	3.5	1.29	0.73	0.54	2.6	2.01	7.5	4.03	8.50	4.45	5.30	3.92	9.30	4.63	14.20
S7	1.78	2.2	0.66	0.52	2.08	2.7	1.74	2.0	4.75	7.00	4.37	5.00	4.63	9.50	5.31	7.30
S8	1.41	1.8	0.88	0.80	2.08	2.7	2.19	2.8	4.48	6.40	4.37	4.90	4.75	9.40	5.42	8.40
S9	1.63	1.9	1.26	0.99	2.46	3.3	2.23	3.2	4.52	7.00	3.73	4.30	4.63	9.10	5.01	8.40
S10	1.78	2.0	2.12	1.1	2.38	2.8	1.33	2.0	4.37	7.20	3.51	4.20	4.48	8.10	4.90	7.20
S11	1.52	2.9	1.96	1.4	1.11	1.7	1.52	1.9	4.30	8.40	3.32	4.40	4.75	7.70	4.30	6.80
S12	1.96	2.4	1.52	1.3	2.01	2.5	1.14	2.0	4.03	7.90	3.32	4.20	4.71	8.20	4.78	7.70
S13	1.29	2.6	1.86	1.03	1.44	1.8	2.42	2.7	4.37	7.10	5.01	5.00	4.52	7.70	3.96	6.80
S14	1.52	2.6	1.98	1.0	1.82	1.9	2.46	3.6	4.56	7.10	3.62	4.40	4.63	7.60	4.33	6.60
S15	1.63	1.9	1.11	0.86	2.23	2.7	2.72	4.5	4.56	7.10	3.62	4.40	4.63	7.60	4.33	6.60
S16	1.33	2.5	1.52	0.98	0.69	1.0	2.79	6.0	4.15	8.00	5.05	5.60	3.85	8.30	3.62	8.00
S17	1.22	2.7	1.63	0.98	0.58	1.0	2.68	6.2	3.58	6.70	5.08	5.80	4.07	8.80	2.53	4.40
S18	1.82	3.2	1.18	0.64	0.36	0.46	2.19	5.8	3.85	8.40	5.65	6.10	3.85	8.00	3.70	7.60
S19	1.03	2.5	1.29	0.73	0.51	1.5	2.46	7.5	3.36	7.30	5.20	6.10	3.81	8.60	2.34	4.70
S20	1.99	4.1	1.18	0.91	0.69	0.41	1.82	7.0	4.26	8.80	4.71	5.30	3.96	9.20	3.96	11.50
S21	1.98	3.4	0.73	052	0.77	1.3	2.42	8.4	4.56	6.10	5.20	7.00	2.95	8.10	4.11	11.80
S22	2.16	2.9	0.58	0.39	1.03	1.9	2.27	8.3	4.15	7.70	4.30	5.60	3.66	9.60	3.47	11.0
S23	1.97	1.9	1.56	0.99	2.61	2.1	2.08	2.9	4.52	7.00	3.77	4.20	4.63	8.60	4.93	7.80
S24	1.67	1.9	1.48	0.95	2.61	2.2	2.04	2.9	4.56	7.00	3.77	4.30	4.71	8.70	4.93	8.00
S25	1.71	1.9	1.14	0.67	2.42	3.3	2.31	2.9	4.45	6.80	4.18	4.70	4.71	9.30	5.20	8.40
S26	1.29	2.2	1.56	0.85	1.93	2.3	2.38	4.3	4.52	7.00	4.75	5.10	4.15	7.70	4.26	6.30
S27	1.56	1.8	1.11	0.71	2.19	2.6	2.79	4.6	4.45	7.10	4.67	4.90	4.30	8.60	4.33	6.90
S28	1.56	1.9	0.88	0.63	2.04	2.9	2.19	3.1	4.48	6.80	4.45	4.70	4.56	8.60	4.78	7.10
S29	1.74	2.2	0.58	0.39	2.08	2.8	1.74	2.0	4.86	7.10	4.37	5.00	4.63	9.60	5.36	7.30
S30	1.48	2.3	0.92	0.45	1.78	2.5	2.19	4.3	4.41	7.60	4.52	5.20	4.18	9.20	4.37	9.10
S31	1.52	2.0	0.73	0.41	1.18	2.4	1.97	3.4	4.56	7.10	4.56	5.40	4.15	9.30	4.18	7.60
S32	1.99	4.2	1.18	0.95	0.69	0.40	1.82	7.0	4.26	7.80	4.71	5.30	3.96	9.20	3.96	11.50
S33	1.78	2.0	2.12	1.1	2.38	2.8	1.33	2.0	4.37	7.20	3.51	4.20	4.48	8.10	4.90	7.20
S34	1.96	2.5	1.52	1.3	2.01	2.5	1.14	2.0	4.03	7.90	3.32	4.20	4.71	8.20	4.78	9.70
S35	1.59	3.8	1.18	0.75	1.33	2.6	2.87	12.7	2.27	6.30	5.72	5.70	1.67	6.20	1.44	5.80
S36	1.59	3.8	1.18	0.75	1.33	2.6	2.87	12.7	2.27	6.30	5.72	6.70	1.67	7.20	1.44	7.80

######## ########